9-26-2018 2:30 PM

Characterizing the Cortical Contributions to Working Memory-Guided Obstacle Locomotion

Carmen Wong
The University of Western Ontario

Supervisor
Lomber, Stephen G.
The University of Western Ontario

Graduate Program in Neuroscience
A thesis submitted in partial fulfillment of the requirements for the degree in Doctor of Philosophy

Recommended Citation
Wong, Carmen, "Characterizing the Cortical Contributions to Working Memory-Guided Obstacle Locomotion" (2018). *Electronic Thesis and Dissertation Repository*. 5716.
https://ir.lib.uwo.ca/etd/5716

Abstract

While walking in complex environments, the ability to acquire information about objects in our surroundings is essential for successful obstacle negotiation. Furthermore, the ease with which most animals can traverse cluttered terrain while grazing, exploring, or hunting is facilitated by the capacity to store obstacle information in working memory (WM). However, the underlying neural substrates supporting such complex behaviours are poorly understood. Therefore, the goal of this thesis is to examine the neural underpinnings of WM-guided obstacle negotiation in the walking cat.

Obstacle locomotion was studied in two main paradigms, characterized by whether obstacle presence was detected via vision or touch. In both paradigms, walking was delayed following foreleg obstacle clearance. When walking resumed, elevated hindleg stepping demonstrated that animals successfully remembered the obstacle beneath them.

The tactile paradigm was first examined to assess the ability of animals to remember an unexpected obstacle over which the forelegs had tripped. Such tactile input to the forelegs was capable of producing a robust, long-lasting WM of the obstacle, similar to what has been previously described using the visual paradigm. Next, to assess whether regions of the brain associated with spatial representation and movement planning contribute to these behaviours, parietal area 5 was reversibly deactivated as visual or tactile obstacle WM was tested. Such deactivations resulted in substantial WM deficits precluding successful avoidance in both paradigms.

To further characterize this cortical contribution, neural activity was then recorded with multi-electrode arrays implanted in area 5. While diverse patterns of task-related modulation were observed, only a small proportion of neurons demonstrated WM-related activity. These neurons exhibited the hallmark property of sustained delay period activity associated with WM maintenance, and were able to reliably discern whether or not the animal had stepped over an obstacle prior to the delay. Therefore, only a specialized subset of area 5 neurons is capable of maintaining stable representations of obstacle information in WM.

Altogether, this work extends our understanding of WM-guided obstacle locomotion in the cat. Additionally, these findings provide insight into the neural circuitry within the posterior parietal cortex, which likely supports a variety of WM-guided behaviours.

Keywords

Walking, Obstacle Avoidance, Working Memory, Cat, Posterior Parietal Cortex, Area 5, Cortical Cooling, Cryoloop, Electrophysiology, Neural Activity

Statement of Co-Authorship

All data collection, analysis, and writing of the manuscripts that comprise this doctoral thesis dissertation were primarily conducted by the author of this thesis, Carmen Wong. Dr. Keir Pearson assisted with the experimental design and editing of the manuscripts for Chapters 3 and 4. Gary Wong assisted in the data collection and analysis for the manuscript for Chapter 3. Dr. Stephen Lomber provided expertise and supervision during all stages of work, including the experimental design and manuscript edits for all chapters.

Acknowledgments

This work would not have been possible without the unwavering support, encouragement, and graciousness of my supervisor, Dr. Stephen Lomber. I struggle to find ample words to articulate my gratitude and fully encapsulate how fortunate I feel to have met him as a naïve undergraduate student. His wisdom, patience, and generosity were invaluable to my development throughout graduate school. He’s one of the good ones.

I also feel very fortunate that Dr. Lomber met Dr. Keir Pearson at a conference many years ago. I am thankful for the technical expertise and trust in continuing his work that Dr. Pearson has offered me throughout this process.

The insights, challenges, criticisms, and reassurances that members of my advisory committee provided have also been essential to this work. I thank Dr. Brian Allman, Dr. Brian Corneil, Dr. Paul Gribble, and Dr. David Sherry for sparing their time and imparting their knowledge.

To the members of the Cerebral Systems Lab throughout the years (Dr. Nicole Chabot, Pam Nixon, Gary Wong, Dr. Blake Butler, Stephen Gordon, Paisley Barnes, Melanie Kok, Dr. Daniel Stolzberg): thank you for your technical support, words of wisdom, amusing anecdotes, and sympathetic ears.

To Nelson: your insistence for bad puns, dancing offbeat, racing me on runs, and supplying sushi have been constant sources of annoyance, entertainment, motivation, and comfort that have helped me retain a sense of sanity and normalcy.

Table of Contents

List of Figures

Chapter 1

1 General Introduction

The intricate neural computations required for complex locomotion in naturalistic environments are often taken for granted, given the relative ease with which most animals can traverse cluttered and uneven terrain. For example, most people can walk through busy crowds without bumping into other people or objects while carrying on a conversation with a friend, or looking down at their phone. Quadrupedal animals can successfully step over an obstacle with all four limbs despite delaying obstacle clearance between their legs as they graze, explore new terrain, or track prey in complex environments. These obstacle locomotor behaviours are facilitated by the ability to store information about an obstacle in working memory. In quadrupeds, this stored information is especially important for guiding hindleg clearance as foreleg clearance results in the obstacle passing under the body, preventing any further visual input. Instead, these animals rely on information about the obstacle maintained internally within working memory in order to guide their hindlegs over it.

Such complex computations necessitate supraspinal involvement, implicating regions of motor and posterior parietal cortices (Takakusaki 2013; Drew and Marigold 2015). However, as locomotor control research has been largely focused on studying spinal control mechanisms, the cortical contributions to working memory-guided obstacle locomotion remain relatively less defined. Additionally, working memory is typically assessed in explicitly instructed paradigms, often in movement-restricted subjects. Thus our understanding of working memory-guided behaviours in a more naturalistic setting also requires further examination.

This thesis is aimed at elucidating the cortical contributions to working memory-guided obstacle negotiation in the cat. In doing so, we can assess the interplay between systems involved in locomotor control and working memory. As such, I first review the fundamental properties of locomotor control systems. Mechanisms of working memory-guided behaviours will then be discussed, before summarizing what is already known about working memory-guided obstacle locomotion.

1.1 Locomotor control systems in the walking cat

In order for an animal to move throughout its environment, locomotor control systems generate rhythmic alternating movements of the body for walking, crawling, swimming, or flying. Given the aims of this thesis, I focus here on locomotion in the cat, as well as humans, which involves fairly stereotyped, repetitive activations of a large number of muscles to produce the swing and stance phases for walking. These patterns of muscle contractions may be considered as involving four phases to comprise swing and stance (Engberg and Lundberg 1969). Flexion (F) of the hip, knee, and ankle joints lifts the foot from the ground during the first half of the swing phase. This is followed by extension (E1) at the hip, knee, and ankle to move the foot ahead of the body in preparation for stance. Extension of ankle and knee extensor muscles in early stance (E2) enables the transfer of weight to allow the body to move over the foot. Finally, extension at the hip, knee, and ankle (E3) propels the body forward. This overall sequence of rhythmic muscle contractions for stepping is produced by circuitry within the spinal cord. The resulting locomotor rhythm is readily adaptable, and responds to proprioceptive and tactile inputs reflexively via spinal pathways for rapid adjustments. Descending signals from brainstem locomotor regions act upon this spinal locomotor circuitry to initiate walking and regulate locomotor speed. Furthermore, in complex locomotor tasks often involving visuomotor control, descending signals from motor and posterior parietal cortices can adapt the locomotor rhythm in a feedforward manner. These levels of locomotor control are reviewed below.

1.1.1 Spinal locomotor circuitry

Three control circuits responsible for rhythm-generation, left-right pattern-generation, and flexor-extensor pattern-generation coexist within the spinal cord of limbed mammals, and are regulated by proprioceptive and tactile inputs relayed through the spinal circuitry (Kiehn 2006).

1.1.1.1 Rhythm-generating circuits

Early studies of the spinalized and deafferented decerebrate cat by Brown (1911) first demonstrated the ability of the spinal cord to produce patterns of rhythmic, alternating flexor and extensor muscle activity without descending command signals from supraspinal structures. He proposed that mutually inhibitory flexor and extensor 'half-centres', termed central pattern generators (CPGs), must exist within the spinal cord to produce rhythmic activation patterns required for stepping (Jones et al. 2011). These CPG networks are comprised of motor neurons innervating synergistic muscle groups of limb flexors or extensors, interconnected with premotor interneurons (Armstrong 1988; Krouchev et al. 2006). Such spinal CPG circuitry determines the appropriate sequences of muscle activation for the generation of motor patterns in all animals (Grillner 2006). Rhythmogenicity may arise through individual pacemaker mechanisms permitting some neurons to display inherent rhythmic bursting capabilities. For example, optogenetic activation of excitatory glutamatergic neurons in the lumbar spinal cord initiates and maintains rhythmic locomotor-like activity, with the appropriate flexor-extensor alternation and left-right alternation (Hägglund et al. 2010). Such glutamatergic neurons in the spinal cord can drive CPG network activity and determine the locomotor tempo via ipsilateral projections onto motor neurons (Jordan et al. 2008). Alternatively, rhythmogenicity may be achieved through a network mechanism as a result of interactions between neurons, possibly associated with persistent sodium currents (Tazerart et al. 2007).

1.1.1.2 Left-right pattern-generating circuits

The coordination of movements between both sides of the body is achieved via commissural neurons, with axons crossing the midline. Both direct and indirect crossed inhibition supports alternating, or out-of-phase, muscle activity required for walking or trotting. Direct inhibition is facilitated by inhibitory commissural neurons acting on motor neurons or interneurons, while indirect inhibition is achieved through excitatory commissural neurons acting on premotor interneurons. Our understanding of left-right pattern-generating circuits has been recently advanced, with a series of studies involving the genetic inactivation of V0 neurons, a distinct type of commissural neurons characterized by the early expression of the transcription factor Developing Brain Homeobox 1 (Talpalar et al. 2013; Bellardita and Kiehn 2015). Mice lacking V0 neurons cannot produce left-right alternating gaits at all locomotor frequencies (Talpalar et al. 2013). Instead, such knock out models can only produce synchronous locomotor patterns like bounding (Bellardita and Kiehn 2015). Furthermore, with selective speed-related deficits, inhibitory V0 neurons are proposed to support left-right alternation for walking, while excitatory V0 neurons maintain alternation for trotting. These left-right alternating circuits are suppressed or overridden at greater locomotor speeds (bounding) by V0-independent synchronous left-right circuits. However, the particular type of commissural neuron recruited for crossed excitation to produce left-right synchronicity for bounding remains to be determined.

1.1.1.3 Flexor-extensor pattern-generating circuits

In addition to left-right alternation, locomotion for limbed animals requires the alternating activation of flexor and extensor muscle synergies in order for a limb to produce a step. Such intralimb coordination is achieved via pairs of reciprocally inhibiting neurons acting on the same joint. Termed reciprocal-Ia-inhibitory neurons, these cells respond to changes in muscle length detected via Ia afferents from the muscle spindles in the flexor or extensor muscles around the joint. Detected changes in the flexor muscles reciprocally inhibit the antagonist motor neurons innervating the extensor muscles, and vice versa (Hultborn 1976). Reciprocal-Ia-inhibitory neurons are also regulated by Renshaw cells within the gray matter of the spinal cord (McCrea et al. 1980). As inhibitory interneurons receiving excitatory collaterals from motor neurons, Renshaw cells related to flexor motor neurons fire maximally during middle and late flexion, while Renshaw cells related to extensor motor neurons respond maximally during late extension (Pratt and Jordan 1987). Such activation represents a negative feedback mechanism, which likely facilitates the transition between antagonistic phases of activation for flexor-extensor alternation.

While reciprocal-Ia-inhibitory neurons and Renshaw cells were originally included in the spinal rhythm generating network, recent studies of genetic knockout models support an alternative, separate model of organization involving two classes of interneurons for flexor-extensor alternation. Synaptic inactivation of two types of reciprocal-Ia-inhibitory neurons, V1 interneurons (derived from progenitor cells expressing the engrailed homeobox 1 transcription factor) and V2b interneurons (derived from progenitor cells expressing the GATA binding protein 2 transcription factor), results in an inability to produce flexor-extensor alternation (Zhang et al. 2014). Furthermore, genetic ablation of V1 interneurons results in limb hyperflexion while ablation of V2b interneurons results in limb hyperextension, demonstrating the distinct contributions of V1 and V2b interneurons to ensuring proper and timely limb extension and flexion, respectively (Britz et al. 2015). Despite the lack of flexor-extensor alternation in transgenic mice lacking V1- and V2b-inhibition, the motor rhythm persists with preserved left-right alternation (Zhang et al. 2014). This supports a two-level CPG model consisting of distinct rhythm-generation and pattern-generation levels, whereby V1 and V2b interneurons support flexor-extensor alternation for adequate pattern formation (Shevtsova and Rybak 2016).

1.1.1.4 Spinal regulation of locomotor networks

The involvement of Ia afferents conveying changes in muscle length to spinal interneurons for flexor-extensor alternation provides only one example of the role of proprioception for locomotion. Both stretch-sensitive muscle spindles and force-sensitive Golgi tendon organs are activated as the leg muscles contract for locomotion, and may facilitate the transitions between the swing and stance phases (Pearson 2007). Early work from Grillner and Rossignol (1978) suggested that proprioceptive input from flexor hip muscles conveying hip position may increase flexor activation of the leg to enhance the swing phase. Furthermore, electrical stimulation of Golgi tendon organ 1b afferents from knee and ankle extensors during flexion terminates flexor activity and initiates an extensor burst during fictive locomotion in decerebrate spinalized cats (Conway et al. 1987). In contrast, stimulation of group I afferents to the extensors during an extensor burst prolongs extension, delaying the subsequent flexor burst. Such influence on central rhythm generators demonstrates the role of proprioceptive inputs on the reflex regulation of stepping. Furthermore, recent work from Akay et al. (2014) dissociates between the two types of proprioceptive inputs by genetically eliminating feedback from the muscle spindles or Golgi tendon organs in transgenic mice. This study demonstrates the role of muscles spindles predominantly on flexor activation influencing the swing-to-stance transition, and the involvement of both muscles spindles and Golgi tendon organs in regulating extensor activation influencing the stance-to-swing transition.

In addition to such proprioceptive regulation of spinal locomotor circuitry, tactile inputs to the feet or legs can also modulate spinal locomotor networks. For example, if an animal trips over an unexpected obstacle, the sudden contact of the foot or leg during the swing phase elicits the stumbling corrective reaction (Forssberg 1979). In both spinalized (Andersson et al. 1978) and intact cats (Buford and Smith 1993), rapid and reflexive activation of ipsilateral knee flexors and ankle extensors lifts the leg and foot above the obstacle to ensure proper obstacle avoidance (Prochazka et al. 1978; Wand et al. 1980). Additionally, activation of contralateral extensor muscles, termed crossed extension, maintains stability of the animal without interrupting forward locomotion (Forssberg et al. 1977). When tactile stimulation is instead applied during the stance phase, extensor muscles are first inhibited then excited, resulting in no overall change in extension. However, the subsequent swing phase features limb hyperflexion and crossed extension to support successful obstacle avoidance. Importantly, as these reflexive activations are present in chronically spinalized cats, the circuitry enabling these rapid adjustments exist within the spinal locomotor circuitry.

1.1.2 Supraspinal control of locomotion

The basic motor pattern for stepping produced by this spinal circuitry is regulated by supraspinal structures, which work to activate and refine locomotor patterns in response to feedback from the limbs and sensory input of the environment.

1.1.2.1 Descending signals initiate walking

In the cat, three major locomotor regions, comprised of the mesencephalic locomotor region, subthalamic locomotor region, and cerebellar locomotor region, have been identified in the brainstem, hypothalamus, and cerebellum, respectively (Takakusaki 2013). Analogous supraspinal locomotor structures are present in the human as mental imagery of locomotion results in similar regions of activation revealed with functional MRI (Jahn et al. 2008).

Early work by Shik et al. (1969) in the decerebrate cat revealed that electrical stimulation of the mesencephalic locomotor region (MLR), comprised of the pedunculopontine tegmental nucleus and the cuneiform nucleus, initiates stepping. Furthermore, increasing the intensity of stimulation increases the locomotor rhythm, allowing an animal to progress from walking to trotting to galloping with progressively stronger electrical stimulation. Such stimulation of the MLR is subsequently relayed via the medullary reticular formation (MRF) to activate interneurons in spinal locomotor networks, as cooling induced deactivation of the MRF prevents MLR-initiated stepping (Shefchyk et al. 1984). Furthermore, as intrathecal infusion of glutamate receptor antagonists in the lumbar spinal cord also inhibits MLR-initiated locomotion, such circuitry is mediated by descending glutamatergic reticulospinal pathways (Douglas et al. 1993).

Within the hypothalamus, electrical stimulation of the subthalamic locomotor region (SLR) can likewise activate spinal locomotor circuitry to initiate stepping (Mori et al. 1989) via the MRF directly or indirectly through the MLR (Sinnamon and Stopford 1987). As a part of the hypothalamus, SLR initiated stepping may be associated with emotional locomotor behaviours for feeding, fleeing, or defensive or aggressive actions (Narita et al. 2002). Additionally, electrical stimulation of the cerebellar locomotor region (CLR) can also evoke locomotion in the decerebrate cat (Mori et al. 1999). Like the MLR and SLR, the CLR can activate spinal locomotor circuitry via reticulospinal pathways from the MRF (Mori et al. 1998). Furthermore, as CLR stimulation also activates vestibulospinal cells, the cerebellum can integrate mechanisms for locomotor initiation and postural control (Orlovsky 1972a). Thus despite the apparent redundancy of the coexistence of three locomotor initiating centres, the activation of each individual region and, subsequently, the downstream locomotor circuitry, may be motivated by different needs of the animal.

While electrical stimulation of these three locomotor regions can initiate stepping in the decerebrate cat, disinhibition of basal ganglia circuitry is required for the initiation of locomotion in an intact animal. In the cat, GABAergic projections from the substantia nigra tonically inhibit the MLR (Takakusaki et al. 2003). Thus activation of dopaminergic striatal neurons within the basal ganglia (Ryczko and Dubuc 2017) is required to disinhibit glutamatergic neurons of the MLR (Roseberry et al. 2016) in order to initiate movement. Such circuitry elucidated in cat and rodent models is conserved in humans, as a deficiency in dopamine precludes this disinhibition, leading to the locomotor deficits seen in Parkinson’s disease (Rolland et al. 2009). Furthermore, a recent study using positron emission tomography (PET) to examine the involvement of supraspinal structures to imagined locomotion demonstrates activation of the basal ganglia when imagined walking is initiated (Malouin et al. 2003).

1.1.2.2 Visuomotor coordination involves the motor cortex, posterior parietal cortex, and cerebellum

With locomotor control research largely focused on elucidating spinal and subcortical mechanisms of walking, a thorough understanding of the cortical contributions to locomotion remains to be attained. However, complex locomotor behaviours dependent on visuomotor coordination have been shown to involve both the motor and posterior parietal cortices (Drew and Marigold 2015), as well as the cerebellum (Morton and Bastian 2004).

The motor cortex contributes to the execution of gait modifications for complex locomotion. Electrophysiological recordings of pyramidal tract neurons in the motor cortex demonstrate increased firing activity as an animal progresses from rest to slow walking (Armstrong and Drew 1984). Furthermore, experiments involving microstimulation of the pyramidal tract of decerebrate cats (Orlovsky 1972b) or the motor cortex of intact cats (Armstrong and Drew 1985) demonstrate differentially modulated locomotor rhythms depending on the phase of the step cycle during which stimulation was applied. If the contralateral foreleg is mid-swing, motor cortical stimulation prolongs the swing phase. However, if applied during the stance phase, motor cortical stimulation initiates a new swing phase. These effects are dependent on stimulation strength, with weaker stimulation unable to produce such changes in the onset or offset of muscle activity. Therefore, descending motor signals may override the existing locomotor rhythm to reset the step cycle, depending on the strength or duration of the signal.

Such motor cortical control is employed during complex locomotion. While lesions to motor cortex do not preclude simple stepping on smooth, unobstructed surfaces, visually-guided locomotor tasks are impaired (Drew et al. 1996). For example, cats can no longer step from rung to rung on a horizontal ladder following bilateral transection of the pyramidal tracts (Liddell and Phillips 1944). Additionally, inactivation of the motor cortex via pharmacological means or with lesions also impairs obstacle locomotion (Beloozerova and Sirota 1993). Such deficits are attributed to errors in paw placement, suggesting a role of the motor cortex in end point control for visually-guided locomotion. In support of this, pyramidal tract neurons in the motor cortex demonstrate increased firing activity during ladder locomotion relative to over ground walking (Armstrong and Marple-Horvat 1996). Such modulation is greatest in the late swing-early stance phase of contralateral foreleg steps, as the foot must be accurately placed onto a ladder rung. Similarly, in comparison to unobstructed walking, pyramidal tract neurons demonstrate increased activity for obstructed locomotion (Beloozerova and Sirota 1993), aligned to contralateral foreleg (Drew 1993) or hindleg (Widajewicz et al. 1994) steps over the obstacle. As these modulations were observed during, and not prior to, the step cycle where the cat stepped over an obstacle, the motor cortex is involved in the execution, and not planning, of visually-guided gait modifications (Drew et al. 2008).

In contrast, modulated activity observed in the posterior parietal cortex (PPC) occurs in advance of visually-guided gait modifications. As such, the PPC is implicated in the planning of visually-guided locomotor tasks (Drew and Marigold 2015). Modulated PPC activity has been observed with a variety of complex locomotor tasks, including stepping on a horizontal ladder, obstructed locomotion, and walking along a narrow path (Beloozerova and Sirota 2003). Furthermore, a visual dissociation task conducted during treadmill locomotion was developed by Lajoie and Drew (2007), where an obstacle was attached to a second, flanking treadmill belt to allow the obstacle to move at a speed different from that of the treadmill. In this visually dissociated setting, cats successfully adapt stepping for obstacle clearance two to three steps leading up to the obstacle. However, lesions to area 5 within the PPC impair these anticipatory step adjustments, resulting in animals frequently hitting the obstacle. Such errors in paw placement leading up to the obstacle implicate the PPC in the precise control of stepping prior to visually-guided gait modifications.

Subsequent electrophysiological recordings from parietal area 5 aimed to examine this further. Unlike motor cortex recordings, PPC neurons modulate their firing activity two to three steps prior to obstacle clearance (Andujar et al. 2010; Lajoie et al. 2010). Furthermore, unlike motor cortical neurons that are modulated in relation to contralateral steps in either lead or trail conditions over an obstacle (Drew 1993), most PPC neurons demonstrate increased activity with the lead foreleg step over an obstacle, regardless of whether the leading limb is ipsilateral or contralateral to the recording site (Andujar et al. 2010; Lajoie et al. 2010). Additionally, Marigold and Drew (2017) demonstrated distinct populations within area 5 that respond to estimates of obstacle location relative to the body in terms of time-to-contact or distance-to-contact measures, regardless of whether the ipsilateral or contralateral foreleg led obstacle clearance.

As such patterns of neural modulation implicate the PPC in visually-guided gait modifications, it its worth differentiating such contributions from visual responses to the obstacle itself. In these studies, while area 5 activity was modulated two to three steps before the obstacle, the obstacle was visible well before any changes in neural activity. Additionally, the majority of modulated area 5 activity prior to visually-guided gait modifications continue throughout a period of brief visual occlusion (Marigold and Drew 2011). Thus altogether, these studies demonstrate a role of the PPC in the planning of visually-guided gait modifications for obstacle locomotor behaviours in the cat. Similar implications for human PPC involvement in obstructed locomotion have been revealed with recent PET and electroencephalography (EEG) studies via imagined (Malouin et al. 2003) or treadmill walking (Gwin et al. 2011; Wagner et al. 2014), respectively.

As the PPC projects to all regions of motor cortex (Babb et al. 1984; Yumiya and Ghez 1984; Andujar and Drew 2007), modulated area 5 activity associated with planning step adjustments for obstacle locomotion may be relayed to the motor cortex for the implementation and execution of visually-guided gait modifications. Alternatively, signals from the PPC may be relayed subcortically to the cerebellum (Glickstein 2000), which also contributes to the control of complex locomotion. Cerebellar nuclear neurons and Purkinje cells are modulated rhythmically with ladder locomotion (Marple-Horvat and Criado 1999). These cells are also implicated in visually-guided coordination as they respond when a rung on a horizontal ladder is moved as an animal approaches (Armstrong and Marple-Horvat 1996). Furthermore, cerebellar damage results in errors in feedforward control, with overshooting trajectory errors during obstacle locomotion in the rat (Aoki et al. 2013), and disrupted predictive motor adaptations to split treadmill walking in humans (Morton and Bastian 2006).

Thus altogether, the motor cortex, PPC, and cerebellum comprise the supraspinal locomotor control centres, which can adapt stepping for complex, visually-dependent locomotor tasks. With a relatively limited focus on understanding these cortical contributions to complex locomotion, even fewer have evaluated mechanisms underlying working memory-guided locomotion. As such, the aim of this dissertation is to extend our understanding of complex locomotor behaviours requiring working memory. Working memory has been studied extensively in human and non-human primates performing various cognitive or delayed behavioural tasks. These studies have been integral to our understanding of working memory, but the applicability of concepts and mechanisms elucidated from such work to obstacle locomotor behaviours requires further study. Therefore, I next describe the established concepts of working memory-guided behaviours, before examining the relatively newer and smaller field of working memory-guided obstacle locomotion.

1.2 Working memory-guided behaviours

The ability to temporarily store information in working memory allows an animal to perform multiple goal directed behaviours simultaneously (Miller et al. 1960; D’Esposito and Postle 2015). For example, as a cat steps over the various pens, notebooks, and electronic devices on a graduate student’s cluttered desk, the cat may pause to inspect a particular item. When the cat has decided the item is no longer interesting, he can continue traversing the desk and exploring new items while remembering to step over previously encountered objects. The ability to store information about the size, shape, and location of an object in working memory facilitates this exploratory behaviour. Working memory is a type of short-term memory that involves the storage and manipulation of information (Baddeley 2003; Leavitt et al. 2017). Semantic, sensory, or motor information may be encoded into working memory to facilitate a variety of different cognitive and or behavioural tasks (D'Esposito and Postle 2015).

Neural correlates of working memory were first described in the prefrontal cortex of macaques performing a delayed response task (Fuster and Alexander 1971). In this paradigm, each animal watched as a food reward was placed behind one of two visually-occluding blocks. The blocks were then hidden from view throughout a delay period, during which the animals were required to remember the location of the reward in order to accurately obtain the reward following the delay. Neurons that demonstrated increased activity that was sustained throughout the delay period when the blocks were hidden were presumed to be involved in working memory processes facilitating this task. Such sustained delay period activity has been subsequently demonstrated to be related to specific task-relevant properties of a remembered visual stimulus, including its location (Funahashi et al. 1989, 1993) or colour (Quintana and Fuster 1999). Such stimulus-specific responses persisting in the absence of the stimulus is thought to be achieved via reverberatory excitation between neurons (Wang 2001) mediated by the slow kinetics of NMDA receptors (Wang 1999; Wang et al. 2013). Furthermore, silencing such activity through the deactivation of prefrontal regions via lesions (Goldman et al. 1971) or cooling (Bauer and Fuster 1976) results in working memory-related task deficits. Thus altogether, sustained delay period activity is classically regarded as a potential mechanism for encoding information into working memory in order to guide future behaviours. However, as will be subsequently discussed, the relevance of sustained delay period activity specifically for working memory has become an increasingly contentious issue.

1.2.1 Neuroanatomy of working memory

Working memory involves multiple regions of the brain. In particular, sustained delay period activity has been described in numerous neural populations recorded from subdivisions of prefrontal and parietal cortices, the basal ganglia, as well as regions of early sensory cortex (Leavitt et al. 2017).

Since the seminal study by Fuster and Alexander (1971), the prefrontal cortex has garnered the focus of working memory research. As previously discussed, sustained delay period activity has been reported in numerous regions of prefrontal cortex using a variety of different working memory tasks (see Leavitt et al. (2017) for an extensive review). Additionally, disruption of delay period activity via electrical stimulation reduces performance on a working memory-dependent oculomotor task (Sobotka et al. 2005). The attenuation or complete lack of sustained delay period activity observed in errors trials (Bolkan et al. 2017) further demonstrates the necessity of such activity for the successful execution of working memory tasks. In contrast to maintained representations described in more posterior brain regions, neural representations maintained within the prefrontal cortex are often more complex or abstract in nature. For example, while neurons in the inferior temporal cortex respond selectively to certain visual stimuli of a delayed matching to sample working memory task, neurons recorded in the prefrontal cortex are less stimulus-selective (Miller et al. 1996). Instead, prefrontal neurons convey information about whether a given stimulus matches the initially presented sample. Similarly, prefrontal neural populations have also been demonstrated to retain category-level representations (Meyers et al. 2008) or previously learned associations (Stokes et al. 2013) of presented visual stimuli.

In conjunction with the prefrontal cortex, the parietal cortex has also been implicated in working memory tasks. In a study recording neural responses from the PPC or prefrontal cortex, cooling-induced deactivation of one region modulates responses recorded in the other during a delayed saccade task (Chafee and Goldman-Rakic 2000). As such, both the PPC and prefrontal cortex are often both implicated in working memory-related tasks (Chafee and Goldman-Rakic 1998). However, distinctions have been observed between parietal and prefrontal cortical involvement in working memory (Qi et al. 2010; Zhou et al. 2012; Masse et al. 2017). For example, prefrontal neural activity is prone to distractors presented during a working memory delay (Jacob and Nieder 2014). While remembered target information is quickly restored in prefrontal neural activity following interference, activity related to the remembered target recorded from the ventral intraparietal area is completely resilient to distracting stimuli. Thus parietal and prefrontal cortices may play distinct, but complementary roles in maintaining and retrieving task-relevant information, respectively. In this view, information stored in working memory in parietal cortical structures is accessed or retrieved by prefrontal cortical structures.

Additionally, the basal ganglia is another structure shown to be responsible for gating working memory encoding, ensuring that only task-relevant information is stored (Frank et al. 2001; D'Ardenne et al. 2008; McNab and Klingberg 2008). As such, caudate neurons in the macaque also demonstrate delay period activity preceding working memory-guided saccades (Hikosaka et al. 1989). The elimination of such involvement in patients with basal ganglia lesions results in deficits in visual working memory independent of the hemifield in which a visual stimulus is presented (Voytek and Knight 2010).

Given the wealth of studies reporting sustained delay period activity across numerous regions of the brain, it is important to articulate that working memory is a distributed process, whereby no brain structures are unique to or specific to working memory (Eriksson et al. 2015). Instead, working memory employs large scale networks involving multiple regions across the cerebral cortex (Fuster and Bressler 2012). The use of functional MRI (fMRI) to examine blood oxygenation level dependent (BOLD) responses as correlates of neural activity have been particularly integral to examining working memory-related networks. For example, BOLD activity observed in sensory regions is correlated with activity in the prefrontal cortex, parietal cortex, and the striatum during the delay of a working memory facial recognition task (Gazzaley et al. 2004). Additionally, a separate fMRI study revealed co-activation of prefrontal and posterior parietal cortices throughout the working memory delay period of a visual object recognition task (Pollmann and von Cramon 2000). These patterns of correlated BOLD activity observed in working memory studies are facilitated by the inherent connectivity between functionally correlated brain regions (Le Bihan et al. 2001). As such, employing diffusion tensor imaging (DTI) to examine white matter connectivity has accordingly revealed correlations between performance on a working memory task and the integrity of white matter pathways connecting the prefrontal, parietal, and temporal cortices (Charlton et al. 2010).

1.2.2 Delay period activity may not be required for working memory

While extensive work has centred around this sustained activity model, whereby task-relevant information is retained via persistent neural activity across a delay period (Curtis and D'Esposito 2003; Funahashi 2015), an emerging view asserts that such delay period activity may not be required for working memory (Ikkai and Curtis 2011). Recently, fMRI studies have been employing multivariate pattern analysis (MVPA) to permit a more sensitive measure of the involvement of a particular brain region to a given behaviour (Mahmoudi et al. 2012; Hebart and Baker 2017). Unlike traditional univariate analysis which examines the activity of each voxel separately, MVPA examines the BOLD activity of a cluster of neighbouring voxels in order to assess whether a particular brain region encodes certain task-relevant information. With such methods, information about a visual stimulus can be decoded from delay period activity in early visual areas lacking sustained delay period activity classically associated with working memory (Harrison and Tong 2009; Riggall and Postle 2012; Emrich et al. 2013). In contrast, such task-relevant information cannot be decoded from frontal, prefrontal, and parietal areas demonstrating robust delay period activity (Postle 2015). Furthermore, studies reporting delay period activity in tasks without a mnemonic component suggest that sustained delay period activity may represent other task-related processes (Sreenivasan et al. 2014). Thus the relevance of sustained delay period activity specifically for working memory has been called into question.

Instead, recent electrophysiological recordings examining population level activity propose an alternative model of working memory coding. In contrast to stable sustained spiking activity discussed previously, highly dynamic activity within prefrontal neurons across a working memory delay has been reported in various high-level cognitive tasks (Meyers et al. 2008; Stokes et al. 2013), as well as simple delayed saccade paradigms (Spaak et al. 2017). Despite such dynamicism, cross-temporal decoding analyses demonstrate stable representations of task-relevant information maintained across the delay (Barak et al. 2010; Stokes 2015). Such dynamic coding is thought to be facilitated by rapid mechanisms of Hebbian plasticity that transiently alter synaptic connectivity

(Mongillo et al. 2008; Eriksson et al. 2015). For example, short-term potentiation results in the increased probability of synaptic vesicle release in response to repetitive tetanic stimulation to the presynaptic neuron, mediated by the increase in calcium concentration at the axon terminal (Fiebig and Lansner 2017). Such synaptic changes do not result in persistent activity that may be sustained throughout a working memory delay, but may be readily engaged when a delayed response is finally cued. Furthermore, such ‘activity-silent’ models of working memory permit a more energy efficient method of information coding that does not require lengthy periods of high-energy neural activation (Stokes 2015).

To continue this debate between sustained versus dynamic delay period activation underlying working memory, most researchers opt to study the macaque prefrontal cortex during delayed oculomotor response tasks (Stokes et al. 2013; Murray et al. 2017). However, examinations of other working memory-guided behaviours in alternative animal models may provide further insight into the neural underpinnings of working memory.

1.3 Working memory-guided obstacle locomotion

Mechanisms of working memory have typically been examined in movement restricted, explicitly instructed testing paradigms in both human and non-human primates. However, McVea and Pearson (2006) devised an elegantly simple task to examine obstacle working memory in the freely moving cat. This paradigm leverages naturalistic behaviours whereby quadrupedal animals may delay obstacle clearance between their four legs as they graze, explore new terrain, or track prey in complex environments. In an experimental setting, food is used to encourage cats to step over an obstacle with only their forelegs. Hindleg obstacle clearance is delayed by allowing the animals to eat while straddling the obstacle between their forelegs and hindlegs. As the animals are distracted with food, the obstacle is removed before walking resumes. Increased hindlimb flexion relative to unobstructed stepping demonstrates the persistence of a working memory of the obstacle to guide hindleg clearance following delays tested up to 10 minutes. Furthermore, hindleg step height scales appropriately with obstacle height, as working memory-guided hindleg steps over a lower obstacle are attenuated relative to stepping over a higher obstacle. Additionally, hindleg step trajectories are inversely related to the starting position of the step relative to the distance from the obstacle, demonstrating reasonable accuracy for the remembered obstacle location beneath the body. Interestingly, if obstacle clearance is instead delayed just before foreleg clearance, the resulting hindleg steps are lower than when obstacle clearance is delayed after the forelegs have stepped over the obstacle (McVea and Pearson 2007). Thus overall, foreleg obstacle clearance is essential for establishing a robust working memory of obstacle size and position relative to the animal.

Interestingly, despite small forward or backward steps taken during the delay, trajectories of subsequent hindleg stepping following the delay reflect the updated starting location of the step (Pearson and Gramlich 2010). Such spatial updating of obstacle location under the body demonstrates the dynamic nature of this working memory circuitry. As passive movements of the paw during the delay by an experimenter can similarly update step trajectory, proprioceptive information about limb position without efference motor copies of step adjustments during the delay may facilitate the spatial updating of the remembered obstacle location for hindleg step trajectory. While such proprioceptive and visually-dependent gait modifications for working memory-guided obstacle avoidance have been described behaviourally, the ability to remember and use tactile information about an obstacle remains unexamined. As introduced earlier, tactile inputs to the feet and legs can induce the stumbling corrective reaction to allow an animal to rapidly and reflexively step over an unexpected obstacle. While such swiftness may be valued in certain contexts, an animal may opt to delay obstacle clearance, for example, as it hunts or hides from a predator. Thus the ability to store information about an obstacle sensed through touch is just as important as the ability to store visual or proprioceptive information regarding an obstacle. However, such capabilities remain to be assessed experimentally.

Additionally, the neural correlates supporting working memory-guided obstacle locomotor behaviours warrant further examination. Studies of neural activity related to interlimb coordination for visually-guided obstacle locomotion recorded from the PPC of the cat have provided initial insight into the possible mechanisms of this obstacle working memory circuitry. Distinct groups of neurons with modulated activity between obstacle clearance of the two forelegs, between one of the forelegs and one of the hindlegs, or between the two hindlegs may provide information about obstacle location relative to the limbs (Andujar et al. 2010; Lajoie et al. 2010; Pearson and Gramlich 2010). Accordingly, within parietal area 5, neurons with elevated activity between the passage of the forelegs and hindlegs over an obstacle demonstrate sustained activation if hindleg clearance is delayed (Lajoie et al. 2010). As lesions to this region of area 5 results in attenuated hindleg stepping indicative of working memory deficits (McVea et al. 2009), such neurons demonstrating sustained delay period activity provide a potential neural substrate for obstacle working memory. However, such potential neural correlates warrant more thorough examination. For example, whether area 5 contributes similarly to both visually-dependent and visually-independent obstacle working memory is unknown. Furthermore, the potential for dynamic processes underlying obstacle information encoding in working memory in the walking cat remain to be assessed.

1.4 Thesis overview

Overall, the ability of locomotor control systems to adapt gait for complex behaviours involving working memory has only garnered focus in relatively recent years. Therefore, the aims of this thesis are to answer five main questions: (1) Is obstacle working memory dependent on vision, or can cats remember an unexpected obstacle over which the forelegs have tripped? (2) Is this memory-guided stumbling correction mediated by parietal area 5? (3) Does area 5 contribute similarly when the animal first sees the obstacle without tripping over it? (4) Is area 5 involved specifically in the acquisition or maintenance of obstacle information in working memory? And lastly, (5) what are the neural correlates of this area 5 contribution?

In **Chapter 2**, I describe the use of cooling induced deactivations to examine cortical contributions to this behaviour. Furthermore, I describe the two testing paradigms used to examine obstacle working memory, characterized by whether obstacle presence was detected via vision or touch. While the obstacle is visible as an animal approaches in the former, the obstacle is covertly introduced in order to trip the forelegs in the latter. This tactile-dependent task was used to evaluate working memory-guided obstacle negotiation in a visually-independent manner in **Chapter 3**. Additionally, cooling induced cortical deactivations were used to demonstrate the role of parietal area 5 in this tactile-dependent paradigm. In **Chapter 4**, obstacle working memory is then compared between visual and tactile tasks. Furthermore, I leverage the ability to temporally restrict cortical deactivations with cooling in order to examine area 5 contributions to distinct phases of obstacle working memory acquisition and maintenance in both visual and tactile paradigms. The neural correlates underlying these behaviours are subsequently examined in **Chapter 5**. Electrophysiological recordings via chronically implanted multi-electrode arrays revealed a subpopulation of area 5 neurons capable of maintaining stable representations of obstacle-related information throughout a working memory delay. Finally, findings from these previous chapters are compiled and discussed in the overall framework of obstacle locomotion in **Chapter 6**.

1.5 References

Akay T, Tourtellotte WG, Arber S, Jessell TM. 2014. Degradation of mouse locomotor pattern in the absence of proprioceptive sensory feedback. Proc Natl Acad Sci USA. 111:16877–16882.

Andersson O, Forssberg H, Grillner S, Lindquist M. 1978. Phasic gain control of the transmission in cutaneous reflex pathways to motoneurones during “fictive” locomotion. Brain Res. 149:503–507.

Andujar J-E, Drew T. 2007. Organization of the projections from the posterior parietal cortex to the rostral and caudal regions of the motor cortex of the cat. J Comp Neurol. 504:17–41.

Andujar J-E, Lajoie K, Drew T. 2010. A contribution of area 5 of the posterior parietal cortex to the planning of visually guided locomotion: limb-specific and limb-independent effects. J Neurophysiol. 103:986–1006.

Aoki S, Sato Y, Yanagihara D. 2013. Lesion in the lateral cerebellum specifically produces overshooting of the toe trajectory in leading forelimb during obstacle avoidance in the rat. J Neurophysiol. 110:1511–1524.

Armstrong DM. 1988. The supraspinal control of mammalian locomotion. J Physiol. 405:1–37.

Armstrong DM, Drew T. 1984. Discharges of pyramidal tract and other motor cortical neurones during locomotion in the cat. J Physiol. 346:471–495.

Armstrong DM, Drew T. 1985. Forelimb electromyographic responses to motor cortex stimulation during locomotion in the cat. J Physiol. 367:327–351.

Armstrong DM, Marple-Horvat DE. 1996. Role of the cerebellum and motor cortex in the regulation of visually controlled locomotion. Can J Physiol Pharmacol. 74:443–455.

Babb RS, Waters RS, Asanuma H. 1984. Corticocortical connections to the motor cortex from the posterior parietal lobe (areas 5a, 5b, 7) in the cat demonstrated by the retrograde axonal transport of horseradish peroxidase. Exp Brain Res. 54:476–484.

Baddeley A. 2003. Working memory: looking back and looking forward. Nat Rev Neurosci. 4:829–839.

Barak O, Tsodyks M, Romo R. 2010. Neuronal population coding of parametric working memory. J Neurosci. 30:9424–9430.

Bauer RH, Fuster JM. 1976. Delayed-matching and delayed-response deficit from cooling dorsolateral prefrontal cortex in monkeys. J Comp Physiol Psychol. 90:293–302.

Bellardita C, Kiehn O. 2015. Phenotypic characterization of speed-associated gait changes in mice reveals modular organization of locomotor networks. Curr Biol. 25:1426–1436.

Beloozerova IN, Sirota MG. 1993. The role of the motor cortex in the control of accuracy of locomotor movements in the cat. J Physiol. 461:1–25.

Beloozerova IN, Sirota MG. 2003. Integration of motor and visual information in the parietal area 5 during locomotion. J Neurophysiol. 90:961–971.

Bolkan SS, Stujenske JM, Parnaudeau S, Spellman TJ, Rauffenbart C, Abbas AI, Harris AZ, Gordon JA, Kellendonk C. 2017. Thalamic projections sustain prefrontal activity during working memory maintenance. Nat Neurosci. 20:987–996.

Britz O, Zhang J, Grossmann KS, Dyck J, Kim JC, Dymecki S, Gosgnach S, Goulding M. 2015. A genetically defined asymmetry underlies the inhibitory control of flexor-extensor locomotor movements. Elife. 4.

Brown TG. 1911. The Intrinsic Factors in the Act of Progression in the Mammal. Proc R Soc B Biol Sci.

Buford JA, Smith JL. 1993. Adaptive control for backward quadrupedal walking. III. Stumbling corrective reactions and cutaneous reflex sensitivity. J Neurophysiol. 70:1102–1114.

Chafee M V, Goldman-Rakic PS. 1998. Matching patterns of activity in primate prefrontal area 8a and parietal area 7ip neurons during a spatial working memory task. J Neurophysiol. 79:2919–2940.

Chafee M V, Goldman-Rakic PS. 2000. Inactivation of parietal and prefrontal cortex reveals interdependence of neural activity during memory-guided saccades. J Neurophysiol. 83:1550–1566.

Charlton RA, Barrick TR, Lawes INC, Markus HS, Morris RG. 2010. White matter pathways associated with working memory in normal aging. Cortex. 46:474–489.

Conway BA, Hultborn H, Kiehn O. 1987. Proprioceptive input resets central locomotor rhythm in the spinal cat. Exp Brain Res. 68:643–656.

Curtis CE, D’Esposito M. 2003. Persistent activity in the prefrontal cortex during working memory. Trends Cogn Sci. 7:415–423.

D’Ardenne K, McClure SM, Nystrom LE, Cohen JD. 2008. BOLD responses reflecting dopaminergic signals in the human ventral tegmental area. Science. 319:1264–1267.

D’Esposito M, Postle BR. 2015. The Cognitive Neuroscience of Working Memory. Annu Rev Psychol. 66:115–142.

Douglas JR, Noga BR, Dai X, Jordan LM. 1993. The effects of intrathecal administration of excitatory amino acid agonists and antagonists on the initiation of locomotion in the adult cat. J Neurosci. 13:990–1000.

Drew T. 1993. Motor cortical activity during voluntary gait modifications in the cat . I . cells related to the forelimbs. J Neurophysiol. 70:179–199.

Drew T, Andujar JE, Lajoie K, Yakovenko S. 2008. Cortical mechanisms involved in visuomotor coordination during precision walking. Brain Res Rev. 57:199–211.

Drew T, Jiang W, Kably B, Lavoie S. 1996. Role of the motor cortex in the control of visually triggered gait modifications. Can J Physiol Pharmacol. 74:426–442.

Drew T, Marigold DS. 2015. Taking the next step: cortical contributions to the control of locomotion. Curr Opin Neurobiol. 33:25–33.

Emrich SM, Riggall AC, Larocque JJ, Postle BR. 2013. Distributed patterns of activity in sensory cortex reflect the precision of multiple items maintained in visual short-term memory. J Neurosci. 33:6516–6523.

Engberg I, Lundberg A. 1969. An electromyographic analysis of muscular activity in the hindlimb of the cat during unrestrained locomotion. Acta Physiol Scand. 75:614–630.

Eriksson J, Vogel EK, Lansner A, Bergström F, Nyberg L. 2015. Neurocognitive architecture of working memory. Neuron. 88:33–46.

Fiebig F, Lansner A. 2017. A Spiking Working Memory Model Based on Hebbian Short-Term Potentiation. J Neurosci. 37:83–96.

Forssberg H. 1979. Stumbling corrective reaction: a phase-dependent compensatory reaction during locomotion. J Neurophysiol. 42:936–953.

Forssberg H, Grillner S, Rossignol S. 1977. Phasic gain control of relexes from the dorsum of the paw during spinal locomotion. Brain Res. 132:121–139.

Frank MJ, Loughry B, O'Reilly RC. 2001. Interactions between frontal cortex and basal ganglia in working memory: A computational model. Cogn Affect Behav Neurosci. 1:137–160.

Funahashi S. 2015. Functions of delay-period activity in the prefrontal cortex and mnemonic scotomas revisited. Front Syst Neurosci. 9:2.

Funahashi S, Bruce CJ, Goldman-Rakic PS. 1989. Mnemonic coding of visual space in the monkey's dorsolateral prefrontal cortex. J Neurophysiol. 61:331–349.

Funahashi S, Chafee M V, Goldman-Rakic PS. 1993. Prefrontal neuronal activity in rhesus monkeys performing a delayed anti-saccade task. Nature. 365:753–756.

Fuster JM, Alexander GE. 1971. Neuron activity related to short-term memory. Science. 173:652–654.

Fuster JM, Bressler SL. 2012. Cognit activation: a mechanism enabling temporal integration in working memory. Trends Cogn Sci. 16:207–218.

Gazzaley A, Rissman J, D'Esposito M. 2004. Functional connectivity during working memory maintenance. Cogn Affect Behav Neurosci. 4:580–599.

Glickstein M. 2000. How are visual areas of the brain connected to motor areas for the sensory guidance of movement? Trends Neurosci. 23:613–617.

Goldman PS, Rosvold HE, Vest B, Galkin TW. 1971. Analysis of the delayed-alternation deficit produced by dorsolateral prefrontal lesions in the rhesus monkey. J Comp Physiol Psychol. 77:212–220.

Grillner S. 2006. Biological pattern generation: the cellular and computational logic of networks in motion. Neuron. 52:751–766.

Grillner S, Rossignol S. 1978. On the initiation of the swing phase of locomotion in chronic spinal cats. Brain Res. 146:269–277.

Gwin JT, Gramann K, Makeig S, Ferris DP. 2011. Electrocortical activity is coupled to gait cycle phase during treadmill walking. Neuroimage. 54:1289–1296.

Hägglund M, Borgius L, Dougherty KJ, Kiehn O. 2010. Activation of groups of excitatory neurons in the mammalian spinal cord or hindbrain evokes locomotion. Nat Neurosci. 13:246–252.

Harrison SA, Tong F. 2009. Decoding reveals the contents of visual working memory in early visual areas. Nature.

Hebart MN, Baker CI. 2017. Deconstructing multivariate decoding for the study of brain function. Neuroimage.

Hikosaka O, Sakamoto M, Usui S. 1989. Functional properties of monkey caudate neurons. I. Activities related to saccadic eye movements. J Neurophysiol. 61:799–813.

Hultborn H. 1976. Transmission in the pathway of reciprocal Ia inhibition to motoneurones and its control during the tonic stretch reflex. Prog Brain Res. 44:235–255.

Ikkai A, Curtis CE. 2011. Common neural mechanisms supporting spatial working memory, attention and motor intention. Neuropsychologia. 49:1428–1434.

Jacob SN, Nieder A. 2014. Complementary roles for primate frontal and parietal cortex in guarding working memory from distractor stimuli. Neuron. 83:226–237.

Jahn K, Deutschländer A, Stephan T, Kalla R, Hüfner K, Wagner J, Strupp M, Brandt T. 2008. Supraspinal locomotor control in quadrupeds and humans. Prog Brain Res. 171:353–362.

Jones JG, Tansey EM (Tilli), Stuart DG. 2011. Thomas Graham Brown (1882–1965): Behind the scenes at the cardiff institute of physiology. J Hist Neurosci. 20:188–

209.

Jordan LM, Liu J, Hedlund PB, Akay T, Pearson KG. 2008. Descending command systems for the initiation of locomotion in mammals. Brain Res Rev. 57:183–191.

Kiehn O. 2006. Locomotor circuits in the mammalian spinal cord. Annu Rev Neurosci. 29:279–306.

Krouchev N, Kalaska JF, Drew T. 2006. Sequential activation of muscle synergies during locomotion in the intact cat as revealed by cluster analysis and direct decomposition. J Neurophysiol. 96:1991–2010.

Lajoie K, Andujar J-E, Pearson KG, Drew T. 2010. Neurons in area 5 of the posterior parietal cortex in the cat contribute to interlimb coordination during visually guided locomotion: a role in working memory. J Neurophysiol. 103:2234–2254.

Lajoie K, Drew T. 2007. Lesions of area 5 of the posterior parietal cortex in the cat produce errors in the accuracy of paw placement during visually guided locomotion. J Neurophysiol. 97:2339–2354.

Le Bihan D, Mangin JF, Poupon C, Clark CA, Pappata S, Molko N, Chabriat H. 2001. Diffusion tensor imaging: concepts and applications. J Magn Reson Imaging. 13:534–546.

Leavitt ML, Mendoza-Halliday D, Martinez-Trujillo JC. 2017. Sustained activity encoding working memories: not fully distributed. Trends Neurosci. 40:328–346.

Liddell EGT, Phillips CG. 1944. Pyramidal section in the cat. Brain. 67:1–9.

Mahmoudi A, Takerkart S, Regragui F, Boussaoud D, Brovelli A. 2012. Multivoxel pattern analysis for FMRI data: a review. Comput Math Methods Med. 2012:961257.

Malouin F, Richards CL, Jackson PL, Dumas F, Doyon J. 2003. Brain activations during motor imagery of locomotor-related tasks: a PET study. Hum Brain Mapp. 19:47–

62.

Marigold DS, Drew T. 2011. Contribution of cells in the posterior parietal cortex to the planning of visually guided locomotion in the cat: effects of temporary visual interruption. J Neurophysiol. 105:2457–2470.

Marigold DS, Drew T. 2017. Posterior parietal cortex estimates the relationship between object and body location during locomotion. Elife. 6ie28143.

Marple-Horvat DE, Criado JM. 1999. Rhythmic neuronal activity in the lateral cerebellum of the cat during visually guided stepping. J Physiol. 518:595–603.

Masse NY, Hodnefield JM, Freedman DJ. 2017. Mnemonic Encoding and Cortical Organization in Parietal and Prefrontal Cortices. J Neurosci. 37:6098–6112.

McCrea D, Pratt C, Jordan LM. 1980. Renshaw cell activity and recurrent effects on motoneurons during fictive locomotion. J Neurophysiol. 44:475–488.

McNab F, Klingberg T. 2008. Prefrontal cortex and basal ganglia control access to working memory. Nat Neurosci. 11:103–107.

McVea DA, Pearson KG. 2006. Long-lasting memories of obstacles guide leg movements in the walking cat. J Neurosci. 26:1175–1178.

McVea DA, Pearson KG. 2007. Stepping of the forelegs over obstacles establishes long-lasting memories in cats. Curr Biol. 17:R621–R623.

McVea DA, Taylor AJ, Pearson KG. 2009. Long-lasting working memories of obstacles established by foreleg stepping in walking cats require area 5 of the posterior parietal cortex. J Neurosci. 29:9396–9404.

Meyers EM, Freedman DJ, Kreiman G, Miller EK, Poggio T. 2008. Dynamic population coding of category information in inferior temporal and prefrontal cortex. J Neurophysiol. 100:1407–1419.

Miller EK, Erickson C a, Desimone R. 1996. Neural mechanisms of visual working memory in prefrontal cortex of the macaque. J Neurosci. 16:5154–5167.

Miller G, Galanter E, Pribram K. 1960. Plans and the structure of behavior: Holt, Rinehart and Winston, Inc., New York.

Mongillo G, Barak O, Tsodyks M. 2008. Synaptic theory of working memory. Science. 319:1543–1546.

Mori S, Matsui T, Kuze B, Asanome M, Nakajima K, Matsuyama K. 1998. Cerebellar-induced locomotion: reticulospinal control of spinal rhythm generating mechanism in cats. Ann N Y Acad Sci. 860:94–105.

Mori S, Matsui T, Kuze B, Asanome M, Nakajima K, Matsuyama K. 1999. Stimulation of a restricted region in the midline cerebellar white matter evokes coordinated quadrupedal locomotion in the decerebrate cat. J Neurophysiol. 82:290–300.

Mori S, Sakamoto T, Ohta Y, Takakusaki K, Matsuyama K. 1989. Site-specific postural and locomotor changes evoked in awake, freely moving intact cats by stimulating the brainstem. Brain Res. 505:66–74.

Morton SM, Bastian AJ. 2004. Cerebellar control of balance and locomotion. Neurosci. 10:247–259.

Morton SM, Bastian AJ. 2006. Cerebellar contributions to locomotor adaptations during splitbelt treadmill walking. J Neurosci. 26:9107–9116.

Murray JD, Bernacchia A, Roy NA, Constantinidis C, Romo R, Wang X-J. 2017. Stable population coding for working memory coexists with heterogeneous neural dynamics in prefrontal cortex. Proc Natl Acad Sci. 114:394–399.

Narita K, Murata T, Honda K, Nishihara M, Takahashi M, Higuchi T. 2002. Subthalamic locomotor region is involved in running activity originating in the rat ventromedial hypothalamus. Behav Brain Res. 134:275–281.

Orlovsky GN. 1972a. Activity of vestibulospinal neurons during locomotion. Brain Res.

46:85–98.

Orlovsky GN. 1972b. The effect of different descending systems on flexor and extensor activity during locomotion. Brain Res. 40:359–371.

Pearson KG. 2007. Role of sensory feedback in the control of stance duration in walking cats. 57.

Pearson KG, Gramlich R. 2010. Updating neural representations of objects during walking. Ann N Y Acad Sci. 1198:1–9.

Pollmann S, von Cramon DY. 2000. Object working memory and visuospatial processing: functional neuroanatomy analyzed by event-related fMRI. Exp Brain Res. 133:12–22.

Postle BR. 2015. The cognitive neuroscience of visual short-term memory. Curr Opin Behav Sci.

Pratt CA, Jordan LM. 1987. Ia inhibitory interneurons and Renshaw cells as contributors to the spinal mechanisms of fictive locomotion. J Neurophysiol. 57:56–71.

Prochazka A, Sontag KH, Wand P. 1978. Motor reactions to perturbations of gait: proprioceptive and somesthetic involvement. Neurosci Lett. 7:35–39.

Qi X-L, Katsuki F, Meyer T, Rawley JB, Zhou X, Douglas KL, Constantinidis C. 2010. Comparison of neural activity related to working memory in primate dorsolateral prefrontal and posterior parietal cortex. Front Syst Neurosci. 4:12.

Quintana J, Fuster JM. 1999. From perception to action: temporal integrative functions of prefrontal and parietal neurons. Cereb Cortex. 9:213–221.

Riggall AC, Postle BR. 2012. The Relationship between Working Memory Storage and Elevated Activity as Measured with Functional Magnetic Resonance Imaging. J Neurosci.

Rolland A-S, Tandé D, Herrero M-T, Luquin M-R, Vazquez-Claverie M, Karachi C, Hirsch EC, François C. 2009. Evidence for a dopaminergic innervation of the pedunculopontine nucleus in monkeys, and its drastic reduction after MPTP intoxication. J Neurochem. 110:1321–1329.

Roseberry TK, Lee AM, Lalive AL, Wilbrecht L, Bonci A, Kreitzer AC. 2016. Cell-type-specific control of brainstem locomotor circuits by basal ganglia. Cell. 164:526–537.

Ryczko D, Dubuc R. 2017. Dopamine and the brainstem locomotor networks: from lamprey to human. Front Neurosci. 11.

Shefchyk SJ, Jell RM, Jordan LM. 1984. Reversible cooling of the brainstem reveals areas required for mesencephalic locomotor region evoked treadmill locomotion. Exp Brain Res. 56:257–262.

Shevtsova NA, Rybak IA. 2016. Organization of flexor–extensor interactions in the mammalian spinal cord: insights from computational modelling. J Physiol. 594:6117–6131.

Shik ML, Severin F V, Orlovsky GN. 1969. Control of walking and running by means of electrical stimulation of the mesencephalon. Electroencephalogr Clin Neurophysiol. 26:549.

Sinnamon HM, Stopford CK. 1987. Locomotion elicited by lateral hypothalamic stimulation in the anesthetized rat does not require the dorsal midbrain. Brain Res. 402:78–86.

Sobotka S, Diltz MD, Ringo JL. 2005. Can delay-period activity explain working memory? J Neurophysiol. 93:128–136.

Spaak E, Watanabe K, Funahashi S, Stokes MG. 2017. Stable and dynamic coding for working memory in primate prefrontal cortex. J Neurosci. 37:6503–6516.

Sreenivasan KK, Curtis CE, D’Esposito M. 2014. Revisiting the role of persistent neural activity during working memory. Trends Cogn Sci. 18:82–89.

Stokes MG. 2015. “Activity-silent” working memory in prefrontal cortex: a dynamic coding framework. Trends Cogn Sci. 19:394–405.

Stokes MG, Kusunoki M, Sigala N, Nili H, Gaffan D, Duncan J. 2013. Dynamic Coding for Cognitive Control in Prefrontal Cortex. Neuron. 78:364–375.

Takakusaki K. 2013. Neurophysiology of gait: From the spinal cord to the frontal lobe. Mov Disord. 28:1483–1491.

Takakusaki K, Habaguchi T, Ohtinata-Sugimoto J, Saitoh K, Sakamoto T. 2003. Basal ganglia efferents to the brainstem centers controlling postural muscle tone and locomotion: a new concept for understanding motor disorders in basal ganglia dysfunction. Neuroscience. 119:293–308.

Talpalar AE, Bouvier J, Borgius L, Fortin G, Pierani A, Kiehn O. 2013. Dual-mode operation of neuronal networks involved in left-right alternation. Nature. 500:85–88.

Tazerart S, Viemari J-C, Darbon P, Vinay L, Brocard F. 2007. Contribution of persistent sodium current to locomotor pattern generation in neonatal rats. J Neurophysiol. 98:613–628.

Voytek B, Knight RT. 2010. Prefrontal cortex and basal ganglia contributions to visual working memory. Proc Natl Acad Sci USA. 107:18167–18172.

Wagner J, Solis-Escalante T, Scherer R, Neuper C, Müller-Putz G. 2014. It’s how you get there: walking down a virtual alley activates premotor and parietal areas. Front Hum Neurosci. 8.

Wand P, Prochazka A, Sontag KH. 1980. Neuromuscular responses to gait perturbations in freely moving cats. Exp Brain Res. 38:109–114.

Wang M, Yang Y, Wang C-J, Gamo NJ, Jin LE, Mazer JA, Morrison JH, Wang X-J, Arnsten AFT. 2013. NMDA receptors subserve persistent neuronal firing during working memory in dorsolateral prefrontal cortex. Neuron. 77:736–749.

Wang XJ. 1999. Synaptic basis of cortical persistent activity: the importance of NMDA receptors to working memory. J Neurosci. 19:9587–9603.

Wang XJ. 2001. Synaptic reverberation underlying mnemonic persistent activity. Trends Neurosci. 24:455–463.

Widajewicz W, Kably B, Drew T. 1994. Motor cortical activity during voluntary gait modifications in the cat. II. Cells related to the hindlimbs. J Neurophysiol. 72:2070–2089.

Yumiya H, Ghez C. 1984. Specialized subregions in the cat motor cortex: anatomical demonstration of differential projections to rostral and caudal sectors. Exp Brain Res. 53:259–276.

Zhang J, Lanuza GM, Britz O, Wang Z, Siembab VC, Zhang Y, Velasquez T, Alvarez FJ, Frank E, Goulding M. 2014. V1 and v2b interneurons secure the alternating flexor-extensor motor activity mice require for limbed locomotion. Neuron. 82:138–150.

Zhou X, Katsuki F, Qi X-L, Constantinidis C. 2012. Neurons with inverted tuning during the delay periods of working memory tasks in the dorsal prefrontal and posterior parietal cortex. J Neurophysiol. 108:31–38.

Chapter 2

2 Reversible cooling-induced deactivations to study cortical contributions to obstacle memory in the walking cat[1]

2.1 Summary

Complex locomotion in naturalistic environments requiring careful coordination of the limbs involves regions of the parietal cortex. The following protocol describes the use of reversible cooling-induced deactivation to demonstrate the role of parietal area 5 in memory-guided obstacle avoidance in the walking cat.

2.2 Abstract

On complex, naturalistic terrain, sensory information about an environmental obstacle can be used to rapidly adjust locomotor movements for avoidance. For example, in the cat, visual information about an impending obstacle can modulate stepping for avoidance. Locomotor adaptation can also occur independent of vision, as sudden tactile inputs to the leg by an expected obstacle can modify the stepping of all four legs for avoidance. Such complex locomotor coordination involves supraspinal structures, such as the parietal cortex. This protocol describes the use of reversible, cooling-induced cortical deactivation to assess parietal cortex contributions to memory-guided obstacle locomotion in the cat. Small cooling loops, known as cryoloops, are specially shaped to deactivate discrete regions of interest to assess their contributions to an overt behavior. Such methods have been used to elucidate the role of parietal area 5 in memory-guided obstacle avoidance in the cat.

---

[1] A version of this chapter is published as:

Wong C, Lomber SG (2017). Reversible cooling-induced deactivations to study cortical contributions to obstacle memory in the walking cat. Journal of Visualized Experiments doi:10.3791/56196.

2.3 Introduction

On naturalistic, uneven terrain, sensory information about an obstacle, which can be acquired via vision or touch, can rapidly modify locomotion for avoidance. This careful coordination of stepping movements involves multiple cortical regions (Takakusaki 2013; Drew and Marigold 2015). For example, areas of motor cortex (Beloozerova and Sirota 1993; Drew 1993) and parietal cortex (Beloozerova and Sirota 2003; McVea et al. 2009; Lajoie et al. 2010) have been implicated during complex locomotor tasks such as obstacle avoidance. In quadrupedal animals, step modulations required for obstacle avoidance must extend to both the forelegs and hindlegs. If forward locomotion is delayed between foreleg and hindleg obstacle clearance (which may arise as an animal treads carefully through a complex, naturalistic environment stalking prey), information about the obstacle maintained in memory is used to guide hindleg stepping over the obstacle once walking resumes.

Experimental techniques aimed to deactivate discrete cortical areas can be used to study cortical contributions to memory-guided obstacle locomotion. Cooling-induced cortical deactivation provides a reversible, reliable, and reproducible method for assessing cortical contributions to an overt behaviour (Lomber et al. 1999). Cryoloops made from stainless steel tubing are shaped specifically to the cortical area of interest, ensuring highly selective and discrete deactivation loci. Once implanted, chilled methanol pumped through the lumen of a cryoloop cools the region of cortex directly beneath the loop to <20 ˚C. Below this critical temperature, synaptic transmission is inhibited in the region of cortex directly beneath the loop. Such deactivation can be reversed simply by ceasing the flow of methanol. This method has been used to study cortical contributions to sensory processing and behaviours (Lomber et al. 1994, 2010; Lomber and Payne 2000a; Lomber and Malhotra 2008; Antunes and Malmierca 2011; Coomber et al. 2011; Carrasco et al. 2015; Kok et al. 2015; Malmierca et al. 2015), as well as the motor control of saccadic eye movements (Peel et al. 2014) and memory-guided obstacle locomotion (Wong et al. 2018).

The purpose of this protocol is to use reversible cooling-induced deactivations to assess the involvement of parietal cortical areas for locomotor coordination in the cat. Specifically, memory-guided obstacle locomotion was examined with or without active parietal cortex. These methods have been used to successfully demonstrate the role of parietal area 5 in memory-guided obstacle avoidance in the walking cat (Wong et al. 2018).

2.4 Protocol

All procedures were conducted in compliance with the National Research Council's Guide for the Care and Use of Laboratory Animals (eighth edition; 2011) and the Canadian Council on Animal Care's Guide to the Care and Use of Experimental Animals (1993), and were approved by the University of Western Ontario Animal Use Subcommittee of the University Council on Animal Care. The following procedure can be applied to experiments studying cortical contributions to locomotor control in the walking cat.

2.4.1 Apparatus

1. Construct the apparatus used to assess obstacle memory.
   NOTE: The apparatus consists of a 2.43 m long, 29 cm wide walkway enclosed by 18 cm high clear acrylic walls (Fig. 2.1). A narrow slot halfway along the apparatus allows a 25.8 cm wide x 3 mm thick obstacle to be raised onto or removed from the walkway using a lever mounted underneath the walking surface.
2. To ensure that attention of the animal is maintained on eating, avoid using the hand to raise or lower the obstacle. Instead, the obstacle can be raised or lowered using the experimenter's leg to move the lever underneath the walkway, allowing the experimenter to continue feeding the animal.
3. Properly maintain the lever system to ensure that the obstacle can be raised or lowered soundlessly.
4. Use a small elevated platform (23 cm long x 23 cm wide x 16 cm high) upon which soft food is placed, to guide movements of the animal.

Figure 2.1 Diagram depicting the camera, cooling equipment, and walking apparatus used to assess obstacle memory in the cat.

A 2.43 m long, 29 cm wide walkway is enclosed by 18 cm high clear Plexiglas walls. Halfway along the walkway, a 25.8 cm wide 3 mm thick obstacle can be raised on the walkway through a narrow slot using a lever mounted underneath the walkway. For each trial, the animal is placed a couple of steps from the obstacle in the starting area of the walkway. Food is placed on a small elevated platform (23 cm long x 23 cm wide x 16 cm high) on the far side of the obstacle slot opposite to the starting area. All trials are recorded via an Ethernet camera mounted on top of a tripod and saved on a laptop. This figure has been modified from Wong et al. (2018).

Figure 2.1

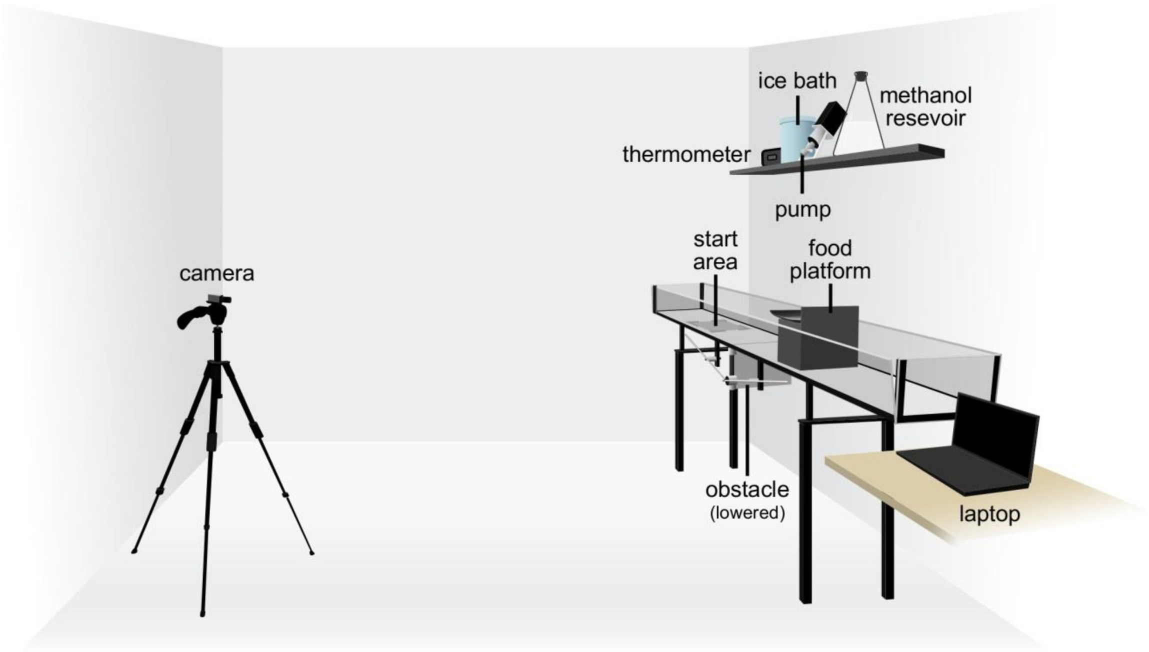
ice bath
methanol resevoir
thermometer
pump
start area
food platform
camera
obstacle (lowered)
laptop

5. Record all trials using an ethernet camera (54 frames/s) mounted on a tripod 1.85 m away from the midline of the walkway.

2.4.2 Training Procedures

NOTE: For successful data acquisition, a period of training preceding behavioral testing ensures that each animal is properly acclimated to the testing room and apparatus. Repeated exposure to a novel environment will aid in reducing startling or other stressful behaviors. Acclimation may vary between animals and may require 1-2 months of training. Initial acclimation sessions may be up to 5 min in length depending on the focus and motivation of the animal to eat. Subsequent sessions should aim to increase the duration of time that the animal is motivated to work (typically around 20-25 min)

1. Acquire mature (>6 months of age) domestic short hair cats from a commercial laboratory breeder of any weight or sex.

   NOTE: Motivation to work for food and a cooperative disposition comprise the selection criteria when considering which animals should be included in the study.
2. Acclimate each animal to wearing a harness to which a 1 m long leash is attached. Anchor the leash to a shelf above the walkway over the midpoint of the walkway.

   NOTE: This allows the animal to walk along the central portion of the apparatus without any tension, thus encouraging the animal to remain within this portion of the apparatus. Establishing such boundaries is helpful for working with a moving test subject.
3. Place the animal onto the walkway, allowing it to eat from the platform upon which soft food is placed.

   NOTE: One aim of this initial training is to ensure that the animal readily follows the food platform when moved forwards, and can walk comfortably with the harness and leash. The use of soft food as positive reinforcement encourages the animal to remain focused throughout each training or testing session, and promotes a comfortable working environment.
4. Ensure that the animal is comfortable with handling, including instances where the animal must be moved to the start area of the walkway.

2.4.3 Behavioural Training and Testing Protocol

NOTE: The obstacle memory is assessed in two paradigms: a visually-dependent obstacle memory task, and a tactile-dependent obstacle memory task. Both paradigms should be used during initial training and subsequent testing.

1. Visual obstacle memory

1. To assess the visual obstacle memory, raise the obstacle onto the walkway (Fig. 2.2A). Place the platform on the far side of the obstacle. Place the animal in the start area of the walkway.
2. Allow the animal to approach the food, stepping over the obstacle with only its forelegs in order to eat from the platform.
3. As the animal continues to eat, lower the obstacle such that it becomes flush with the walkway to prevent any further visual or tactile inputs.
4. Following a variable delay period, move the food forwards again to encourage the animal to resume walking; this delay can be less than 1 s to upwards of 2 min.
   Importantly, perform trials where the obstacle is absent in order to prevent habituation to the obstacle and development of a learned avoidance response. In such visual obstacle-absent trials, ensure that the obstacle is not raised onto the walkway before placing the animal in the start area of the walkway.
5. Observe hindleg stepping in obstacle-present and obstacle-absent trials to verify typical locomotor behaviors and intact visual obstacle memory prior to cooling. Ensure that the animal can clear the obstacle without contact, and that stepping of all four legs is significantly elevated in obstacle-present trials.
   NOTE: Watching videos of training trials may assist in this verification.

2. Tactile obstacle memory

1. To assess the tactile obstacle memory, ensure that the obstacle is not raised onto the walkway before placing the animal in the start area of the walkway (Fig. 2.2B).
2. Allow the animal to walk towards the food platform placed on the far side of the obstacle slot.

Figure 2.2 Diagram depicting both visual and tactile obstacle memory tasks and the step measurements used to assess obstacle memory in the walking cat.

(A) To assess visual obstacle memory, the obstacle is raised onto the walkway as the animal approaches the food platform. After stepping over the obstacle with only its forelegs, the animal is allowed to eat from the platform, as the obstacle is lowered covertly becoming flush with the surface of the walkway. Following a variable delay period, the food is moved forwards to encourage the animal to resume walking.

(B) To assess tactile obstacle memory, the obstacle is not raised onto the walkway as the animal approaches the food platform. As the animal eats, the obstacle is raised silently onto the walkway directly beneath the food platform. The food is moved forwards causing the forelegs of the animal to contact the obstacle before stepping over it. The animal is allowed to continue eating from the food platform while straddling the obstacle between its forelegs and hindlegs. During this time, the obstacle is covertly lowered from the walkways. The food is moved forward once again to encourage the animal to resume walking. Hindleg steps are measured to assess obstacle memory.

(C) Stepping is assessed in both visual and tactile obstacle memory paradigms by measuring the peak step height, step clearance, and the horizontal distance between the peak of each step and the obstacle.

Figure 2.2

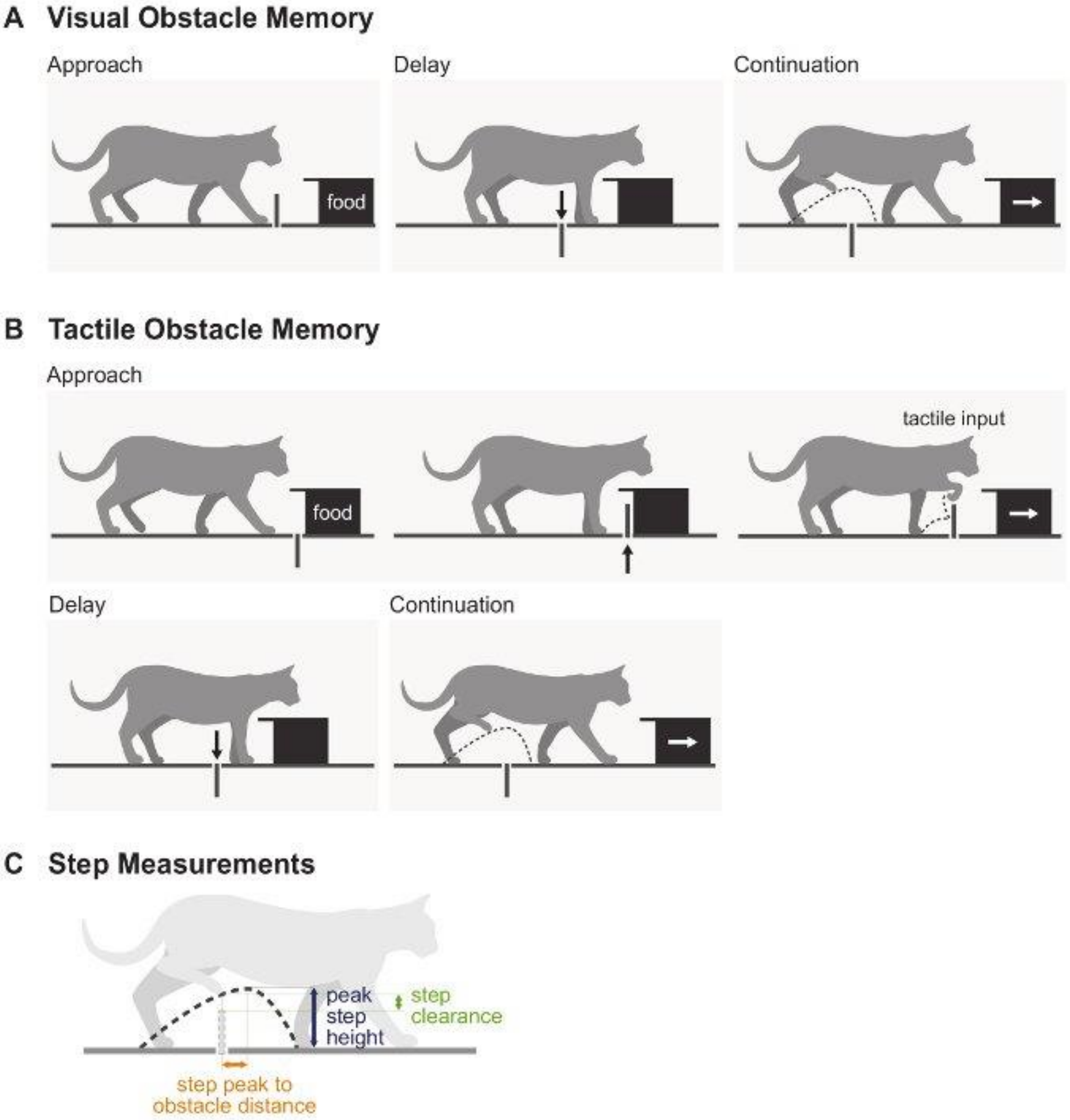
A Visual Obstacle Memory
Approach
Delay
Continuation
food
B Tactile Obstacle Memory
Approach
food
tactile input
Delay
Continuation
C Step Measurements
peak
step
height
step
clearance
step peak to
obstacle distance

3. As the animal eats, raise the obstacle onto the walkway beneath the food dish, preventing any visual input of the obstacle.
4. As the food is moved forwards, note that the animal should contact the obstacle with their forelegs before stepping over it.
5. Allow the animal to continue eating while straddling the obstacle between their fore- and hindlegs. During this time, lower the obstacle so that it becomes flush with the walkway to prevent any further visual or tactile inputs.
6. Following a variable delay period, move the food forwards once again to encourage the animal to resume walking.
7. Importantly, perform trials where the obstacle is absent and no foreleg contact occurs for preventing habituation to the obstacle and development of a learned avoidance response.
    a. In these tactile obstacle-absent trials, have the animal approach and eat from the food platform, as described in step 2.1. However, raise and lower the obstacle (step 2.3) before moving the food forward in step 2.4. Ensure that a similar delay period where the animal is allowed to continue eating (step 2.5) precedes the final continuation of locomotion (step 2.6).
8. Observe the hindleg stepping in the obstacle-present and obstacle-absent trials to verify normal locomotor behaviors and intact visual obstacle memory prior to cooling.

2.4.4 Video Analyses

NOTE: To assess obstacle memory, analyses during initial training and subsequent testing after cooling loop implantation involve quantifying the peak step height, step clearance, and the horizontal distance between the toe and obstacle at the peak of each step for both visual and tactile paradigms (Fig. 2.2C).

1. Analyze the videos using custom written scripts.
2. For every trial, track each foot by marking the position of the toe closest to the camera throughout each step.
3. Measure the peak step height as the perpendicular distance between the toe and the surface of the walkway at the highest point in each step trajectory (Fig. 2.2C).

4. In the obstacle-present trials, measure the step clearance as the step height directly above the obstacle slot subtracted by the height of the obstacle.
5. Additionally, measure the horizontal distance between the toe and the obstacle at the peak of each step in the obstacle-present trials.
6. Confirm that the obstacle memory capabilities are intact prior to the cooling loop implantation by verifying that the peak step height is elevated in the obstacle-present trials in comparison to stepping in the obstacle-absent trials.

2.4.5 Cooling loop (Cryoloop) Implantation

1. Implant cryoloops bilaterally over areas 5 and 7 according to previously reported surgical procedures (Lomber et al. 1999; Fig. 2.3).
2. In brief, for each hemisphere, perform a craniotomy and durotomy from Horsley-Clarke coordinates (Horsley and Clarke 1908) A15 to A25 to expose the juncture of the ansate and lateral sulci.
3. Position individual cooling loops shaped from 23-gauge stainless steel hypodermic tubing with the loop in direct contact with the cortical surface of parietal area 5 or 7.
4. Secure the base of each cryoloop to the skull with dental acrylic anchored to the stainless steel screws.
5. Close the craniotomies with additional dental acrylic; draw up the skin margins up to the acrylic edges and suture together.

2.4.6 Cortical Cooling Protocol

1. Experimental setup

NOTE: Before bringing the animal into the testing room, the cooling circuit is prepared and tested. The cooling circuit consists of a methanol reservoir with an intake tube (3.2 mm O.D., 1.6 mm I.D.), a reciprocating piston pump, and dry ice bath connected via polytetrafluoroethylene tubing (1.6 mm O.D., 0.5 mm I.D.; Fig. 2.4). Additionally, a digital thermometer is required.

Figure 2.3 Schematic of the cryoloop.

The cryoloop consists of a protective cap, which fits over the inlet and outlet tubes. These tubes run through a threaded post and form the loop that sits in direct contact with the cortical surface over the region of interest. A microthermocouple is soldered at the union of the loop to measure the cryoloop temperature. Its wires run back up through the heat-shrink tubing (which also wraps the stainless steel tubing) and are attached to a connector. The entire assembly is secured to the skull with dental acrylic.

Figure 2.3

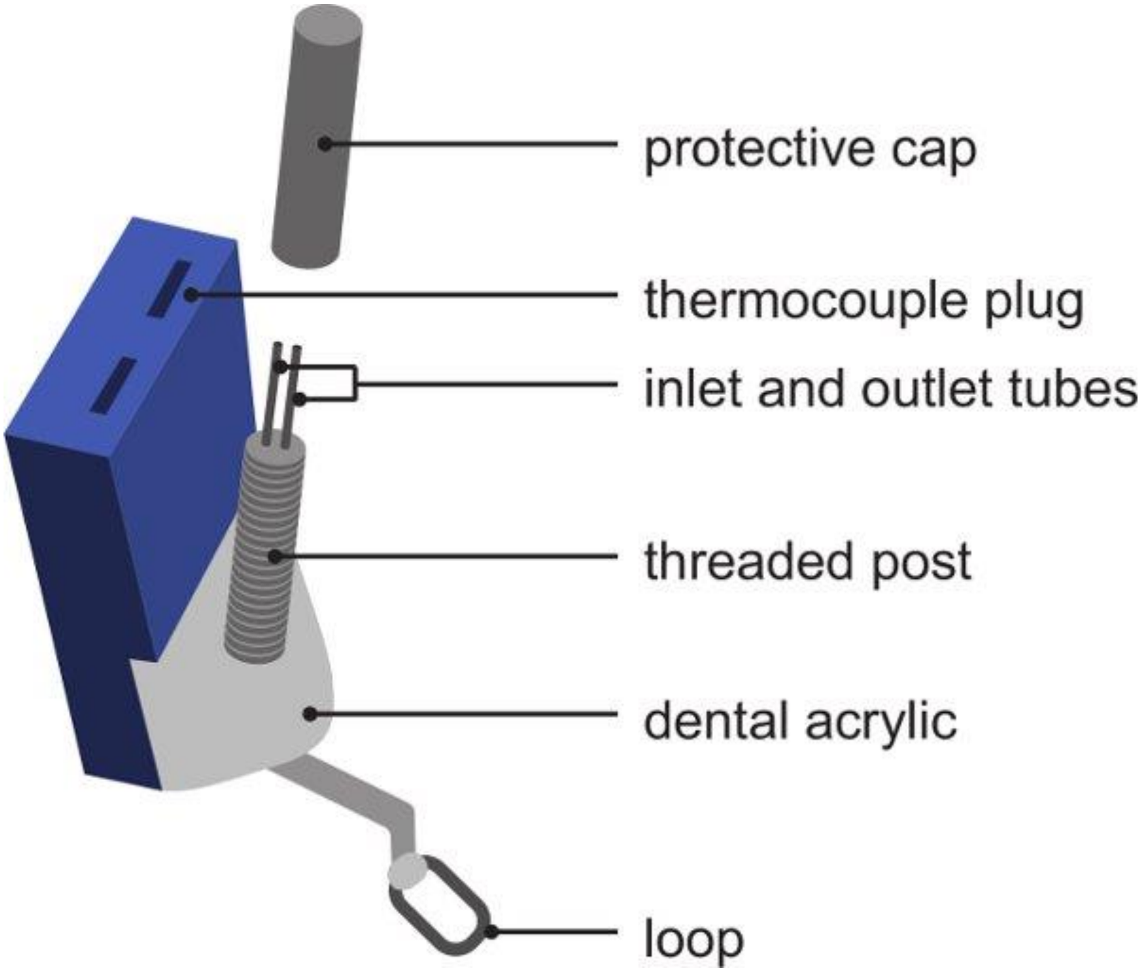
protective cap
thermocouple plug
inlet and outlet tubes
threaded post
dental acrylic
loop

Figure 2.4 The cooling circuit.

The cooling circuit consists of the methanol reservoir, reciprocating piston pump, ice bath, thermometer, and cryoloop. To cool, the pump draws methanol up from the reservoir through the intake tube (1.6 mm I.D.). The methanol exits the pump through the polytetrafluoroethylene tubing (0.5 mm I.D.) and is pumped through to the dry ice bath, where the flowing methanol in the tubing is cooled to -75 °C. The chilled methanol then exits the ice bath and runs through the attached cryoloop before returning to the methanol reservoir. This cryoloop may be a dummy loop (not implanted) used during initial setup, or may be an implanted cryoloop in a test animal. The cryoloop is also connected to a digital thermometer to record loop temperature throughout behavioral testing.

Figure 2.4

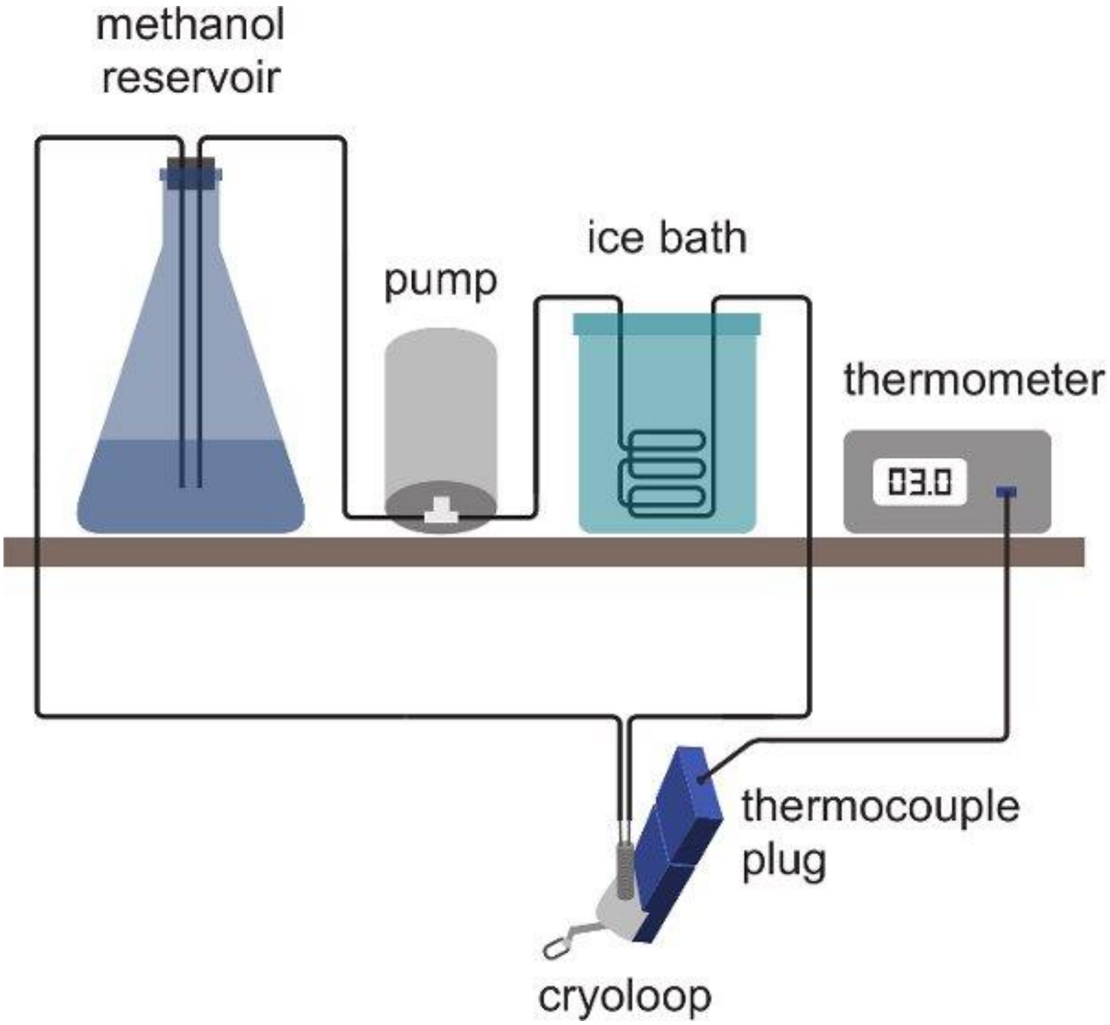
methanol reservoir
pump
ice bath
thermometer
03.0
thermocouple plug
cryoloop

1. Add 500 cc dry ice to 200 mL of methanol in the ice bath. Fit tubing ends snugly over the inlet and outlet of a dummy cryoloop to complete the cooling circuit.
2. Attach the thermocouple plug to a digital thermometer for continuous temperature monitoring using a cable composed of two male thermocouple connectors and a thermocouple wire. Ensure that the length of this cable is sufficient to reach the head of the animal when one end is plugged into the thermometer.
3. Turn on the piston pump using the switch.

   NOTE: Methanol should be drawn up from the reservoir, passed through the pump to the dry ice bath where the flowing methanol in the tubing will be cooled to -75 °C. The chilled methanol will then exit the ice bath and run through the attached cryoloop before returning to the methanol reservoir.
4. Ensure that the pump setting, length of tubing within the ice bath, and length of tubing from the ice bath to the dummy loops are optimal such that the dummy cryoloop temperature can reach a steady state around -5.0 °C.

   NOTE: Such temperatures achieved during this initial setup are often sufficient for achieving test temperatures of 3.0 ± 1.0 °C when the same system is used to cool an implanted cryoloop. Difficulty in attaining sufficient cooling can be solved by adjusting the speed of the pump, increasing the length of tubing submerged within the ice bath, and/or minimizing the length of tubing from the ice bath to the cryoloop.
5. If necessary, lengthen a section of tubing by threading the end of the tube through a tube end fitting and flange the end of the tube with a flanging tool. Attach tubing of a desired length with a similarly flanged end using a connector.
6. Verify that all connections are snug and no leaks are present. Once satisfied with the initial setup, switch the pump off, and remove the dummy cryoloop; the circuit is now prepared for a test animal.

2. Behavioural testing

1. Place the animal on the testing apparatus. Slide the harness over the head and secure the strap snuggly around the animal. Attach the leash.

2. Remove the protective cap of the implanted cryoloop to expose the inlet and outlet tubes. Fit tubing ends snugly over the inlet and outlet tubes of the cryoloop. Connect the thermocouple plug to the digital thermometer.
3. Begin the testing session with a visual (step 3.1) or tactile (step 3.2) obstacle memory trial. Follow with additional trials of all four types (visual obstacle-present, visual obstacle-absent, tactile obstacle-present, tactile obstacle-absent) in a random fashion.

   NOTE: A typical testing session consists of a 'warm' block of trials, where memory-guided obstacle avoidance is observed in the absence of cooling to establish baseline measures.
4. Switch on the piston pump, and wait for the cryoloop to reach a temperature of 3.0 ± 1.0 °C (1-2 min). Then, run a 'cool' block of trials after the piston pump has been switched on. During this block of trials, if needed, assess contributions of the cooled area to memory-guided. Ensure that the temperature of the cryoloop is maintained at 3.0 ± 1.0 °C throughout the entire block.

   NOTE: All four trial types should be randomly interspersed throughout the block.
5. Run a final 'rewarm' block of trials after the piston pump has been switched off, and the cryoloop has returned to its original temperature.

   NOTE: Baseline stepping behavior is re-established during this block. Again, all four trial types should be randomly interspersed throughout the block.

3. Clean-up

1. When the behavioral testing is concluded, remove the tubing from inlet and outlet tubes. Be conscious of residual methanol that may drip from the tubing ends and may irritate the animal.
2. Ensure that the protective cap is replaced. Remove the leash and harness before returning the animal to the colony. Trim the tubing ends (3-4 mm) using a tubing cutter to prevent leaky connections on the next testing day.

2.4.7 Verifying the Extent of Cooling

1. At the end of behavioural testing, confirm that the extent of deactivation is restricted to the region of cortex directly beneath each cryoloop using previously reported techniques (Lomber et al. 1999).

   NOTE: This can be verified with thermocline mapping (Lomber et al. 2010) or with a thermal imaging camera (Carrasco et al. 2015; Kok et al. 2015; Wong et al. 2018).

2.5 Representative Results

This protocol has been successfully used to examine parietal cortex contributions to obstacle memory in the walking cat (Wong et al. 2018). In this study, cryoloops were implanted bilaterally over parietal areas 5 and 7 in three adult (>6 M) female cats (Fig. 2.5A). Animals were assessed in the tactile obstacle memory paradigm in the absence of cooling (warm, control condition), or when area 5 or 7 was bilaterally deactivated.

The representative results from that study demonstrate that when area 5 was bilaterally cooled, hindleg stepping was significantly attenuated in obstacle-present trials (Figure 2.5D, blue). In the warm condition, the mean peak step height for leading and trailing hindlegs was 9.5 ± 2.2 cm and 8.0 ± 2.1 cm, respectively. When area 5 was cooled, peak step height for leading and trailing hindlegs was significantly reduced to 4.3 ± 2.2 cm ($p < 0.0001$) and 3.4 ± 1.4 cm ($p < 0.0001$), respectively. Peak step height of the forelegs in obstacle-present trials or of any leg in obstacle-absent trials was not affected by area 5 deactivation. Similarly, peak step height for any leg in either obstacle-present or obstacle-absent trials did not differ from the warm condition when area 7 was deactivated.

Furthermore, hindleg step clearance was similarly affected when area 5 was deactivated. In comparison to both warm and area 7 cooled conditions, step clearance was reduced to 4.7 ± 2.2 cm in the leading hindleg step ($p < 0.0001$; Fig. 2.5G) and −5.6 ± 1.4 cm in the trailing hindleg step ($p < 0.0001$). Additionally, step trajectory of the trailing hindleg was affected by area 5 deactivation, as the peak occurred before the obstacle, unlike stepping in warm and area 7 cooled conditions (Fig. 2.5G).

Figure 2.5 Reversible, cooling-induced deactivation of parietal area 5 results in obstacle memory deficits.

(A) Lateral view of the right hemisphere of the cat cerebrum showing cryoloops implanted directly over parietal areas 5 (blue) and 7 (green) examined in Wong et al. (2018). D: dorsal, A: anterior.

(B-E) Bar plots depicting mean step height ± SD for the obstacle-present (B, D) and obstacle-absent trials (C, E) for the forelegs (B, C) and hindlegs (D, E) for warm (red), area 5 cooled (blue), and area 7 cooled conditions (green). Step height was significantly reduced in both the leading and trailing hindlegs in the obstacle-present trials when area 5 was deactivated.

(F) Bar plot depicting mean hindleg step clearance ± SD for each cooling condition. Area 5 deactivation resulted in reduced clearance for both leading and trailing hindleg steps.

(G) Bar plot depicting the mean horizontal distance between the peak of each step and the obstacle for each cooling condition. When area 5 was cooled, step trajectories were more variable and differed significantly from warm and area 7 cooled conditions. $*p<0.005$, $**p<0.0001$, n.s.: not significant. This figure has been modified from Wong et al. (2018).

Figure 2.5

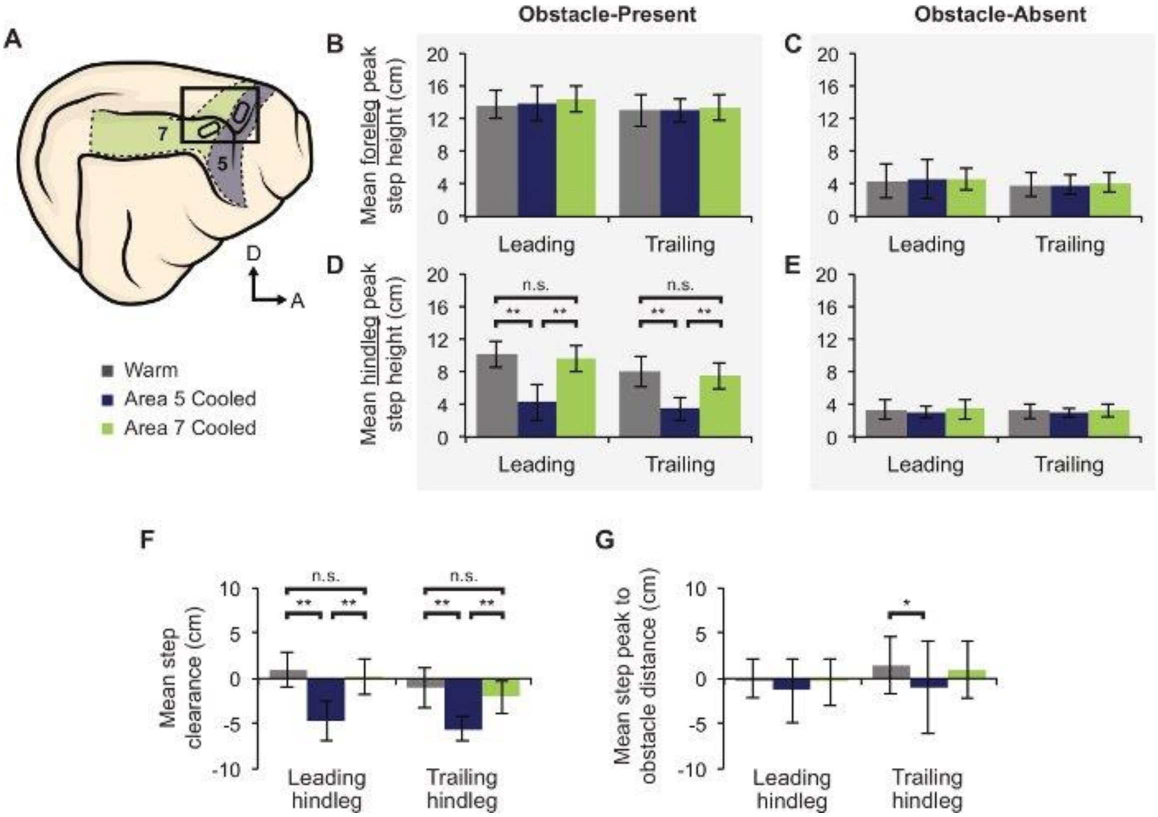
A
7
5
D
A
■ Warm
■ Area 5 Cooled
■ Area 7 Cooled
Obstacle-Present
Obstacle-Absent
B
C
Mean foreleg peak step height (cm)
20
16
12
8
4
0
Leading
Trailing
D
E
Mean hindleg peak step height (cm)
n.s.
**
Leading
Trailing
F
Mean step clearance (cm)
10
5
0
-5
-10
n.s.
**
Leading hindleg
Trailing hindleg
G
Mean step peak to obstacle distance (cm)
*
Leading hindleg
Trailing hindleg

Altogether, such changes in peak step height, step clearance, and step trajectory indicated profound obstacle memory deficits when area 5 was deactivated. Importantly, as area 5 deactivation only altered the characteristics of hindleg stepping in obstacle-present trials and did not impair the ability to make stepping movements, these observed changes in locomotion reflect memory, not motor deficits. Furthermore, thermal imaging performed at the conclusion of behavioural testing confirmed that cooling was restricted to area 5 or 7 when each loop was individually cooled for each hemisphere (Fig. 2.6). Thus overall, these results demonstrate the contributions of parietal area 5 to memory-guided obstacle locomotion in the cat.

2.6 Discussion

The described paradigm employs cooling-induced deactivations of discrete cortical areas using the cryoloop in order to study memory-guided obstacle locomotion in the cat. The visual and tactile obstacle memory paradigms are fairly simple for animals to execute as they exploit naturalistic locomotor behaviours that occur with minimal effort when an animal is motivated to follow a moving food source. Thus the majority of the training period is devoted to acclimating the animal the testing room and cooling equipment. Most animals require repeated exposure to wearing the harness and being tethered via the leash before walking comfortably and naturally on the apparatus. Additionally, during testing, the sound of the piston pump may distract or startle the animal. Completing the cooling circuit with the dummy cryoloop and running the pump during initial training can allow the animal to acclimate to the sound of the pump.

Additionally, the cortical cooling protocol may be adapted for use in alternative behavioural testing paradigms in other experimental animals. Regardless of the exact behavioural task used, the following considerations will facilitate data collection when cortical cooling is used for a variety of different paradigms. For any experimental task, despite sufficient training prior to testing, there will likely be a limited time for testing before the animal becomes restless. Therefore, ample time devoted to ensure proper set-up and troubleshooting prior to bringing the animal into the testing room will optimize subsequent data collection. Difficulty attaining sufficient cooling can be addressed by adjusting the pump speed. However, attention should be paid to the increasing pressure

Figure 2.6 Thermal imaging used to confirm restricted deactivation of area 5 or 7 during cooling.

(A) Photograph depicting cryoloops in contact with parietal areas 5 and 7 of the right hemisphere. Top is dorsal, right is anterior. Dashed line represents border between parietal areas 5 and 7.

(B-C) Thermal images of the parietal cortical surface photographed when the cryoloop over area 5 (B) or area 7 (C) was cooled to 3 °C. This figure has been modified from Wong et al. (2018).

Figure 2.6

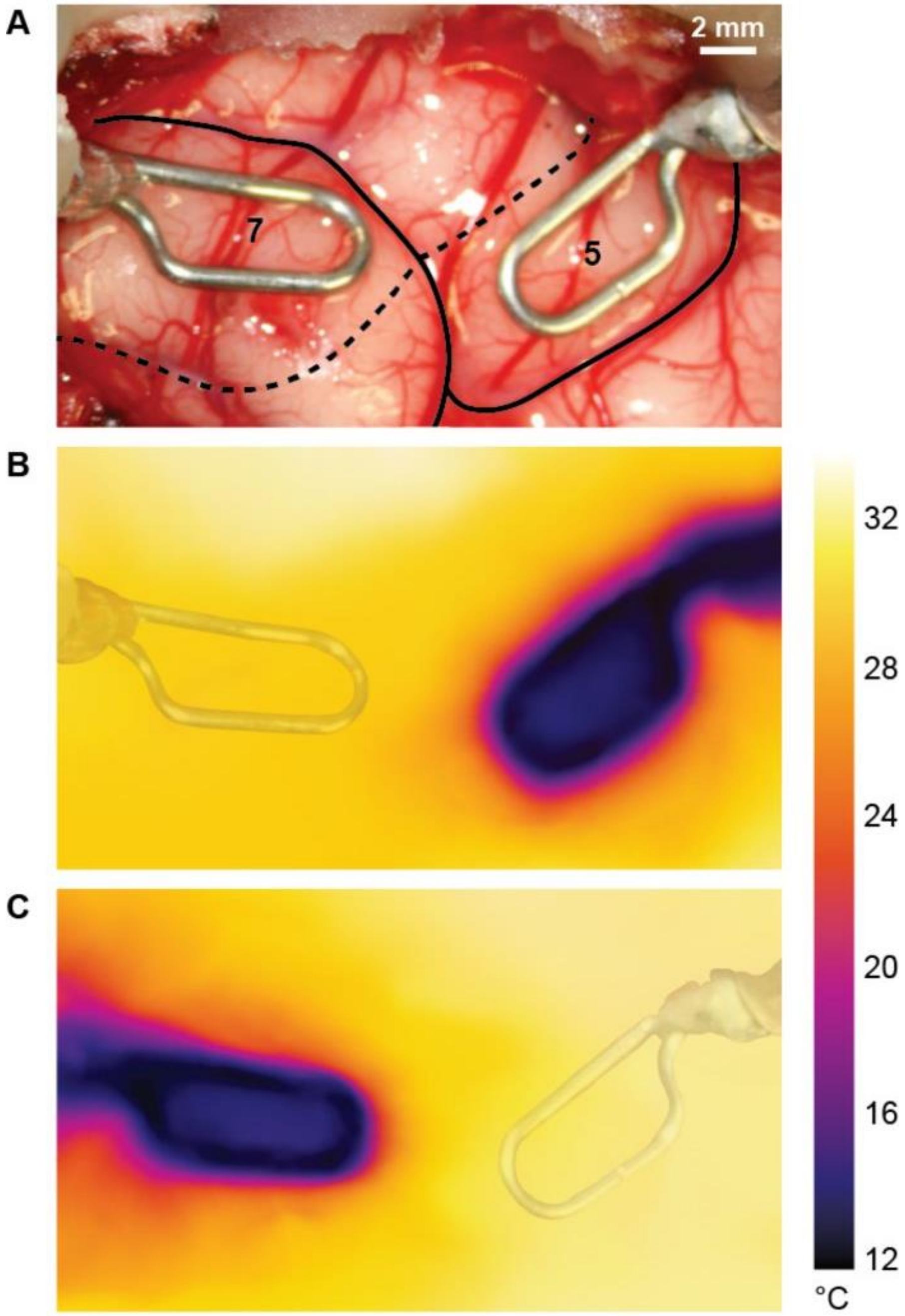

that may result the tubing being forced off the inlet or outlet tubes of the cryoloop. Alternatively, the length of tubing submerged in the ice bath may be increased to enable more time to chill the flow of methanol within the tubes. Additionally, ensuring that the length of tubing from the point of exit from the ice bath to the cryoloop is as short as possible will minimize loss of cooling. However, this distance must also be long enough to allow sufficient range of locomotion for a given behavioural paradigm. Tubing may be insulated with flexible foam wrapping to optimize cooling efficiency. Such wrapping can also prevent drops of condensation that form around the tubing from falling on the animal, which may irritate or startle the animal.

During testing, ensuring a snug fit of the tubing over the inlet and outlet tubes of the cryoloop can make connecting the cryoloop difficult. Wearing a nitrile or latex glove can provide better grip of the Teflon tubing. Ensuring that the animal is comfortable and patient while the experimenter attaches the tubing is essential. Food may be used to keep the animal stationary and content.

Cryoloops can be routinely cooled yielding highly reproducible changes in behaviour when a particular area is deactivated. By assessing the same task in the presence and absence of cortical deactivation within the same animal, the overall number of animals used may be reduced. Furthermore, the extent of cooling may be manipulated to further specify cortical contributions to a specific behaviour. For example, both unilateral and bilateral deactivations can be performed in the same animal to examine possible lateralization effects of a behavior. Additionally, the degree of cooling can be varied to examine laminar contributions. By cooling cryoloops at the cortical surface to 3.0 ± 1.0 °C, all six layers of cortex directly beneath each loop are cooled to <20 °C, inhibiting neuronal spiking activity (Lomber and Payne 2000b). Alternatively, cryoloops can be cooled to 8.0 ± 1.0 °C, which selectively cools only the supragranular cortical layers below this critical temperature of 20 °C. Assessing behaviours with such superficial cortical deactivation as well as full cortical deactivation may permit translaminar dissociations of cortical function (Lomber et al. 2007).

Overall, the cooling system requires minimal maintenance. Tubing and connectors of the cooling circuit should be checked regularly for leaks. The methanol within the reservoir should be replaced weekly to ensure that the methanol is free from particulate matter. Implanted cryoloops also require minimal maintenance. The margins are cleaned periodically with a 3% hydrogen peroxide solution followed by a surgical scrub solution. With proper use and care, implanted cryoloops can be cooled routinely for many years. These cortical cooling procedures can be adapted to other behavioral paradigms (Lomber and Payne 2000a; Lomber and Malhotra 2008; Lomber et al. 2010) or electrophysiological recording preparations (Carrasco et al. 2015; Kok et al. 2015) in alternative animal models (Antunes and Malmierca 2011; Coomber et al. 2011; Johnston et al. 2014; Peel et al. 2014).

2.7 References

Antunes FM, Malmierca MS. 2011. Effect of auditory cortex deactivation on stimulus-specific adaptation in the medial geniculate body. J Neurosci. 31:17306–17316.

Beloozerova IN, Sirota MG. 1993. The role of the motor cortex in the control of accuracy of locomotor movements in the cat. J Physiol. 461:1–25.

Beloozerova IN, Sirota MG. 2003. Integration of motor and visual information in the parietal area 5 during locomotion. J Neurophysiol. 90:961–971.

Carrasco A, Kok MA, Lomber SG. 2015. Effects of core auditory cortex deactivation on neuronal response to simple and complex acoustic signals in the contralateral anterior auditory field. Cereb Cortex. 25:84–96.

Coomber B, Edwards D, Jones SJ, Shackleton TM, Goldschmidt J, Wallace MN, Palmer AR. 2011. Cortical inactivation by cooling in small animals. Front Syst Neurosci. 5:53.

Drew T. 1993. Motor cortical activity during voluntary gait modifications in the cat . I . cells related to the forelimbs. J Neurophysiol. 70:179–199.

Drew T, Marigold DS. 2015. Taking the next step: cortical contributions to the control of locomotion. Curr Opin Neurobiol. 33:25–33.

Horsley V, Clarke RH. 1908. The structure and function of the cerebellum examined by a new method. Brain Behav Evol. 31:45–124.

Johnston K, Koval MJ, Lomber SG, Everling S. 2014. Macaque dorsolateral prefrontal cortex does not suppress saccade-related activity in the superior colliculus. Cereb Cortex. 24:1373–1388.

Kok MA, Stolzberg D, Brown TA, Lomber SG. 2015. Dissociable influences of primary auditory cortex and the posterior auditory field on neuronal responses in the dorsal zone of auditory cortex. J Neurophysiol. 113:475–486.

Lajoie K, Andujar J-E, Pearson KG, Drew T. 2010. Neurons in area 5 of the posterior parietal cortex in the cat contribute to interlimb coordination during visually guided locomotion: a role in working memory. J Neurophysiol. 103:2234–2254.

Lomber SG, Cornwell P, Sun J, Macneil MA, Payne BR. 1994. Reversible inactivation of visual processing operations in middle suprasylvian cortex of the behaving cat. Proc Natl Acad Sci USA. 91:2999–3003.

Lomber SG, Malhotra S. 2008. Double dissociation of “what” and “where” processing in auditory cortex. Nat Neurosci. 11:609–616.

Lomber SG, Malhotra S, Hall AJ. 2007. Functional specialization in non-primary auditory cortex of the cat: areal and laminar contributions to sound localization. Hear Res. 229:31–45.

Lomber SG, Meredith MA, Kral A. 2010. Cross-modal plasticity in specific auditory cortices underlies visual compensations in the deaf. Nat Neurosci. 13:1421–1427.

Lomber SG, Payne BR. 2000a. Contributions of cat posterior parietal cortex to visuospatial discrimination. Vis Neurosci. 17:701–709.

Lomber SG, Payne BR. 2000b. Translaminar differentiation of visually guided behaviors revealed by restricted cerebral cooling deactivation. Cereb Cortex. 10:1066–1077.

Lomber SG, Payne BR, Horel JA. 1999. The cryoloop: An adaptable reversible cooling deactivation method for behavioral or electrophysiological assessment of neural function. J Neurosci Methods. 86:179–194.

Malmierca MS, Anderson LA, Antunes FM. 2015. The cortical modulation of stimulus-specific adaptation in the auditory midbrain and thalamus: a potential neuronal correlate for predictive coding. Front Syst Neurosci. 9:19.

McVea DA, Taylor AJ, Pearson KG. 2009. Long-lasting working memories of obstacles established by foreleg stepping in walking cats require area 5 of the posterior parietal cortex. J Neurosci. 29:9396–9404.

Peel TR, Johnston K, Lomber SG, Corneil BD. 2014. Bilateral saccadic deficits following large and reversible inactivation of unilateral frontal eye field. J Neurophysiol. 111:415–433.

Takakusaki K. 2013. Neurophysiology of gait: From the spinal cord to the frontal lobe. Mov Disord. 28:1483–1491.

Wong C, Wong G, Pearson KG, Lomber SG. 2018. Memory-guided stumbling correction in the hindlimb of quadrupeds relies on parietal area 5. Cereb Cortex. 28:561–573.

Chapter 3

3 Memory-guided stumbling correction in the hindlimb of quadrupeds relies on parietal area 5[2]

3.1 Abstract

In complex environments, tripping over an unexpected obstacle evokes the stumbling corrective reaction, eliciting rapid limb hyperflexion to lift the leg over the obstruction. While stumbling correction has been characterized within a single limb in the cat, this response must extend to both forelegs and hindlegs for successful avoidance in naturalistic settings. Furthermore, the ability to remember an obstacle over which the forelegs have tripped is necessary for hindleg clearance if locomotion is delayed. Therefore, memory-guided stumbling correction was studied in walking cats after the forelegs tripped over an unexpected obstacle. Tactile input to only one foreleg was often sufficient in modulating stepping of all four legs when locomotion was continuous, or when hindleg clearance was delayed. When obstacle height was varied, animals appropriately scaled step height to obstacle height. As tactile input without foreleg clearance was insufficient in reliably modulating stepping, efference, or proprioceptive information about modulated foreleg stepping may be important for producing a robust, long-lasting memory. Finally, cooling-induced deactivation of parietal area 5 altered hindleg stepping in a manner indicating that animals no longer recalled the obstacle over which they had tripped. Altogether, these results demonstrate the integral role area 5 plays in memory-guided stumbling correction.

---

[2] A version of this chapter is published as:

Wong C, Wong G, Pearson KG, Lomber SG (2018). Memory-guided stumbling correction in the hindlimb of quadrupeds relies on parietal area 5. Cerebral Cortex doi: 10.1093/cercor/bhw391

3.2 Introduction

Locomotor control systems responsible for moving an animal through a complex environment must be able to compensate for changes in terrain or sudden perturbations. For example, tripping over an unexpected obstacle evokes the “stumbling corrective reaction” (Forssberg 1979) to prevent falling and ensure proper obstacle avoidance without interrupting forward locomotion (Prochazka et al. 1978; Wand et al. 1980). Sudden contact of the foot or leg with an obstacle during the swing phase of a step results in activation of knee flexors and ankle extensors to ensure that the leg and foot are lifted above the obstacle (Andersson et al. 1978; Buford and Smith 1993). Such rapid readjustments of step trajectory are present in the locomotor system even before the onset of walking in human infants (Lam et al. 2003), and are evident in both bipedal (Eng et al. 1994; Van Wezel et al. 1997; Zehr et al. 1997, 1998; Schillings et al. 2000) and quadrupedal animals (Drew and Rossignol 1987; McVea and Pearson 2007a). In quadrupeds, stumbling correction in response to cutaneous inputs to the forelegs must extend to both the forelegs and hindlegs for successful obstacle avoidance. Previous studies have focused on kinematic and electromyographic responses exclusively within either a foreleg or hindleg following tactile or electrical stimulation to the same leg. However, the ability of tactile inputs to only one leg to modify stepping of all four limbs for stumbling correction in a naturalistic setting remains to be examined.

While spinal reflex pathways and central pattern generators within the spinal cord can produce and adapt locomotion on simple even terrain (Takakusaki 2013; Kiehn 2016), supraspinal cortical structures contribute to locomotor control in more complex settings (Drew and Marigold 2015). For example, the posterior parietal cortex is involved in coordinating correct paw placement required to step around or over an obstacle in the environment (Marigold et al. 2011). Recent work has also demonstrated the ability of animals to store visual information about an obstacle in memory used to modify stepping if locomotion is interrupted (McVea and Pearson 2006; Whishaw et al. 2009). Such obstacle memory has been shown to be particularly robust when the forelegs, but not the hindlegs, have cleared an obstacle, suggesting that efference motor commands of enhanced foreleg flexion, proprioceptive feedback from muscle receptors, or both may be important for establishing long-lasting memories to guide subsequent hindleg stepping (McVea and Pearson 2007b). Electrophysiological experiments (Andujar et al. 2010; Lajoie et al. 2010) and cortical inactivation studies employing lesions (McVea et al. 2009) or cooling-induced deactivations (Wong et al. 2015) have implicated parietal area 5 in such memory-guided obstacle locomotion. Specifically, as a cat steps over an obstacle with its forelegs, increased neuronal activity in area 5 is sustained as long as the cat remains straddling the obstacle between its fore- and hindlegs (Lajoie et al. 2010). As persisting neural activity is believed to temporally bridge the gap between sensory stimuli (such as visual input of an obstacle) and contingent memory-guided actions (Curtis and D'Esposito 2003), such sustained activity likely reflects a representation of the obstacle being held in memory. Thus lesions or cooling-induced deactivations of this area result in deficits in this visually-dependent obstacle memory, as evidenced by altered hindlimb stepping indicating that cats could no longer recall an obstacle over which the forelegs had stepped (McVea et al. 2009; Wong et al. 2015). However, these memory impairments were temporally dependent as hindleg obstacle avoidance was unaltered when locomotion was continuous. Stepping was only modified if forward locomotion was paused after foreleg obstacle clearance, demonstrating the necessity of parietal area 5 for coordinating delayed hindleg stepping over a remembered obstacle.

A similar temporal relationship between parietal cortex involvement and memory-guided stepping may be present for stumbling correction if hindleg clearance does not immediately follow foreleg clearance. As stumbling correction persists following lower spinal transection in walking cats, neural circuitry within the spinal cord is possibly sufficient for this reflexive reaction during continuous locomotion (Forssberg et al. 1977; Miller et al. 1977). However, if locomotion is delayed or interrupted, the ability to remember an obstacle over which an animal has tripped has yet to be examined. In the case of an animal stalking prey on natural terrain, stepping movements are often slow and deliberate, and can be interrupted by long pauses to minimize the risk of exposure to prey and other predators. During such behaviors, it is imperative that information about uneven terrain and potential obstacles gained via tactile inputs to the leg or paw can be maintained in memory while gaze is maintained on moving prey. The ability to use this memory to modify movements when stepping resumes would be essential for successful hunting in these animals.

Therefore, the purpose of this study was to examine the ability of walking cats to remember an obstacle over which they have tripped. Tactile input to at least one of the forelegs from an unexpected obstacle was used to evoke the stumbling corrective reaction. Subsequent hindleg steps were measured when hindleg clearance immediately followed foreleg clearance (continuous locomotion), or when hindleg clearance was delayed (interrupted locomotion). To determine if specific characteristics of the obstacle were retained, memory-guided stumbling correction over obstacles of different heights was examined. To assess the relative contributions of tactile sensory input and foreleg obstacle clearance (and concomitant efference motor signals and/or proprioceptive inputs), locomotion was also interrupted immediately after foreleg obstacle contact, but before foreleg clearance. Finally, to assess parietal cortical contributions to memory-guided stumbling correction, cooling loops were placed bilaterally over parietal area 5. While all cats demonstrated the ability to remember an obstacle over which they had tripped in the absence of cortical cooling, deactivation of area 5 resulted in significantly diminished obstacle memory. Altogether, these experiments demonstrate the critical role of parietal area 5 in the memory-guided coordination required for avoidance after tripping over an unexpected obstacle.

3.3 Materials and Methods

3.3.1 Overview

Memory-guided stumbling correction was examined in 5 adult (>6 M) female domestic cats obtained from a commercial breeding facility (Liberty Labs, NY). Animals were housed in an enriched colony environment and provided with water ad libitum. Food intake was regulated during testing days when moist food was provided. Additionally, animals were offered dry food for 1 h at the end of each day. Following characterization of memory-guided stumbling correction, parietal contributions to obstacle memory were examined in 3 animals. Each animal received bilateral cryoloops over parietal areas 5 and 7. Memory-guided stumbling correction was subsequently assessed when each area was bilaterally cooled. When behavioral testing was completed, cryoloops were exposed on the surface of the brain and a thermal imaging camera was used to capture the extent of cortical deactivation. Animals were then perfused and the brains were fixed and removed from the cranium. Brains were then frozen, coronally sectioned, and processed for Nissl, cytochrome oxidase, and SMI-32. Reconstructions of deactivation loci were compared with areal boundaries revealed with SMI-32 to confirm accurate cryoloop placement. All procedures were conducted in compliance with the National Research Council's *Guide for the Care and Use of Laboratory Animals* (eighth edition; 2011) and the Canadian Council on Animal Care's *Guide to the Care and Use of Experimental Animals* (1993), and were approved by the University of Western Ontario Animal Use Subcommittee of the University Council on Animal Care.

3.3.2 Apparatus

Each cat was trained to walk along a walkway (2.43 m long × 29 cm wide) enclosed by 18 cm high clear Plexiglas walls, similar to the apparatus used by McVea et al. (2009; Fig. 3.1). Halfway along the apparatus, a 25.8 cm wide × 3 mm thick obstacle could be silently raised onto or removed from the walkway through a slot using a lever mounted underneath the walking surface. The obstacle was raised to heights of either 8.7 cm or 4.8 cm in different trials to assess the specificity of object characteristics being retained. The 4.8 cm high obstacle was raised or lowered slower than the 8.7 cm high obstacle in order to match the time required to introduce or remove the higher obstacle. The lever mechanism was examined daily to ensure that the obstacle could be raised or lowered soundlessly at the required speeds, and was lubricated to ensure silence if necessary. Soft food was placed on an elevated platform (23 cm long × 23 cm wide × 16 cm high) at a height to encourage the animal to remain standing as it ate. During preliminary training, the experimenter used her hand to raise and lower the obstacle using a lever mounted to the underside of the walkway. However, as cats appeared to notice arm movements used to control the obstacle, the experimenter instead used her leg to move the lever controlling the obstacle. This permitted the experimenter to continue using her hands to feed the animal, ensuring that attention of the animal was maintained on eating. This method was found to effectively introduce and remove the obstacle without detectable

Figure 3.1 Equipment and apparatus for obstacle memory testing.

Each animal would walk along a 243 cm long × 29 cm wide runway enclosed by 18 cm high Plexiglas walls towards a 16 cm high platform on top of which food was placed. A 25.8 cm wide × 3 mm thick obstacle could be raised onto or removed from the runway using a lever mounted underneath the walking surface to a height of 8.7 cm or 4.8 cm. An ethernet camera mounted onto a tripod was placed 185 cm from the side of the walking apparatus aligned to the obstacle position. All trials were recorded and saved to a laptop using Contemplas (Kempten, GER) motion analysis software.

Figure 3.1

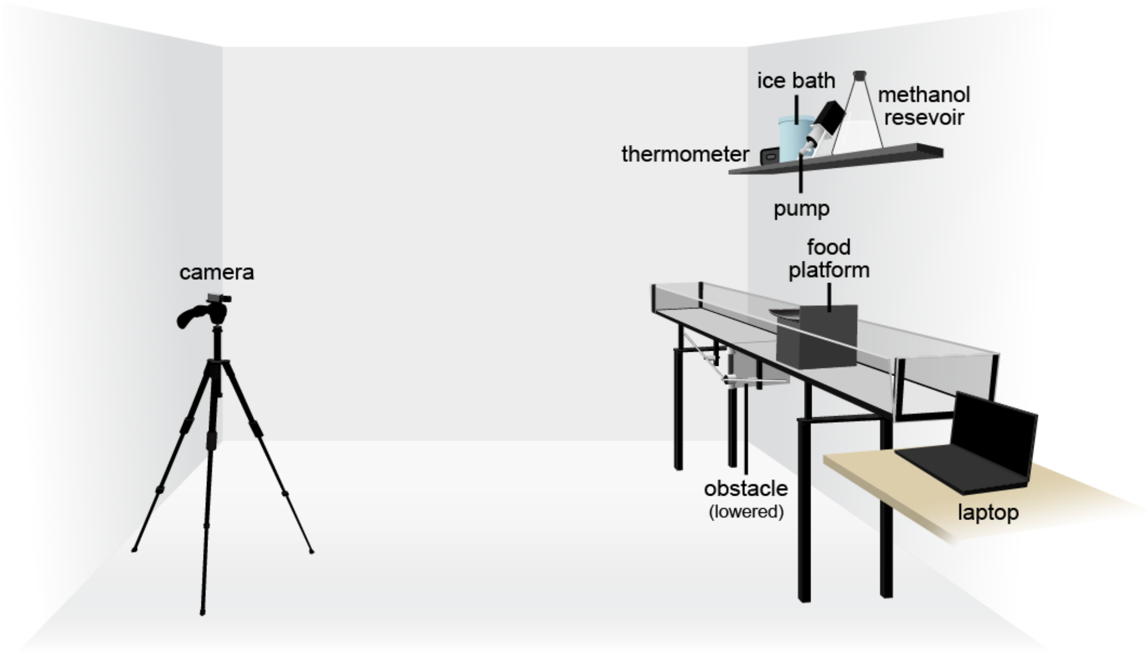
ice bath
methanol
resevoir
thermometer
pump
food
platform
camera
obstacle
(lowered)
laptop

sound, and without drawing attention to movements of the experimenter's leg beneath the walkway. An ethernet camera mounted on a tripod was placed 1.85 m from the side of the walkway and aligned to where the obstacle was raised onto and lowered from the walkway. All trials were recorded at 54 frames per second using Contemplas (Kempten, GER) motion detection software. By examining stepping in all cats, it was verified that introducing the obstacle in this manner did not prevent the forelegs from contacting the obstacle prior to clearing it, demonstrating that the animals were unaware of that the obstacle had been introduced.

3.3.3 Behavioural Testing Procedures

To assess memory-guided stumbling correction, each animal approached food placed on the elevated platform in the absence of any obstacle. As the animal ate, the obstacle was silently raised onto the walkway beneath the food dish to prevent visual input of the obstacle. The food was then moved forwards causing the animal to contact the obstacle with their forelegs before stepping over it. As the animal continued eating while straddling the obstacle between their fore- and hindlegs, the obstacle was lowered covertly becoming flush with the walkway to prevent further visual or tactile inputs. Following a variable delay period, the food was moved forwards to encourage the animal to resume walking. By introducing the obstacle in this manner, the stumbling corrective reaction was reliably elicited in an unexpected manner, without providing any visual input of the obstacle prior to foreleg contact. Subsequent hindleg stepping either immediately followed foreleg obstacle clearance (continuous locomotion), or was delayed for up to 2 min. A “tactile input only” variation was also used to assess the contributions of foreleg obstacle clearance to obstacle memory. In these trials, each animal approached the food platform in the absence of any obstacle. As the animal ate, obstacle was covertly raised onto the walkway beneath the platform. The food was then carefully moved forwards, causing the animal to contact the obstacle with at least one of its forelegs. Immediately following tactile input, the food was carefully moved backwards to encourage the animal to resume its stance and prevent foreleg movement over the obstacle. As the animal continued eating in this position, the obstacle was removed, before moving the food forwards again to encourage the animal to resume walking.

To prevent habituation to the obstacle and development of a learned avoidance response, trials where the obstacle was present were interspersed with trials where the obstacle was absent. The lack of elevated stepping observed in obstacle absent trials demonstrated the lack of habituation to the presence of the obstacle, and use of tactilely acquired memory on a trial to trial basis in obstacle present conditions. In obstacle present trials, intact obstacle memory demonstrated by an average hindleg step height exceeding the height of the obstacle was confirmed in all animals ($n = 3$) prior to cooling loop implantation.

3.3.4 Surgical Procedures

Cryoloops were implanted bilaterally over areas 5 and 7 according to previously reported surgical procedures (Lomber et al. 1999, 2010; Lomber and Payne 2000a, 2000b; Lomber and Malhotra 2008). Cooling loops were individually shaped from 23-gauge stainless steel hypodermic tubing to conform to each area examined. A microthermocouple was soldered to each loop, which was connected to a digital thermometer to continuously monitor cooling loop temperature throughout all behavioral testing.

3.3.5 Memory Testing and Reversible Cooling Deactivation

Following surgical implantation and approximately 2 weeks of recovery, obstacle memory was tested in 3 animals, using the initial variation of the memory task where the forelegs contacted the 8.7 cm high obstacle before stepping over it. Each testing day began with trials conducted in the absence of any cooling (warm condition). This was followed by a second “cooling block”, where histological grade methanol was drawn up from a reservoir, pumped through a dry ice bath to cool the flowing methanol, through the lumen of a cooling loop, and back to the reservoir. The flow of chilled methanol through the lumen of a cooling loop serves to silence neuronal activity in the region of cortex directly beneath the loop (Lomber et al. 1999). Parietal loops were cooled to 3.0 ± 1.0 °C to completely deactivate all cortical layers (Lomber and Payne 2000a, 2000b). A final “warm” block followed to re-establish baseline stepping. Cooling loop temperatures were monitored closely throughout testing by connecting the microthermocouple to a thermometer to confirm the duration and depth of deactivation. Each testing block consisted of trials where the obstacle was present interspersed with trials where the obstacle was absent.

3.3.6 Data Analysis

Videos were analyzed using custom written scripts in Matlab (MathWorks, Natick, MA). Peak foreleg and hindleg step height was measured as the perpendicular distance between the toe and the walking surface when the toe reached the highest point in the step. Additionally, step clearance was measured as the step height directly above the lowered obstacle in obstacle present trials. The horizontal distance between the toe and obstacle at the peak of each step was also measured in obstacle present trials. Toe position was also tracked throughout each step to determine peak step velocity and total movement times. To assess the ability of tactile input to the forelegs to modify stepping of all four limbs for obstacle avoidance, a three-way ANOVA was conducted to examine the effects of the obstacle condition (present or absent), step order (leading or trailing), and leg (foreleg or hindleg) on step height. Due to significant interaction effects, follow-up *t*-tests were used to compare step height for each step between obstacle present and obstacle absent trials. A Bonferroni correction was applied to account for multiple comparisons, and statistical significance was accepted at $P < 0.0125$. Linear regression models were computed to assess the effect of increasing the duration of the delay on hindleg step height. To assess the ability to scale step height to obstacle height, a one-way multivariate ANOVA was used to compare the effect of obstacle condition (high, low, or absent) on step height for all four legs. Linear regression models were computed to assess the effect of increasing delay duration on hindleg step height for low obstacle trials. Paired *t*-tests were conducted to compare step clearance and the step peak to obstacle distance between high and low obstacle conditions. To assess the role of foreleg obstacle clearance on obstacle memory, a one-way multivariate ANOVA was conducted to assess the effect of tactile condition (tactile input with foreleg clearance, tactile input without foreleg clearance, or no tactile input) on step height for all four legs. Linear regression models were computed to assess the effect of delay on hindleg step height for tactile only trials. Finally, to assess parietal cortex contributions to memory-guided stumbling correction, a one-way multivariate ANOVA was conducted to assess the effect of cooling condition (warm (no cooling), area 5 cooled, or area 7 cooled) on step height for all four legs in obstacle present and obstacle absent trials. Linear regression models were computed to assess the effect of delay on hindleg step height for warm and area 7 cooled conditions. Due to nonlinearity, a power function was used to fit the relationship between step height and delay for the area 5 cooled condition. Additionally, a one-way multivariate ANOVA was conducted to assess the effect of cooling condition on step clearance, the step peak to obstacle distance, movement time, and peak step velocity. A Bonferroni correction was applied to account for multiple comparisons, and statistical significance was accepted at $P < 0.00625$. When statistical differences were detected, post hoc Tukey's tests were conducted.

3.3.7 Terminal Procedures

Following all behavioral testing, each cat was anesthetized with sodium pentobarbital (25–30 mg/kg, i.v.) and a craniotomy was made to expose the implanted cooling loops on the surface of the brain. Each cryoloop was individually cooled to the same temperature used during behavioral testing (3.0 ± 1.0 °C) and photographed with a thermal imaging camera to capture the extent of deactivation (Fig. 3.2). After each area was photographed, anesthesia was deepened with sodium pentobarbital (40 mg/kg, i.m.) and the animal was transcardially perfused. The brain was removed, frozen and cut in 60 µm coronal sections and collected serially. Sections from the first of five series, separated by 300 µm intervals, were processed with Nissl stain. Series 2 was processed with cytochrome oxidase. Nissl and cytochrome oxidase stained sections were examined to ensure that repeated deactivations did not alter the cortical structure of parietal areas cooled over the testing period. Series 3 was processed with the monoclonal antibody SMI-32 (Covance, Emeryville, CA) for areal border delineation. Series 4 and 5 were retained as spares to process with any of the above methods as need. Reacted sections were mounted onto gelatinized slides, cleared and coverslipped.

Figure 3.2 Thermal images taken of the dorsolateral surface of parietal cortex showing the extent of deactivation of each individual cortical loop.

(A) Cooling loops in contact with areas 5 and 7 of the right hemisphere photographed with a camera attached to a surgical microscope.

(B) Thermal image of the parietal surface when the cryoloop over area 5 was cooled to 3 °C. A translucent image of the cryoloop over area 7 has been superimposed to indicate its position. A color-coded temperature scale is provided on the right.

(C) Thermal image of the parietal surface when the cryoloop over area 7 was cooled to 3 °C. A translucent image of the cryoloop over area 5 has been superimposed to indicate its position.

Figure 3.2

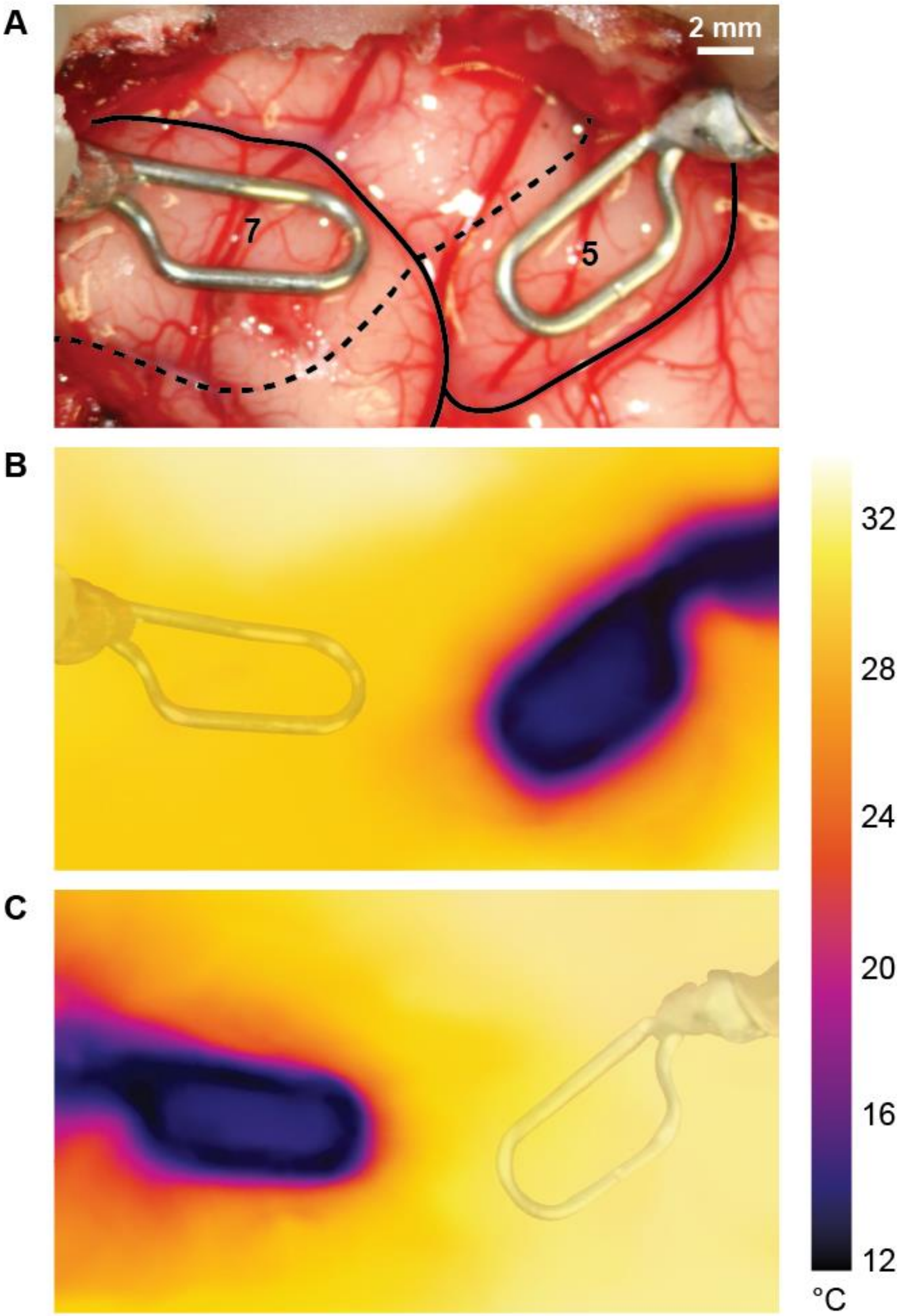

3.3.8 Cooling Deactivation Assessment

Alignment of deactivation sites with area 5 or 7 was confirmed in each animal by comparing thermal photographs with Nissl and SMI-32 processed tissue. In the region of cortex directly beneath each cooling loop, area 7 was characterized by weaker SMI-32 labeling in layers III and V, relative to dense labeling present in anteriorly adjacent area 5, and ventrally adjacent anteromedial lateral suprasylvian area (van der Gucht et al. 2001). Additionally, the increase in cortical thickness, particularly in layer III, defined the transition from area 5 to area 7 along the suprasylvian gyrus (Andujar and Drew 2007). Area 5 and area 7 borders delineated in SMI-32 stained sections, and assessment of thermal photographs taken of exposed cryoloops during cooling confirmed that deactivation loci were contained within each area of interest, with minor spread into flanking cortices (Fig. 3.2).

3.4 Results

3.4.1 Persisting Obstacle Memory Modulates Hindleg Stepping

To determine whether cats (*n* = 5) could remember the presence of an unseen obstacle over which they tripped, the stumbling corrective reaction was evoked by causing the forelegs to contact an unexpected obstacle during the swing phase of a step (Fig. 3.3A). Such contact was followed by rapid hyperflexion of the forelegs over the obstacle. The obstacle was then covertly removed to prevent further tactile or visual inputs. Locomotion was either continuous, allowing hindleg steps to immediately follow foreleg obstacle clearance, or interrupted, delaying hindleg steps for intervals ranging from a couple of seconds to upwards of 2 min. Trials where the obstacle was present were interspersed with trials where the obstacle was absent to prevent habituation to the presence of the obstacle and development of a learned avoidance response. Foreleg and hindleg step heights were measured and compared between obstacle present and obstacle absent trials to assess memory-guided stumbling correction.

In all five animals, tactile input to the forelegs successfully modulated stepping in all limbs during both continuous and delayed locomotion. In 46% of obstacle present trials, sudden contact of only one foreleg with the obstacle was sufficient in modulating

Figure 3.3 Memory of an obstacle can be used to modulate stepping to ensure avoidance after tripping over an unexpected obstacle.

(A) Memory-guided stumbling correction was assessed by covertly raising an 8.7 cm high obstacle onto the walking surface beneath a food platform from which an animal ate. The food was then moved forwards causing the animal to contact the obstacle with their forelegs before stepping over it. As the animal continued eating, the obstacle was lowered becoming flush with the walkway to prevent further visual or tactile inputs. Following a variable delay period, the food was moved forwards to encourage the animal to resume walking.

(B) Pie chart depicting the proportion of obstacle present trials by type of foreleg tactile input. While both forelegs contacted the obstacle in 54% of trials, tactile input to only one foreleg was sufficient in modulating stepping in 46% of obstacle present trials.

(C,D) Bar plots depicting mean peak step height ± standard deviation (SD) for leading and trailing foreleg steps (C) and hindleg steps (D) in obstacle present (black) and obstacle absent trials (gray). Step height was significantly higher in obstacle present conditions for both the forelegs and hindlegs, regardless of the order of stepping.

(E,F) Scatter plots depicting peak step height versus delay duration for leading (E) and trailing hindleg steps (F), and the gradual decline in step height over time. Dashed horizontal line indicates obstacle height (8.7 cm); gray horizontal line and shaded bar indicates the mean ± SD hindleg step height in obstacle absent trials. Solid line represents the linear regression line with the equation, coefficient of determination, and corresponding *P* value shown. $^*P < 0.0001$

Figure 3.3

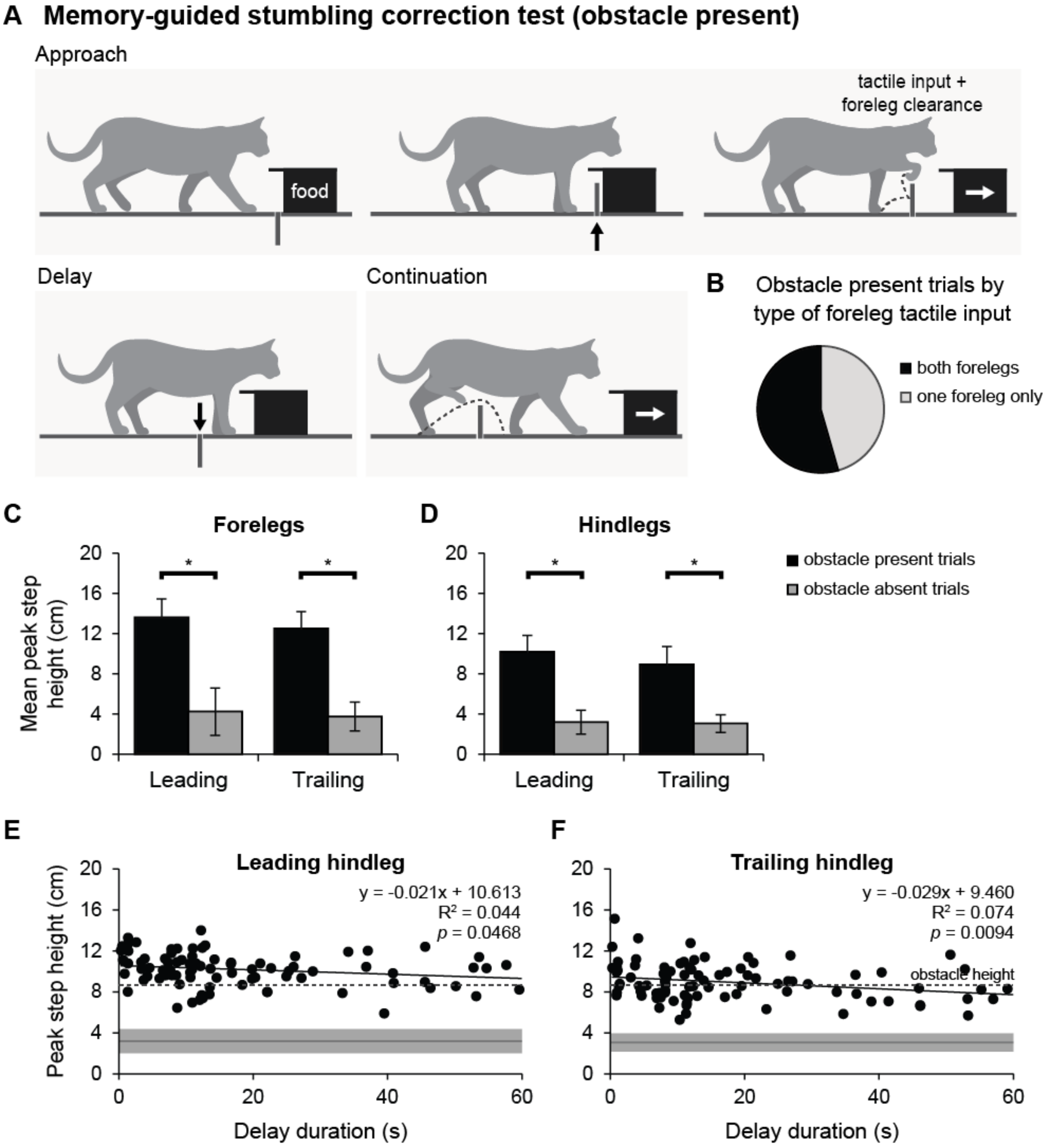
A Memory-guided stumbling correction test (obstacle present)
Approach
food
tactile input +
foreleg clearance
Delay
Continuation
B Obstacle present trials by type of foreleg tactile input
■ both forelegs
□ one foreleg only
C
Forelegs
Mean peak step height (cm)
20
16
12
8
4
0
*
*
Leading
Trailing
D
Hindlegs
■ obstacle present trials
■ obstacle absent trials
E
Leading hindleg
y = -0.021x + 10.613
R² = 0.044
p = 0.0468
Peak step height (cm)
Delay duration (s)
0
20
40
60
F
Trailing hindleg
y = -0.029x + 9.460
R² = 0.074
p = 0.0094
obstacle height

stepping of all limbs (Fig. 3.3B, grey). In the remaining 54% of obstacle present trials, obstacle contact with one foreleg did not preclude contact with the other foreleg, resulting in obstacle contact with both forelegs (Fig. 3.3B, black). A three-way ANOVA conducted to examine the effects of the obstacle condition (present or absent), step order (leading or trailing), and leg (foreleg or hindleg) on step height revealed a significant interaction between all three factors ($F(1, 592) = 8.20$, $p = 0.004$), and significant two-way interactions between obstacle condition and step order ($F(1, 592) = 10.66$, $p = 0.001$), and obstacle condition and stepping leg ($F(1, 592) = 165.02$, $p < 0.0001$). Thus to determine if tactile input to the forelegs could modulate stepping of all four legs, the height of each step was compared between obstacle present and obstacle absent trials. In obstacle present trials, mean step heights of leading (13.6 ± 1.8 cm; Fig. 3.3C) and trailing foreleg steps (12.5 ± 1.7 cm) were significantly higher than in obstacle absent trials (leading: 4.2 ± 2.4 cm, $t(89) = 29.0$, $p < 0.0001$; trailing: 3.7 ± 1.4, $t(89) = 35.2$, $p < 0.0001$). Similarly, mean step heights of leading (10.2 ± 1.6 cm; Fig. 3.3D) and trailing hindleg steps (8.9 ± 1.8 cm) were significantly higher than in obstacle absent trials (leading: 3.2 ± 1.2 cm, $t(89) = 35.2$, $p < 0.0001$; trailing: 3.1 ± 0.9, $t(89) = 26.9$, $p < 0.0001$), demonstrating the ability of all animals to remember the obstacle. Additionally, linear regressions were performed to characterize the effect of increasing the duration of the delay on hindleg step height. Delay was found to be a significant predictor of step height for both leading ($R^2(1, 88) = 0.044$, $p = 0.0468$; Fig. 3.3E) and trailing hindleg steps ($R^2(1, 88) = 0.074$, $p = 0.009$; Fig. 3.3F), with negative linear functions describing the gradual decline in step height with increasing delays. However, hindlegs steps remained significantly higher in obstacle present trials (Fig. 3.3D), demonstrating the persisting, yet gradually decaying property of obstacle memory. Altogether, these results demonstrate the capacity of walking cats to remember an obstacle over which they have tripped, and their ability to use this memory to modulate stepping during continuous or interrupted obstacle negotiation.

3.4.2 Memory-guided Stepping Reflects Obstacle Characteristics

To further examine the precision of memory-guided stumbling correction, a lower obstacle was used to assess whether step height would scale to obstacle height. A one-way multivariate ANOVA revealed a significant effect of obstacle condition (high, low, or absent) on step height (F(8, 468) = 131.81, $p < 0.0001$). Step height of all four legs was significantly affected by the different obstacle conditions (leading foreleg: F(2, 237) = 329.39, $p < 0.0001$; trailing foreleg: F(2, 237) = 632.76, $p < 0.0001$; leading hindleg: F(2, 237) = 346.00, $p < 0.0001$; trailing hindleg: F(2, 237) = 219.57, $p < 0.0001$). Post hoc Tukey tests indicated that step height differed significantly between high obstacle (8.7 cm) trials, low obstacle (4.8 cm) trials, and obstacle absent trials for leading foreleg steps, trailing foreleg steps, and leading hindleg steps ($p < 0.0001$ for all comparisons), demonstrating the specificity of step modulation for each condition. In low obstacle trials, leading and trailing foreleg steps were on average 11.8 ± 2.5 cm and 10.0 ± 1.7 cm high, respectively (Fig. 3.4A). Mean leading and trailing hindleg step heights were 8.2 ± 1.3 cm and 7.1 ± 1.3 cm, respectively (Fig. 3.4B). Similar to trials with the high obstacle, negative linear functions described the gradual decline in step height with increasing delays for both leading ($R^2(1, 77) = 0.0526$, $p = 0.0420$; Fig. 3.4C) and trailing hindleg steps in low obstacle trials ($R^2(1, 77) = 0.0718$, $p = 0.0169$; Fig. 3.4D). However, both forelegs contacted the low obstacle in only 18% of trials (Fig. 3.4E, black), while tactile input to only one foreleg in the remaining 82% of low obstacle trials was sufficient in modulating stepping of all legs (Fig. 3.4E, grey). Step clearance, or the difference between obstacle height and step height directly over the obstacle, also differed, with significantly greater mean clearances over the lower obstacle for both leading ($t(89) = -5.6$, $p < 0.0001$; Fig. 3.4F) and trailing hindleg steps ($t(89) = -6.8$, $p < 0.0001$). However, the mean distance between the peak of each step and the obstacle did not differ significantly for leading and trailing hindleg steps between high and low obstacle trials (Fig. 3.4G). In both obstacle present conditions, the leading hindleg step tended to peak before the obstacle, while the trailing hindleg step tended to reach its maximal height after passing the obstacle. Overall, these results reinforce the ability of walking cats to retain specific information about an obstacle over which they have tripped and modulate stepping accordingly to remembered obstacle height.

Figure 3.4 Memory-guided obstacle avoidance can scale to obstacle height.

(A,B) Bar plots depicting mean peak step height ± SD for leading and trailing foreleg steps (A) and hindleg steps (B) in high obstacle trials (8.7 cm high obstacle, black), low obstacle trials (4.8 cm high obstacle, dark gray), and obstacle absent trials (gray). Step height differed significantly between all obstacle conditions for leading and trailing steps.

(C,D) Scatter plots depicting peak step height versus delay duration for leading (C) and trailing hindleg steps (D) for low obstacle trials. Similar to high obstacle trials, step height gradually declined with time. Dashed horizontal line indicates obstacle height (4.8 cm); gray horizontal line and shaded bar indicates the mean ± SD hindleg step height in obstacle absent trials. Solid line represents the linear regression line with the equation, coefficient of determination, and corresponding *P* value shown.

(E) Pie chart depicting that in 82% of obstacle present trials, obstacle contact with only one foreleg was sufficient in modulating stepping for low obstacle locomotion.

(F) Bar plots depicting mean step clearance for obstacle present conditions for leading (left) and trailing (right) hindleg steps. Step clearances were significantly greater in low obstacle trials.

(G) Bar plots depicting mean horizontal distance between the peak of each step and the obstacle which did not differ between obstacle present conditions for leading (left) and trailing (right) hindleg steps. $^*P < 0.0001$.

Figure 3.4

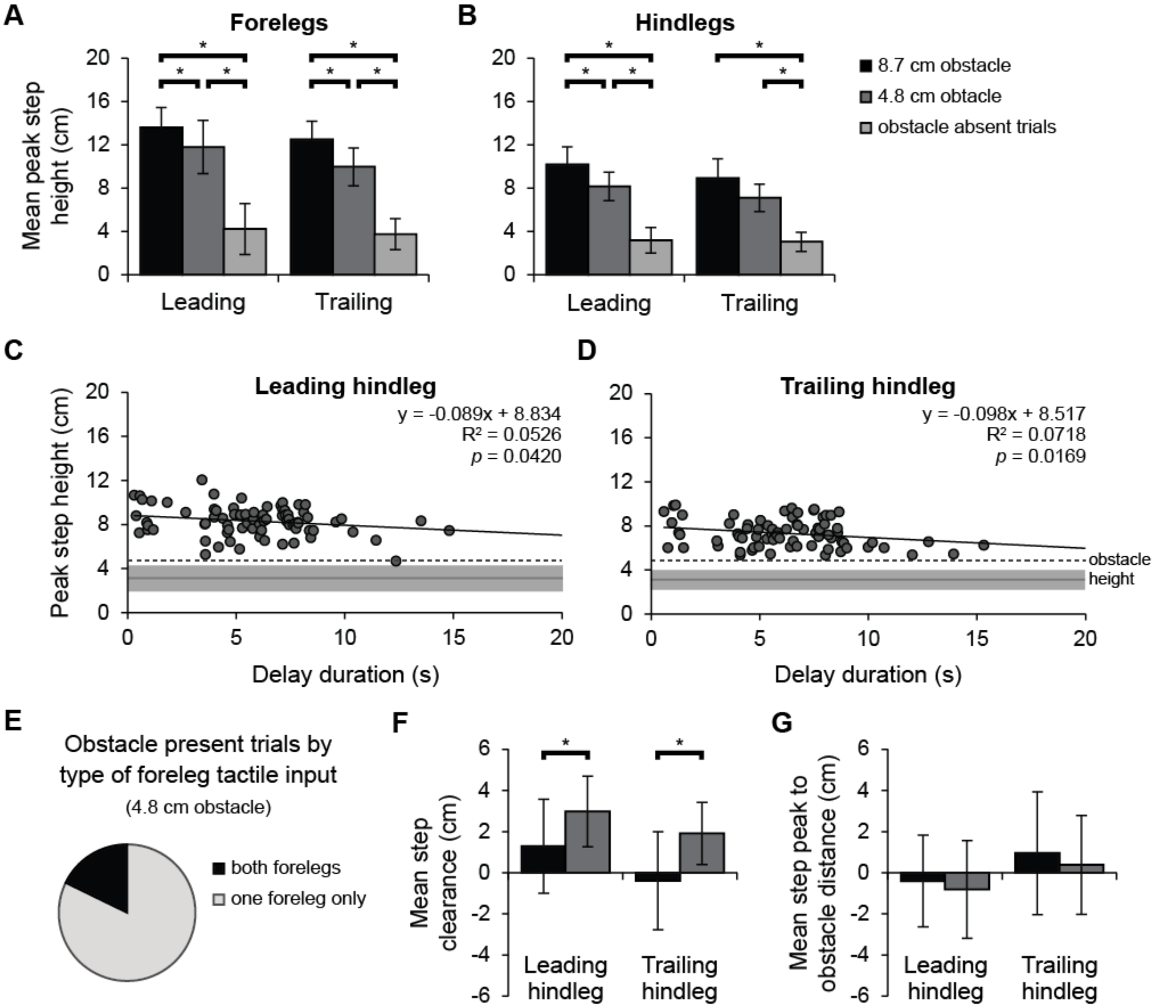
A
Forelegs
Mean peak step height (cm)
20
16
12
8
4
0
Leading
Trailing
*
B
Hindlegs
■ 8.7 cm obstacle
▨ 4.8 cm obtacle
□ obstacle absent trials
C
Leading hindleg
y = -0.089x + 8.834
R^2 = 0.0526
p = 0.0420
Peak step height (cm)
Delay duration (s)
0
5
10
15
20
D
Trailing hindleg
y = -0.098x + 8.517
R^2 = 0.0718
p = 0.0169
obstacle
height
E
Obstacle present trials by type of foreleg tactile input
(4.8 cm obstacle)
■ both forelegs
□ one foreleg only
F
Mean step clearance (cm)
6
4
2
0
-2
-4
-6
Leading hindleg
Trailing hindleg
G
Mean step peak to obstacle distance (cm)

3.4.3 Tactile Input without Foreleg Obstacle Clearance is Insufficient for Memory-guided Stumbling Correction

To assess the role of foreleg movement over a tripped obstacle in establishing memory of that obstacle, a set of “tactile only” trials prevented foreleg obstacle clearance after contacting the obstacle (Fig. 3.5A). Such conditions did not reliably modulate stepping in a similar manner to previously examined obstacle present conditions. A one-way multivariate ANOVA revealed a significant effect of tactile condition (tactile input with foreleg clearance, tactile input without foreleg clearance, or no tactile input) on step height (F(8, 418) = 96.56, $p < 0.0001$). Step height of all four legs was significantly affected by the different tactile conditions (leading foreleg: F(2, 212) = 229.13, $p < 0.0001$; trailing foreleg: F(2, 212) = 475.46, $p < 0.0001$; leading hindleg: F(2, 212) = 193.21, $p < 0.0001$; trailing hindleg: F(2, 212) = 139.05, $p < 0.0001$). In comparison to trials where foreleg clearance followed obstacle contact, mean step height was significantly reduced to 6.6 ± 3.1 cm ($p < 0.0001$; Fig. 3.5B) and 5.2 ± 2.2 cm ($p < 0.0001$) for leading and trailing foreleg steps, respectively, in tactile only trials. Leading and trailing hindleg steps were also significantly reduced to 6.0 ± 2.9 cm ($p < 0.0001$;Fig. 3.5C) and 4.7 ± 2.0 cm ($p < 0.0001$), respectively. However, steps in tactile only trials remained significantly higher than steps in obstacle absent trials ($p < 0.0001$ for both leading and hindleg trailing steps). Stepping in tactile only trials was highly variable, with standard deviations of 3.1 and 2.0 cm for leading and trailing hindleg step heights, respectively. In comparison, standard deviations for leading and trailing hindleg step heights in original obstacle present condition were 1.6 and 1.8 cm, respectively. The highly variable nature of stepping in tactile only trials is further demonstrated in scatter plots of step height over time, where the negative linear correlation between peak step height and delay duration characterized in previous obstacle present conditions is nonexistent (Fig. 3.5D-E). Variation in step height was not dependent on where the forelegs contacted the obstacle (Fig. 3.5F-H). In high (Fig. 3.5F) and low obstacle conditions (Fig. 3.5G), tactile input from the top of the obstacle or well below the full height of the obstacle was sufficient in modulating peak hindleg step height. However, in tactile only trials (Fig. 3.5H), even contacting the top of the obstacle was insufficient in reliably modulating step height for obstacle avoidance. Altogether, poor obstacle memory

Figure 3.5 Tactile input without foreleg obstacle clearance is insufficient for memory-guided stumbling

(A) “Tactile only” trials similarly involved raising an 8.7 cm high obstacle beneath the food platform as an animal ate. The food was carefully moved forwards causing the animal to contact the obstacle with their forelegs. The food was then immediately shifted backwards to prevent the forelegs from stepping over the obstacle, and encourage resumption of stance. As the animal continued eating, the obstacle was lowered becoming flush with the walkway, before moving the food forwards to encourage the animal to resume walking.

(B,C) Bar plots depicting mean peak step height ± SD for leading and trailing foreleg steps (B) and hindleg steps (C) in trials where the forelegs contacted the obstacle and stepped over it (black), obstacle absent trials (gray), and tactile only trials (light gray). Step height differed significantly between all conditions for leading and trailing steps.

(D,E) Scatter plots depicting peak step height versus delay duration for leading (D) and trailing hindleg steps (E) for tactile only trials. Peak step heights were dramatically varied, falling above and well below the height of the obstacle. Unlike trials where foreleg clearance followed obstacle contact, peak step height did not significantly correlate with delay. Dashed horizontal line indicates obstacle height (8.7 cm); gray horizontal line and shaded bar indicates the mean ± SD hindleg step height in obstacle absent trials.

(F–H) Scatter plots depicting peak step height versus the highest point of obstacle contact for obstacle present trials (high obstacle-F, low obstacle-G) and tactile only trials (H). $*P < 0.0001$.

Figure 3.5

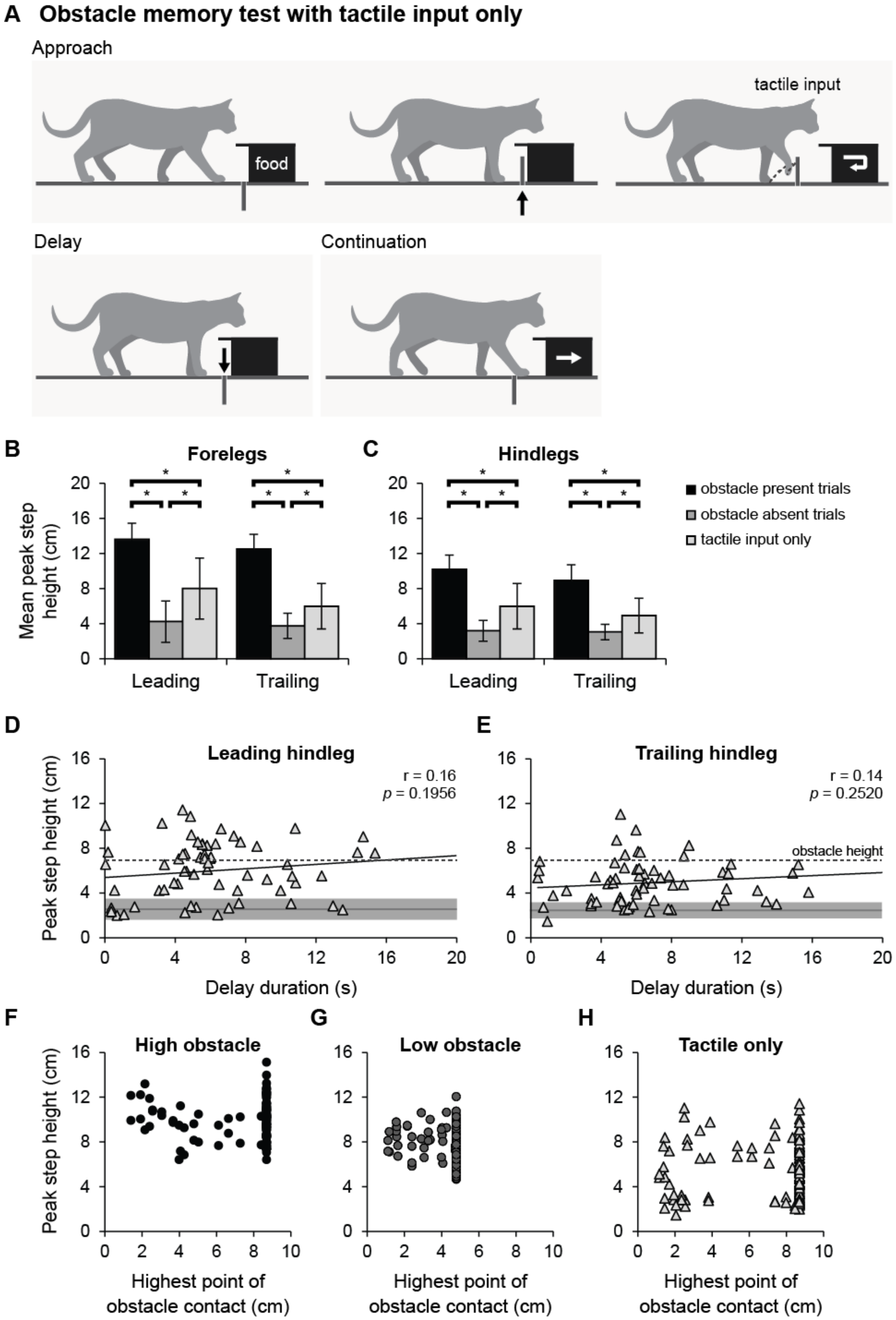
A Obstacle memory test with tactile input only
Approach
food
tactile input
Delay
Continuation
B
Forelegs
C
Hindlegs
*
Mean peak step height (cm)
20
16
12
8
4
0
Leading
Trailing
■ obstacle present trials
■ obstacle absent trials
□ tactile input only
D
Leading hindleg
r = 0.16
p = 0.1956
E
Trailing hindleg
r = 0.14
p = 0.2520
obstacle height
Peak step height (cm)
Delay duration (s)
0
4
8
12
16
20
F
High obstacle
G
Low obstacle
H
Tactile only
Highest point of obstacle contact (cm)
0
2
4
6
8
10

in tactile only trials demonstrates the critical contributions of foreleg clearance following obstacle contact to establishing a robust obstacle memory used to modulate stepping.

3.4.4 Memory-guided Stumbling Correction Depends on Parietal Area 5

The ability to scale step height to obstacle height, and the importance of the forelegs stepping over an obstacle in establishing robust memories have been similarly described in assessments of visually acquired obstacle memory used by walking animals to retain information about an obstacle they observe in their path. Previous lesion work and electrophysiological experiments implicate parietal area 5 in visually obtained obstacle memories used to guide the hindlegs over an obstacle which the forelegs have stepped. To evaluate parietal cortex contributions to memory-guided stumbling correction, cryoloops (Lomber et al. 1999) were implanted bilaterally over parietal area 5, and an adjacent parietal region, area 7, in three cats (Fig. 3.6A). Following cooling loop implantation, all subjects demonstrated intact memory of the obstacle in the absence of cortical cooling (warm control condition; Fig. 3.6B,D, red). However, while foreleg stepping in obstacle present and obstacle absent conditions did not differ with cooling-induced deactivation of area 5 (Fig. 3.6B-C, blue), hindleg stepping was significantly attenuated in obstacle present trials (Fig. 3.6D-E, blue). A two-way ANOVA conducted to examine the effect of the cooling condition (warm, area 5 cooled, or area 7 cooled) and obstacle condition (present or absent) on step height revealed a significant interaction between the two factors (F(8, 882) = 38.16, $p < 0.0001$). Further analysis of step height for each cooling condition for each obstacle condition revealed significant differences in step height for leading foreleg steps (F(5, 444) = 513.23, $p < 0.0001$), trailing foreleg steps (F(5, 444) = 877.40, $p < 0.0001$), leading hindleg steps (F(5, 444) = 355.60, $p < 0.0001$), and trailing hindleg steps (F(5, 444) = 258.64, $p < 0.0001$). In comparison to either the warm or area 7 cooled condition, when area 5 was cooled, mean step height was reduced to 4.3 ± 2.2 cm ($p < 0.0001$) and 3.4 ± 1.4 cm ($p < 0.0001$) for leading and trailing hindleg steps, respectively. Furthermore, unlike stepping in warm trials, peak step height did not demonstrate a linear relationship with delay duration (compare Fig. 3.6-F,I with G,J). If animals were permitted to walk continuously over the obstacle while area 5

Figure 3.6 Memory-guided stumbling correction is dependent on parietal area 5.

(A) Lateral view of the cat cerebrum showing parietal areas 5 and 7 examined in the current study. D – dorsal, A – anterior.

(B–E) Bar plots depicting mean step height ± SD for obstacle present (B,D) and obstacle absent trials (C,E) for the forelegs (B,C) and hindlegs (D,E) for warm (red), area 5 cooled (blue), and area 7 cooled conditions (green). Step height was significantly reduced in both the leading and trailing hindlegs in obstacle present trials when area 5 was deactivated.

(F–K) Scatter plots depicting step height versus delay duration for leading and trailing hindleg steps for each of the 3 cooling conditions. In contrast to the negative linear relationship between step height and time observed in warm (F,I) and area 7 cooled conditions (H,K), the rapid decay in step height with increasing delays when area 5 was deactivated was best modeled with a power function (G,J). For each scatter plot, solid lines represent the linear or power regression line with the equation, coefficient of determination, and corresponding P value shown.

(L) Bar plot depicting mean hindleg step clearance ± SD for each cooling condition. Area 5 deactivation resulted in reduced clearance for both leading and trailing hindleg steps.

(M) Bar plot depicting the mean horizontal distance between the peak of each step and the obstacle for each cooling condition. When area 5 was cooled, step trajectories were more variable and differed significantly from warm and area 7 cooled conditions. (N) Reduction in mean movement time ± SD with area 5 cooling reflects difference in step height shown in obstacle present conditions. Movement times were unaffected by cortical cooling in obstacle absent conditions.

(O) Mean peak velocity ± SD was unaffected by cortical cooling. $^*P < 0.005$, $^{**}P < 0.0001$.

Figure 3.6

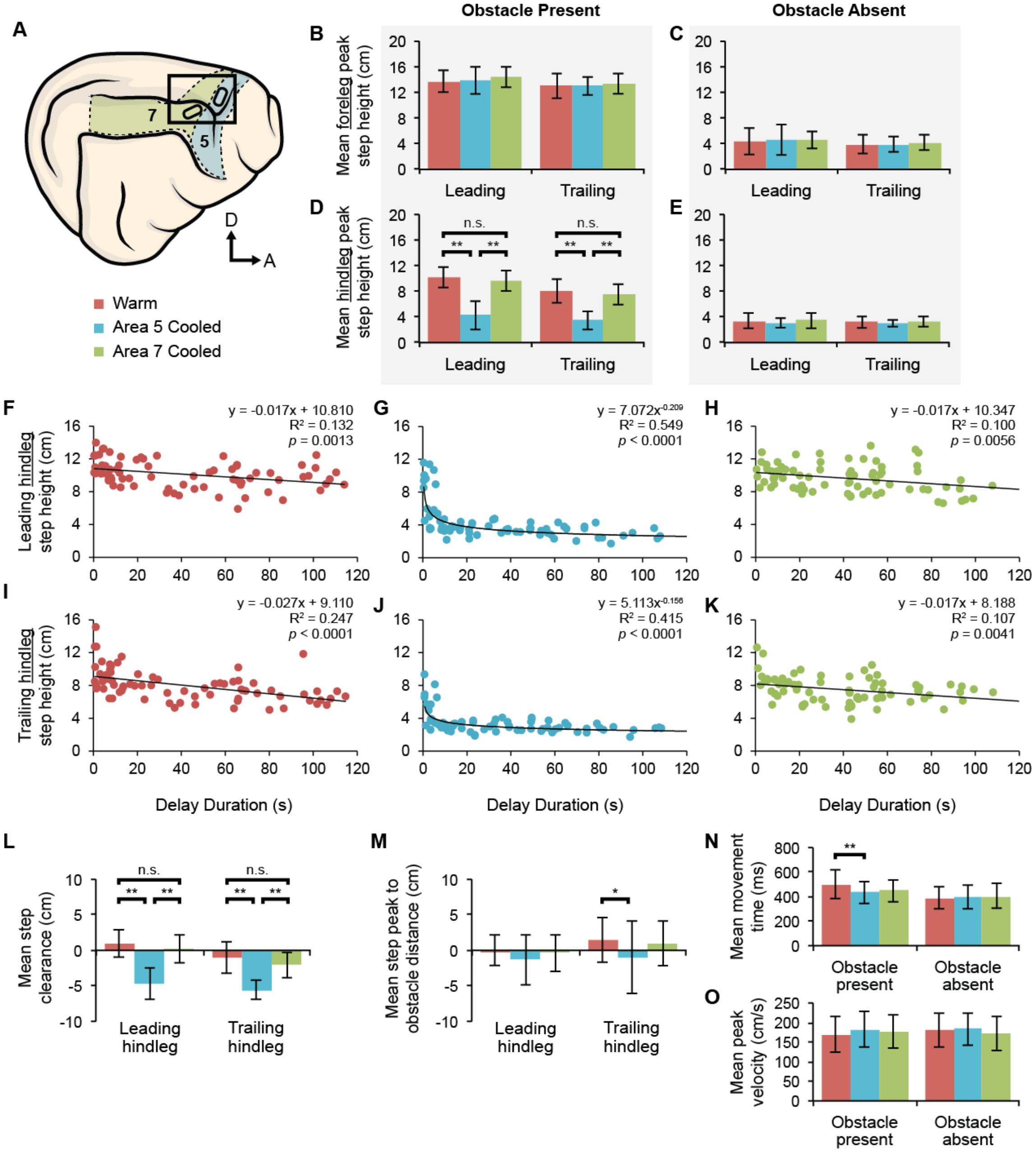
A
7
5
D
A
Warm
Area 5 Cooled
Area 7 Cooled
Obstacle Present
Obstacle Absent
B
C
Mean foreleg peak step height (cm)
20
16
12
8
4
0
Leading
Trailing
D
E
Mean hindleg peak step height (cm)
n.s.
**
**
F
G
H
I
J
K
y = -0.017x + 10.810
R² = 0.132
p = 0.0013
y = 7.072x-0.209
R² = 0.549
p < 0.0001
y = -0.017x + 10.347
R² = 0.100
p = 0.0056
y = -0.027x + 9.110
R² = 0.247
p < 0.0001
y = 5.113x-0.156
R² = 0.415
p < 0.0001
y = -0.017x + 8.188
R² = 0.107
p = 0.0041
Leading hindleg step height (cm)
Trailing hindleg step height (cm)
0
20
40
60
80
100
120
Delay Duration (s)
L
Mean step clearance (cm)
10
5
0
-5
-10
Leading hindleg
Trailing hindleg
M
Mean step peak to obstacle distance (cm)
*
N
Mean movement time (ms)
800
600
400
200
0
Obstacle present
Obstacle absent
O
Mean peak velocity (cm/s)
250
200
150
100
50
0

was deactivated, stepping above or around the height of the obstacle, particularly in leading hindleg steps, indicated intact memory-guided obstacle locomotion. However, hindleg step height decayed rapidly with increasing delays. This relationship was best modeled with a power function for both leading ($R^2(1, 73) = 0.549$, $p < 0.0001$; Fig. 3.6G) and trailing hindleg step heights ($R^2(1, 73) = 0.451$, $p < 0.0001$; Fig. 3.6J). Similarly, there was also an effect of cooling condition on step clearance for both leading ($F(2, 222) = 170.81$, $p < 0.0001$) and trailing hindleg steps ($F(2, 222) = 126.05$, $p < 0.0001$). In comparison to either warm or area 7 cooled conditions, area 5 deactivation significantly reduced leading and trailing step clearances to -4.7 ± 2.2 cm ($p < 0.0001$; Fig. 3.6L) and -5.6 ± 1.4 cm ($p < 0.0001$), respectively. Additionally, there was also a significant effect of cooling condition on the step peak to obstacle distance for trailing hindleg steps ($F(2, 222) = 7.85$, $p < 0.0001$). Deactivation of area 5 significantly altered step trajectory in relation to the obstacle, as trailing steps tended to peak before the obstacle in comparison to stepping in the warm condition ($p = 0.001$; Fig. 3.6M). In contrast, memory-guided stumbling correction appeared unaffected when area 7 was deactivated (Fig. 3.6, green). Mean step height, the linear relationship between step height and delay duration, step clearance, and the distance between step peak and the obstacle did not differ between area 7 cooled trials and warm trials. Cortical cooling of neither area 5 nor area 7 affected movement times in obstacle absent conditions (Fig. 3.6N), or peak step velocity in either obstacle present or obstacle absent trials (Fig. 3.6O). Reduction in mean movement time with area 5 cooling reflects attenuated step height in obstacle present conditions (Fig. 3.6N). Thus any observed alterations in hindlimb locomotion were not a result of impaired motor capabilities. Therefore, deactivation of area 5, but not an adjacent region within area 7, resulted in impaired memory of an obstacle over which the forelegs have tripped.

3.5 Discussion

These results demonstrate the ability of walking cats to adapt stepping following an unexpected trip over an unseen obstacle to ensure avoidance. In the absence of any cortical deactivations, tactile input to just one foreleg could modify stepping of all four limbs, even when hindleg clearance was interrupted for delays tested up to 120 s. Such memory-guided behavior reflected properties of the obstacle encountered, and is particularly robust when the forelegs not only contact the obstacle, but subsequently step over it. However, deactivation of area 5 resulted in altered hindleg stepping, indicating that animals no longer remembered the obstacle over which they had tripped. Altogether, these results demonstrate the contributions of parietal area 5 to memory-guided stumbling correction.

3.5.1 Memory-Guided Locomotion in the Cat

While previous work characterized mechanical and electrical consequences to stumbling within a single leg following tactile or electrical stimulation to the same leg (Forssberg 1979; Drew and Rossignol 1987; McVea and Pearson 2007a), obstacle avoidance in naturalistic settings must be a coordinated response involving all moving limbs. The present work demonstrates the capacity for brief, but salient tactile inputs to just one foreleg to influence stepping of all four legs. Typically, interlimb coordination is thought to be mediated by long ascending propriospinal neurons in the lumbar spinal cord whose axons terminate in cervical regions (English et al. 1985). These neurons produce a caudorostral excitability gradient that couples foreleg rhythmic generators in the cervical cord to hindleg rhythmic generators in the lumbar region (Juvin et al. 2005). However, the present study demonstrates the ability of altered forelimb stepping to modify subsequent hindlimb movements. Thus there must be complementary descending influences within the spinal cord that permit rapid hindlimb movement modulation following forelimb modulation during continuous locomotion following a sudden trip.

Since animals examined in the present study were previously familiarized with the obstacle in a separate study of visually-guided obstacle locomotion, it is possible that tactile contact invoked a visually-acquired memory of obstacle height retained from other testing, which could be used to guide movements for avoidance. While possible, previously acquired visual information is unlikely to be the only source of sensory information guiding movements. In some trials, despite the paw contacting the obstacle near its base, the evoked hyperflexion and resulting trajectory was insufficient in clearing the obstacle, resulting in the paw or leg contacting the top edge of the obstacle. This suggests that the initial paw contact was insufficient in invoking visually-acquired information about obstacle height, or that such information was insufficient in modifying foreleg stepping for successful clearance. Additional corrective movements resulting in additional tactile inputs from the obstacle demonstrate the use of tactile information acquired on a trial to trial basis. Furthermore, observations of cats that were not trained for the current study as they explored cluttered laboratory settings demonstrated appropriate step modifications for obstacle avoidance when the foreleg unexpectedly encountered an object. Altogether, these trials and observations demonstrate the ability of animals to use tactile information acquired about an unfamiliar obstacle upon stumbling to modify stepping for avoidance, independent of any previously attained information about the obstacle.

Overall, the observed attributes of memory-guided stumbling correction are similar to a visually obtained obstacle memory previously described in walking cats. If an animal is paused after the forelegs, but not the hindlegs, have stepped over an obstacle visibly in its path, memory of the obstacle is used to coordinate hindleg stepping when walking is resumed (McVea and Pearson 2006; Whishaw et al. 2009). Similar to our tactile only trials, this “visual” obstacle memory is particularly robust when the forelegs step over the observed obstacle (McVea and Pearson 2007c), suggesting that both “tactile” and “visual” obstacle memory may rely on efference motor commands of foreleg movements, or proprioceptive feedback from the forelegs for establishing long-lasting representations of an obstacle. Furthermore, step height was significantly reduced in both the forelegs and hindlegs in tactile only trials, which was similarly reported in previous “visual only” conditions. Thus despite sensing the presence of an obstacle via vision or touch, animals are likely to forget about the obstacle after even a short delay if they have not yet physically engaged with it. Projections from primary motor cortex to parietal cortex (Yumiya and Ghez 1984; Kang et al. 1986) may convey efference motor information regarding foreleg stepping, which could be integrated with sensory information about an obstacle (Beloozerova and Sirota 2003) from somatosensory or visual areas (Avendaño et al. 1988), and proprioceptive feedback from foreleg joint receptors via somatosensory cortical areas (Mackie et al. 1996) to produce a long-lasting memory.

Another similarity between tactilely and visually obtained obstacle memories is the ability to retain specific properties of an obstacle. Specifically, the ability to scale stepping appropriately after bumping into obstacles of different heights is also evident after seeing objects of different heights. For example, when an obstacle was placed in the path of a walking cat, the average height of hindleg steps over the obstacle was appropriately lower when a 3 cm high obstacle was used, in comparison to a 7 cm high obstacle (McVea and Pearson 2006). Similarly, in humans, trailing leg steps scaled appropriately when stepping over obstacles of different heights, even when trailing leg steps were delayed following leading leg steps for delays examined up to 2 minutes (Lajoie et al. 2012). This reflection of obstacle properties in visually or tactilely obtained memory indicates that modulated hindleg stepping is not merely a coarsely preprogrammed avoidance response. Instead, pertinent obstacle properties, like height and location, obtained via the somatosensory or visual modality, are held in memory when locomotion is delayed or interrupted and used to coordinate future actions. Additional differences in step clearance and the proportion of obstacle present trials based on foreleg tactile input further demonstrate distinctions between memory-guided stumbling correction over a high or low obstacle. In general, after tripping over the lower obstacle, adapting stepping successfully for avoidance appears more efficient, with a greater proportion of trials where obstacle contact with only one foreleg was sufficient in modulating stepping. In contrast, contacting the higher obstacle with one foreleg did not prevent the other foreleg from tripping over the obstacle in more than half of trials examined. This may reflect a default response following tactile input to one foreleg to lift the uncontacted foreleg a certain height in attempt for avoidance. In low obstacle trials, this default height is sufficient in clearing the obstacle. However, in high obstacle trials, this default height is insufficient in clearing the obstacle and inevitably results in contact of the trailing foreleg with the obstacle before it is lifted above and over the obstacle. This additional tactile input and subsequent motor correction may provide or reinforce information about obstacle height via sensory and efference motor pathways discussed previously.

In contrast to studies of memory-guided action in humans and non-human primates that typically assess retention following a few seconds, the observed obstacle memory retention following delays tested up to 2 minutes highlights the durability of this memory system in the cat. However, it is notable that hindleg steps frequently undershoot the obstacle, particularly for the trailing hindleg in high obstacle trials, and especially following longer memory delays. In humans, memory-guided obstacle avoidance has also been described to be worse in the trailing leg than in the leading leg (Heijnen et al. 2014). While these observations indicate poor memory underlying unsuccessful hindlimb avoidance, this attenuated movement accuracy is a common observation of memory-guided actions studied in many species. In comparison to visually-guided reaching, reduced target overshooting and increased endpoint variability observed with memory-guided reaching (Westwood et al. 2003) are thought to reflect less accurate target representations maintained in the ventral visual stream for memory-guided actions (Goodale and Milner 1992; Goodale et al. 2004). Importantly, while step height was attenuated with increasing delays, stepping was still significantly higher than stepping in obstacle absent trials, demonstrating the persisting, albeit gradually decaying nature of obstacle memory.

3.5.2 Parietal Cortex Cooling Results in Memory, Not Motor Deficits

In cluttered environments, supraspinal structures, such as the parietal and motor cortices, modulate basic locomotor patterns to adapt stepping (Armstrong 1988; Jahn et al. 2008). While cortical contributions to walking have previously been evaluated in visually-dependent memory-guided obstacle avoidance paradigms, this is the first study to demonstrate supraspinal involvement to memory-guided stumbling correction. The present work clearly implicates parietal area 5 for memory-guided stumbling correction, and suggests a greater role when hindleg obstacle clearance is substantially delayed. As the stumbling corrective reaction was initially described in chronic spinal cats (Forssberg et al. 1975), the neural circuitry for this short latency reflexive response primarily resides within spinal networks. Thus preserved memory-guided hindleg stepping when locomotion was continuous was an expected outcome, and demonstrates the ability of an animal to negotiate obstacles independent of parietal cortex contributions for uninterrupted walking. However, if a memory demand is introduced by delaying locomotion after foreleg clearance, such as in the case of an animal walking slowly through brush and trees while stalking prey, area 5 becomes necessary for successful avoidance once walking is resumed.

Importantly, deactivation of area 5 does not have any direct effects on motor capabilities. Foreleg stepping was unaffected by cortical cooling, and the animals examined were able to produce high hindleg steps around or above the height of the obstacle when locomotion was uninterrupted. Following longer delays, area 5 deactivation reduced step height without any evidence of paw dragging, inability to lift the feet, or changes in peak step velocity. Thus altered hindleg stepping was not due to motor impairment, but instead reflects the role of area 5 in obstacle memory. Such deficits in obstacle memory following deactivations to the hindleg region of area 5 provide an example of a specific memory localized to a discrete region of cortex.

As previous lesion and electrophysiological work have demonstrated that area 5 is likewise involved in visually obtained obstacle memory, area 5 appears to contribute to obstacle memory regardless of input sensory modality. Thus area 5 may lie further along the transformative process required to convert relevant sensory information, obtained via vision or touch, to motor commands for appropriate action (Buneo and Andersen 2006). Consequently, while area 5 is often referred to as retaining sensory information about the environment, its neural activity may be better related to motor planning. Electrophysiological recordings revealing modulated area 5 neural activity persisting despite visual occlusion of an obstacle (Lajoie et al. 2010; Marigold and Drew 2011) and often into the beginning of gait modifications for obstacle avoidance (Lajoie et al. 2010) implicate area 5 in motor planning rather than sensory perception. While the methods used for the present study do not directly dissociate the sensory versus motor nature of area 5 contributions to memory-guided stumbling correction, similarities between area 5 involvement in visual and tactile forms of obstacle memory support the notion that area 5 is important for planning movements based on sensory information. Given the repetitive nature of experimental testing, it is possible that upon reencountering a familiar obstacle, a previously successful motor plan of elevated stepping is invoked for obstacle avoidance. However, whether area 5 neural activity described in memory-guided obstacle locomotion represents such invoked motor plans rather than sensory characteristics of the obstacle remains to be demonstrated. Future work directly examining the nature of area 5 contributions to memory-guided stumbling correction may provide further insights into the sensory versus motor debate.

3.6 References

Andersson O, Forssberg H, Grillner S, Lindquist M. 1978. Phasic gain control of the transmission in cutaneous reflex pathways to motoneurones during “fictive” locomotion. Brain Res. 149:503–507.

Andujar J-E, Drew T. 2007. Organization of the projections from the posterior parietal cortex to the rostral and caudal regions of the motor cortex of the cat. J Comp Neurol. 504:17–41.

Andujar J-E, Lajoie K, Drew T. 2010. A contribution of area 5 of the posterior parietal cortex to the planning of visually guided locomotion: limb-specific and limb-independent effects. J Neurophysiol. 103:986–1006.

Armstrong DM. 1988. The supraspinal control of mammalian locomotion. J Physiol. 405:1–37.

Avendaño C, Rausell E, Perez-Aguilar D, Isorna S. 1988. Organization of the association cortical afferent connections of area 5: a retrograde tracer study in the cat. J Comp Neurol. 278:1–33.

Beloozerova IN, Sirota MG. 2003. Integration of motor and visual information in the parietal area 5 during locomotion. J Neurophysiol. 90:961–971.

Buford JA, Smith JL. 1993. Adaptive control for backward quadrupedal walking. III. Stumbling corrective reactions and cutaneous reflex sensitivity. J Neurophysiol. 70:1102–1114.

Buneo CA, Andersen RA. 2006. The posterior parietal cortex: sensorimotor interface for the planning and online control of visually guided movements. Neuropsychologia.

44:2594–2606.

Curtis CE, D'Esposito M. 2003. Persistent activity in the prefrontal cortex during working memory. Trends Cogn Sci. 7:415–423.

Drew T, Marigold DS. 2015. Taking the next step: cortical contributions to the control of locomotion. Curr Opin Neurobiol. 33:25–33.

Drew T, Rossignol S. 1987. A kinematic and electromyographic study of cutaneous reflexes evoked from the forelimb of unrestrained walking cats. J Neurophysiol. 57:1160–1184.

Eng JJ, Winter DA, Patla AE. 1994. Strategies for recovery from a trip in early and late swing during human walking. Exp Brain Res. 102:339–349.

English AW, Tigges J, Lennard PR. 1985. Anatomical organization of long ascending propriospinal neurons in the cat spinal cord. J Comp Neurol. 240:349–358.

Forssberg H. 1979. Stumbling corrective reaction: a phase-dependent compensatory reaction during locomotion. J Neurophysiol. 42:936–953.

Forssberg H, Grillner S, Rossignol S. 1975. Phase dependent reflex reversal during walking in chronic spinal cats. Brain Res. 85:103–107.

Forssberg H, Grillner S, Rossignol S. 1977. Phasic gain control of relexes from the dorsum of the paw during spinal locomotion. Brain Res. 132:121–139.

Goodale MA, Milner AD. 1992. Separate visual pathways for perception and action. Trends Neurosci. 15:20–25.

Goodale MA, Westwood DA, Milner AD. 2004. Two distinct modes of control for object-directed action. Prog Brain Res. 144:131–144.

Heijnen MJH, Romine NL, Stumpf DM, Rietdyk S. 2014. Memory-guided obstacle crossing: More failures were observed for the trail limb versus lead limb. Exp Brain Res. 232:2131–2142.

Jahn K, Deutschländer A, Stephan T, Kalla R, Hüfner K, Wagner J, Strupp M, Brandt T. 2008. Supraspinal locomotor control in quadrupeds and humans. Prog Brain Res. 171:353–362.

Juvin L, Simmers J, Morin D. 2005. Propriospinal circuitry underlying interlimb coordination in mammalian quadrupedal locomotion. J Neurosci. 25:6025–6035.

Kang Y, Endo K, Araki T, Mitani A. 1986. Dual mode of projections from the parietal to the motor cortex in the cat. Exp Brain Res. 62:281–292.

Kiehn O. 2016. Decoding the organization of spinal circuits that control locomotion. Nat Rev Neurosci. 17:224–238.

Lajoie K, Andujar J-E, Pearson KG, Drew T. 2010. Neurons in area 5 of the posterior parietal cortex in the cat contribute to interlimb coordination during visually guided locomotion: a role in working memory. J Neurophysiol. 103:2234–2254.

Lajoie K, Bloomfield LW, Nelson FJ, Suh JJ, Marigold DS. 2012. The contribution of vision, proprioception, and efference copy in storing a neural representation for guiding trail leg trajectory over an obstacle. J Neurophysiol. 107:2283–2293.

Lam T, Wolstenholme C, van der Linden M, Pang MYC, Yang JF. 2003. Stumbling corrective responses during treadmill-elicited stepping in human infants. J Physiol. 553:319–331.

Lomber SG, Malhotra S. 2008. Double dissociation of “what” and “where” processing in auditory cortex. Nat Neurosci. 11:609–616.

Lomber SG, Meredith MA, Kral A. 2010. Cross-modal plasticity in specific auditory cortices underlies visual compensations in the deaf. Nat Neurosci. 13:1421–1427.

Lomber SG, Payne BR. 2000a. Contributions of cat posterior parietal cortex to visuospatial discrimination. Vis Neurosci. 17:701–709.

Lomber SG, Payne BR. 2000b. Translaminar differentiation of visually guided behaviors revealed by restricted cerebral cooling deactivation. Cereb Cortex. 10:1066–1077.

Lomber SG, Payne BR, Horel JA. 1999. The cryoloop: An adaptable reversible cooling deactivation method for behavioral or electrophysiological assessment of neural function. J Neurosci Methods. 86:179–194.

Mackie PD, Zhang HQ, Schmidt RF, Rowe MJ. 1996. Parallel organization of proprioceptive inputs from joint receptors to cortical somatosensory areas I and II in the cat. J Physiol. 494 (Pt 2:529–537.

Marigold DS, Andujar J-E, Lajoie K, Drew T. 2011. Motor planning of locomotor adaptations on the basis of vision: the role of the posterior parietal cortex. Prog Brain Res. 188:83–100.

Marigold DS, Drew T. 2011. Contribution of cells in the posterior parietal cortex to the planning of visually guided locomotion in the cat: effects of temporary visual interruption. J Neurophysiol. 105:2457–2470.

McVea DA, Pearson KG. 2006. Long-lasting memories of obstacles guide leg movements in the walking cat. J Neurosci. 26:1175–1178.

McVea DA, Pearson KG. 2007a. Long-lasting, context-dependent modification of stepping in the cat after repeated stumbling-corrective responses. J Neurophysiol. 97:659–669.

McVea DA, Pearson KG. 2007b. Contextual learning and obstacle memory in the walking cat. Integr Comp Biol. 47:457–464.

McVea DA, Pearson KG. 2007c. Stepping of the forelegs over obstacles establishes long-lasting memories in cats. Curr Biol. 17:R621–R623.

McVea DA, Taylor AJ, Pearson KG. 2009. Long-lasting working memories of obstacles established by foreleg stepping in walking cats require area 5 of the posterior parietal cortex. J Neurosci. 29:9396–9404.

Miller S, Ruit JB, Van der Meché FG. 1977. Reversal of sign of long spinal reflexes dependent on the phase of the step cycle in the high decerebrate cat. Brain Res. 128:447–459.

Prochazka A, Sontag KH, Wand P. 1978. Motor reactions to perturbations of gait: proprioceptive and somesthetic involvement. Neurosci Lett. 7:35–39.

Schillings AM, van Wezel BM, Mulder T, Duysens J. 2000. Muscular responses and movement strategies during stumbling over obstacles. J Neurophysiol. 83:2093–2102.

Takakusaki K. 2013. Neurophysiology of gait: From the spinal cord to the frontal lobe. Mov Disord. 28:1483–1491.

van der Gucht E, Vandesande F, Arckens L. 2001. Neurofilament protein: A selective marker for the architectonic parcellation of the visual cortex in adult cat brain. J Comp Neurol. 441:345–368.

Van Wezel BM, Ottenhoff FA, Duysens J. 1997. Dynamic control of location-specific information in tactile cutaneous reflexes from the foot during human walking. J Neurosci. 17:3804–3814.

Wand P, Prochazka A, Sontag KH. 1980. Neuromuscular responses to gait perturbations in freely moving cats. Exp Brain Res. 38:109–114.

Westwood DA, Heath M, Roy EA. 2003. No evidence for accurate visuomotor memory: systematic and variable error in memory-guided reaching. J Mot Behav. 35:127–133.

Whishaw IQ, Sacrey LAR, Gorny B. 2009. Hind limb stepping over obstacles in the horse guided by place-object memory. Behav Brain Res. 198:372–379.

Wong C, Pearson KG, Lomber SG. 2015. Dissociation of parietal cortex contributions to obstacle memory in walking cats. Program No. 341.11. In: 2015 Neuroscience Meeting Planner. Chicago, IL: Society for Neuroscience. Online.

Yumiya H, Ghez C. 1984. Specialized subregions in the cat motor cortex: anatomical demonstration of differential projections to rostral and caudal sectors. Exp Brain Res. 53:259–276.

Zehr EP, Komiyama T, Stein RB. 1997. Cutaneous reflexes during human gait: electromyographic and kinematic responses to electrical stimulation. J Neurophysiol. 77:3311–3325.

Zehr EP, Stein RB, Komiyama T. 1998. Function of sural nerve reflexes during human walking. J Physiol. 507:305–314.

Chapter 4

4 Contributions of parietal cortex to the working memory of an obstacle acquired visually or tactilely in the locomoting cat[3]

4.1 Abstract

A working memory of obstacles is essential for navigating complex, cluttered terrain. In quadrupeds, it has been proposed that parietal cortical areas related to movement planning and working memory may be important for guiding the hindlegs over an obstacle previously cleared by the forelegs. To test this hypothesis, parietal areas 5 and 7 were reversibly deactivated in walking cats. The working memory of an obstacle was assessed in both a visually-dependent and tactilely-dependent paradigm. Reversible bilateral deactivation of area 5, but not area 7, altered hindleg stepping in a manner indicating that the animals did not recall the obstacle over which their forelegs had stepped. Similar deficits were observed when area 5 deactivation was restricted to the delay during which obstacle memory must be maintained. Furthermore, partial memory recovery observed when area 5 function was deactivated and restored within this maintenance period suggests that the deactivation may suppress, but not eliminate, the working memory of an obstacle. As area 5 deactivations incurred similar memory deficits in both visual and tactile obstacle working memory paradigms, parietal area 5 is critical for maintaining the working memory of an obstacle acquired via vision or touch that is used to modify stepping for avoidance.

---

[3] A version of this chapter is published as:

Wong C, Pearson KG, Lomber SG (2017). Contributions of parietal cortex to the working memory of an obstacle acquired visually or tactilely in the locomoting cat. Cerebral Cortex doi: 10.1093/cercor/bhx186

4.2 Introduction

Neural mechanisms for walking must maintain equilibrium of the moving animal while adapting gait for the environment and the current goals of the animal (Forssberg et al. 1980; Takakusaki 2013; Drew and Marigold 2015). While spinal locomotor networks can generate rhythmic activity in motor neurons for basic gait on a level surface (Grillner 2011; Takakusaki 2013), uneven or cluttered terrain engages supraspinal structures related to motor planning and working memory (Drew et al. 2008; Drew and Marigold 2015). In particular, a working memory of environmental obstacles is essential for navigation in walking mammals. As humans, this memory system affords us the ability to walk through a complex or cluttered setting without looking directly at our feet as we step around or over obstacles (Patla and Vickers 1997; Mohagheghi et al. 2004). In quadrupeds, this memory system is especially important for guiding hindleg stepping. As an obstacle previously cleared by the forelegs is no longer directly visible to the animal once it has passed under the body, a working memory of the obstacle is used to modify subsequent hindleg steps (Wilkinson and Sherk 2005; McVea and Pearson 2006, 2007a; McVea et al. 2009; Whishaw et al. 2009).

Furthermore, such step modulations can also occur without any visual input of an obstacle. A sudden stumble over an unexpected obstacle evokes the stumbling corrective reaction (Forssberg 1979), resulting in limb hyperflexion to lift the leg over an impeding obstacle. Recently, such tactilely acquired working memory of an obstacle was demonstrated to be able to persist for many minutes, and could be used to coordinate appropriate hindleg stepping if forward locomotion was delayed after foreleg clearance (Wong et al. 2018). Moreover, cooling-induced deactivation of parietal area 5 resulted in altered hindleg stepping indicative of a forgotten obstacle. As inactivation of area 5 via lesions results in similar deficits in the working memory of an obstacle acquired visually (McVea et al. 2009), area 5 appears to be important for the working memory of an obstacle, regardless of the sensory modality through which obstacle information is obtained.

Working memory involves the acquisition and maintenance of relevant sensory stimuli used to guide future behaviours (Jonides et al. 2008). Previous electrophysiological recordings in walking cats revealed a population of cells in area 5 that discharge strongly as an obstacle passes beneath the body (Lajoie et al. 2010). If forward progress of the cat is delayed, this increased neural activity is sustained as long as the cat remains straddling the obstacle between its fore- and hindlegs. Such sustained activity during delayed response tasks is regarded as representing the maintenance of relevant sensory stimuli in memory (Fuster and Alexander 1971; Eriksson et al. 2015). Thus area 5 is hypothesized to contribute specifically to maintaining the working memory of an obstacle, although its causal role in working memory maintenance remains to be demonstrated. Furthermore, area 5 contributions to working memory acquisition have yet to be evaluated. While aforementioned studies employing lesions to elucidate area 5 function can only demonstrate overall contributions to working memory-guided obstacle locomotion, transient, temporally controlled cortical deactivations achieved with cooling can be used to dissociate the role of area 5 in working memory acquisition versus maintenance.

In the present study, the working memory of an obstacle previously cleared by the forelegs was examined in walking cats. To assess the role of area 5 in the acquisition and maintenance of the working memory of an obstacle, cooling loops were placed bilaterally over parietal area 5 in three cats. Additionally, control cooling loops were placed bilaterally over an adjacent region of parietal area 7 to ensure that any observed changes in gait following area 5 deactivation were due to the specific cooling of area 5 and not a result of cooling in general. Obstacle working memory was assessed while individually deactivating area 5 or 7. By varying the duration that hindleg obstacle clearance was delayed, parietal cortex contributions to obstacle working memory were assessed in a delay-dependent manner. Additionally, both bilateral and unilateral parietal cortex deactivations were performed in the same animals to assess possible laterality of the working memory system. Finally, by varying the onset and offset of cooling, parietal areas were deactivated throughout memory testing or during specific phases to assess their contributions to obstacle working memory acquisition versus maintenance. Parietal cortex contributions were assessed in both a visually-dependent obstacle working memory test adapted from McVea et al. (2009) and a tactile (visually-independent) test designed to evoke the stumbling corrective reaction (Wong et al. 2018). Altogether, these experiments revealed the critical role of parietal area 5 in maintaining the working memory of an obstacle obtained with or without vision, used to ensure proper obstacle negotiation.

4.3 Materials and Methods

4.3.1 Overview

Parietal cortex contributions to obstacle working memory were examined in three adult (>6M) female domestic cats obtained from a commercial breeding facility (Liberty Labs, NY). All animals were housed in an enriched colony environment. Food intake was regulated during testing days such that moist food was provided during each testing session. Additionally, animals were offered dry food for 1 hour at the end of each day. Water was provided ad libitum. Each animal received bilateral cryoloops over parietal areas 5 and 7. Each area was bilaterally cooled during both visually-dependent and tactilely-dependent obstacle working memory testing paradigms. When behavioural testing was completed, cryoloops were exposed on the surface of the brain and a thermal imaging camera was used to visualize the extent of cortical deactivation. Animals were then perfused and the brains were fixed and removed from the cranium. Brains were then frozen, coronally sectioned, and processed for Nissl, cytochrome oxidase, and SMI-32. Reconstructions of deactivation loci were compared with areal boundaries revealed with SMI-32 to confirm accurate cryoloop placement. All animals were previously examined in a study of memory-guided stumbling correction (Wong et al. 2018). All trials included in the present study are distinct from trials examined in the previous study. All procedures were conducted in compliance with the National Research Council’s *Guide for the Care and Use of Laboratory Animals* (8th edition; 2011) and the Canadian Council on Animal Care’s *Guide to the Care and Use of Experimental Animals* (1993), and were approved by the University of Western Ontario Animal Use Subcommittee of the University Council on Animal Care.

4.3.2 Apparatus

The same apparatus described in Wong et al. (2016, 2017) was used to assess visual and tactile obstacle working memory in the present study. Each cat was trained to walk along an 8-foot long runway. Halfway along the apparatus, an 8.7 cm high obstacle could be raised onto or lowered from the surface using a lever mounted underneath the runway. An ethernet camera mounted on a tripod recorded all trials at 54 frames per second using Contemplas (Kempten, GER) motion detection software.

4.3.3 Obstacle memory testing

To examine visually-dependent obstacle working memory, each animal was trained to walk along a runway towards an obstacle (Fig. 4.1A). Food was placed on an elevated platform on the far side of the obstacle to encourage the animal to step over the obstacle with their forelegs only. Animals were allowed to eat from the platform for delays ranging from less than a second to two minutes. Delays were varied in order to assess any possible delay-dependent effects of obstacle working memory. During this delay, the obstacle was covertly lowered, becoming flush with the walkway, to prevent further visual or tactile inputs. The food was then moved forward to encourage the animal to resume walking and hindlegs steps were observed. Such trials comprised the visual obstacle present condition. Additionally, an equivalent number of trials where the animal approached the food platform on the far side of the lowered obstacle comprised the visual obstacle absent condition. In these control trials, forward progress was similarly delayed for up to two minutes as the animal ate. Stepping in these visual obstacle absent trials was examined to ensure that animals did not develop a learned obstacle avoidance strategy of sustained overstepping regardless of whether the obstacle was present or absent. In both visual obstacle present and obstacle absent conditions, there was never any tactile contact between the cat and the obstacle. The tactile-dependent obstacle working memory paradigm was identical to previously described procedures (Wong et al. 2018). Briefly, each animal approached the food platform in the absence of any obstacle (Fig. 4.1B). As the animal ate, the obstacle was covertly raised onto the walkway directly below the food dish to prevent any visual input of the obstacle. The food was moved to encourage the animal to continue walking forwards, causing the front legs to contact the obstacle before stepping over it. The animal’s interest in food was sufficient in maintaining the gaze forwards, preventing any visual input of the obstacle during the trial. As the animal continued to eat, the obstacle was covertly removed from the walkway, before forward locomotion was again resumed. Such trials comprised the tactile obstacle present

Figure 4.1 Visually-dependent and tactilely-dependent testing paradigms used to assess obstacle working memory.

(A) Schematic depicting the visual obstacle working memory test where each animal would see and step over an 8.7 cm high obstacle with their forelegs to reach food placed on an elevated platform. As the animal ate, the obstacle was covertly lowered becoming flush with the walkway. Following a variable delay period, the food was moved forwards to encourage the animal to resume walking. Hindleg stepping was measured to assess working memory of the obstacle. Horizontal blue and red bars (i-iv) represent variations in cooling onset (blue) and offset (red) used to examine overall parietal cortex contributions to the working memory task as a whole (i), or to distinct phases of working memory acquisition (ii) and working memory maintenance (iii-iv).

(B) Schematic depicting the tactile obstacle working memory test where each animal would approach the food platform in the absence of the obstacle. As the animal ate, it could not see that the obstacle was covertly raised beneath the food platform. By moving the food forward, the forelegs would contact the obstacle before stepping over it. During the subsequent delay period, the obstacle was lowered becoming flush with the walkway. As in the visual obstacle working memory paradigm, hindleg stepping when walking resumed was examined to assess obstacle working memory. Horizontal blue and red bars (i-iii) represent variations in cooling onset (blue) and offset (red) used to examine overall parietal cortex contributions to the working memory task as a whole (i), or to distinct phases of working memory acquisition (ii) and working memory maintenance (iii).

Figure 4.1

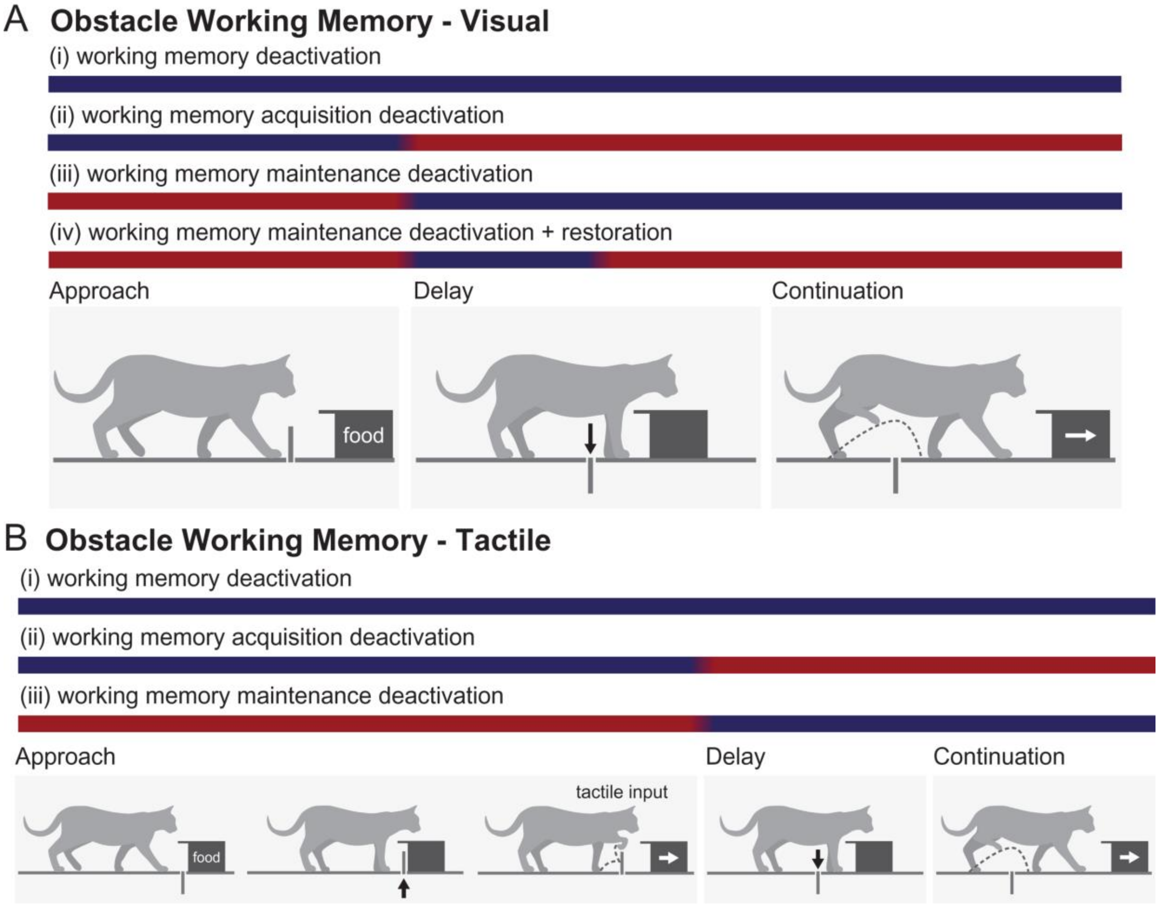
A Obstacle Working Memory - Visual
(i) working memory deactivation
(ii) working memory acquisition deactivation
(iii) working memory maintenance deactivation
(iv) working memory maintenance deactivation + restoration
Approach
Delay
Continuation
food
B Obstacle Working Memory - Tactile
(i) working memory deactivation
(ii) working memory acquisition deactivation
(iii) working memory maintenance deactivation
Approach
tactile input
Delay
Continuation
food

condition. Additionally, trials where the obstacle was raised onto then immediately removed from the walkway during the initial approach comprised the tactile obstacle absent condition. In these control trials, removal of the obstacle precluded any contact. Stepping in these tactile obstacle absent trials was examined to ensure that animals did not develop a learned avoidance response of chronic overstepping.

4.3.4 Surgical Procedures

Cryoloops (Lomber et al. 1999) were implanted bilaterally over areas 5 and 7 (Fig. 4.2) according to previously reported surgical procedures (Lomber et al. 1999, 2010; Lomber and Payne 2000a, 2000b; Lomber and Malhotra 2008).Cooling loops were shaped from 23-guage stainless steel hypodermic tubing to conform to each area examined. For surgical implantation, craniotomies exposed parietal areas 5 and 7 in each hemisphere. Individual cryoloops were positioned with the loop in direct contact with the cortical surface for each area. The base of each loop was secured to the skull with dental acrylic anchored to stainless steel screws, before closing the craniotomies with additional dental acrylic.

4.3.5 Working Memory Testing and Reversible Cooling Deactivation

Following surgical implantation and approximately two weeks of recovery, obstacle working memory was examined using both visual and tactile obstacle memory paradigms. Each testing day began with trials conducted in the absence of any cooling (warm condition). A second block of trials then began with a maintenance phase cooling trial, where cryoloops in contact with the parietal areas were cooled to 3.0 ± 1.0 ˚C to completely deactivate all cortical layers (Lomber and Payne 2000b). In these trials where parietal cortex deactivation was restricted to working memory maintenance, cooling was initiated immediately following foreleg obstacle clearance (Fig. 4.1A-iii, B-iii). Subsequent memory delays lasted around 60 s or longer to allow cortical temperatures to reach 3.0 ± 1.0˚C for complete cortical deactivation. Maintenance phase cooled trials were then followed by more trials where parietal areas remained deactivated throughout the entire obstacle working memory test (Fig. 4.1A-i, B-i). This cooling block ended with

Figure 4.2 Cortical areas deactivated in parietal cortex shown on the right hemisphere of a cat brain.

(A) Lateral view of the right cat cerebrum showing parietal areas 5 and 7 examined in the current study. D—dorsal, A—anterior.

(B) Cooling loops in contact with areas 5 and 7 of the right hemisphere photographed at the time of implantation. Adapted with permission from Wong et al. (2018).

Figure 4.2

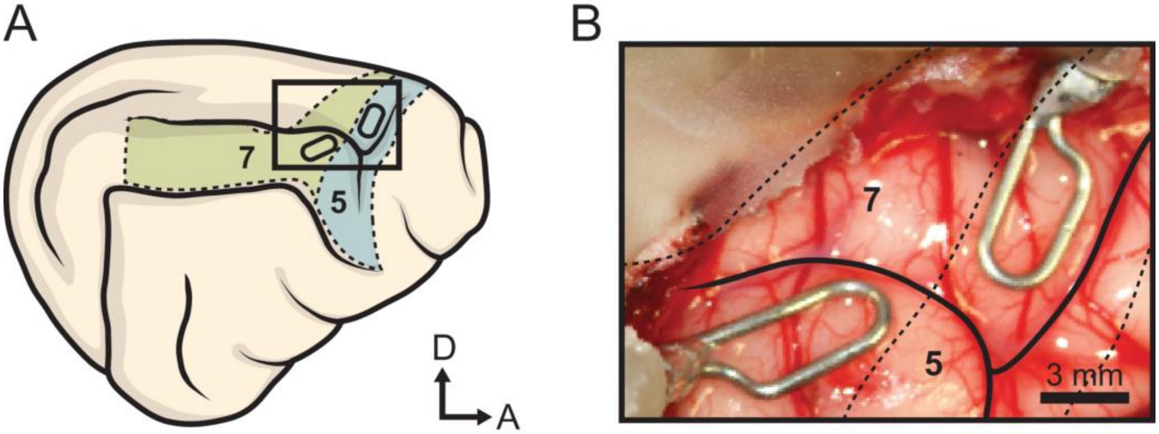

a final acquisition phase cooled trial, where cooling was stopped immediately after foreleg clearance of the obstacle (Fig. 4.1A-ii, B-ii). Once cooling was terminated, memory delays exceeded 60 s to permit restoration of cortical temperature and full functional restoration before walking resumed. A final “warm” block of trials re-established baseline stepping. Cortical temperatures were monitored closely throughout testing to confirm the duration and depth of deactivation. Each testing block consisted of trials where the obstacle was present interspersed with trials where the obstacle was absent for both visual and tactile variations in order to prevent habituation to the obstacle and development of a learned avoidance response. Either bilateral or unilateral deactivations were performed on a given testing day.

4.3.6 Data Analysis

Videos were analyzed using custom written scripts in Matlab (MathWorks, Natick, MA). Steps were tracked by an investigator who was blind with respect to which experimental condition each trial belonged to during video analyses. Step height was measured at the peak of each step as the vertical height of the toe above the walking surface when the toe reached the highest point in the step. Additionally, step clearance was measured as the step height directly above the lowered obstacle. The horizontal distance between the toe and obstacle at the peak of each step was also measured. Trials of the same experimental condition from the three animals were combined for subsequent statistical testing due to similarities in peak step height, step clearance, and the step peak to obstacle distance between all three animals.

To assess working memory-guided obstacle locomotion in visual and tactile obstacle paradigms, step height for each leg was compared between obstacle present and obstacle absent trials, in accordance with previous studies examining obstacle working memory in quadrupedal animals (McVea and Pearson 2006, 2007b; McVea et al. 2009; Whishaw et al. 2009; Setogawa et al. 2014; Wong et al. 2018). This was done for the following reasons: within the warm condition, elevated step height in obstacle present trials in comparison to obstacle absent trials would indicate that the animal accurately remembered the presence of the obstacle, demonstrating intact obstacle working memory. Observing relatively lower step height in obstacle absent trials would also ensure that the animals did not overlearn an avoidance response, and that elevated stepping in obstacle present trials was truly indicative of working memory. Additionally, step height comparisons between obstacle present and obstacle trials when cryoloops were cooled could be used to ensure that parietal cortex deactivations did not induce any motor deficits; any observed attenuations of step height thus reflect deficits in working memory. Thus a one-way multivariate ANOVA was used to compare peak step height for each leg for each trial type (visual-obstacle present, visual-obstacle absent, tactile-obstacle present, tactile obstacle-absent). A Bonferroni correction was applied to account for multiple comparisons and statistical significance was accepted at $P < 0.0125$. For each of the four steps, paired t-tests were conducted to compare step clearances as well as the step peak to obstacle distance between visual and tactile obstacle present trials. Bonferroni corrections were applied to account for multiple comparisons and statistical significance was accepted at $P < 0.0125$.

To assess parietal cortex contributions to obstacle working memory, a one-way multivariate ANOVA was conducted to assess the effect of cooling condition (warm, area 5 bilaterally cooled, or area 7 bilaterally cooled) on peak step height for all four legs in obstacle present and obstacle absent trials. Statistical significance was accepted at $P < 0.00625$ to account for multiple comparisons. Additionally, step clearances and step peak to obstacle distances were compared between the three cooling conditions with one-way multivariate ANOVAs, with significance accepted at $P < 0.0125$. Similar analyses were conducted when cooling was temporally restricted to either working memory acquisition or working memory maintenance phases.

To examine the effects of unilateral deactivation, a two-way multivariate ANOVA was conducted to examine the effects of deactivation locus (left area 5 or right area 5) and leading leg (ipsilateral or contralateral to the site of deactivation) on peak step height. Due to significant interaction effects, unilaterally cooled trials were examined separately according to which hemisphere was cooled, and whether the hindleg ipsilateral or contralateral to the site of cooling was the first to step. For each unilateral cooling condition, peak step heights, step clearances, and the distances between the step peak and obstacle were compared to stepping in warm trials and trials where area 5 was bilaterally deactivated.

4.3.7 Terminal Procedures

Following all behavioural testing, each cat was anesthetized with sodium pentobarbital (25-30 mg/kg, i.v.) and a craniotomy was made to expose the implanted cooling loops on the surface of the brain. Each cryoloop was individually cooled to the same temperature used during behavioural testing (3.0 ± 1.0 °C) and photographed with a thermal imaging camera to capture the extent of deactivation. After each area was photographed, anesthesia was deepened with sodium pentobarbital (40 mg/kg, i.m.) and the animal was transcardially perfused. The brain was removed, frozen and cut in 60 µm coronal sections and collected serially. Sections from the first of five series, separated by 300 µm intervals, were processed with Nissl stain. Series 2 was processed with cytochrome oxidase (Payne and Lomber 1996). Nissl and cytochrome oxidase stained sections were examined to ensure that repeated deactivations did not alter the cortical structure of parietal areas cooled over the testing period. Series 3 was processed with the monoclonal antibody SMI-32 (Covance, Emeryville, CA) for areal border delineation (van der Gucht et al. 2001; Mellott et al. 2010; Wong et al. 2014). Series 4 and 5 were retained as spares to process with any of the above methods as need. Reacted sections were mounted onto gelatinized slides, cleared and coverslipped.

4.3.8 Cooling Deactivation Assessment

Alignment of deactivation sites with area 5 or 7 was confirmed in each animal by comparing thermal photographs with Nissl and SMI-32 processed tissue. Area 5 and area 7 borders delineated in SMI-32 stained sections confirmed that deactivation loci were contained within each area of interest, with minor spread into flanking cortices.

4.4 Results

4.4.1 Visual or tactile information about an obstacle can be used for working memory-guided obstacle locomotion

Working memory-guided obstacle locomotion was assessed in cats (n = 3) using both a visually-dependent and tactile-dependent obstacle working memory paradigm. The height of each step was compared between obstacle present and obstacle absent conditions for both visual and tactile paradigms. A one-way multivariate analysis revealed a significant effect of the trial type (visual-obstacle present, visual-obstacle absent, tactile-obstacle present, tactile obstacle-absent) on peak step height ($F(12, 617) = 165.0$, $P < 0.0001$). Step height of all four legs was significantly affected by trial type (leading foreleg $F(3, 236) = 1148.6$, $P < 0.0001$; trailing foreleg $F(3, 236) = 1383.4$, $P < 0.0001$; leading hindleg $F(3, 236) = 670.5$, $P < 0.0001$; trailing hindleg $F(3, 236) = 268.8$, $P < 0.0001$). For all four legs, post hoc Tukey tests indicated that step height was significantly higher in obstacle present trials for both visual and tactile paradigms (Fig. 4.3A-D). Furthermore, for tactile obstacle present trials, foreleg stepping was significantly higher than stepping in visual obstacle present trials ($P < 0.0001$ for all comparisons), with mean peak step heights of 13.2 ± 1.6 cm and 12.5 ± 1.5 cm for leading and trailing foreleg steps, respectively, in tactile obstacle present trials, and step heights of 11.9 ± 1.2 cm and 11.6 ± 1.0 cm for leading and trailing foreleg steps, respectively, in visual obstacle present trials (Fig. 4.3A-B). The opposite pattern was observed for the leading hindleg step. In tactile obstacle present trials, peak step height for the leading hindleg steps was 9.6 ± 1.5 cm, which was significantly lower than in visual obstacle present trials where mean step height was 10.5 ± 1.7 cm ($P = 0.0014$; Fig. 4.3C). For the trailing hindleg, peak step height did not differ between the visual and tactile paradigms, with mean heights of 7.6 ± 1.4 cm and 7.4 ± 1.7, respectively (Fig. 4.3D).

Additionally, step clearance was measured as the difference between obstacle height and step height directly above the lowered obstacle (Fig. 4.3E). While step clearance was generally similar between visual and tactile obstacle memory paradigms, mean clearance of the trailing foreleg step was significantly higher in tactile trials at 3.0 ± 2.0 cm, in comparison to mean step clearance in visual trials at 2.5 ± 1.0 cm ($P = 0.0062$).

Figure 4.3 Visual or tactile information about an obstacle can be used for working memory-guided obstacle locomotion.

(A–D) Mean peak step height ± SD in obstacle present and obstacle absent trials for both visual and tactile obstacle working memory paradigms for leading foreleg (A), trailing foreleg (B), leading hindleg (C), and trailing hindleg steps (D). For both visual and tactile obstacle present trials, stepping of all 4 legs was significantly elevated over stepping in obstacle absent trials, demonstrating the ability to use visual or tactile information about an obstacle to modify stepping. In obstacle present trials, foreleg stepping was significantly higher in tactile obstacle working memory trials. Conversely, leading hindleg steps were significantly higher in visual obstacle working memory trials, while trailing hindleg steps were similar between the 2 paradigms.

(E) Mean step clearance ± SD for all 4 legs in visual (V) and tactile (T) obstacle present trials. Step clearance only differed between visual and tactile trials for the trailing foreleg, where clearance was significantly higher in the tactile paradigm.

(F) Mean step peak to obstacle distance ± SD for all 4 legs in visual (V) and tactile (T) obstacle present trials. Both leading and trailing forelegs tended to peak later after passing over the obstacle in tactile trials. Conversely, leading hindleg steps tended to peak sooner before passing over the obstacle in visual trials. Step trajectories were similar between visual and tactile paradigms for the trailing hindleg. $^{*}P < 0.0125$, $^{**}P < 0.001$, $^{***}P < 0.0001$.

Figure 4.3

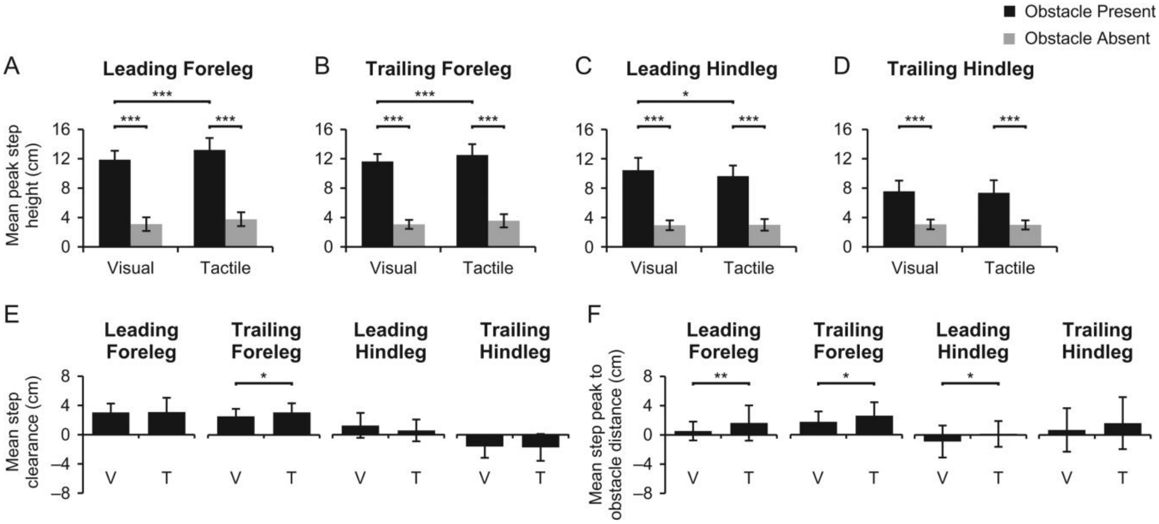
Obstacle Present
Obstacle Absent
A
Leading Foreleg
B
Trailing Foreleg
C
Leading Hindleg
D
Trailing Hindleg
Mean peak step height (cm)
16
12
8
4
0
Visual
Tactile
***
*
E
Leading Foreleg
Trailing Foreleg
Leading Hindleg
Trailing Hindleg
Mean step clearance (cm)
8
4
0
−4
−8
V
T
F
Mean step peak to obstacle distance (cm)
**

Furthermore, the horizontal distance between step peak and the obstacle was measured to assess step trajectory (Fig. 4.3F). Foreleg steps tended to peak further after passing over the obstacle in tactile trials than in visual trials (leading: $P = 0.0008$; trailing: $P = 0.0014$). In contrast, leading hindleg steps tended to peak before passing over the obstacle in visual trials with a mean step peak to obstacle distance of -0.9 ± 2.2 cm, while leading hindleg steps tended to peak just after the obstacle in tactile trials with a mean distance of 0.1 ± 1.8 cm ($P = 0.004$). Step trajectories were similar between visual and tactile trials for the trailing hindleg. Overall, despite the differences between stepping in visual and tactile obstacle memory paradigms, significantly elevated stepping in obstacle present versus obstacle absent trials indicates the ability to use visual or tactile information about an obstacle to modulate stepping for memory-guided obstacle avoidance.

4.4.2 Visual obstacle working memory relies on parietal area 5

To assess parietal cortex contributions to visual obstacle memory, cryoloops implanted over areas 5 or 7 were then bilaterally cooled prior to obstacle approach, and sustained throughout the delay and continuation phases for the visual obstacle memory paradigm (Fig. 4.4A). Such deactivation of neither area 5 nor area 7 affected foreleg stepping in obstacle present or obstacle absent trials (Fig. 4.4B, C). Leading and trailing foreleg steps remained significantly higher in obstacle present trials than in obstacle absent trials whether visual obstacle memory was assessed with parietal areas warm, when area 5 was deactivated, or when area 7 was deactivated ($P < 0.0001$ for all comparisons). However, in comparison to both warm and area 7 cooled conditions, deactivation of area 5 resulted in significantly lower hindleg stepping, with mean peak step heights of 4.7 ± 2.4 cm and 3.2 ± 1.2 cm for leading and trailing hindleg steps, respectively ($P < 0.0001$ for all comparisons; Fig. 4.4D, E). In comparison to obstacle absent trials for any condition, leading hindleg steps remained significantly higher in obstacle present trials when area 5 was deactivated ($P < 0.0001$ for all comparisons; Fig. 4.4D). In contrast, area 5 deactivation reduced trailing hindleg step height such that it no longer differed from stepping in obstacle absent trials (Fig. 4.4E). Differences in leading and trailing hindleg stepping are further visualized by examining scatter plots of peak step height over time (Fig. 4.4F-H). While leading steps are higher than trailing steps in warm and area 7

Figure 4.4 Bilateral deactivation of parietal area 5, but not area 7, results in working memory deficits in the visually dependent obstacle memory test.

(A) Schematic of the visual obstacle working memory paradigm with the blue horizontal bar indicating the use of cooling throughout the entire test.

(B–E) Mean peak step height ± SD in visual obstacle present and obstacle absent trials for leading foreleg (B), trailing foreleg (C), leading hindleg (D), and trailing hindleg steps (E) in warm, area 5 cooled, and area 7 cooled conditions.

(F–H) Scatter plots of peak step height versus delay for leading and trailing hindlegs in warm (F), area 5 cooled (G), and area 7 cooled trials (H). While foreleg steps were unaffected by cooling, deactivation of area 5 resulted in attenuated hindleg step height.

(I–L) Mean step clearance ± SD for all 4 legs in each of the 3 cooling conditions. Area 5 deactivation similarly resulted in reduced hindleg step clearance in comparison to warm and area 7 cooled conditions.

(M–P) Mean step peak to obstacle distance ± SD for all 4 legs in the 3 cooling conditions. Leading step trajectories did not differ between cooling conditions. However, in comparison to area 5 cooled trials, trailing forelegs peaked further from the obstacle after passing over it in area 7 cooled trials. Additionally, while trailing hindleg steps peaked just after passing over the obstacle in warm and area 7 cooled trials, area 5 cooling resulted in steps peaking well before passing over the obstacle. $^{*}P < 0.0125$, $^{***}P < 0.0001$, n.s.—not significant.

Figure 4.4

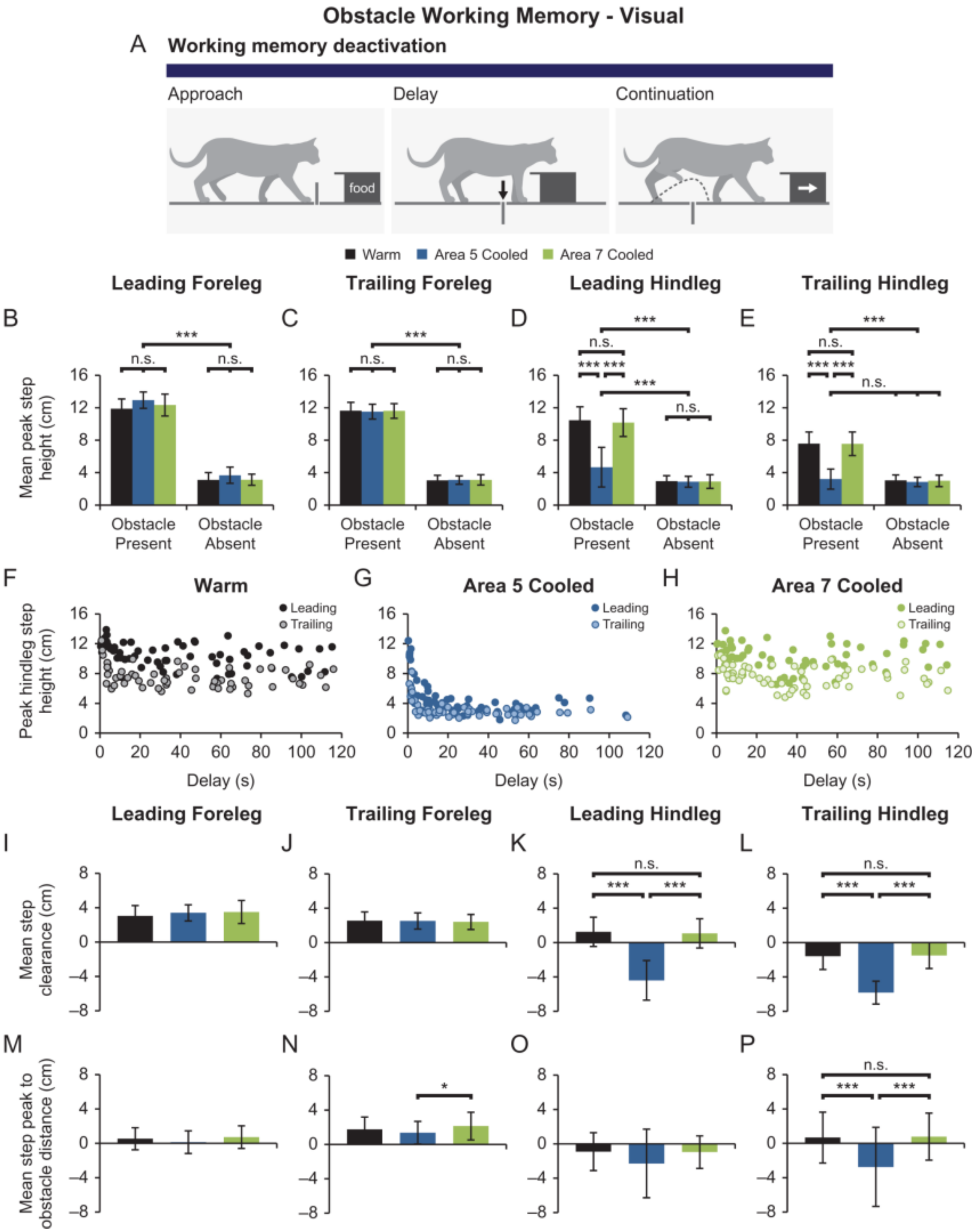
Obstacle Working Memory - Visual
A
Working memory deactivation
Approach
Delay
Continuation
food
Warm
Area 5 Cooled
Area 7 Cooled
Leading Foreleg
Trailing Foreleg
Leading Hindleg
Trailing Hindleg
B
C
D
E
Mean peak step height (cm)
***
n.s.
0
4
8
12
16
Obstacle Present
Obstacle Absent
F
Warm
G
Area 5 Cooled
H
Area 7 Cooled
Peak hindleg step height (cm)
Leading
Trailing
Delay (s)
0
20
40
60
80
100
120
I
J
K
L
Mean step clearance (cm)
8
4
0
−4
−8
M
N
O
P
Mean step peak to obstacle distance (cm)
*

cooled conditions (Fig. 4.4F, H), step height remains relatively stable across delays of up to 2 minutes. When area 5 was deactivated during trials where animals were permitted to walk continuously over the obstacle (such that delays were only a maximum of a few seconds), hindleg steps were similar to obstacle height, indicating intact memory-guided obstacle locomotion. However, as demonstrated by the exponential decay of step height over time (Fig. 4.4G), step height was rapidly attenuated with increasing delays when area 5 was deactivated.

Furthermore, step clearance was similarly affected by parietal cortex deactivation. In comparison to step clearances in the warm condition, neither leading nor trailing foreleg step clearances were affected by bilateral area 5 or area 7 cooling (Fig. 4.4I, J). However, both leading and trailing hindleg step clearances were significantly reduced to -4.4 ± 2.3 cm ($P < 0.0001$) and -5.8 ± 1.3 cm ($P < 0.0001$), respectively, when area 5 was cooled (Fig. 4.4K, L). When area 7 was deactivated, hindleg step clearances did not differ from the step clearances in the warm condition. Additionally, in comparison to the warm condition, foreleg step trajectories were not affected by area 5 or area 7 cooling (Fig. 4.4M, N). However, the mean step peak to obstacle distance was significantly lower when area 5 was cooled in comparison to the area 7 cool condition, with mean distances of 1.4 ± 1.3 cm and 2.1 ± 1.6 cm, respectively ($P = 0.0108$; Fig. 4.4N). While leading hindleg step trajectories did not differ with parietal cortex deactivation (Fig. 4.4O), trailing hindleg steps peaked well before passing the obstacle with a mean step peak to obstacle distance of –2.7 ± 4.6 cm (Fig. 4.4P). In comparison, trailing hindleg steps typically peaked after passing the obstacle in both warm and area 7 cooled conditions, with mean distances of 0.7 ± 3.0 cm ($P < 0.0001$) and 0.8 cm ± 2.7 cm ($P < 0.0001$), respectively. Overall, these alterations in hindleg stepping indicate significant obstacle memory deficits with bilateral parietal area 5, but not area 7, deactivation (Fig. 4.10, row 1).

4.4.3 Area 5 in one hemisphere may affect obstacle locomotion of both hindlegs

In order to evaluate a possible lateralization of area 5 contributions to obstacle memory, area 5 was deactivated unilaterally. Leading and trailing hindleg steps appeared to be differentially affected by unilateral cooling depending on whether the leading hindleg was ipsilateral or contralateral the site of area 5 deactivation. Thus a two-way multivariate ANOVA was conducted to examine the effects of deactivation locus (left area 5 or right area 5) and leading hindleg (ipsilateral or contralateral to the site of deactivation) on peak step height. This revealed a significant interaction between deactivation locus and leading leg ($F(2, 224) = 8.1, P = 0.0004$). Further analyses of unilateral area 5 contributions to obstacle memory compared hindleg stepping between warm and bilateral area 5 cooled conditions for both left and right area 5 cooled trials according to the identity of the leading hindlimb (Fig. 4.5). The results of left area 5 deactivations are detailed here; however, note that hindleg stepping is similarly affected by right area 5 deactivations (Fig. 4.5, right).

For trials where left area 5 was cooled and the ipsilateral (left) hindleg led, a one-way multivariate analysis revealed a significant effect of the cooling condition (warm, bilateral area 5 deactivation, or left area 5 deactivation) on peak step height ($F(4, 366) = 112.4$, $P < 0.0001$; Fig. 4.5A). Both leading ($F(2, 164) = 138.6$, $P < 0.0001$) and trailing ($F(2, 164) = 132.9$, $P < 0.0001$) hindleg step height were significantly affected by the cooling condition. Post-hoc Tukey tests revealed that while bilateral area 5 deactivation resulted in significantly reduced leading and trialing hindleg step height in comparison to the warm condition ($P < 0.0001$), step height was only significantly reduced in the contralateral (right) trailing hindleg when left area 5 was cooled ($P < 0.0001$). Notably, trailing step height was not reduced to the same extent as in the bilateral deactivation condition, as trailing step height was significantly higher when left area 5 was cooled and the left hindleg led ($P < 0.0001$). Peak step height of the ipsilateral (left) leading hindleg did not differ from the warm condition. In contrast, when left area 5 was cooled and the contralateral (right) hindleg led, both leading and trailing hindleg step heights were significantly reduced in comparison to the warm condition (Fig. 4.5B). Peak step height of the contralateral (right) leading hindleg was significantly reduced to 5.4 ± 2.6 cm ($P < 0.0001$ in comparison to warm), such that it did not differ from leading hindleg step height when area 5 was bilaterally deactivated. However, despite a significant reduction in step height to a mean of 6.5 ± 2.6 cm ($P = 0.0076$ in comparison to the warm

Figure 4.5 Obstacle working memory deficits following unilateral area 5 deactivation were dependent on which hindleg led.

(A,B) Mean peak step height ± SD for leading and trailing hindleg steps in warm obstacle present trials, trials where area 5 was bilaterally cooled, or trials where left area 5 was cooled and the ipsilateral (A) or contralateral (B) hindleg led.

(C,D) Mean peak step height ± SD for leading and trailing hindleg steps when right area 5 was cooled and the ipsilateral (C) or contralateral (D) hindleg led compared to warm and bilateral area 5 cooled conditions.

(E,F) Mean step clearance ± SD for leading and trailing hindleg steps when left area 5 was cooled and the ipsilateral (E) or contralateral (F) hindleg led compared to warm and bilateral cooled conditions.

(G,H) Mean step clearance ± SD for leading and trailing hindleg steps when right area 5 was cooled and the ipsilateral (G) or contralateral (H) hindleg led compared to warm and bilateral cooled conditions. Regardless of whether area 5 was cooled in the left or right hemisphere, when the ipsilateral hindleg led, step height and clearance was significantly attenuated in the contralateral hindleg only. However, stepping of both legs was affected when the contralateral hindleg led.

(I–L) Mean step peak to obstacle distance ± SD for leading and trailing hindleg steps. In comparison to bilateral area 5 deactivation, unilateral cooling did not affect trailing hindleg trajectory relative to the warm condition. $*P < 0.0125$, $**P < 0.001$, $***P < 0.0001$, n.s. – not significant.

Figure 4.5

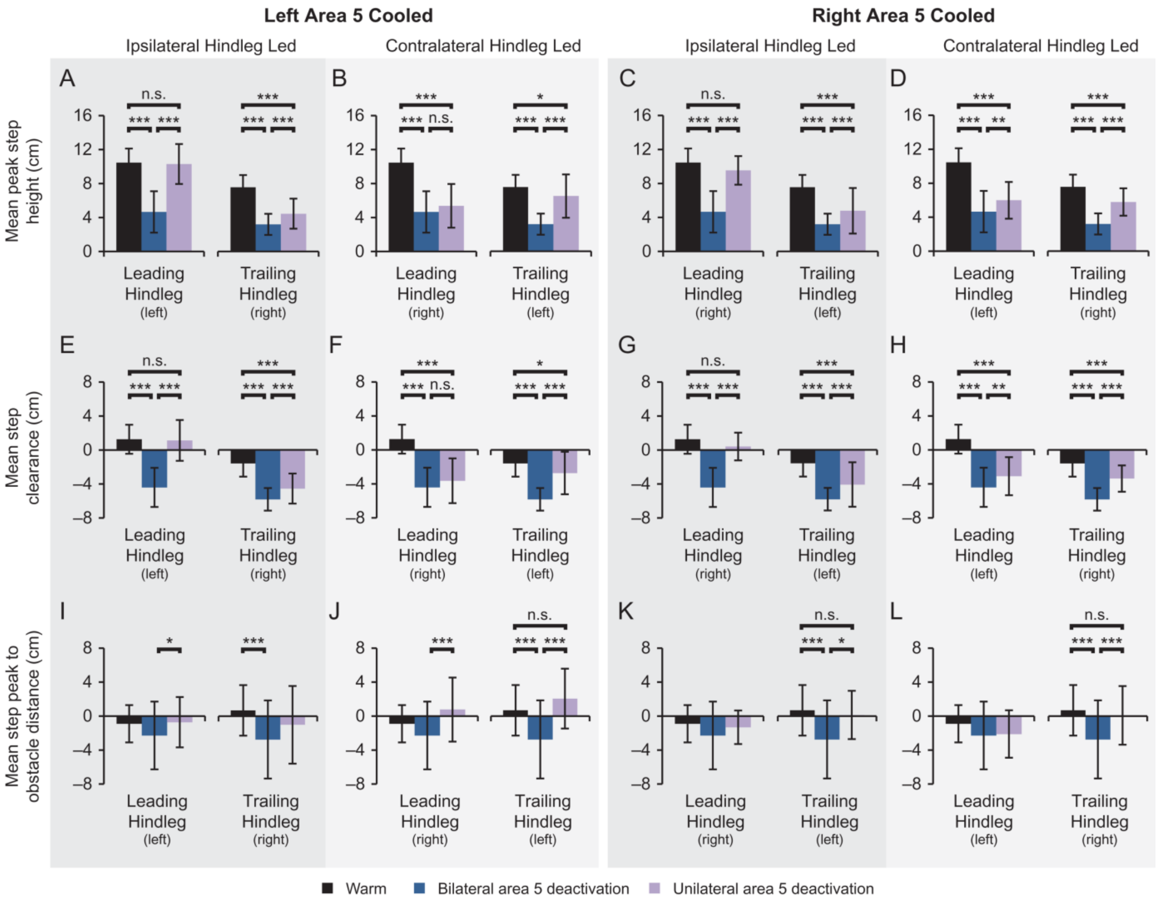
Left Area 5 Cooled
Right Area 5 Cooled
Ipsilateral Hindleg Led
Contralateral Hindleg Led
Ipsilateral Hindleg Led
Contralateral Hindleg Led
A
B
C
D
E
F
G
H
I
J
K
L
Mean peak step height (cm)
Mean step clearance (cm)
Mean step peak to obstacle distance (cm)
Leading Hindleg (left)
Trailing Hindleg (right)
Leading Hindleg (right)
Trailing Hindleg (left)
n.s.
***
*
**
■ Warm
■ Bilateral area 5 deactivation
■ Unilateral area 5 deactivation

condition), ipsilateral (left) trailing hindleg steps remained significantly higher than trailing hindleg steps when area 5 was bilaterally deactivated ($P < 0.0001$). Accordingly, changes in step clearance paralleled changes in peak step height with unilateral area 5 deactivations (Fig. 4.5E-H). Overall, in comparison to the warm condition, step clearance was only significantly reduced in trailing hindleg steps if the ipsilateral hindleg led ($P < 0.0001$ for both comparisons; Fig. 4.5E, G); ipsilateral leading step clearances were unaffected. However, step clearance was significantly reduced in both hindlegs if the hindlimb contralateral to the site of deactivation led ($P < 0.0001$ in comparison to the warm condition for both comparisons; Fig. 4.5F, H). For example, when left area 5 was cooled, step clearance of the contralateral (right) leading hindleg was reduced to -3.6 ± 2.6 cm such that it did not differ from clearance of the leading hindleg in bilaterally cooled trials (Fig. 4.5F). In contrast, clearance of the ipsilateral (right) trailing hindleg was significantly higher than in bilaterally cooled trials ($P < 0.0001$). Furthermore, when left area 5 was cooled and the ipsilateral hindleg led, leading hindleg steps peaked significantly closer to the obstacle than when area 5 was bilaterally cooled ($P = 0.0152$, Fig. 4.5I). When the contralateral hindleg led and left area 5 was cooled, both leading and trailing steps peaked after passing the obstacle unlike bilaterally cooled trials ($P < 0.0001$ for both comparisons; Fig. 4.5J).

Altogether, pronounced memory deficits restricted to the contralateral trailing leg when the ipsilateral hindlimb led suggest that area 5 in one hemisphere may be essential for guiding the contralateral leg over a remembered obstacle (Fig. 4.10, row 2). However, similar memory deficits in both leading and trailing hindleg steps when the contralateral leg led suggest that leading hindlimb steps can influence trailing hindlimb steps (Fig. 4.10, row 3). Ultimately, memory-guided obstacle avoidance likely involves bilateral area 5 contributions.

4.4.4 Area 5 is necessary for memory maintenance, but insufficient for working memory acquisition

To further specify cortical contributions to obstacle memory, parietal areas were bilaterally deactivated during different phases of the visual obstacle memory test (Figs. 4.6-4.8). First, we examined the effect of deactivating area 5 during the initial approach towards the obstacle, encompassing the memory acquisition phase (Fig. 4.6A). A one-way multivariate ANOVA revealed a significant effect of the cooling condition on peak step height ($F(10, 856) = 116.9$, $P < 0.0001$). With mean peak step heights of 7.7 ± 2.7 cm and 5.2 cm for leading and trailing hindlegs, respectively, steps following bilateral area 5 deactivation during memory acquisition remained significantly lower than steps in time-matched warm trials ($P < 0.0001$ for both comparisons). However, both leading and trailing steps remained significantly higher than stepping in all obstacle absent trials ($P < 0.0001$ for all comparisons). Consequently, leading and trailing step clearances were also significantly lower in comparison to time-matched warm trials ($P < 0.0001$ for both comparisons, Fig. 4.6D-E). In contrast, area 7 deactivation restricted to obstacle memory acquisition did not affect step height or step clearance in comparison to the warm condition. Furthermore, step trajectories were similar between cooling conditions in obstacle present trials, as the mean step peak to obstacle distance did not differ significantly between warm or acquisition cooled trials or area 5 or area 7 (Fig. 4.6F-G). Thus in comparison to the marked changes in hindleg stepping with bilateral area 5 deactivation throughout the entire visual obstacle memory paradigm, acquisition phase deactivation of area 5 resulted in partial or incomplete deficits in obstacle memory (Fig. 4.10, row 4).

Next, the effect of deactivating area 5 during the delay was examined to assess parietal cortex contributions to obstacle memory maintenance (Fig. 4.7A). In these trials, maintenance phase deactivation of area 5 resulted in hindleg step heights similar to those observed in obstacle absent trials (Fig. 4.7B-C). In comparison to both time-matched warm trials and trials where area 7 was deactivated during memory maintenance, leading and trailing steps were significantly lower, with mean step heights of 3.5 ± 0.9 cm and 3.6 cm ± 1.0 cm, respectively ($P < 0.0001$ for all comparisons). Mean step clearances were consequently reduced to -5.1 ± 1.1 cm and -5.7 ± 0.7 cm for leading and trailing hindlegs, respectively, which were both significantly lower than step clearances in warm and area 7 cooled trials ($P < 0.0001$ for all comparisons; Fig. 4.7D-E). While the distance between the leading step peak and obstacle did not differ significantly between cooling conditions, trailing steps peaked before the obstacle in area 5 maintenance cooled trials, which differed significantly from both warm and area 7 maintenance cooled trials ($P <$

Figure 4.6 Bilateral cortical cooling was restricted to the approach phase to assess cortical contributions to the acquisition of visual obstacle memory.

(A) Schematic of the visual obstacle memory paradigm with the blue and red horizontal bar depicting the restriction of cooling (blue) to the approach phase of the task.

(B,C) Mean peak step heights ± SD of leading (B) and trailing (C) hindlegs for each cooling condition for trials where the obstacle was present or absent. While area 5 deactivation during memory acquisition attenuated hindleg step height relative to warm and area 7 cooled conditions, steps remained significantly higher than stepping in obstacle absent trials.

(D,E) Mean step clearance ± SD of leading (D) and trailing (E) hindlegs for each cooling condition. Acquisition phase cooling of area 5 significantly reduced hindleg step clearances in comparison to warm and area 7 cooled conditions.

(F,G) Mean step peak to obstacle distance ± SD for leading (F) and (G) trailing hindlegs did not differ between conditions. ***$P < 0.0001$, n.s.—not significant.

Figure 4.6

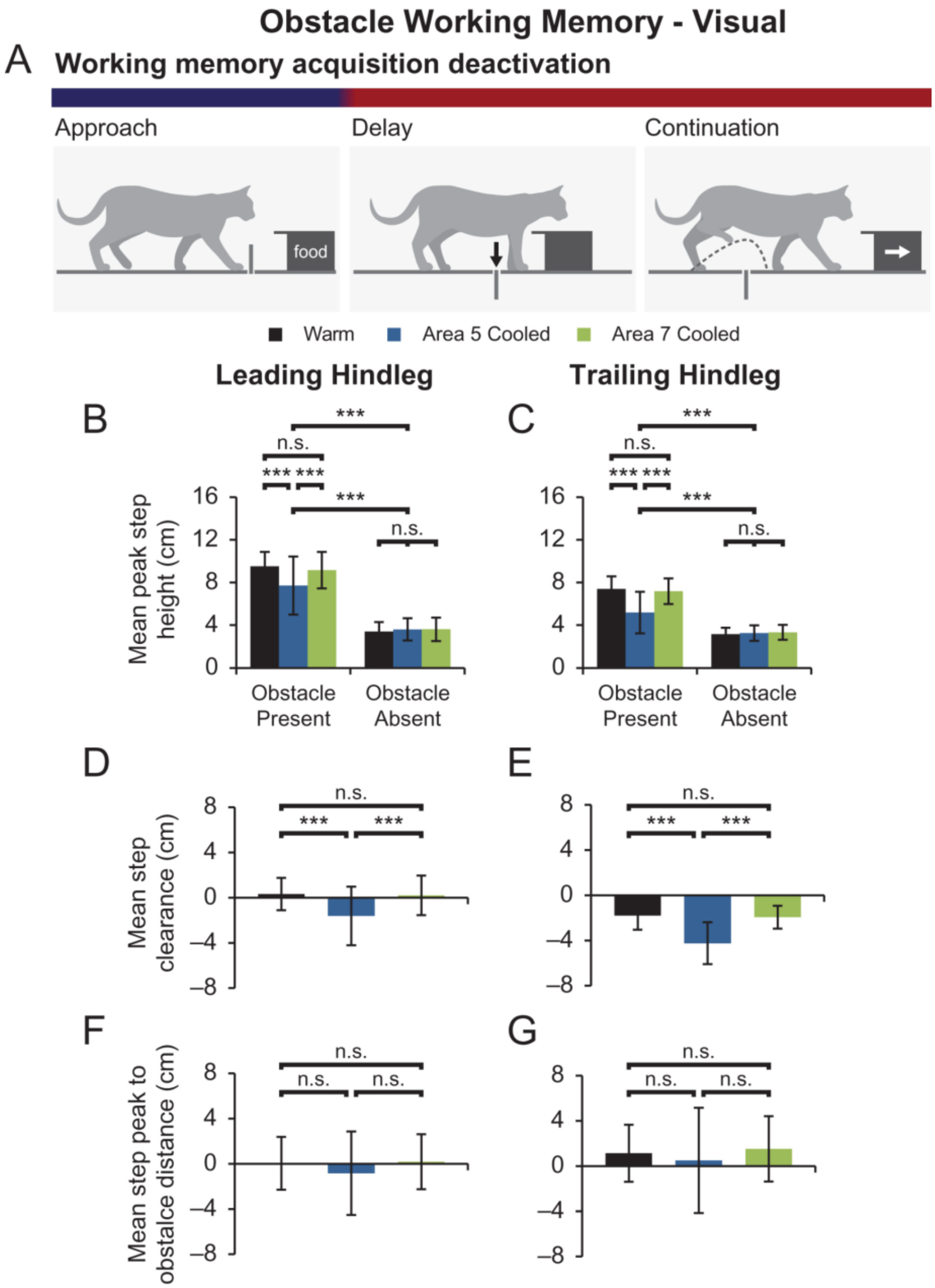
Obstacle Working Memory - Visual
A
Working memory acquisition deactivation
Approach
Delay
Continuation
food
■ Warm
■ Area 5 Cooled
■ Area 7 Cooled
Leading Hindleg
Trailing Hindleg
B
C
Mean peak step height (cm)
16
12
8
4
0
***
n.s.
*** ***
***
n.s.
Obstacle Present
Obstacle Absent
D
E
Mean step clearance (cm)
8
4
0
−4
−8
n.s.
*** ***
F
G
Mean step peak to obstalce distance (cm)
n.s.
n.s. n.s.

Figure 4.7 Bilateral cortical cooling was initiated during the delay phase to assess cortical contributions to the maintenance of visual obstacle memory.

(A) Schematic of the visual obstacle memory paradigm with the red and blue horizontal bar depicting the initiation of cooling (blue) during the delay phase of the task.

(B,C) Mean peak step heights ± SD of leading (B) and trailing (C) hindlegs for each cooling condition for trials where the obstacle was present or absent.

(D,E) Mean step clearance ± SD of leading (D) and trailing (E) hindlegs for each cooling condition. Maintenance phase cooling of area 5 resulted in significantly reduced hindleg step heights and clearances.

(F,G) Mean step peak to obstacle distance ± SD for leading (F) and (G) trailing hindlegs for each condition. While leading hindleg step trajectories did not differ between conditions, area 5 deactivation resulted in trailing hindleg steps peaking sooner before passing over the obstacle. ***$P < 0.0001$, n.s.—not significant.

Figure 4.7

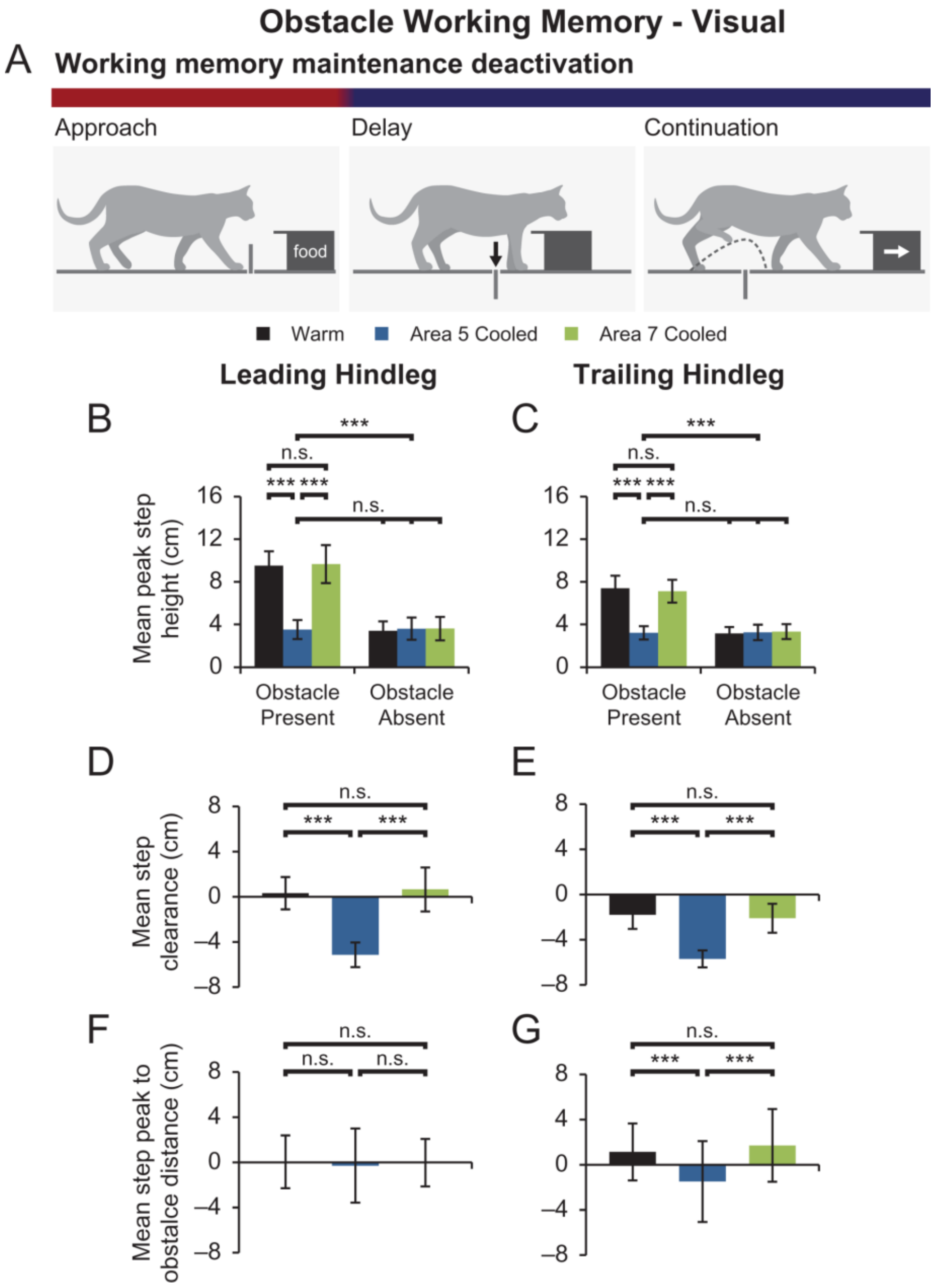
Obstacle Working Memory - Visual
A
Working memory maintenance deactivation
Approach
Delay
Continuation
food
■ Warm
■ Area 5 Cooled
■ Area 7 Cooled
Leading Hindleg
Trailing Hindleg
B
C
***
n.s.
*** ***
n.s.
Mean peak step height (cm)
16
12
8
4
0
Obstacle Present
Obstacle Absent
D
E
Mean step clearance (cm)
8
4
0
−4
−8
F
G
Mean step peak to obstalce distance (cm)

0.0001 for both comparisons; Fig. 4.7F-G). Overall, these changes in hindleg stepping were similar to those observed when area 5 was cooled throughout the entire visual obstacle memory task. Thus deactivation of area 5, but not 7, during memory maintenance was sufficient in reproducing memory deficits observed when area 5 was deactivated throughout the entire memory test (Fig. 4.10, row 5).

Finally, parietal areas were deactivated and reactivated within the memory maintenance phase (Fig. 4.8A). Memory delays ranged from 140 s to around 240 s to permit complete cortical deactivation and subsequent restoration of neural activity before walking resumed. Additional warm trials were conducted to ensure comparisons between trials with similar memory delays. Area 5 deactivation and reactivation during memory maintenance resulted in mean step heights of 6.9 ± 1.7 cm and 5.0 ± 1.1 cm for leading and trailing legs, respectively, which was significantly lower than stepping in both time-matched warm trials (leading: 9.1 ± 1.7 cm, $P < 0.0001$; trailing: 6.9 ± 1.6 cm, $P < 0.0001$; Fig. 4.8B-C), and trials where area 7 was deactivated and reactivated during memory maintenance (leading: 9.0 ± 1.3 cm, $P < 0.0001$; trailing: 6.2 ± 1.4 cm, $P < 0.0001$). Consequently, such area 5 deactivation and reactivation resulted in leading and trailing step clearances of -2.1 ± 1.8 cm and -4.0 ± 1.1 cm, respectively, which were both significantly lower in comparison to the warm condition ($P < 0.0001$ for both comparisons; Fig. 4.8D-E). While leading hindleg step clearances similarly differed between area 5 and area 7 cooled trials (Fig. 4.8D), trailing hindleg step clearances were not differentially affected by area 5 or area 7 deactivation and reactivation during memory maintenance (Fig. 4.8E). Furthermore, the distance between the step peak and obstacle did not differ significantly between any of the three cooling conditions (Fig. 4.8F-G). Overall, area 5 deactivation and reactivation during memory maintenance resulted in partial or incomplete memory deficits, similar to those observed when area 5 was deactivated during obstacle memory acquisition (Fig. 4.10, row 6).

4.4.5 Area 5 contributes similarly to tactile obstacle working memory

To compare parietal cortex involvement between visual and tactile obstacle memory, areas 5 or 7 were bilaterally deactivated throughout the entire tactile obstacle memory

Figure 4.8 Bilateral cortical deactivation and reactivation during the memory maintenance phase of the visual obstacle memory paradigm.

(A) Schematic of the visual obstacle memory paradigm with the red and blue horizontal bar depicting the onset and offset of cooling (blue) during the delay phase of the task.

(B,C) Mean peak step heights ± SD of leading (B) and trailing (C) hindlegs for each cooling condition for trials where the obstacle was present or absent. While area 5 deactivation and reactivation during memory maintenance attenuated hindleg step height relative to warm and area 7 cooled conditions, steps remained significantly higher than stepping in obstacle absent trials.

(D,E) Mean step clearance ± SD of leading (D) and trailing (E) hindlegs for each cooling condition. Area 5 deactivation and reactivation during memory maintenance resulted in significantly reduced hindleg step clearances in comparison to warm and area 7 cooled conditions.

(F–G) Mean step peak to obstacle distance ± SD for leading (F) and (G) trailing hindlegs did not differ between conditions. ***$P < 0.0001$, n.s.—not significant.

Figure 4.8

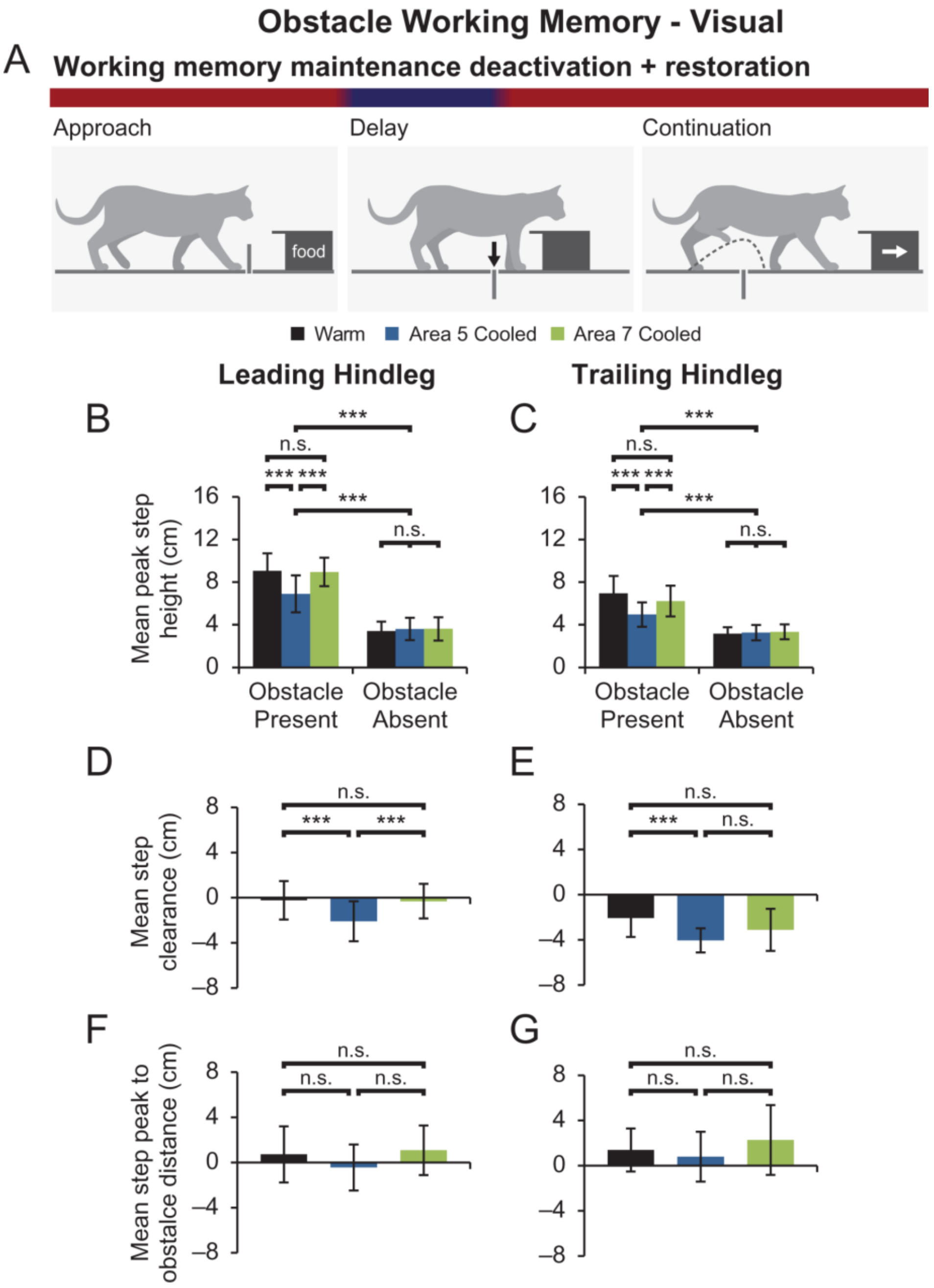
Obstacle Working Memory - Visual
A
Working memory maintenance deactivation + restoration
Approach
Delay
Continuation
food
Warm
Area 5 Cooled
Area 7 Cooled
Leading Hindleg
Trailing Hindleg
B
C
Mean peak step height (cm)
16
12
8
4
0
***
n.s.
Obstacle Present
Obstacle Absent
D
E
Mean step clearance (cm)
8
4
0
−4
−8
F
G
Mean step peak to obstalce distance (cm)

paradigm, or specifically during memory acquisition or memory maintenance (Fig. 4.9A). While deactivation of neither area 5 nor area 7 throughout the entire tactile obstacle memory paradigm affected stepping of the forelegs, both leading and trailing hindleg step height was significantly reduced to 4.7 ± 2.4 cm and 3.2 ± 1.2 cm, respectively, for obstacle present trials in comparison to both warm and area 7 cooled conditions ($P < 0.0001$ for all comparisons; Fig.4.9B-C). Moreover, area 5 deactivation resulted in hindleg step heights in obstacle present trials that did not differ significantly from obstacle absent trials. Such memory deficits were similar to those observed in visual obstacle memory trials (Fig. 4.9D-E). For leading hindleg steps, area 5 deactivation resulted in a 55.4% reduction from step height measured in visual trials performed warm, and a 63.1% reduction from step height measured in tactile trials performed warm (Fig. 4.9D). In contrast, area 7 deactivation resulted in 2.8% and 2.7% reduction from step height in warm visual and warm tactile trials, respectively. Similarly, trailing hindleg step height was reduced by 57.7% and 62.2% when area 5 was cooled during visual and tactile trials, respectively (Fig. 4.9E). In contrast, area 7 deactivation during visual and tactile trials only reduced trailing hindleg step height by 0.2% and 4.2%, respectively. Thus in both visual and tactile obstacle memory paradigms, deactivation of area 5, but not 7, resulted in profound obstacle memory deficits (Fig. 4.10, rows 1 and 7).

When area 5 deactivation was restricted to the memory acquisition phase of the tactile paradigm, leading and trailing hindleg step heights were significantly reduced to 5.5 ± 2.2 cm and 4.5 ± 1.7 cm for obstacle present trials, in comparison to warm time-matched trials (leading: 9.1 ± 2.3 cm, $P < 0.0001$, Fig. 8F; trailing: 7.3 ± 1.9 cm, $P < 0.0001$, Fig. 4.9F-G). However, these steps remained significantly higher than steps in obstacle absent trials ($P < 0.0001$ for all comparisons), suggesting only partial or incomplete deficits in the memory of obstacle height. Overall, such changes in hindleg step height represented a 40.0% and 38.6% reduction from leading and trailing step height, respectively, in time-matched tactile warm trials (Fig. 9*H*,*I*). In contrast, area 5 deactivation during visual memory acquisition resulted in a 19.0 % and 30.0 % reduction from leading and trailing step height, respectively, in time-matched visual trials. Area 7 deactivation during memory acquisition did not substantially reduce step height, with only a 3.7% and 2.6% reduction in leading step height in visual and tactile trials, respectively, and a 3.1% and

Figure 4.9 Bilateral deactivation of parietal area 5 during the tactile obstacle memory paradigm results in deficits similar to those observed in the visual obstacle memory paradigm.

(A) Schematic of the tactile obstacle memory paradigm with blue and red horizontal bars depicting the duration of cooling extending throughout the entire task (i), or restriction of cooling (blue) to the approach phase (ii) or delay and continuation phases of the task (iii).

(B,C) Mean peak step height ± SD of leading (B) and trailing (C) hindlegs for obstacle present and obstacle trials performed with parietal areas warm (no cooling), or when area 5 or area 7 was bilaterally deactivated.

(D,E) Deactivation of area 5, but not 7, resulted in substantial reductions from leading (D) and trailing (E) hindleg step height observed in warm obstacle present trials for both visual and tactile paradigms.

(F–I) Area 5 deactivation restricted to the memory acquisition phase of the tactile obstacle memory test attenuated hindleg stepping in obstacle present trials. The percent reduction in step height from warm trials was greater in tactile trials for both hindlegs. However, deficits were not as pronounced as in trials where area 5 was cooled throughout the entire task.

(J–M) Area 5 deactivation restricted to the memory maintenance phase of the tactile paradigm attenuated hindleg stepping in obstacle present trials to a similar extent in visual and tactile paradigms. Deficits were similar to those observed when area 5 was cooled throughout the entire task. ***$P < 0.0001$, n.s.—not significant.

Figure 4.9

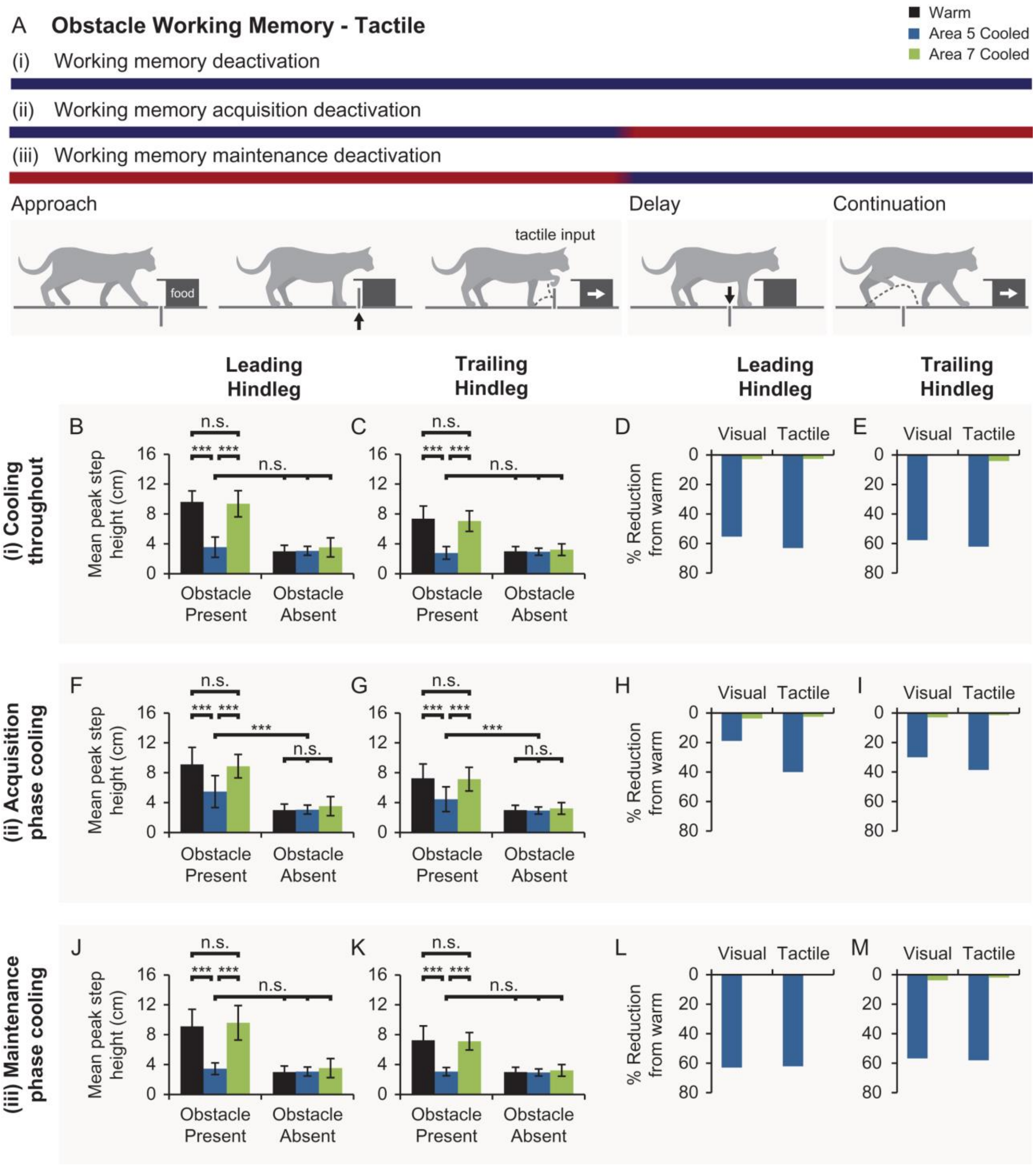
A
Obstacle Working Memory - Tactile
■ Warm
■ Area 5 Cooled
■ Area 7 Cooled
(i) Working memory deactivation
(ii) Working memory acquisition deactivation
(iii) Working memory maintenance deactivation
Approach
Delay
Continuation
food
tactile input
Leading Hindleg
Trailing Hindleg
Leading Hindleg
Trailing Hindleg
(i) Cooling throughout
(ii) Acquisition phase cooling
(iii) Maintenance phase cooling
B
C
D
E
F
G
H
I
J
K
L
M
Mean peak step height (cm)
16
12
8
4
0
n.s.
***
Obstacle Present
Obstacle Absent
% Reduction from warm
Visual
Tactile
0
20
40
60
80

1.5% reduction in trailing step height in visual and tactile trials, respectively (also see Fig. 10 rows 4 and 8).

When area 5 was deactivated during the tactile memory maintenance phase, both leading and trailing hindleg steps were significantly reduced to peak heights of 3.5 ± 0.8 cm and 3.0 ± 0.6 cm, respectively, relative to both warm and area 7 maintenance cooled trials ($P < 0.0001$ for all comparisons; Fig. 4.9J-K). As in trials where area 5 was cooled throughout the entire task, tactile maintenance cooling of area 5 resulted in attenuated leading and trailing step heights such that they did not differ from stepping in obstacle absent trials. Such memory deficits were similar to those observed in the visual obstacle memory paradigm (Fig. 4.9L-M; compare Fig. 4.10 rows 5 and 9). Maintenance phase deactivation of area 5 resulted in a 62.9% and 62.1% reduction from leading hindleg step height in time-matched warm visual and tactile trials, respectively. Trailing hindleg steps were reduced by 56.7% and 58.1% when area 5 deactivation was restricted to visual and tactile obstacle memory maintenance, respectively. In contrast, maintenance phase deactivation of area 7 resulted in leading and trailing hindleg step heights that were actually 1.7% and 5.3% higher than time-matched warm trials. Trailing hindleg steps were reduced by a mere 3.8% and 2.0% when area 7 was deactivated during visual and tactile obstacle memory maintenance, respectively.

Overall, deactivation of area 5, but not 7, resulted in profound obstacle memory deficits for both visual and tactile paradigms (Fig. 4.10). While memory deficits were similar when area 5 was cooled throughout obstacle memory paradigms or restricted to memory maintenance, step heights were reduced to a lesser extent when area 5 deactivation was restricted to obstacle memory acquisition, especially in the visual paradigm.

4.5 Discussion

These results demonstrate parietal cortex contributions to a working memory system required for hindleg obstacle avoidance in quadrupeds. While area 7 has little or no contribution to obstacle memory, altered hindleg stepping following deactivation of area 5 demonstrates the critical role of area 5 in maintaining the working memory of an

Figure 4.10 Summary diagram illustrating the dissociation of parietal cortex contributions to obstacle memory.

Deactivation of area 5, but not area 7, resulted in altered hindleg step height and trajectories demonstrative of impaired obstacle memory. ↓↓—complete deficit; ↓—incomplete deficit.

Figure 4.10

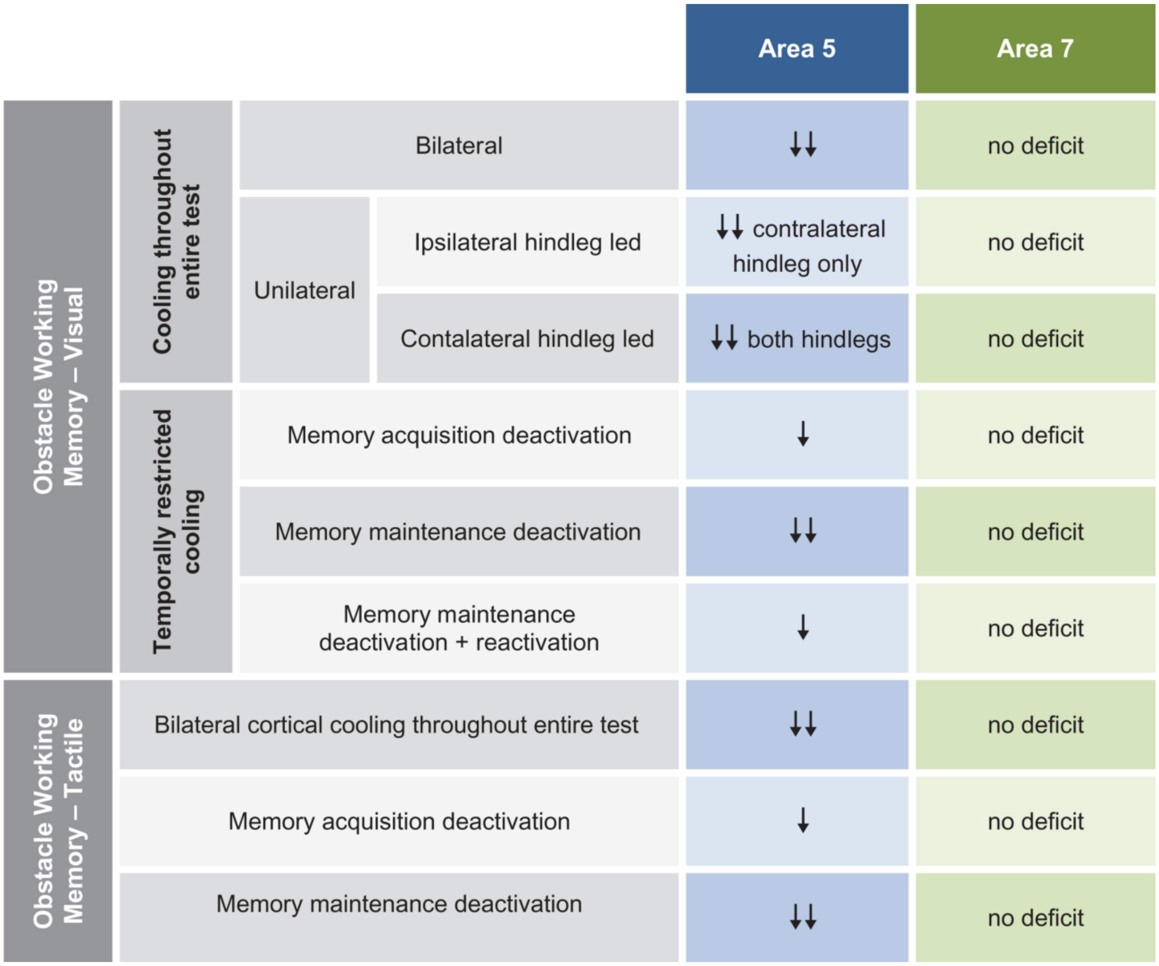

				Area 5	Area 7
Obstacle Working Memory – Visual	Cooling throughout entire test	Bilateral		↓↓	no deficit
		Unilateral	Ipsilateral hindleg led	↓↓ contralateral hindleg only	no deficit
			Contalateral hindleg led	↓↓ both hindlegs	no deficit
	Temporally restricted cooling	Memory acquisition deactivation		↓	no deficit
		Memory maintenance deactivation		↓↓	no deficit
		Memory maintenance deactivation + reactivation		↓	no deficit
Obstacle Working Memory – Tactile	Bilateral cortical cooling throughout entire test			↓↓	no deficit
	Memory acquisition deactivation			↓	no deficit
	Memory maintenance deactivation			↓↓	no deficit

obstacle acquired visually or tactilely (Fig. 4.10). Furthermore, incomplete working memory deficits or partial working memory recovery following restoration of area 5 function during visual working memory maintenance suggests that maintenance phase deactivations may suppress but not eliminate obstacle working memory. Furthermore, partial working memory deficits following acquisition phase deactivation of area 5 suggest that area 5 is necessary but insufficient for acquiring the working memory of an obstacle. As this simple behavioural task involves mechanisms related to locomotion, motor planning, working memory, and spatial representation of the environment, the observed memory deficits strongly implicate area 5 in all of these processes.

4.5.1 Working memory-guided obstacle avoidance can rely on vision or somatosensation

In comparison to stepping in obstacle absent trials, elevated stepping of all four legs in visual and tactile obstacle present trials demonstrates the ability to use visual or tactile information about an obstacle to modify leg movements for avoidance. Moreover, elevated hindleg stepping following delays tested up to 2 minutes illustrates the ability to retain information about an obstacle in memory. In both visual and tactile obstacle present trials, foreleg steps exceeded the height of the obstacle by around 3 cm, ensuring an adequate margin of safety between the foot and obstacle (Patla et al. 1991). Furthermore, in tactile trials, contact with the obstacle produced higher foreleg steps relative to foreleg stepping modified by visual input of the obstacle. Additionally, trailing foreleg step clearance was also higher in tactile obstacle present trials, and both forelegs steps peaked later after passing over the obstacle following tactile input. These differences in foreleg stepping can be attributed to the reflexive activation of shoulder and wrist flexors upon foreleg contact, which withdraw the foreleg from the obstacle (Andersson et al. 1978). This rapid compensatory response mediated by spinal locomotor mechanisms ensures that the legs are lifted well above the obstacle for avoidance (Forssberg 1979). In contrast, visual inputs acquired at least two steps before the obstacle can adjust stepping in a feedforward manner (Drew et al. 1996; Patla and Vickers 1997; Mohagheghi et al. 2004). Resulting steps are therefore not as excessively elevated as in tactile trials, demonstrating more efficient obstacle locomotion without incurring extraneous energy costs (Patla et al. 1991).

Foreleg steps were also notably higher than hindleg steps for both visual and tactile obstacle present trials. While foreleg stepping is modified directly by visual inputs or fast reflexive pathways initiated by tactile inputs, hindleg stepping following a delay is modified by memory dependent processes. The resulting attenuation of hindleg step height is similar to the target undershooting bias associated with memory-guided reaching (Westwood et al. 2003). Such target undershooting is thought to reflect uncertainty about target location, and ensures that reaches do not collide with the target incurring time-consuming reversals in movement direction. A similar uncertainty about obstacle size and location likely exists when hindleg clearance is delayed and obstacle information must be retained in working memory. While undershooting leg height would likely result in the foot colliding with the target, less energy is required relative to overshooting obstacle height. As the obstacle used for the present study is relatively benign, attenuated hindleg stepping likely reflects a strategy invoked with uncertainty about obstacle height that opts to minimize energy expenditure given the low risk of serious danger.

In visual obstacle present trials, leading hindleg steps were higher and peaked sooner before passing over the obstacle. In tactile obstacle present trials, having the hindleg peak closer to the actual location of the obstacle may indicate a more accurate representation of obstacle location retained in working memory. However, if steps do not reach their maximal point until after passing the obstacle, the leg may not be elevated sufficiently for clearance by the time it actually reaches the obstacle. Thus having the foot peak sooner in a step may reflect a cautious strategy to maximize the opportunity for successful avoidance. Additionally, with relatively higher leading hindleg step heights and clearances in visual obstacle present trials, obstacle avoidance would be more successful in visual than tactile trials. This may be attributed to a more accurate representation of obstacle height and location acquired visually during the initial approach.

In contrast to differences in leading hindleg steps, trailing hindleg steps did not differ in terms of peak height, clearance, or step peak to obstacle distance between visual and tactile trials. Trailing hindleg steps were also notably lower than leading hindleg steps. With mean step clearances falling below the height of the obstacle, working memory-guided modifications to trailing hindleg steps would have been insufficient for successful obstacle avoidance in either paradigm. In humans, a similar pattern of increased failures in trailing versus leading limb obstacle crossings have been demonstrated in tests of working memory-guided obstacle locomotion (Heijnen et al. 2014). Thus insufficient trailing limb clearance may reflect common limitations of obstacle working memory mechanisms in bipedal and quadrupedal animals, regardless of whether obstacle information is acquired visually or tactilely. Importantly, despite these insufficiencies in step modulation for obstacle clearance, both leading and trailing hindleg steps were significantly elevated in obstacle present trials. Thus despite differences in how obstacle information is acquired, the resulting working memory-guided step modulations may be executed by similar mechanisms, which appear to include parietal area 5.

4.5.2 Area 5 contributes to memory-guided obstacle locomotion regardless of input sensory modality

Within the same animal, deactivating identical sites within area 5 produced similar working memory deficits in visual and tactile paradigms. Furthermore, as temporally restricted deactivations resulted in similar patterns of working memory impairment in both visual and tactile paradigms, area 5 may store information about an obstacle regardless of input sensory modality. While area 5 has been previously examined in studies of visuomotor processing, area 5 in the cat has been traditionally regarded as a higher order somatosensory area (Avendaño et al. 1988). In addition to receiving visual (Squatrito et al. 1981; Avendaño et al. 1988) and corollary motor inputs (Ghosh 1997), area 5 is primed to receive tactile information about an obstacle. Direct projections from primary sensory cortex (Jones and Powell 1970) enable area 5 to respond to cutaneous inputs (Sakata et al. 1973; Scannell et al. 1995), such as the collision of the forelegs with an obstacle. Thus it is perhaps unsurprising that the present study demonstrates the role of area 5 in tasks dependent on visual or tactile information about the environment.

However, it remains to be determined if previously described memory delay-related activity recorded in area 5 during a similar visual obstacle memory task (Lajoie et al. 2010) is similarly present in our tactile variation. Specifically, elucidating whether it is identical or distinct neural populations that are active during visual and tactile variations will provide insights into the nature of the neural signals observed in area 5. For example, if distinct subpopulations of area 5 neurons are recruited for visual and tactile obstacle working memory maintenance, then area 5 may indeed store visual or tactile information about the obstacle, respectively, during the working memory delay. Conversely, if the same group of neurons is recruited regardless of sensory input modality, area 5 may be more closely related to retaining the impending motor intention for elevated hindleg stepping. Alternatively, delay-related neural activity in area 5 may not be purely sensory or purely motor in nature. As the resiliency of visual or tactile obstacle working memory is improved if the forelegs have cleared the obstacle (McVea and Pearson 2007a; Wong et al. 2018), efference motor commands and proprioceptive information about foreleg movements may also contribute to the neural signal observed in area 5 (Lajoie et al. 2012). These diverse inputs to area 5 from visual, somatosensory, and motor cortices could be integrated to form a representation of the body in relation to near objects, or body schema (Graziano and Botvinick 2002; Ivanenko et al. 2011), used to guide locomotor movements. Delay-related neural activity may represent such higher order awareness of the obstacle beneath the body that could be used to modulate hindleg stepping when walking resumes.

4.5.3 Utility of transient, reversible deactivations

While studies employing lesions have been essential in elucidating the functional role of particular brain regions, such permanent damage precludes the ability to assess the contributions of an area to distinct stages of working memory. In the present study, cooling permitted temporal control to cortical deactivations, allowing discrete parietal areas to be switched “on” or “off” during different phases of working memory testing. Restricting area 5 deactivation to the working memory maintenance phase was sufficient in reproducing memory deficits observed when area 5 was cooled throughout visual or tactile tests. Previous electrophysiological recordings in walking cats reported a subset of area 5 cells that exhibit sustained activation when an obstacle passes under the body and remains straddled between the fore- and hindlimbs if forward locomotion is paused (Lajoie et al. 2010) – equivalent to the working memory maintenance phase of the present study. Thus working memory deficits resulting from maintenance phase deactivation are likely due to the silencing of such cells, implicating their direct involvement in maintaining the working memory of an obstacle when locomotion is delayed.

Additionally, area 5 deactivation to the working memory acquisition phase resulted in partial working memory deficits. It must be noted, however, that the temporal resolution of cooling-induced deactivations is admittedly not as precise as optogenetically-induced inhibition (compare with Kopec et al. 2015). While cooling offers greater temporal control to cortical deactivations in comparison to those achieved pharmacologically (compare with Winters and Bussey 2005), a span of about 6 to 16 seconds typically separates cooling onset or offset from the silencing or restoration of neural activity, respectively (Lomber et al. 1999). In comparison, optogenetic approaches ensures inhibition onset and offset within 60 ms of laser stimulation (Kopec et al. 2015). This temporal limitation of cooling-induced deactivation reflects the thermodynamic properties of cortical tissue. As such, the delays used to examine parietal cortex contributions to obstacle working memory maintenance and acquisition were sufficiently long enough to permit deactivation or reactivation of parietal areas following cooling onset or offset, respectively. However, despite these efforts to separate working memory acquisition from maintenance, it is possible that despite terminating cooling immediately following foreleg clearance over the obstacle, neurons remained inactive into the early stages of the working memory maintenance phase. As such, we must acknowledge that the observed partial memory deficits may result from area 5 deactivation during working memory acquisition and early working memory maintenance. Future work employing more temporally precise deactivation techniques will provide further insight into the role of area 5 in obstacle working memory acquisition in the walking cat.

4.5.4 Redundant working memory systems involve multiple brain regions

Obstacle working memory recovery (albeit partial) following restoration of area 5 function during memory maintenance suggests that maintenance phase deactivation of area 5 may suppress, but not completely eliminate the working memory of the obstacle. Such recovery may be possible if information about the obstacle is relayed to area 5 continuously or repetitively during working memory maintenance. This would implicate another region or structure in the working memory circuitry, although the identity of such an area or areas, and its connectivity to area 5 remains elusive. Given the incomplete memory recovery, it is possible that reverberating activity (Hebb 1949; Sejnowski 1999) between area 5 and another area is responsible for maintaining obstacle working memory. This configuration suggests that deactivating area 5 during early working memory maintenance reduces the overall activity of this reverberating circuitry. Thus despite restoring area 5 function later in the maintenance phase, the memory of the obstacle may be incomplete or less robust, resulting in only partial memory recovery. Similarly, partial working memory deficits were observed following acquisition phase area 5 deactivation. Such deficits may arise if cortical cooling interferes with the relay of information about the obstacle to area 5, again implicating another area or region in the working memory system.

The involvement of other brain regions in working memory-related processes would establish functional redundancies that provide safeguarding mechanisms preventing data loss (Li et al. 2016; Yu 2016). As no brain structure appears to be unique or specific to working memory (Eriksson et al. 2015), memory-related processing is likely distributed across and involves multiple brain areas (Fuster and Bressler 2012). In addition to parietal area 5, working memory-guided obstacle locomotion may also recruit prefrontal (Fuster and Alexander 1971; Goldman-Rakic 1995), premotor (Simon et al. 2002; Lorey et al. 2011), and motor cortical areas (Tomasino and Gremese 2016). Furthermore, the possibility of subcortical contributions to working memory-guided obstacle locomotion cannot be overlooked. Transient optogenetic inactivation of both cortical and subcortical brain regions in the rat revealed contributions of a frontal cortical region and the superior colliculus in both the acquisition and maintenance of working memory for orienting (Kopec et al. 2015). Thus while our discrete deactivations of a single area of parietal cortex resulted in behaviourally relevant memory impairments, these results likely demonstrate the role of a single player within a network of multiple areas and regions that mediate working memory-guided obstacle avoidance. Further electrophysiological and anatomical work will aid in identifying other players in the obstacle working memory circuitry.

4.6 References

Andersson O, Forssberg H, Grillner S, Lindquist M. 1978. Phasic gain control of the transmission in cutaneous reflex pathways to motoneurones during “fictive” locomotion. Brain Res. 149:503–507.

Avendaño C, Rausell E, Perez-Aguilar D, Isorna S. 1988. Organization of the association cortical afferent connections of area 5: a retrograde tracer study in the cat. J Comp Neurol. 278:1–33.

Drew T, Andujar JE, Lajoie K, Yakovenko S. 2008. Cortical mechanisms involved in visuomotor coordination during precision walking. Brain Res Rev. 57:199–211.

Drew T, Jiang W, Kably B, Lavoie S. 1996. Role of the motor cortex in the control of visually triggered gait modifications. Can J Physiol Pharmacol. 74:426–442.

Drew T, Marigold DS. 2015. Taking the next step: cortical contributions to the control of locomotion. Curr Opin Neurobiol. 33:25–33.

Eriksson J, Vogel EK, Lansner A, Bergström F, Nyberg L. 2015. Neurocognitive architecture of working memory. Neuron. 88:33–46.

Forssberg H. 1979. Stumbling corrective reaction: a phase-dependent compensatory reaction during locomotion. J Neurophysiol. 42:936–953.

Forssberg H, Grillner S, Halbertsma J. 1980. The locomotion of the low spinal cat. I. Coordination within a hindlimb. Acta Physiol Scand. 108:269–281.

Fuster JM, Alexander GE. 1971. Neuron activity related to short-term memory. Science. 173:652–654.

Fuster JM, Bressler SL. 2012. Cognit activation: a mechanism enabling temporal integration in working memory. Trends Cogn Sci. 16:207–218.

Ghosh S. 1997. Cytoarchitecture of sensorimotor areas in the cat cerebral cortex. J Comp Neurol. 388:354–370.

Goldman-Rakic P. 1995. Cellular basis of working memory. Neuron. 14:477–485.

Graziano MSA, Botvinick MM. 2002. How the brain represents the body: insights from neurophysiology and psychology. In: Prinz W,, Hommel B, editors. Common mechanisms in perception and action: Attention and performance. Oxford: Oxford University Press. p. 136–157.

Grillner S. 2011. Control of Locomotion in Bipeds, Tetrapods, and Fish, Comprehensive Physiology. Hoboken, NJ, USA: John Wiley & Sons, Inc.

Hebb DO. 1949. Organization of Behavior. New York: John Wiley and Sons.

Heijnen MJH, Romine NL, Stumpf DM, Rietdyk S. 2014. Memory-guided obstacle crossing: More failures were observed for the trail limb versus lead limb. Exp Brain Res. 232:2131–2142.

Ivanenko YP, Dominici N, Daprati E, Nico D, Cappellini G, Lacquaniti F. 2011. Locomotor body scheme. Hum Mov Sci. 30:341–351.

Jones EG, Powell TPS. 1970. An anatomical study of converging sensory pathways within the cerebral cortex of the monkey. Brain. 93:793–820.

Jonides J, Lewis RL, Nee DE, Lustig CA, Berman MG, Moore KS. 2008. The mind and brain of short-term memory. Annu Rev Psychol. 59:193–224.

Kopec CD, Erlich JC, Brunton BW, Deisseroth K, Brody CD. 2015. Cortical and subcortical contributions to short-term memory for orienting movements. Neuron.

88:367–377.

Lajoie K, Andujar J-E, Pearson KG, Drew T. 2010. Neurons in area 5 of the posterior parietal cortex in the cat contribute to interlimb coordination during visually guided locomotion: a role in working memory. J Neurophysiol. 103:2234–2254.

Lajoie K, Bloomfield LW, Nelson FJ, Suh JJ, Marigold DS. 2012. The contribution of vision, proprioception, and efference copy in storing a neural representation for guiding trail leg trajectory over an obstacle. J Neurophysiol. 107:2283–2293.

Li N, Daie K, Svoboda K, Druckmann S. 2016. Robust neuronal dynamics in premotor cortex during motor planning. Nature. 532:459–464.

Lomber SG, Malhotra S. 2008. Double dissociation of “what” and “where” processing in auditory cortex. Nat Neurosci. 11:609–616.

Lomber SG, Meredith MA, Kral A. 2010. Cross-modal plasticity in specific auditory cortices underlies visual compensations in the deaf. Nat Neurosci. 13:1421–1427.

Lomber SG, Payne BR. 2000a. Contributions of cat posterior parietal cortex to visuospatial discrimination. Vis Neurosci. 17:701–709.

Lomber SG, Payne BR. 2000b. Translaminar differentiation of visually guided behaviors revealed by restricted cerebral cooling deactivation. Cereb Cortex. 10:1066–1077.

Lomber SG, Payne BR, Horel JA. 1999. The cryoloop: An adaptable reversible cooling deactivation method for behavioral or electrophysiological assessment of neural function. J Neurosci Methods. 86:179–194.

Lorey B, Pilgramm S, Bischoff M, Stark R, Vaitl D, Kindermann S, Munzert J, Zentgraf K. 2011. Activation of the parieto-premotor network is associated with vivid motor imagery--a parametric FMRI study. PLoS One. 6:e20368.

McVea DA, Pearson KG. 2006. Long-lasting memories of obstacles guide leg movements in the walking cat. J Neurosci. 26:1175–1178.

McVea DA, Pearson KG. 2007a. Stepping of the forelegs over obstacles establishes long-lasting memories in cats. Curr Biol. 17:R621–R623.

McVea DA, Pearson KG. 2007b. Contextual learning and obstacle memory in the walking cat. Integr Comp Biol. 47:457–464.

McVea DA, Taylor AJ, Pearson KG. 2009. Long-lasting working memories of obstacles established by foreleg stepping in walking cats require area 5 of the posterior parietal cortex. J Neurosci. 29:9396–9404.

Mellott JG, Van der Gucht E, Lee CC, Carrasco A, Winer JA, Lomber SG. 2010. Areas of cat auditory cortex as defined by neurofilament proteins expressing SMI-32. Hear Res. 267:119–136.

Mohagheghi AA, Moraes R, Patla AE. 2004. The effects of distant and on-line visual information on the control of approach phase and step over an obstacle during locomotion. Exp Brain Res. 155:459–468.

Patla AE, Prentice SD, Robinson C, Neufeld J. 1991. Visual control of locomotion: strategies for changing direction and for going over obstacles. J Exp Psychol Hum Percept Perform. 17:603–634.

Patla AE, Vickers JN. 1997. Where and when do we look as we approach and step over an obstacle in the travel path? NeuroReport. 8:3661–3665.

Payne BR, Lomber SG. 1996. Age dependent modification of cytochrome oxidase activity in the cat dorsal lateral geniculate nucleus following removal of primary visual cortex. Vis Neurosci. 13:805–816.

Sakata H, Takaoka Y, Kawarasaki A, Shibutani H. 1973. Somatosensory properties of neurons in the superior parietal cortex (area 5) of the rhesus monkey. Brain Res. 64:85–102.

Scannell JW, Blakemore C, Young MP. 1995. Analysis of connectivity in the cat cerebral cortex. J Neurosci. 15:1463–1483.

Sejnowski TJ. 1999. The book of Hebb. Neuron. 24:773–776.

Setogawa S, Yamaura H, Arasaki T, Endo S, Yanagihara D. 2014. Deficits in memory-guided limb movements impair obstacle avoidance locomotion in Alzheimer's disease mouse model. Sci Rep. 4:7220.

Simon SR, Meunier M, Piettre L, Berardi AM, Segebarth CM, Boussaoud D. 2002. Spatial attention and memory versus motor preparation: premotor cortex involvement as revealed by fMRI. J Neurophysiol. 88:2047–2057.

Squatrito S, Galletti C, Battaglini PP, Sanseverino ER. 1981. An autoradiographic study of bilateral cortical projections from cat area 19 and lateral suprasylvian visual area. Arch Ital Biol. 119:21–42.

Takakusaki K. 2013. Neurophysiology of gait: From the spinal cord to the frontal lobe. Mov Disord. 28:1483–1491.

Tomasino B, Gremese M. 2016. The cognitive side of M1. Front Hum Neurosci. 10:298.

van der Gucht E, Vandesande F, Arckens L. 2001. Neurofilament protein: A selective marker for the architectonic parcellation of the visual cortex in adult cat brain. J Comp Neurol. 441:345–368.

Westwood DA, Heath M, Roy EA. 2003. No evidence for accurate visuomotor memory: systematic and variable error in memory-guided reaching. J Mot Behav. 35:127–133.

Whishaw IQ, Sacrey LAR, Gorny B. 2009. Hind limb stepping over obstacles in the horse guided by place-object memory. Behav Brain Res. 198:372–379.

Wilkinson EJ, Sherk HA. 2005. The use of visual information for planning accurate steps in a cluttered environment. Behav Brain Res. 164:270–274.

Winters BD, Bussey TJ. 2005. Transient inactivation of perirhinal cortex disrupts encoding, retrieval, and consolidation of object recognition memory. J Neurosci.

25:52–61.

Wong C, Chabot N, Kok MA, Lomber SG. 2014. Modified areal cartography in auditory cortex following early- and late-onset deafness. Cereb cortex. 24:1778–1792.

Wong C, Wong G, Pearson KG, Lomber SG. 2018. Memory-guided stumbling correction in the hindlimb of quadrupeds relies on parietal area 5. Cereb Cortex. 28:561–573.

Yu BM. 2016. Neuroscience: Fault tolerance in the brain. Nature. 532:449–450.

Chapter 5

5 Stable delay period representations in the posterior parietal cortex facilitate working memory-guided obstacle negotiation[4]

5.1 Abstract

In complex environments, information about surrounding obstacles is stored in working memory (WM) and used to coordinate appropriate movements for avoidance. In quadrupeds, this WM system is particularly important for guiding hindleg stepping, as an animal can no longer see the obstacle underneath the body following foreleg clearance. Such obstacle WM involves the posterior parietal cortex (PPC), as deactivation of area 5 incurs WM deficits precluding successful avoidance. However, the neural underpinnings of this involvement remain undefined. To reveal the neural substrates of this behavior, microelectrode arrays were implanted to record neuronal activity in area 5 during an obstacle WM task in cats. Early in the WM delay, neurons were modulated generally by obstacle presence, or more specifically in relation to foreleg step height. Thus information about the obstacle or about foreleg clearance can be retained in WM. In a separate set of neurons, this information was recalled later in the delay in order to plan subsequent hindleg stepping. Such early and late delay period signals were temporally bridged by neurons exhibiting obstacle-modulated activity sustained throughout the delay. These neurons represented a specialized subset of all recorded neurons that maintained stable information coding across the WM delay. Ultimately, these various patterns of task-related modulation enable stable representations of obstacle-related information within the PPC to support successful WM-guided obstacle negotiation in the cat.

---

[4] A version of this chapter is currently in review:

Wong C, Lomber SG. Stable delay period representations in the posterior parietal cortex facilitate working memory-guided obstacle negotiation. Current Biology. Revision requested. Manuscript #D-18-00939.

5.2 Introduction

The extraordinary capabilities of locomotor control systems are illustrated by the ability of animals to traverse complex, naturalistic environments without much conscious effort. Sensory information obtained about obstacles in the environment can be used to modify stepping in a feedforward manner (Patla and Vickers 1997; Mohagheghi et al. 2004; Wilkinson and Sherk 2005) allowing, for example, mountain goats to scale precarious rocky ledges while grazing, foxes to chase prey through a dense forest, or humans to maintain a conversation without colliding into other people or objects while walking through a busy crowd. This relative ease of obstacle locomotor behaviors is facilitated by the ability to store information about an obstacle in working memory (WM) that can be used to coordinate the appropriate movements for avoidance. In quadrupedal animals, obstacle WM is especially important for ensuring hindlimb clearance as the animal can no longer see the obstacle once it has passed under the body. Instead, an internal representation of the obstacle maintained in WM may be used to guide hindleg stepping (McVea and Pearson 2006, 2007a; Whishaw et al. 2009).

This WM system has been studied using an experimental paradigm (McVea and Pearson 2006) that leverages naturalistic behaviours whereby quadrupedal animals may delay obstacle clearance between their four legs as they graze, explore new terrain, or track prey in complex environments. In this experimental paradigm, food is used to encourage cats to walk towards and step over an obstacle with their forelegs. Obstacle clearance is then delayed as the animals eat, during which the obstacle is covertly removed from the walkway. When walking resumes, elevated hindleg stepping observed even after delays tested up to 10 minutes demonstrates a robust, long-lasting WM of the obstacle used to guide hindleg clearance. We previously used cooling-induced cortical deactivations via chronically implanted cryoloops (Lomber et al. 1999; Wong and Lomber 2017) to demonstrate the role of the posterior parietal cortex in this WM-guided behavior (Wong et al. 2017, 2018). Furthermore, by temporally restricting deactivations to the delay in which animals must maintain information about the obstacle in WM, we attributed a role of parietal area 5 in WM maintenance. Such deactivations may preclude activity of parietal area 5 neurons involved in interlimb coordination for visually-guided obstacle locomotion, which have been shown to exhibit sustained activation if obstacle negotiation is delayed between foreleg-hindleg or hindleg-hindleg clearance (Lajoie et al. 2010). However, the neural underpinnings of this WM contribution remain unclear.

WM has been extensively examined often by studying memory-guided eye and arm movements in human and non-human primates (Goldman-Rakic 1995; Pasternak and Greenlee 2005; Leavitt et al. 2017). Neural correlates of WM maintenance were first described in macaque prefrontal neurons that demonstrated elevated activity sustained throughout the delay period of a WM task in the absence of a visual cue (Fuster and Alexander 1971; Kubota and Niki 1971). Such persistent delay period activity thought to represent maintenance of relevant sensory cues and or movement plans in WM have been similarly described in numerous prefrontal (Funahashi et al. 1993; Takeda and Funahashi 2002, 2004) and parietal (Gnadt and Andersen 1988; Koch and Fuster 1989; Murata et al. 1996; Snyder et al. 1997; Fiehler et al. 2011; Singhal et al. 2013) areas. However, more recent work has suggested that stable delay period activity need not be relevant or necessary for WM (Rainer and Miller 2002; Riggall and Postle 2012; Postle 2015; Stokes 2015). Additionally, the activity of individual neurons (Shafi et al. 2007) or entire recording populations (Spaak et al. 2017) can be highly dynamic throughout a delay, and may exhibit a series of rapid state transitions following an instructional cue in a working memory task (Stokes et al. 2013). Such phasic, rather than persistent, modulation occurring momentarily throughout a delay period has been suggested to be important for information encoding and movement planning in WM tasks (Fuster 1984; Quintana and Fuster 1999; Wang et al. 2015).

As these concepts associated with WM have typically been examined in explicitly instructed, movement restricted testing paradigms, the neural correlates of WM and applicability of these concepts in more naturalistic multi-effector behaviours, such as obstacle locomotion, warrants further investigation. While a single study has reported individual neurons exhibiting sustained delay period activation that may serve as a WM correlate of obstacle-related information (Lajoie et al. 2010), the potential for more dynamic coding on the single neuron and population level has yet to be examined.

Furthermore, the specificity and extent of these neural contributions to WM-guided obstacle locomotion require further investigation.

Therefore, in the present study, microelectrode arrays were implanted in the same region of parietal area 5 that elicits obstacle WM deficits when deactivated. The purpose of this work was to determine if WM-guided obstacle negotiation modulates neural activity in parietal area 5 of the cat. Specifically, we aimed to investigate whether area 5 neurons in the cat demonstrate the classic WM property of sustained delay period activity, or instead exhibit phasic delay period modulation. Furthermore, we assessed whether the observed modulation was related to motor output by examining stepping flanking the delay period. The specificity of this WM-related activity was examined by varying the position of the obstacle during the delay, and the sensory modality through which obstacle information was obtained during the approach. Finally, the ability of recorded neurons to discriminate between obstacle conditions throughout a trial was assessed to examine population level coding and dynamicism.

Overall, these recordings revealed multiple possible patterns of obstacle-related and WM-related activity within the posterior parietal cortex of the cat. Sustained or phasic delay period modulation may convey information about the obstacle or step height required for clearance. However, with such patterns of delay period activity comprising a relatively small proportion of all recorded neurons, the presence or absence of the obstacle was only reliably discernable before and after the delay within the dynamic population level activity. In contrast, discriminability remained robust in the subset of neurons exhibiting sustained delay period modulation. Thus altogether, stable representations of obstacle-related information maintained throughout the WM delay in a specialized subset of parietal area 5 neurons support successful WM-guided obstacle negotiation in the cat.

5.3 Methods

5.3.1 Experimental Model and Subject Details

WM-guided obstacle locomotion was examined in two mature (>6M) female cats (Liberty Labs, NY). All procedures were conducted in compliance with the National Research Council's Guide for the Care and Use of Laboratory Animals (eighth edition;

2011) and the Canadian Council on Animal Care's Guide to the Care and Use of Experimental Animals (1993), and were approved by the University of Western Ontario Animal Use Subcommittee of the University Council on Animal Care.

5.3.2 Method Details

5.3.2.1 Behavioral paradigm

Obstacle WM was assessed by comparing obstructed (OP) with unobstructed (OA) locomotion using the same apparatus described previously (Wong and Lomber 2017; Wong et al. 2017, 2018). In OP trials, each animal approached and stepped over a 25.8 cm wide x 8.7 cm high x 3 mm thick obstacle raised onto the surface of the walkway (Fig. 5.1A). Forward locomotion was delayed following foreleg clearance, such that the obstacle was straddled between the forelegs and hindlegs during the delay (foreleg-hindleg (FH) trials). Alternatively, forward locomotion could be delayed after the forelegs and one of the hindlegs had stepped over the obstacle such that the obstacle was straddled between the two hindlegs during the delay (hindleg-hindleg (HH) trials; see Fig. 5.7A). To assess obstacle working memory in a visually independent manner, a tactile variation of obstacle present (TOP) trials was also examined (Wong et al. 2018). In this condition, each animal would approach food placed on an elevated plate in the absence of the obstacle (lowered; see Fig. 5.8A). As the animal ate, the obstacle would be covertly raised onto the walkway directly beneath the food plate to prevent any visual input of the obstacle. The food was then moved forwards to encourage the animal to resume locomotion, resulting in the forelegs contacting the unexpected obstacle before stepping over it. Forward locomotion was then delayed in a similar manner to foreleg-hindleg trials, with the obstacle in between the forelegs and hindlegs beneath the body. For all three OP variations, the obstacle was covertly lowered to become flush with the walkway during the delay to prevent any further visual or tactile inputs. Locomotion was resumed at the end of the delay by moving the food forward. In unobstructed trials, locomotion was similarly delayed with the lowered (absent) obstacle. All trials were digitally recorded at 50 frames/s for subsequent frame-by-frame analyses to denote start and end frames for each delay period and step. Each recording session consisted of at least 10 OP trials, and 10 OA trials. When HH testing was conducted, a minimum of 10

Figure 5.1 Experimental task and microelectrode array placement in parietal area 5.

(A) Schematic depicting an obstacle present trial where each animal would approach and step over an obstacle with its forelegs. Forward locomotion was then delayed, during which the obstacle was covertly removed before walking continued. Hindleg step height was measured and compared to stepping observed in obstacle absent trials to assess working memory.

(B) Bar plots depicting mean step height ± SEM for foreleg and hindleg steps in approach and continuation phases. Relative to obstacle absent trials, foreleg and hindleg stepping was significantly elevated during obstacle present approach and continuation, respectively.

(C) Lateral view of the cat cerebrum depicting right parietal area 5 in green with the array placement indicated in white. Black rectangle outlines location of image in (D). D – dorsal, A – anterior.

(D) Photograph taken during surgical implantation depicting the placement of the floating microelectrode array relative to the ansate and lateral sulci indicated in dashed lines. Black horizontal scale bar = 3 mm.

Figure 5.1

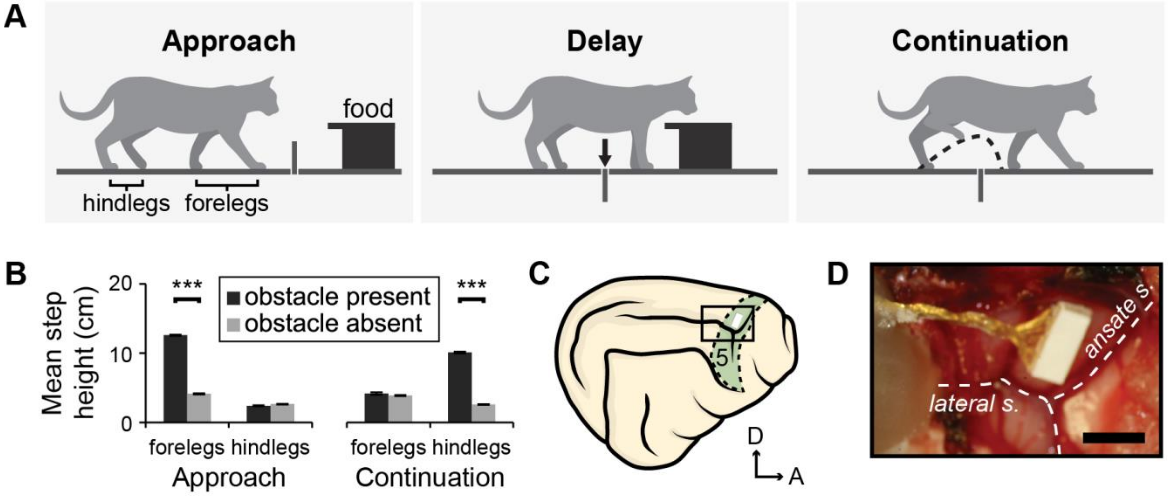
A
Approach
food
hindlegs
forelegs
Delay
Continuation
B
Mean step height (cm)
20
10
0
***
obstacle present
obstacle absent
***
forelegs
hindlegs
Approach
forelegs
hindlegs
Continuation
C
5
D
A
D
ansate s.
lateral s.

of these trials were completed. Given the propensity for animals to develop a learned avoidance response to repeated foreleg obstacle contact (McVea and Pearson 2007b), TOP trials were completed no more than 5 times throughout a single recording session. Thus the subset of units included in the TOP analysis was dependent on unit stability (see below) to ensure that a minimum of 10 TOP trials were included in the statistical analyses.

5.3.2.2 Microelectrode arrays and implantation

Under general anaesthesia, a 32 electrode floating microelectrode array (FMA; MicroProbes for Life Science, Gaithersburg, MD) was implanted in parietal area 5 of each hemisphere, at the junction of the ansate and lateral sulci, to mimic placement of cryoloops in previous studies (Wong et al. 2017, 2018). Each animal was anesthetized using sodium pentobarbital (25 mg/kg to effect i.v.) or alfaxan (4-6 mg/kg to effect i.v.) and intubated. A craniotomy was made over each hemisphere between coordinates A15-A25 and L2-L14 (Horsley and Clarke 1908). Bone screws were placed around each craniotomy to anchor dental acrylic. For each craniotomy, the dura was cut and reflected to better visualize parietal area 5 in order to plan the placement of each array and its connector. To place the array, the wax coating protecting the electrodes was first removed with warm saline. A vacuum inserter tool (MicroProbes) attached to a stereotaxic surgical arm held the array while the connector was held by the experimenter. The stereotaxic arm was used to slowly lower the array into the cortex, with brief waiting periods in between small increments to circumvent cortical dimpling. Once the ceramic substrate of the array contacted the cortical surface, the array was held in place with blunt forceps before disabling the vacuum. Using dental acrylic, the array wire was anchored to a nearby point on the skull ensuring sufficient slack between the array and anchor point, before anchoring the connector. The dura was then replaced and the craniotomy was covered in Gelfoam before closing with dental acrylic. The contralateral array was then implanted using similar procedures. Each animal was provided with standard postoperative care and experienced an uneventful recovery.

Each array had an interelectrode distance of 400 μm, impedance of about 0.5 MΩ, and electrode lengths that varied between 0.9-1.5 mm. During each recording session, neural signals from the array were passed through a ZIF-clip headstage (ZC32; Tucker-Davis Technologies, Alachua, FL), filtered from 0.1 to 10,000 Hz, amplified (x10,000), digitized at ~25kHz (RZ5; Tucker-Davis Technologies), and saved to disk for offline analysis.

5.3.2.3 Spike sorting

Spike activity was detected offline by first isolating spiking activity with an acausal filter between 700 and 7000 Hz. The common average reference was then computed and subtracted from all electrode channels (Ludwig et al. 2009). A threshold set at 4 times the standard deviation of the filtered signal using 10 second chunks of data was applied for spike detection (Quiroga et al. 2004). Spike waveforms were then aligned by their largest peak, and extracted with their timestamps. For each electrode channel, waveforms were then de-noised and sorted in Offline Sorter (Plexon, Dallas TX) using T-Distribution Expectation Maximization. Waveforms and timestamps of isolated units were then exported for subsequent analyses.

5.3.2.4 Determining unit stability across recording sessions

Unit stability was assessed in a manner similar to Richardson et al. (Richardson et al. 2012). The stability analysis ensured that a stable unit that was recorded on multiple days was not included as separate units in the total recording population. For each isolated unit within a recording session, three attributes were used to assess between-session stability: the mean spike waveform (MSW), interspike interval histogram (ISIH) (Chen and Fetz 2005; Dickey et al. 2009), and perievent spike rate (PESR). The ISIH was constructed using 100 bins uniformly spaced on a logarithmic scale from 0.1 ms to 10 s. The PESR was constructed as the spike rate in 50 ms bins across three perievent windows (-1.0 to 0 s to delay onset (approach), 0 to 1.0 s following delay onset (delay), and 0 to 1.0 s following delay end (continuation)) concatenated together and averaged over OP trials completed within each session.

Next, the similarity between attributes for each pair of units across all channels and sessions was examined. To compare the similarity of MSWs, Pearson's correlation coefficient (CC) was computed for each pair. To compare the similarity of ISIHs, the

Kolmogorov-Smirnov (KS) statistic was computed for each pair. Pearson’s correlation coefficient was also computed to compare the similarity of PESRs. For each of the three attributes, the similarity statistics were compiled for all pairs of units recorded on different channels. Since the same unit could not be recorded on multiple channels given the interelectrode distance of 400 μm, the similarity statistics of paired units from different channels comprised the “true negative” populations. To determine whether a pair of units recorded on the same channel was the same unit, the proportion of the “true negative” population of MSW CCs that was greater than that of the MSW CC of the given pair was determined. Similarly, the proportion of the “true negative” population of PESR CCs that was greater than that of the pair was determined. Additionally, the proportion of the “true negative” population of ISIH KSs that was less than the given pair was determined. The probability of unit stability for the pair (P) was computed as the product between these three proportions. Significant pairings ($P < 0.001$) were grouped to determine the total number of days for which a stable unit was present to ensure that trials from the appropriate days were included in subsequent analyses. An example of a unit deemed stable for 5 days from these analyses is depicted in Figure 5.2. Note the similarities in the three attributes, MSW, ISIH, and PESR across all 5 days (Fig. 5.2A-C). Additionally, note the similarities in raster plots and histograms of unit activity aligned to delay starts of FH trials recorded on days 2 and 3 (Fig. 5.2D,G). Likewise, the similarities between raster plots and histograms of HH delay aligned activity from days 2 and 3 (Fig. 5.2E,H), and the similarities between OA plots from days 2 and 3 (Fig. 5.2F,I) demonstrate the effectiveness of the unit stability analyses.

5.3.3 Quantification and Statistical Analysis

For each isolated unit, mean firing rates were first compared between OP and OA trials during the approach, delay, and continuation phases of each trial with a two-way ANOVA to assess possible effects of obstacle condition (present or absent) and trial phase (approach, delay, continuation). If a significant interaction effect was detected, firing rates were subsequently compared between obstacle conditions with an unpaired t-test for each of the three phases. Given the three comparisons between obstacle conditions during approach, delay, and continuation, statistical significance was accepted

Figure 5.2 Example unit determined to be stable across 5 consecutive recording days.

(A-C) Different coloured lines indicate the mean spike waveform (MSW; A), interspike interval histogram (ISIH; B), and perievent spike rate (PESR; C) recorded on different days for this unit.

(D-I) Histograms and perievent raster plots recorded on day 2 (D-F, red) and day 3 (G-I, blue). Between the two depicted recording days, note the similarities in the histograms and rasters aligned to obstacle present foreleg-hindleg (FH) trials (D,G), obstacle present hindleg-hindleg (HH) trials (E,H), and obstacle absent trials (F,I).

Figure 5.2

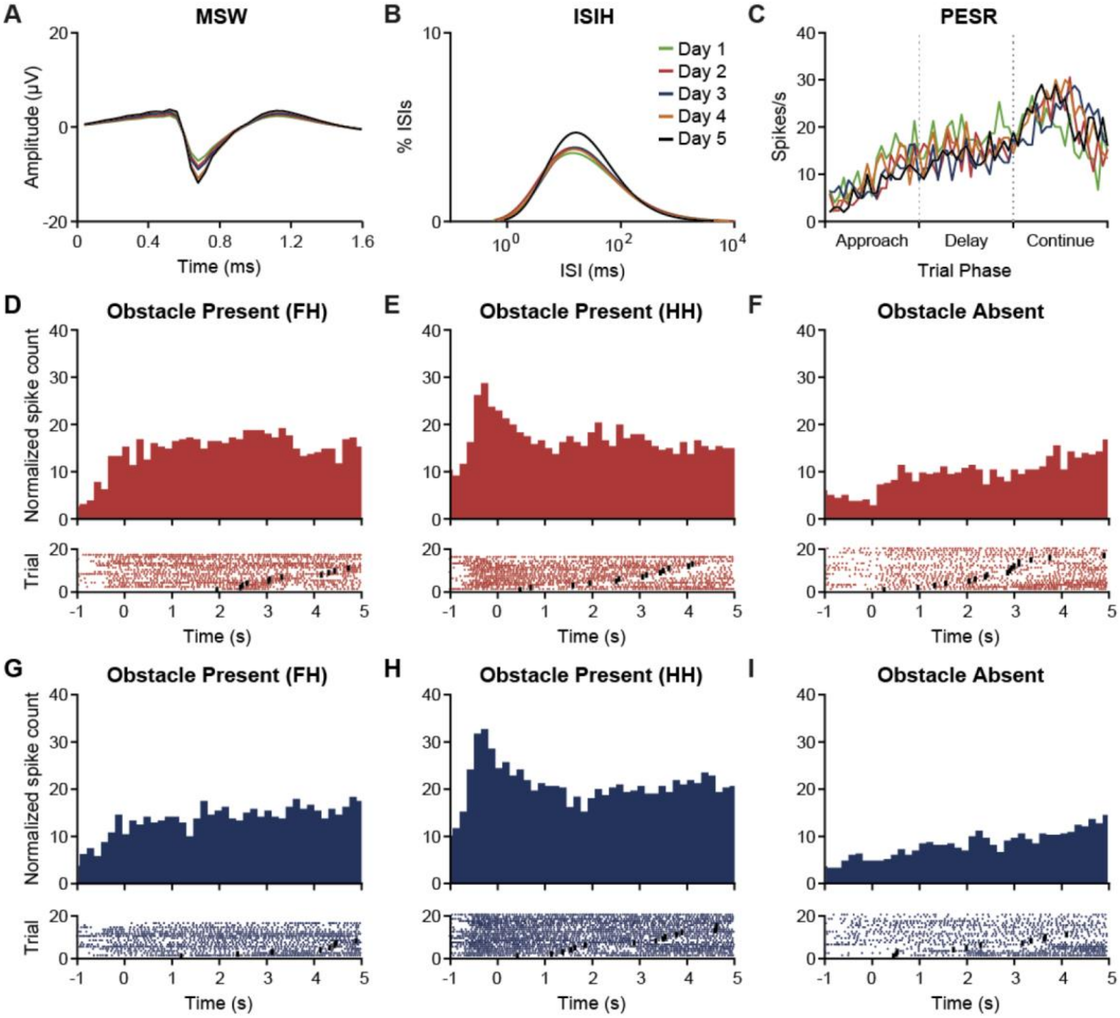
A
MSW
Amplitude (μV)
Time (ms)
B
ISIH
% ISIs
ISI (ms)
Day 1
Day 2
Day 3
Day 4
Day 5
C
PESR
Spikes/s
Approach
Delay
Continue
Trial Phase
D
Obstacle Present (FH)
E
Obstacle Present (HH)
F
Obstacle Absent
Normalized spike count
Trial
Time (s)
G
Obstacle Present (FH)
H
Obstacle Present (HH)
I
Obstacle Absent
Normalized spike count
Trial
Time (s)

at a Bonferroni corrected *p* value of 0.0167. For units that demonstrated obstacle-modulated activity during the delay, Pearson's correlation coefficient was computed to assess the relationship between delay period activity and step height of the leading and trailing forelegs preceding the delay, and the leading and trailing hindlegs following the delay. As the majority of posterior parietal neurons are modulated in relation to leading steps over an obstacle, regardless of whether the lead limb is ipsilateral or contralateral to the recording site (Andujar et al. 2010; Lajoie et al. 2010), the analyses used in the present study examined trials where the leading limb could be ipsilateral or contralateral to the recording array.

Additionally, to assess phasic WM-related delay activity, spike rates during the first and last second of the delay for trials with delays of 2 s or more were compared between obstacle conditions using unpaired t-tests. For obstacle-modulated units during early or late delay periods, the relationship between early or late delay period activity, respectively, and step height was similarly assessed by computing Pearson's correlation coefficient.

To assess the specificity of obstacle modulation, unit activity was subsequently compared between FH, HH, and OA trials. A two-way ANOVA was used to assess possible effects of obstacle condition (FH, HH, OA) and trial phase (approach, delay, continuation) on the activity of each unit. Delay period modulation was further examined for units demonstrating significant interaction effects by comparing firing rates between obstacle conditions with a one-way univariate ANOVA. The relationship between delay period activity, respectively, and step height was assessed by computing Pearson's correlation coefficient for units demonstrating modulated delay period activity. Additionally, to assess the visual dependency of obstacle modulation, early, late, and whole delay period activity was similarly compared between VOP, TOP, and OA trials.

Finally, to examine population level activity, discriminability and dynamicism were assessed with methods similar to Spaak et al. (2017). Briefly, all OP (FH) trials and OA trials were randomly assigned to one of two independent splits. Within each split, the difference between mean firing rates for OP and OA conditions was computed for each neuron. The correlation between these differences between the two splits for all neurons provides a measure of the ability of the recording population to discriminate between OP and OA trials. Discriminability was assessed across two hundred time points comprising the second before and after delay starts or delay ends, constituting the approach-delay and delay-continuation epochs, respectively. Significance was assessed using permutation tests where OP and OA trial designations were randomly shuffled 1000 times. Additionally, to assess the dynamicism or stability in obstacle information coding, the difference in mean firing rates at one time point was correlated to differences at every other time point, resulting in a 200 x 200 matrix for each epoch. While highly correlated differences across all time points between splits indicates stable working memory coding, poorly correlated differences across all time points indicates optimal discriminability only between neighbouring time points, and therefore, dynamic working memory coding. Thus dynamicism was indicated by significant off-diagonal reduction from on-diagonal values. Significance was assessed using permutation tests where off- and on-diagonal values were randomly shuffled 1000 times. For detailed methodology and formulas, please refer to Spaak et al. (2017).

5.4 Results

5.4.1 Modulated posterior parietal cortex activity during WM-guided obstacle negotiation

Neural activity was recorded from parietal area 5 of two cats during both obstructed and unobstructed locomotion. To examine WM-guided obstacle avoidance, each trial was composed of three phases: the approach, delay, and continuation. Previous examinations of this paradigm demonstrated that foreleg obstacle clearance establishes robust, long-lasting working memories of the obstacle used to guide delayed hindleg clearance (McVea and Pearson 2007a). Therefore, during trials where the obstacle was present (OP), the initial approach phase consisted of the animals stepping over the obstacle with only their forelegs (Fig. 5.1A). Obstacle clearance was then delayed before clearance of the hindlegs. For the present analyses, the start of the delay was defined as the time at which a stationary stance was assumed following trailing foreleg clearance, typically occurring after one to two subsequent hindleg steps. During the delay, the obstacle was covertly removed from between the forelegs and hindlegs before walking resumed. In comparison to trials where the obstacle was absent (OA), elevated hindleg step height observed during the continuation phase of OP trials demonstrated the ability of animals to remember the obstacle over which the forelegs had stepped (Fig. 5.1B; McVea and Pearson 2006; Wong and Lomber 2017; Wong et al. 2017).

To assess the neural contributions of parietal area 5 to this WM-guided behavior, 32-channel floating microelectrode arrays were chronically implanted in the same region of area 5 that when deactivated elicits WM deficits (Fig. 5.1C,D) (McVea et al. 2009; Wong et al. 2017, 2018). Electrode lengths varied from 0.9 to 1.5 mm. One array was placed in area 5 of each hemisphere for both animals. Neural activity was recorded from one array at a time as animals performed the WM task. A total of 810 units were recorded over a period of ~2 months: of the 396 units recorded from Cat 1, 204 units were recorded from the left hemisphere; of the 414 units recorded from Cat 2, 254 were in the left hemisphere. The number of units recorded from electrodes of each length did not differ between electrode lengths (p = 0.47; Fig. 5.3A).

For each unit, a two factor ANOVA was used to assess the effects of the obstacle (present or absent) and phase of the trial (approach, delay, continuation) on mean firing rate (Fig. 5.4). Most neurons (83%; 672/810) demonstrated task-related activity, with significant effects of trial phase, obstacle condition, both, or phase x obstacle interactions. Among them, a total of 349/810 units, comprising 43% of the recording population, were significantly modulated by trial phase Fig. 5.4A). These units were recorded from all electrodes (Fig. 5.4A). Of these phase modulated units, 103/349 neurons (30%) were differentially modulated for phases where the animal was walking (approach, continuation) versus standing (delay; Fig. 5.4B). In contrast, 197/810 units (24% of the total recording population) were modulated by the presence of the obstacle (Fig. 5.4C). These units were recorded from more medial and anterior electrodes. Of these obstacle modulated units, the activity of 122/197 neurons (62%) was elevated for the OP condition, while the remaining 38% of neurons were suppressed. Additionally, 132/810 units (16%), recorded from more medial electrodes, demonstrated significant effects of both the obstacle and trial phase (Figure 5.4E).

Figure 5.3 Mean number of units recorded from electrodes of each length.

(A) For all recorded units (n = 810), the mean number of units recorded from electrodes of each length did not differ between electrode lengths (p = 0.47). Black bars represent the mean number of units, while the white circles depict the number of units recorded from each array from each animal.

(B) For units demonstrating modulated activity across the whole delay (n = 99), the mean number of units recorded from electrodes of each length did not differ between electrode lengths (p = 0.64).

(C) For units demonstrating modulated activity during the early delay period (n = 114), the mean number of units recorded from electrodes of each length did not differ between electrode lengths (p = 0.97).

(D) For units demonstrating modulated activity during the late delay period (n = 100), the mean number of units recorded from electrodes of each length did not differ between electrode lengths (p = 0.37).

Figure 5.3

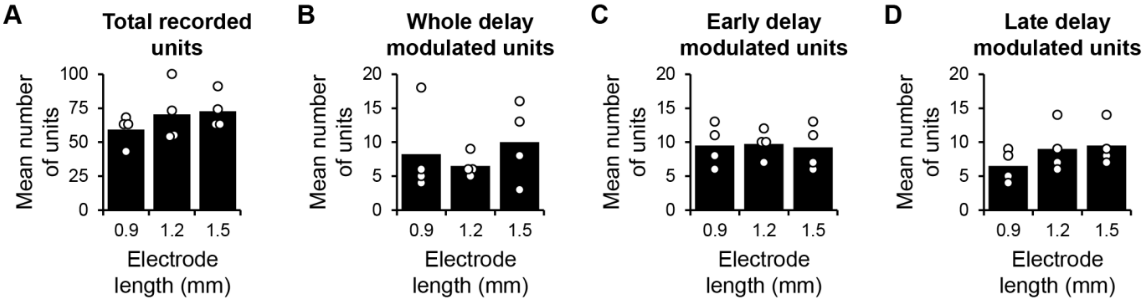
A
Total recorded units
Mean number of units
100
75
50
25
0
0.9
1.2
1.5
Electrode length (mm)
B
Whole delay modulated units
Mean number of units
20
15
10
5
0
0.9
1.2
1.5
Electrode length (mm)
C
Early delay modulated units
Mean number of units
20
15
10
5
0
0.9
1.2
1.5
Electrode length (mm)
D
Late delay modulated units
Mean number of units
20
15
10
5
0
0.9
1.2
1.5
Electrode length (mm)

Figure 5.4 Trial phase and obstacle modulated neurons within area 5.

(A-B) Two-factor ANOVA revealed significant effects of the phase of the trial for 349 units. (A) Array plot where each colored square corresponds to one of 32 electrodes, relative to the placement of the array along the ansate and lateral sulci. Different colors represent the number of phase modulated neurons recorded on that electrode according to the color scale below. M – medial, A – anterior. Overall, phase modulated neurons were recorded across all electrodes. (B) Example unit representing the majority of units (30%) differentially modulated for phases where the animal was walking versus standing. Activity of this unit during approach (t = -1 to 0 s relative to delay start, left) and continuation (t = 0 to 1 s relative to delay end, right) was elevated relative to delay period activity.

(C-D) The activity of 197 units, recorded from more medial and anterior electrodes, was modulated by obstacle presence. (D) Example unit demonstrating attenuated obstacle present (OP) activity relative to obstacle absent OA) activity.

(E-F) The activity of 132 units, located towards the medial edge of the array, was modulated by both phase and obstacle condition. (F) Example unit that demonstrated elevated activity for the continuation phase, relative to the approach and delay. Additionally, activity of this unit was elevated during the OP condition.

(G-J) Of the 258 units with significant phase x obstacle interaction effects, the activity of 150 units was modulated by the obstacle during the approach phase (G). (H) The activity of 99 units, recorded predominantly from more lateral electrodes, was modulated by the obstacle during the delay phase. These units were across all sampled cortical depths. (I) The activity of 88 units was modulated by the obstacle during the delay phase. (J) Diagram depicting the number of obstacle modulated units within each phase. Neurons could be modulated by obstacle presence during one, two, or all three phases of the task.

Figure 5.4

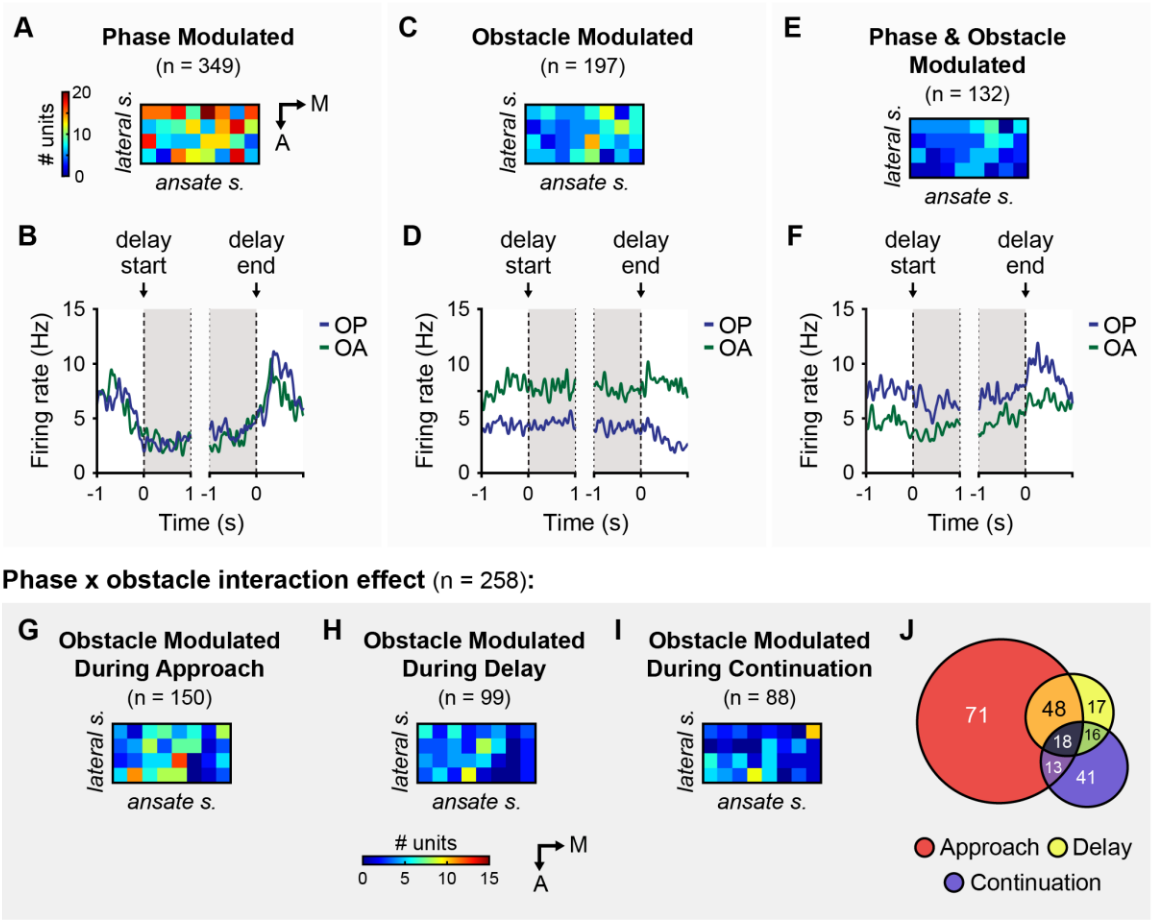
A
Phase Modulated
(n = 349)
units
20
10
0
lateral s.
ansate s.
M
A
C
Obstacle Modulated
(n = 197)
lateral s.
ansate s.
E
Phase & Obstacle Modulated
(n = 132)
lateral s.
ansate s.
B
D
F
delay start
delay end
Firing rate (Hz)
15
10
5
0
-1
0
1 -1
0
Time (s)
OP
OA
Phase x obstacle interaction effect (n = 258):
G
Obstacle Modulated During Approach
(n = 150)
H
Obstacle Modulated During Delay
(n = 99)
I
Obstacle Modulated During Continuation
(n = 88)
lateral s.
ansate s.
units
0
5
10
15
M
A
J
71
48
17
18
16
13
41
Approach
Delay
Continuation

The two factor ANOVAs also revealed significant obstacle x phase interaction effects for 258/810 units (32%). These units demonstrated more complex patterns of phase- and obstacle-modulation. Neural activity of each of these units was subsequently compared between OP and OA for each of the three phases (Fig. 5.4G-I). Note that a given unit could differ between obstacle conditions for one, two, or all phases of testing (Fig. 5.4J).

5.4.2 Obstacle-modulated activity sustained throughout the delay period during the obstacle WM task

Delay period activity was further examined in the 258 units that demonstrated significant interaction effects between trial phase and obstacle condition. Within the recording population, 12% of units (99/810) were modulated by the obstacle throughout the delay period (Fig. 5.5). These units were recorded more prevalently from lateral electrodes (Fig. 5.5A), from electrodes of each length (Fig. 5.3B). Of these neurons, 53% (52/99) demonstrated elevated delay period activity for the OP condition. Additionally, the delay period activity of 37% (37/99) of these neurons was correlated with step height (Fig. 5.5B). Specifically, delay period activity of 13% (13/99) of obstacle-modulated neurons was correlated with leading foreleg step height, while 12% (12/99) of neurons were correlated with trailing foreleg step height (Fig. 5.5C). Delay period activity was also correlated with leading and trailing hindleg step height in 18% (18/99) and 16% (16/99) of these neurons, respectively. Thus overall, a small proportion of delay period obstacle modulation was related to stepping prior to or following the delay. However, the majority of the observed delay period modulation lacked such movement-correlated responses, instead simply signaling whether the obstacle was present or absent.

For example, the neuron depicted in Figures 5.5D–G exhibited elevated activity during the approach (28.2 ± 0.7 Hz) and delay (24.2 ± 0.6 Hz) of OP trials, relative to the OA condition (approach: 16.2 ± 1.0 Hz, $p = 7.2 \times 10^{-19}$; delay: 14.9 ± 0.8 Hz, $p = 1.2 \times 10^{-17}$). Comparisons of OP and OA rasters with unit activity aligned to delay starts at $t = 0$ s demonstrates elevated activity sustained throughout the OP delay phase (Fig. 5.5E). Note that the offset of this elevated activity was tightly coupled to the delay ends (red vertical lines) across trials of various delay durations (see also Fig. 5.5F). Such elevated activity

Figure 5.5 Sustained obstacle-modulated activity throughout the delay of an obstacle working memory task.

(A) The activity of 99 units, recorded from most electrodes, was modulated by the obstacle throughout the delay period.

(B) Within this group of neurons with obstacle-modulated activity sustained throughout the delay, 37% of neurons demonstrated delay period activity correlated with step height.

(C) Delay period activity correlated with hindleg stepping was more prevalent than with foreleg stepping.

(D-G) Example unit with elevated activity during the approach and delay phases of obstacle present (OP) trials relative to the obstacle absent (OA) condition. (D) Bar plot depicting mean firing rates ± SEM for the approach, delay, and continuation phases of OP (blue) and OA (green) conditions. *** $p < 0.0001$. In raster plots (E) and spike density functions (F) of unit activity aligned to delay starts at $t = 0$ s, neural activity was elevated throughout the approach and delays of OP trials relative to OA trials. The offset of OP delay activity was tightly coupled to delay ends, indicated by red vertical lines in raster plots, across delays of various durations. Trials are ranked ordered according to delay duration. (G) Delay period activity was not correlated with step height of the leading or trailing forelegs (FL), or the leading or trailing hindlegs (HL).

Figure 5.5

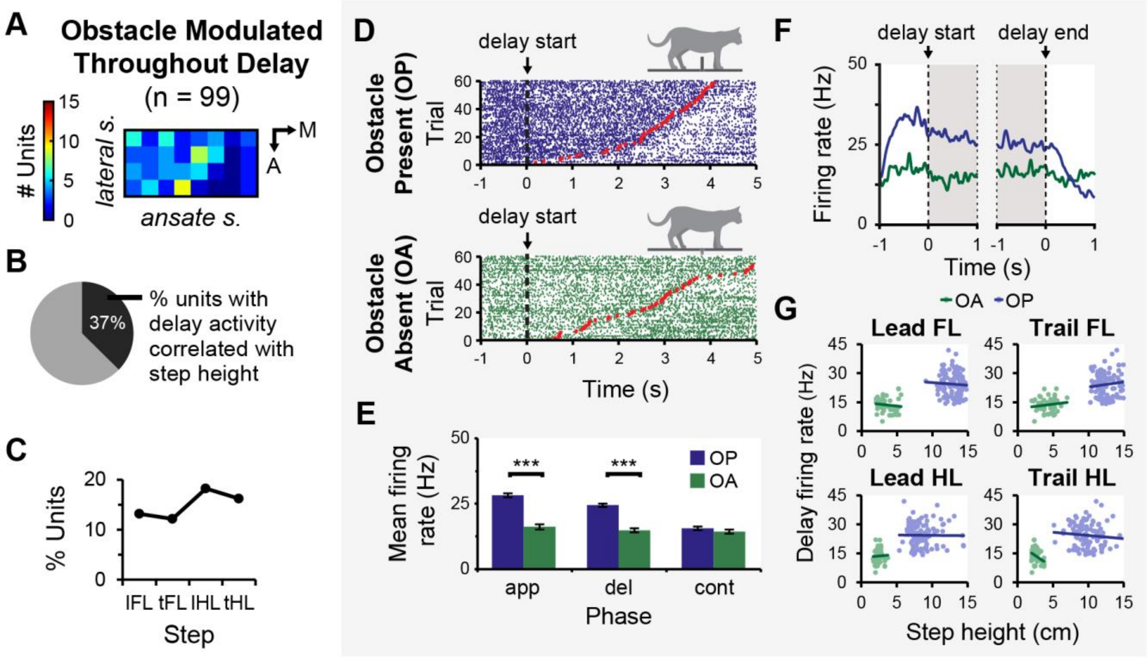
A
Obstacle Modulated Throughout Delay
(n = 99)
Units
15
10
5
0
lateral s.
ansate s.
M
A
B
37%
% units with delay activity correlated with step height
C
% Units
20
10
0
lFL tFL lHL tHL
Step
D
delay start
Obstacle Present (OP)
Trial
60
40
20
0
-1 0 1 2 3 4 5
delay start
Obstacle Absent (OA)
Trial
60
40
20
0
-1 0 1 2 3 4 5
Time (s)
E
Mean firing rate (Hz)
50
25
0
***
***
OP
OA
app
del
cont
Phase
F
delay start
delay end
Firing rate (Hz)
50
25
0
-1 0 1 -1 0 1
Time (s)
G
OA
OP
Lead FL
Trail FL
Lead HL
Trail HL
Delay firing rate (Hz)
45
30
15
0
0 5 10 15
Step height (cm)

persisting throughout a delay preceding a WM-guided action represents a characteristic hallmark associated with WM maintenance described in numerous other studies (Fuster and Alexander 1971; Goldman-Rakic 1995; Curtis and D'Esposito 2003; Funahashi 2015). Additionally, the relationship between step heights and delay period firing rates was examined (Fig. 5.5G). Note the separation in OP (blue) and OA (green) step height clusters for leading and trailing foreleg steps, as well as leading and trailing hindleg steps, demonstrating the difference in step height between the two obstacle conditions. Furthermore, as similarly reported in a previous study (Wong et al. 2018), step height variability (cluster spread) is greater for the hindlegs than the forelegs, demonstrating increased endpoint variability observed in other work comparing memory-guided versus immediate actions (Westwood et al. 2003). Finally, like the majority of neurons with sustained obstacle-modulated delay activity, delay period activity was not significantly correlated with the height of the preceding foreleg steps or proceeding hindleg steps (Fig. 5.5G).

5.4.3 Phasic delay period modulation represents the encoding or recall of obstacle or step height information

In addition to sustained activation persisting throughout a WM delay, recent studies of WM-guided behaviours have reported phasic delay period activation, which may also be important for WM (Quintana and Fuster 1999; Wang et al. 2015). Modulated activity peaking early during a WM delay is presumed to represent sensory encoding of task relevant information, while modulated activity peaking later in the delay is thought to be motor-related and important for preparing the action following the delay.

Thus early and late delay period activity was compared between OP and OA trials during the first and last second of the delay phase, respectively (Fig. 5.6A). The activity of 114/810 units was modulated by obstacle presence selectively during the first second of the delay; these units did not demonstrate significant obstacle modulation sustained throughout the total delay period. These units were recorded from most electrodes across the arrays (Fig. 5.6A), in equal proportions from electrodes of each length (Fig. 5.3C). The early delay activity of 50% of these units (57/114) was elevated for OP trials.

Figure 5.6 Phasic obstacle-modulated activity restricted to the early or late delay period.

(A) The activity of 114 units, recorded from most electrodes, was modulated by the obstacle only during the first second of the delay.

(B) Of these early delay modulated neurons, 28% demonstrated early delay period activity correlated with step height.

(C) Early delay period activity correlated with foreleg stepping was more prevalent than with hindleg stepping.

(D-F) Example unit with elevated activity specifically during the early delay. (D) Spike density functions of unit activity relative to delay starts (left) and ends (right) in obstacle present (OP; blue) and obstacle absent (OA; green) conditions. (E) Bar plots depicting mean firing rate ± SEM for the first and last seconds of OP and OA delays. *** $p < 0.0001$. (F) Scatter plots depicting early delay period firing rates significantly correlated with leading foreleg step height ($r = 0.40$, $^{**}p = 0.0008$). Early delay period activity was not correlated with stepping of the other legs.

(G) The activity of 150 units, mainly recorded from more medial electrodes, was modulated by the obstacle only during the last second of the delay.

(H) Of these late delay modulated neurons, 29% demonstrated late delay period activity correlated with step height.

(I) Late delay period activity correlated with leading limb steps was more prevalent than with trailing limb steps.

(J-L) Example unit with elevated activity specifically during the late delay. (J) Spike density functions of unit activity relative to delay starts (left) and ends (right) in OP and OA conditions. (K) Bar plots depicting mean firing rate ± SEM for the first and last seconds of OP and OA delays ($^{*}p < 0.05$). (L) Scatter plots depicting late delay period firing rates correlated with leading ($r = 0.22$, $^{*}p = 0.010$) and trailing ($r = 0.18$, $^{*}p = 0.037$) hindleg step heights only.

Figure 5.6

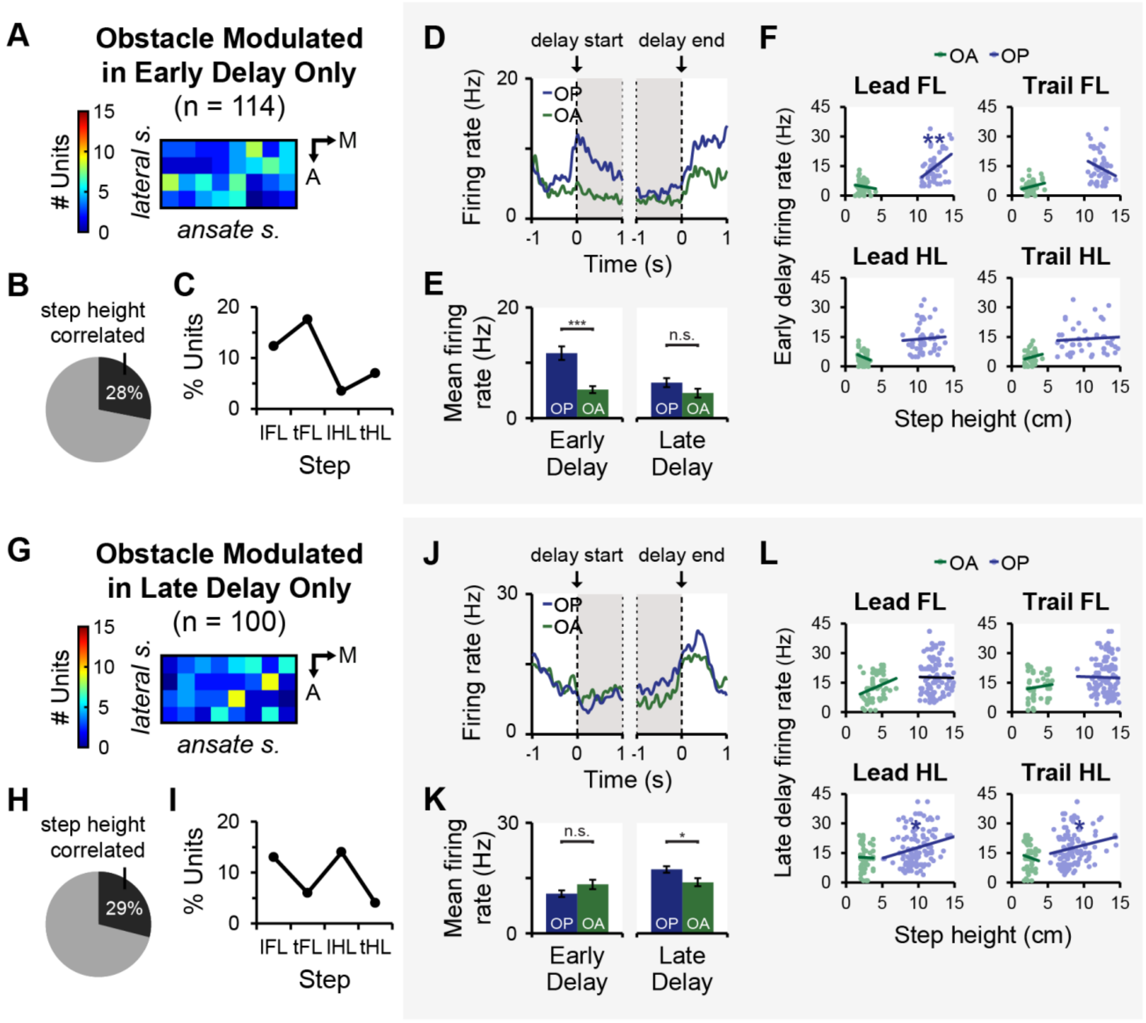
A
Obstacle Modulated
in Early Delay Only
(n = 114)
Units
15
10
5
0
lateral s.
ansate s.
M
A
B
step height
correlated
28%
C
% Units
20
10
0
lFL tFL lHL tHL
Step
D
delay start
delay end
OP
OA
Firing rate (Hz)
20
0
-1 0 1 -1 0 1
Time (s)
E
Mean firing rate (Hz)
20
0
***
n.s.
OP OA
OP OA
Early Delay
Late Delay
F
OA OP
Lead FL
Trail FL
Lead HL
Trail HL
Early delay firing rate (Hz)
45
30
15
0
0 5 10 15
**
Step height (cm)
G
Obstacle Modulated
in Late Delay Only
(n = 100)
Units
15
10
5
0
lateral s.
ansate s.
M
A
H
step height
correlated
29%
I
% Units
20
10
0
lFL tFL lHL tHL
Step
J
delay start
delay end
OP
OA
Firing rate (Hz)
30
0
-1 0 1 -1 0 1
Time (s)
K
Mean firing rate (Hz)
30
0
n.s.
*
OP OA
OP OA
Early Delay
Late Delay
L
OA OP
Lead FL
Trail FL
Lead HL
Trail HL
Late delay firing rate (Hz)
45
30
15
0
0 5 10 15
*
*
Step height (cm)

Additionally, the early delay period activity of 28% (32/114) of these neurons was correlated with step height (Fig. 5.6B). Specifically, early delay period activity was correlated with leading and trailing foreleg step heights in 12% (14/114) and 18% (20/114) of units, respectively (Fig. 5.6C). In contrast, early delay period activity was correlated with leading and trailing hindleg step height in only 4% (4/114) and 7% (8/114) of neurons, respectively. Therefore, as observed in the subset of neurons with obstacle-modulated activity sustained throughout the delay, the majority of early delay period obstacle modulation was not correlated with step height, instead signaling the general presence of the obstacle. Within the small proportion of early delay period modulation that was related to stepping, activity related to foreleg step height preceding the delay rather than hindleg step height following the delay was more prevalent.

For example, relative to the OA condition, the activity of the neuron depicted in Figures 5.6D–F was elevated during the early, but not late, delay period for the OP condition ($p = 2.3 \times 10^{-5}$). Mean firing rate was reduced from 11.7 ± 1.2 Hz in the early OP delay to 6.4 ± 0.8 Hz in the late OP delay. In contrast, mean firing rate was relatively stable in the OA condition, at 5.2 ± 0.6 Hz in the early delay, and 4.5 ± 0.8 Hz in the late delay. Furthermore, early delay period activity was significantly correlated with leading foreleg step height in the OP condition ($r = 0.40$, $p = 0.0008$; Fig. 5.6F).

Additionally, 100 neurons were obstacle-modulated selectively during the last second of the delay; these units did not demonstrate significant obstacle modulation sustained throughout the entire delay period. These units were recorded across almost all electrodes across the arrays (Fig. 5.6G), from electrodes of each length (Fig. 5.3D). The late delay activity of 59% of these units (59/100) was elevated for OP trials. Furthermore, the late delay period activity of 29% (29/100) of these neurons was correlated with step height (Fig. 5.6H). Specifically, late delay period activity was correlated with leading and trailing foreleg step heights in 13% (13/100) and 6% (6/100) of units, respectively (Fig. 5.6I). Additionally, late delay period activity was correlated with leading and trailing hindleg step height in 14% (14/100) and 4% (4/100) of neurons, respectively. Therefore, as observed in the previous subgroups of neurons with early or sustained obstacle-modulated delay activity, the majority of late delay period obstacle modulation was not correlated with step height, instead signaling the general presence of the obstacle. Within the small proportion of late delay period modulation that was related to motor output, activity related to leading, rather than trailing, steps prior to or following the delay was the most prevalent.

For example, relative to the OA condition, activity of the neuron depicted in Figures 5.6J–L was elevated during the late, but not early, delay period for the OP condition (p = 0.021). Mean firing rate increased from 10.7 ± 0.9 Hz in the early delay to 17.3 ± 0.9 Hz in the late delay. In contrast, mean firing rate was relatively stable in the OA condition, at 13.3 ± 1.3 Hz in the early delay, and 13.9 ± 1.1 Hz in the late delay. Furthermore, late delay period activity was significantly correlated with leading (r = 0.22, p = 0.010; Fig. 5.6L) and trailing (r = 0.18, p = 0.037) hindleg step height in the OP condition.

Thus overall, in addition to the 12% (99/810) of area 5 neurons demonstrating sustained delay period obstacle modulation, a separate subset of neurons comprising 14% (114/810) of the recording population demonstrated only early delay period obstacle modulation, while 12% (100/810) demonstrated only late delay period modulation. The majority of obstacle-modulated activity within each of these three groups of neurons was unrelated to stepping, likely signaling the presence or awareness of the obstacle in WM. However, obstacle-modulated activity that was related to foreleg step height may represent the encoding or recall of information regarding foreleg clearance early or late in the delay, respectively, in order to guide hindleg clearance. Additionally, obstacle-modulated activity related to hindleg step height may represent motor processes directly related to elevating hindleg stepping for obstacle avoidance.

5.4.4 Delay period activity may signal obstacle clearance progress

In order to examine the specificity of obstacle modulated activity in area 5, we examined unit activity during a variation of OP trials. Forward locomotion was delayed after the forelegs and one of the hindlegs cleared the obstacle, such that the obstacle was straddled between the hindlegs during the delay (OP-HH trials, Fig. 5.7A). Neural activity during OP-HH trials was compared to OA trials, as well as the original OP variation where the

Figure 5.7 Posterior parietal cortex may monitor the progress of obstacle clearance.

(A) Schematic depicting an obstacle present hindleg-hindleg (HH) trial where obstacle clearance was delayed between passage of the two hindlegs over the obstacle.

(B) Diagram depicting the number of units that differed between the three obstacle conditions during the delay.

(C-E) Example neuron representing one of 36 units in (B) (overlapping green wedge) that demonstrated elevated activity for HH trials (orange) relative to the FH (blue) and OA (green) conditions. Delay period activity during HH trials was significantly correlated with step height of the trailing foreleg ($r = -0.52$, $^{***}p = 2.2 \times 10^{-6}$) and leading hindleg ($r = 0.42$, $^{**}p = 0.0003$). Note that this delay period activity was attenuated in the continuation phase, while the activity during FH trials peaked during this final phase.

(F-H) Example neuron representing one of 16 units in (B) (central overlapping wedge) that demonstrated elevated activity during the delay of both types of obstacle present trials relative to the OA condition. Delay period activity was significantly higher in HH than FH trials. Note HH delay activity was then attenuated in the continuation phase, while FH activity continued to increase, peaking later in continuation. Delay period activity during FH trials was significantly correlated with step height of only the trailing foreleg ($r = 0.28$, $^{**}p = 0.004$). HH delay period activity was not correlated to step height of any leg.

Figure 5.7

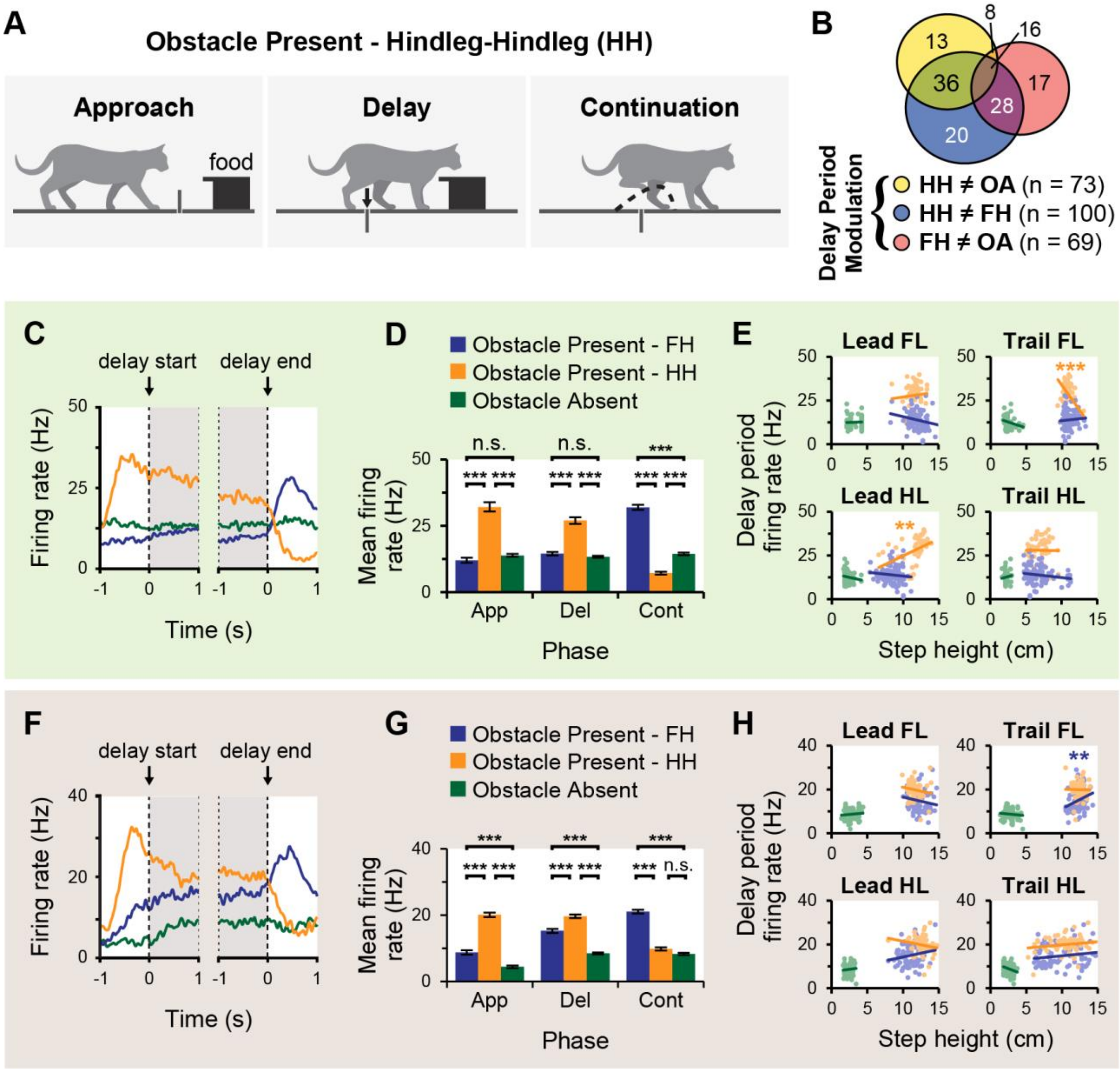
A
Obstacle Present - Hindleg-Hindleg (HH)
Approach
Delay
Continuation
food
B
13
8
16
36
17
28
20
Delay Period Modulation
○ HH ≠ OA (n = 73)
○ HH ≠ FH (n = 100)
○ FH ≠ OA (n = 69)
C
delay start
delay end
Firing rate (Hz)
50
25
0
-1
0
1
-1
0
1
Time (s)
D
■ Obstacle Present - FH
■ Obstacle Present - HH
■ Obstacle Absent
n.s.
n.s.
***
Mean firing rate (Hz)
50
25
0
App
Del
Cont
Phase
E
Lead FL
Trail FL
Lead HL
Trail HL
***
**
Delay period firing rate (Hz)
50
25
0
0
5
10
15
Step height (cm)
F
delay start
delay end
Firing rate (Hz)
40
20
0
-1
0
1
-1
0
1
Time (s)
G
■ Obstacle Present - FH
■ Obstacle Present - HH
■ Obstacle Absent
***
n.s.
Mean firing rate (Hz)
40
20
0
App
Del
Cont
Phase
H
Lead FL
Trail FL
Lead HL
Trail HL
**
Delay period firing rate (Hz)
40
20
0
0
5
10
15
Step height (cm)

obstacle was straddled between the forelegs and hindlegs during the delay (OP-FH condition). A total of 404 units were recorded during sessions where all three trial types were performed.

Delay period activity was examined in 234 units that demonstrated significant interaction effects between trial phase and obstacle condition. Relative to OA trials, the activity of 31% (73/234) of these units differed during the delay period of OP-HH trials (Fig. 5.7B, yellow circle). Additionally, 43% (100/234) of units differed between the two OP conditions during the delay (Fig. 5.7B, blue circle). Within these two groups, the activity of 36 units differed selectively for HH trials relative to both of the other conditions, with similar delay activity between FH and OA trials (Fig. 5.7B, green overlapping wedge).

For example, the neuron depicted in Fig. 5.7C–E demonstrated elevated activity throughout the delay of HH trials relative to the other two conditions. Mean firing rate during HH delays was 27.0 ± 1.3 Hz, which was significantly higher than both FH (14.5 ± 0.6 Hz, $p = 9.6 \times 10^{-10}$) and OA (13.3 ± 0.4 Hz, $p = 9.6 \times 10^{-10}$) delay activity (Fig. 5.4D); FH delay activity did not differ from OA delay activity (p = 0.30). Furthermore, HH delay period activity was significantly correlated with step height of the trailing foreleg (r = -0.52, $^{***}p = 2.2 \times 10^{-6}$, Fig. 5.7E) and leading hindleg (r = 0.42, $^{**}p = 0.0003$). Additionally, note that this delay period activity was attenuated in the subsequent continuation phase, while the activity during FH trials peaked during this final phase (Fig. 5.7C). Such patterns of modulation may reflect the response of this neuron to the coordinated passage of the leading and trailing hindlegs over the obstacle. This modulation is therefore evident in the continuation phase of FH trials, and may be sustained if trailing hindleg clearance is interrupted, as in the delay of HH trials.

In contrast to such units that differed selectively for HH trials, 8/234 neurons demonstrated similar delay period obstacle modulation in both FH or HH trials (Fig. 5.7B, orange overlapping wedge). These units were therefore modulated by obstacle presence regardless of where the obstacle was relative to the body or progress of obstacle clearance during the delay.

Additionally, a small subset of neurons differed between all three obstacle conditions (n = 16, Fig. 5.7B, central overlapping wedge). For example the neuron depicted in Figures 5.7F–H demonstrated elevated activity for both types of OP trials relative to the OA condition. However, delay period activity was significantly higher in HH than FH trials ($p = 2.9 \times 10^{-9}$), with mean firing rates of 19.7 ± 0.5 Hz and 15.3 ± 0.6 Hz, respectively. Delay period activity during FH trials was significantly correlated with step height of only the trailing foreleg (r = 0.28, $**p = 0.004$). HH delay period activity was not correlated to step height of any leg. Interestingly, note that HH delay activity was then attenuated in the continuation phase, while FH activity continued to increase, peaking later in continuation. Unlike the neuron depicted above, this neuron increased its activity with the clearance of each additional leg, returning only to baseline (OA activity levels) once the trailing hindleg initiated its clearing step. Therefore, while some area 5 neurons may respond to the passage of a particular limb or coordinated pair of limbs over an obstacle (Fig. 5.7C–E), other neurons may monitor the overall progress of clearance to ensure complete and successful obstacle avoidance (Fig. 5.7F–H).

5.4.5 Sensory-specific obstacle modulation was attenuated across the delay

Previous studies demonstrated that when area 5 is deactivated, WM deficits in a visually-independent tactile obstacle memory task are similar to those observed in a visually-dependent paradigm (Wong et al. 2017). Therefore, in the present study, neural activity recorded in area 5 was compared between visual and tactile obstacle memory tasks to assess the sensory specificity of obstacle modulation. In tactile obstacle present (TOP) trials, each animal approached the food plate in the absence of the obstacle (lowered; Fig. 5.8A). The obstacle was then raised onto the walkway directly beneath the food plate to prevent any visual input of the obstacle. When the food was advanced, the forelegs of the animal inevitably tripped over the unexpected obstacle. This tactile input, independent of any visual input thus informed the animal about the presence of the obstacle. Hindleg obstacle clearance was then delayed in a similar manner to the visual obstacle present (VOP) condition (Fig. 5.1A), before walking resumed.

Figure 5.8 Sensory modality specific and non-specific obstacle modulation in cat area 5.

(A) Schematic depicting a tactile obstacle present (TOP) trial where the obstacle was raised covertly onto the walkway during the approach. This resulted in the forelegs tripping over the unexpected obstacle. Hindleg obstacle clearance was then delayed in a similar manner to Fig. 5.1A.

(B) Diagram depicting the number of units that differed between the three obstacle conditions during the delay.

(C) Example neuron representing one of 5 units in (B) (green overlapping wedge) that exhibited elevated delay period activity for TOP trials relative to both VOP and OA conditions, demonstrating modulation specifically when the animal tripped over the obstacle without seeing it.

(D) Example neuron representing one of 22 units in (B) (orange overlapping wedge) that exhibited similar delay activity in VOP and TOP trials, demonstrating non-specific modulation regardless of whether the obstacle was first seen or felt.

(E) The number of units modulated by the different obstacle conditions during the early delay period differed by the late delay period, such that there were very few units differentially modulated by the visual and tactile conditions by the end of the delay. Colors correspond to groupings in (B).

Figure 5.8

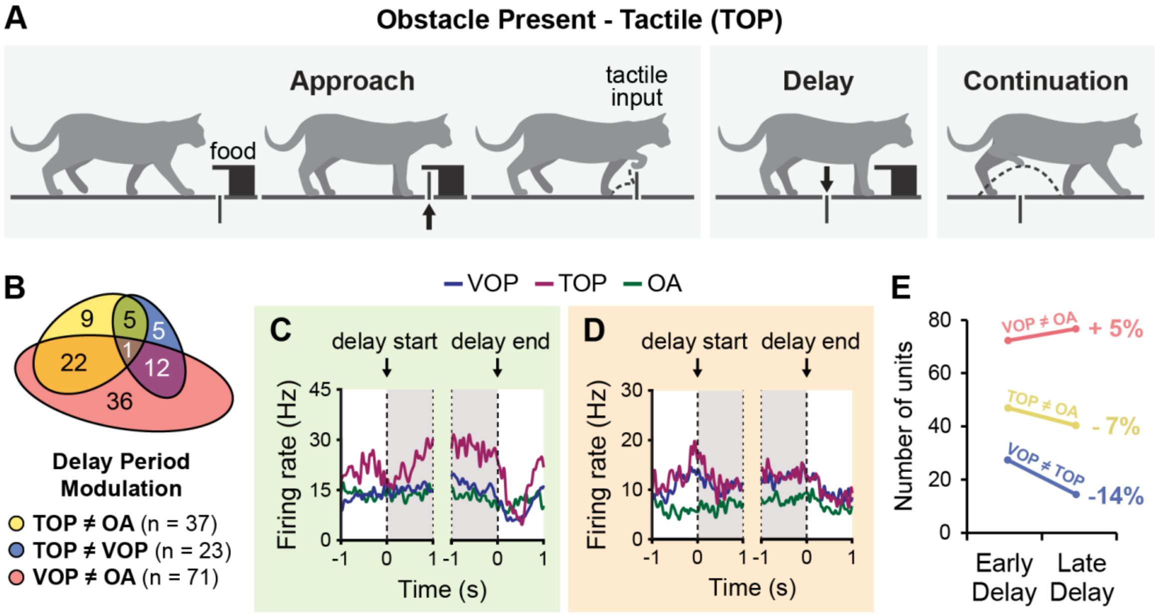
A
Obstacle Present - Tactile (TOP)
Approach
food
tactile input
Delay
Continuation
B
9
5
5
22
1
12
36
Delay Period Modulation
○ TOP ≠ OA (n = 37)
○ TOP ≠ VOP (n = 23)
○ VOP ≠ OA (n = 71)
VOP
TOP
OA
C
delay start
delay end
Firing rate (Hz)
45
30
15
0
-1
0
1
-1
0
1
Time (s)
D
delay start
delay end
Firing rate (Hz)
30
20
10
0
-1
0
1
-1
0
1
Time (s)
E
Number of units
80
60
40
20
0
VOP ≠ OA
+ 5%
TOP ≠ OA
- 7%
VOP ≠ TOP
-14%
Early Delay
Late Delay

A total of 265 units were recorded during sessions where all three trial types were performed. Relative to OA trials, the activity of 14% (37/265) of units differed during the delay period of tactile trials (Fig. 5.8B, yellow oval). Additionally, 9% (23/265) of units differed between visual and tactile OP conditions during the delay (Fig. 5.8B, blue oval). Within these two groups, the activity of 5 units differed selectively for TOP trials relative to both of the other conditions, with similar delay activity between VOP and OA trials (Fig. 5.8B, green overlapping wedge). For example, the neuron depicted in Figure 5.8C demonstrated elevated activity throughout the delay of TOP trials relative to the other two conditions. This neuron represents one of the few units (2%; 5/265) modulated specifically when the animal tripped over the obstacle without seeing it.

In contrast, 8% (22/265) of units were similarly modulated by the obstacle in visual and tactile trials (Fig. 5.8B, orange overlapping wedge). For example, the neuron depicted in Figure 5.8D exhibited similar delay activity in VOP and TOP conditions that was elevated in comparison to the OA condition. Such non-sensory specific modulation may signal the presence of the obstacle regardless of whether the obstacle was first seen or felt.

Further examination of early and late periods of the delay revealed dynamic, phasic modulatory patterns. Overall, the total proportion of units significantly modulated by obstacle condition was reduced from 35% (93/265) to 25% (65/265) from the early to late delay periods. However, the percentage of neurons comprising each of the three major groups of modulation depicted in Figure 5.8B varied across the delay. The proportion of units that differed between VOP and OA trials increased slightly by 5% (from 67/93 to 50/65; Fig. 5.8E, red). The proportion of units that differed between TOP and OA trials was attenuated by 7% (from 44/93 to 26/65; Fig. 5.8E, yellow). In contrast, the proportion of units that differed between VOP and TOP trials was markedly reduced by 14% (from 26/93 to 9/65; Fig. 5.8E, blue), resulting in very few units (n = 9) capable of differentiating between sensory conditions by the late delay period.

5.4.6 Periods of stable and dynamic population level coding can discriminate between obstacle conditions

To assess population level recruitment for obstacle working memory, a multivariate analysis method (Stokes et al. 2013; Spaak et al. 2017) was used to examine neural activity recorded during the first comparison of OP and OA trials (Fig. 5.9). All OP and OA trials were randomly assigned to one of two independent splits (A or B). The difference between mean firing rates in OP and OA conditions for each neuron was then computed for each independent split. The ability of recorded area 5 neurons to discriminate between OP and OA conditions is reflected in the correlation of these differences between the two splits. Discriminability was measured across both the approach-delay and delay-continuation epochs. For all recorded neurons, discriminability was significantly elevated throughout the approach phase (Fig. 5.9A(i)). In contrast, significant discriminability was sporadic during the early delay period (Fig. 5.9A(i)), and the ability to distinguish between obstacle conditions from examining population level activity was essentially absent in the late delay period (Fig. 5.9A(ii)). Robust discriminability was restored in the final continuation phase. In contrast, for neurons demonstrating modulated activity throughout the delay, discriminability was significantly elevated during all three phases (Fig. 5.9B(i)– (ii)).

For each epoch examined, firing rate differences between obstacle conditions at each time point was correlated with the difference in firing rate at every time point. Note that the diagonal of each resulting matrix in Figures 5.9(iii) and (iv) therefore depicts the discriminability in Figures 5.9A(i) and (ii). Analysis of cross-temporal discriminability can provide a measure of how dynamic or stationary the discriminative representation is by comparing on- and off-diagonal values (Spaak et al. 2017). Significant off-diagonal reduction from on-diagonal values indicates optimal discriminability only between neighbouring time points, thus demonstrating dynamic population coding across time.

Within the total recording population, significant off-diagonal reduction was observed during the approach (Fig. 5.6A(v)) and continuation phases only (Fig. 5.6A(vi)). This pattern was also evident within the subpopulation of neurons modulated throughout the whole delay period. Therefore, obstacle-related information coding during approach and

Figure 5.9 Population and subpopulation level discriminability and dynamicism.

(A) For all recorded units, discriminability plots across (i) approach-delay epochs and (ii) delay-continuation epochs depict the ability of the recorded population to reliably discern between obstacle present and obstacle absent trials during approach and continuation phases. Blue horizontal bars indicate periods of significantly elevated discriminability. (iii – iv) Colour coded plots depicting discriminability across the two epochs, measured as the correlation of differences between neural activity in obstacle present and obstacle absent conditions between all combinations of time points. Green outlines indicate off-diagonal reduction, a measure of dynamicism, which was significant during approach and continuation phases only (see below). (v-vi) Dynamicism plots depicting the dynamicism index across time for the two corresponding epochs. Green horizontal bars indicate periods of significant dynamicism.

(B) Similar discriminability and dynamicism plots for units with modulated activity sustained throughout the delay. Note the robust discriminability maintained across all three test phases, and lack of significant dynamicism, or stable information coding during the delay period.

Figure 5.9

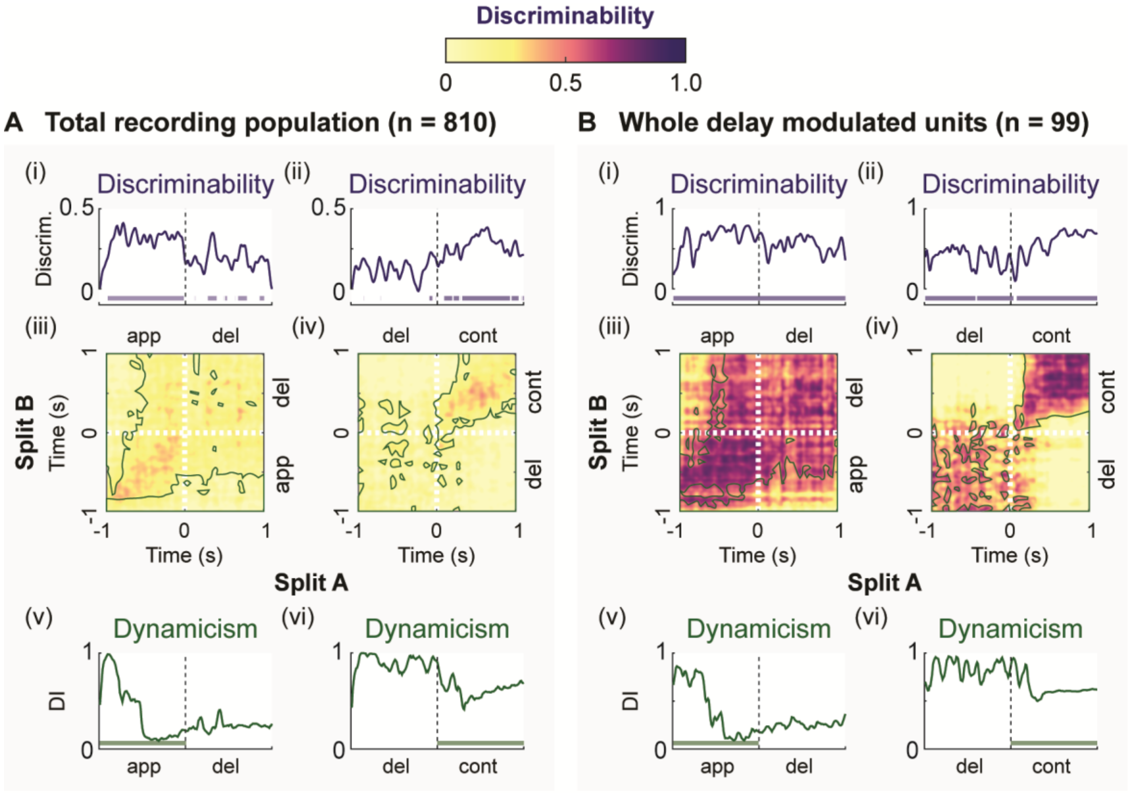
Discriminability
0
0.5
1.0
A Total recording population (n = 810)
B Whole delay modulated units (n = 99)
(i)
Discriminability
(ii)
Discriminability
Discrim.
0.5
0
1
(iii)
(iv)
app
del
cont
Split B
Time (s)
-1
0
1
Time (s)
Split A
(v)
Dynamicism
(vi)
Dynamicism
DI
app
del
cont

continuation phases was supported by dynamic population level activity. In contrast, there was no significant off-diagonal reduction during the delay in the whole recording population or subpopulation of delay modulated units. Thus altogether, obstacle-related information is reliably discriminable throughout the delay in only a small subset of area 5 neurons that are capable of maintaining stable representations of obstacle information in WM.

5.5 Discussion

This report describes the neural correlates of WM-guided obstacle locomotion in the posterior parietal cortex of the cat. Multiple combinations of phase- and obstacle-dependent modulation were observed in over 800 area 5 neurons. This demonstrates the ability of parietal area 5 to signal when the animal is walking or standing, when the animal is walking towards or over an obstacle, or when the animal is standing over the obstacle if clearance is delayed. Furthermore, distinct subsets of neurons exhibited characteristic properties of WM, including both sustained and phasic delay period modulation associated with WM maintenance, or information encoding and movement planning, respectively. In assessing the relevance of such individual neurons on population level coding, obstacle information was only reliably discernable across approach and continuation phases. However, neurons exhibiting sustained delay period modulation represent a specialized subset of area 5 neurons capable of maintaining stable representations of obstacle information in WM. As previous work demonstrated WM deficits precluding successful avoidance when a comparable region of area 5 was deactivated during the delay (McVea et al. 2009; Wong et al. 2017, 2018), neurons capable of stable WM maintenance are likely necessary for such behaviors.

This study extends upon previous electrophysiological work demonstrating the role of the posterior parietal cortex in complex locomotion. Neural activity recorded from cat area 5 is modulated during a variety of complex locomotor tasks, including stepping on a horizontal ladder, walking along a narrow path, as well as obstructed locomotion (Beloozerova and Sirota 2003). Furthermore, during treadmill locomotion, lesions to this region of parietal cortex impair anticipatory step adjustments necessary for adapting stepping to an obstacle moving towards an animal at a speed different from that of the treadmill (Lajoie and Drew 2007). Neural recordings during this visual dissociation task revealed corresponding anticipatory modulations of area 5 activity two to three steps prior to obstacle clearance (Andujar et al. 2010; Lajoie et al. 2010). Furthermore, work from Lajoie et al. (Lajoie et al. 2010) represents the first and only other study to examine neural activity during working memory-guided obstacle locomotion. Our identification of neurons demonstrating modulated activity selectively throughout the delay of FH or HH trials complements their identification of a possible working memory correlate for obstacle-related information maintained within parietal area 5. Additionally, the present work examining phasic delay activity, neural activity related to stepping, contributions to tactile obstacle memory, and population level discriminability and dynamicism represent novel efforts to further our understanding of this obstacle working memory system.

Within the recorded population, a total of 38% of area 5 neurons demonstrated obstacle modulated activity during the early (14%), late (12%), or whole (12%) delay period. As the same stance was maintained during both OP and OA delays, this modulated delay period activity may represent the retention of information about the obstacle that is no longer visible to the animal. Neurons from each of these subgroups were recorded in equal proportions from electrodes of each length, suggesting that working memory-related cells may be evenly distributed across superficial and deep cortical layers of area 5 in the cat. However, this lack of laminar specificity, especially for neurons with sustained modulation throughout the delay period, contrasts with previous work demonstrating sustained spiking activity and working memory encoding restricted to superficial layers of macaque prefrontal and premotor areas (Markowitz et al. 2015; Bastos et al. 2018). These differences in laminar organization may arise from brain region-dependent or species-dependent factors. Such laminar specific functions of working memory gating and encoding attributed to deep and superficial cortical layers, respectively, may permit the more complex, cognitive working memory tasks often examined in primates. Interestingly, obstacle-modulated responses demonstrated in superficial layers in the present work also contrasts previous work demonstrating low activity from layer III of cat area 5 during locomotion (Beloozerova et al. 2011). However, the working memory-dependent nature of the task observed in the present work may underlie this discrepancy.

Note that any inferences about laminar-specific responses in the present work should be met with hesitation. We acknowledge the limitations of using the length of the electrode from which a neuron was recorded as a proxy for the cortical layer in which the neuron resides. Unintended and or unavoidable variations in the angle or depth of array insertion preclude a direct or consistent correspondence between electrode length and recording depth. Thus future recordings in conjunction with a multi-laminar probe to enable current source density analysis may provide further insight into the laminar organization of working memory circuitry in the cat.

Interestingly, as 31% of these obstacle-modulated neurons demonstrated delay period activity related to step height, this modulation may reflect the difference in foreleg and or hindleg stepping before and after the delay, respectively, of OP versus OA trials. Such responses to elevated foreleg stepping prior to the delay can be afforded by proprioceptive inputs relayed to area 5 via projections from primary sensory areas (Vogt and Pandya 1978; Pearson and Powell 1985; Avendaño et al. 1988; Scannell et al. 1995; Mori et al. 1996). Conversely, step-related responses may be facilitated by neural representations of motor commands, known as efference copy (von Holst and Mittelstaedt 1950) or corollary discharge (Sperry 1950), that predict and prime the system for sensory consequences of the signaled movement (Poulet and Hedwig 2006). Projections from motor cortical areas to parietal regions (Parkinson et al. 2010), including area 5 in the cat (Yumiya and Ghez 1984), may facilitate the relay of efference copies of motor programs for elevated stepping to area 5.

Such efference motor information regarding elevated foreleg as well as hindleg stepping may underlie the ability of a single neuron to exhibit delay activity related to both foreleg and hindleg stepping. Additionally, as previously demonstrated, foreleg obstacle clearance is required for establishing a robust WM of obstacle information to guide hindleg clearance (McVea and Pearson 2007). Furthermore, hindleg step height following a WM delay scales accordingly with obstacle height (McVea and Pearson 2006), and by extension, foreleg step height. Thus a neuron with activity correlated to both foreleg and hindleg stepping may represent an efficient coding mechanism ensuring successful hindleg clearance of an obstacle over which the forelegs have stepped.

Given the diverse sensory and motor inputs to area 5, it is also possible that foreleg step-related delay period modulation may originate from both proprioceptive inputs and motor efference copies. For example, area 5 neurons that respond to passive joint manipulation are even more responsive during active movements, demonstrating an integration of both sensory and motor inputs (Mountcastle et al. 1975). Correspondingly, previous work has demonstrated that in comparison to trials where the animal is delayed just before the forelegs have stepped over an obstacle, obstacle memory is more robust when the animal is delayed after foreleg clearance (McVea and Pearson 2007b; Wong et al. 2018). These studies suggest that the efference copies of motor commands for elevated foreleg stepping, or the resulting proprioceptive foreleg feedback, or both, are important for WM-guided obstacle locomotion.

As such, delay period modulation related to foreleg obstacle clearance, especially during the early delay period, may encode this information into WM in order to guide the hindlegs over the same obstacle following the delay. Similarly, in previous WM studies, early delay period modulation has been attributed to the encoding of task-relevant information in macaque prefrontal neurons (Quintana and Fuster 1999; Takeda and Funahashi 2002, 2004; Wang et al. 2015). In addition to such neurons associated with information encoding (or “sensory-coupled cue cells”), previous studies also describe a separate group of “preparatory set cells”, which increase their activity throughout a WM delay (Wang et al. 2015). This late delay period modulation is often attuned to the WM-guided action following the delay, such as the direction of a saccade (Watanabe and Funahashi 2007) or manual response (Quintana and Fuster 1999), and can be exhibited as a ‘ramping’ of neural activity towards the end of a fixed delay (Barak et al. 2010). Notably, as only 12% of neurons demonstrated such activity, this limited proportion of late delay period modulation is likely due to the variability in delay periods assessed to allow for the examination of more naturalistic obstacle locomotor behaviours. However, with the majority of OP and OA trials spanning between 3 to 5 seconds (30% and 27%, respectively; see Fig. 5.10), animals may have been able to anticipate end of the delay with reasonable accuracy. While we would expect a greater proportion of neurons to demonstrate late delay period modulation if this obstacle locomotor task were overtrained with a fixed delay period, this remains to be further assessed.

Figure 5.10 Distribution of working memory delay durations examined.

(A) Histogram depicting the distribution of working memory delay durations tested for obstacle present trials. Working memory was assessed in trials consisting of delays of at least 2 s.

(B) Histogram depicting the distribution of working memory delay durations tested for obstacle absent trials.

Figure 5.10

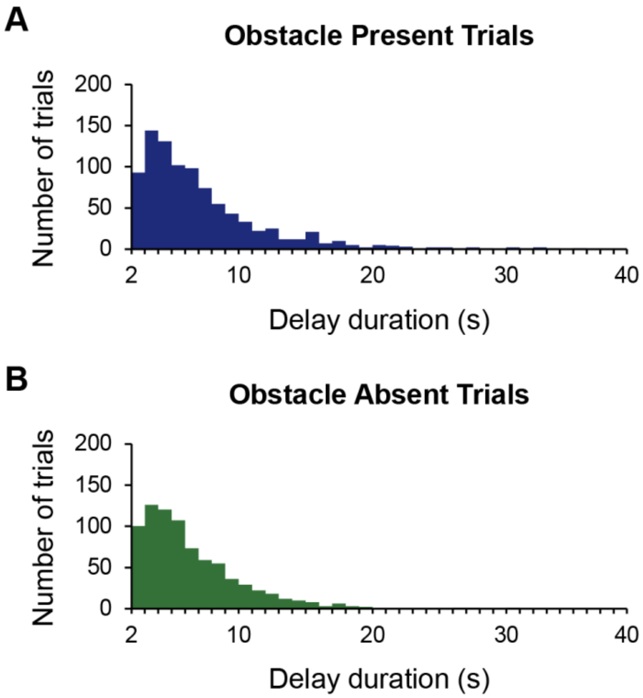
A
Obstacle Present Trials
Number of trials
200
150
100
50
0
2
10
20
30
40
Delay duration (s)
B
Obstacle Absent Trials
Number of trials
200
150
100
50
0
2
10
20
30
40
Delay duration (s)

Nonetheless, 48% of late delay modulation observed in the present study was correlated with lead hindleg step height following the delay. Interestingly, 45% of late delay modulation was correlated with lead foreleg height. Thus information about leading foreleg steps may be recalled towards the end of the delay in order to plan subsequent hindleg stepping. Such modulation within area 5 neurons in supragranular layers may be relayed via its profuse projections to motor cortex (Babb et al. 1984; Kang et al. 1986; Mori 1997) to modulate movement commands for stepping. Alternatively, neurons were recorded in infragranular layers may relay step-related information to the cerebellum, which has also been demonstrated to be involved in visually guided movements (Armstrong and Marple-Horvat 1996; Marple-Horvat and Criado 1999; Morton and Bastian 2006), including obstacle locomotion (Aoki et al. 2013). Furthermore, the cross-temporal integration of these early and late delay activities may be facilitated by neurons demonstrating obstacle modulated activity sustained throughout the delay (Curtis and Lee 2010).

However, note that the activity of the majority of delay period modulation was not correlated with step height of any of the four legs. Thus the majority of sustained or phasic delay period modulation within area 5 may not represent a specific motor plan. Instead, such responses likely reflect the ability of area 5 neurons to estimate the relationship between the obstacle and the animal (Andujar et al. 2010; Lajoie et al. 2010; Drew and Marigold 2015; Marigold and Drew 2017). Neurons signaling the time- or distance-to-contact during continuous locomotion (Marigold and Drew 2017) would convey critical information if locomotion is interrupted and obstacle clearance is delayed. This information may thus represent the nature of information encoded in working memory for the tasks examined in the present work. Furthermore, such coding may permit a more advantageous strategy allowing an animal to change its movement plan following a delay if necessary. For example, if a predator or other threat is suddenly detected and the animal no longer wants to continue walking forward, hindleg obstacle clearance becomes unnecessary. Instead, obstacle modulated activity within area 5 may allow the forelegs to step back over the remembered obstacle, allowing the animal to change its course of direction while still negotiating the obstacle successfully.

Additionally, the possibility of area 5 neurons to be modulated selectively by a particular phase of the task, the presence of the obstacle, or by various combinations of phase and obstacle related factors may confer another encoding strategy. Neural populations exhibiting complex combinations of task- and behavior-related modulation are described as demonstrating mixed selectivity (Fusi et al. 2016), which has been described in macaque prefrontal (Rigotti et al. 2013; Jacob and Nieder 2014; Blackman et al. 2016) and posterior parietal (Raposo et al. 2014; Zhang et al. 2017) cortex. In comparison to a population of neurons demonstrating single selectivity, the readout of a population with mixed selectivity where different aspects of a task are encoded in a distributed manner provides a more efficient method of encoding a diverse repertoire of behavioral outputs. Thus mixed selectivity revealed by examining a select number of experimental tasks allows a discrete population of neurons to encode the variety of naturalistic behaviors an animal may require. As such, parietal area 5 neurons do not contribute singularly to WM-guided obstacle locomotion, and the heterogeneous patterns of modulation observed likely enable the cat to perform a plethora of complex behaviors beyond what was tested in the present study.

We also observed that neurons involved in interlimb coordination for continuous obstacle locomotion may demonstrate sustained activity if obstacle clearance of those limbs is delayed. For example, increased activation of the neuron in Figure 5C during FH continuation likely corresponds to the coordinated, sequential passage of both hindlegs over the obstacle. Such activation is sustained during the HH delay when trailing hindleg clearance is interrupted. Similarly, neurons activated for hindleg-hindleg coordination as well as foreleg-hindleg coordination during treadmill obstacle locomotion have also been reported to demonstrate sustained activation if trailing or leading hindleg clearance, respectively, is delayed (Lajoie et al. 2010). Therefore, these groups of neurons described previously and in the present study demonstrate a recognized WM concept whereby neurons involved in the sensory perception or motor planning for non-delayed behaviors may be similarly involved in WM processes if that behavior is delayed (Mansouri et al. 2015).

We also probed the sensory specificity of obstacle-modulated delay activity in area 5. Of the 90 neurons with modulated delay activity when comparing the visual and tactile tasks, 24% of neurons responded similarly to the presence of the obstacle, regardless of whether the animal selectively saw or felt the obstacle during the approach. As such, these units may not be involved in interlimb coordination or retain sensory specific information about the obstacle, but may represent the general awareness of the obstacle held in WM. However, such sensory non-selective neurons represented the minority of modulated neurons in the comparison of VOP and TOP conditions. With the majority of delay modulated units demonstrating differential delay activity for VOP versus OA conditions (71/90, 89%), area 5 seems to be primarily driven by visual obstacle information. However, 41% (37/90) of neurons did respond to tactile obstacle information. The percentage of these neurons responding to either visual or tactile obstacle information was relatively stable across the delay, fluctuating by only 5% or 7%, respectively.

In contrast, the percentage of neurons differentiating between visual and tactile conditions was reduced by 14% by the late delay period. Similarly, in a previous WM study examining prefrontal neural modulation, the proportion of neurons demonstrating delay activity differentially modulated by a visual versus tactile remembered stimulus was attenuated from 69% to 2% of cells during the early to late periods, respectively, of a WM delay (Wang et al. 2015). While the attenuation in parietal cortex neurons observed in the present study was markedly less, the reduced sensory differentiation likely reflects the minimal need to remember whether the animal first saw or felt the obstacle late in the delay. Instead, late delay activity that differentiates simply between whether an obstacle is present or absent is likely sufficient and important for ensuring subsequent hindleg clearance.

Thus overall, WM-guided obstacle locomotion revealed dynamic patterns of delay period modulation in parietal area 5. Early delay period modulation may represent WM encoding of visual or tactile information about the obstacle, or information about foreleg stepping adequate for clearance. As the delay progresses, the sensory specificity of obstacle-related modulation is attenuated. Information about the obstacle or prior foreleg stepping may be recalled later in the delay in order to guide hindleg stepping over the same obstacle. In addition to these groups of early and late delay modulated units, neurons demonstrating obstacle modulation sustained throughout the delay period may bridge these phasic responses. While such neurons comprised relatively modest proportions of the total recording population, obstacle information coding was stable in population level delay activity. While these observed patterns of modulation exemplify characteristic properties of WM that have been described extensively in human and non-human primates performing various saccadic and manual tasks, the present work demonstrates their relevance in the cat performing a locomotor task. Furthermore, as quadrupedal obstacle locomotion necessitates multi-limb coordination, neurons typically associated with interlimb coordination for continuous obstacle negotiation may also demonstrate sustained activation if obstacle clearance is delayed. The overall heterogeneity of task- and obstacle-related modulation observed within a relatively small region of parietal cortex is likely important for allowing an animal to safely and successfully negotiate an obstacle. Additionally, such mixed selectivity likely enables this circuitry to contribute to a variety of actions beyond obstacle locomotion necessary for naturalistic behaviors in the real world.

5.6 References

Andujar J-E, Lajoie K, Drew T. 2010. A contribution of area 5 of the posterior parietal cortex to the planning of visually guided locomotion: limb-specific and limb-independent effects. J Neurophysiol. 103:986–1006.

Aoki S, Sato Y, Yanagihara D. 2013. Lesion in the lateral cerebellum specifically produces overshooting of the toe trajectory in leading forelimb during obstacle avoidance in the rat. J Neurophysiol. 110:1511–1524.

Armstrong DM, Marple-Horvat DE. 1996. Role of the cerebellum and motor cortex in the regulation of visually controlled locomotion. Can J Physiol Pharmacol. 74:443–455.

Avendaño C, Rausell E, Perez-Aguilar D, Isorna S. 1988. Organization of the association cortical afferent connections of area 5: a retrograde tracer study in the cat. J Comp Neurol. 278:1–33.

Babb RS, Waters RS, Asanuma H. 1984. Corticocortical connections to the motor cortex from the posterior parietal lobe (areas 5a, 5b, 7) in the cat demonstrated by the retrograde axonal transport of horseradish peroxidase. Exp Brain Res. 54:476–484.

Barak O, Tsodyks M, Romo R. 2010. Neuronal population coding of parametric working memory. J Neurosci. 30:9424–9430.

Bastos AM, Loonis R, Kornblith S, Lundqvist M, Miller EK. 2018. Laminar recordings in frontal cortex suggest distinct layers for maintenance and control of working memory. Proc Natl Acad Sci. 115:1117–1122.

Beloozerova IN, Nilaweera WU, Viana di Prisco G, Sirota M, Marlinski V. 2011. Sparse locomotion-related activity of cortico-cortical projection from parietal area 5 to motor cortex. In: 2011 Neuroscience Meeting Planner. Society for Neuroscience. Washington, DC. p. Online.

Beloozerova IN, Sirota MG. 2003. Integration of motor and visual information in the parietal area 5 during locomotion. J Neurophysiol. 90:961–971.

Blackman RK, Crowe DA, DeNicola AL, Sakellaridi S, MacDonald AW, Chafee M V. 2016. Monkey Prefrontal Neurons Reflect Logical Operations for Cognitive Control in a Variant of the AX Continuous Performance Task (AX-CPT). J Neurosci. 36:4067–4079.

Chen D, Fetz EE. 2005. Characteristic membrane potential trajectories in primate sensorimotor cortex neurons recorded in vivo. J Neurophysiol. 94:2713–2725.

Curtis CE, D'Esposito M. 2003. Persistent activity in the prefrontal cortex during working memory. Trends Cogn Sci. 7:415–423.

Curtis CE, Lee D. 2010. Beyond working memory: the role of persistent activity in decision making. Trends Cogn Sci. 14:216–222.

Dickey AS, Suminski A, Amit Y, Hatsopoulos NG. 2009. Single-unit stability using chronically implanted multielectrode arrays. J Neurophysiol. 102:1331–1339.

Drew T, Marigold DS. 2015. Taking the next step: cortical contributions to the control of locomotion. Curr Opin Neurobiol. 33:25–33.

Fiehler K, Bannert MM, Bischoff M, Blecker C, Stark R, Vaitl D, Franz VH, Rösler F. 2011. Working memory maintenance of grasp-target information in the human posterior parietal cortex. Neuroimage. 54:2401–2411.

Funahashi S. 2015. Functions of delay-period activity in the prefrontal cortex and mnemonic scotomas revisited. Front Syst Neurosci. 9:2.

Funahashi S, Chafee M V, Goldman-Rakic PS. 1993. Prefrontal neuronal activity in rhesus monkeys performing a delayed anti-saccade task. Nature. 365:753–756.

Fusi S, Miller EK, Rigotti M. 2016. Why neurons mix: High dimensionality for higher cognition. Curr Opin Neurobiol.

Fuster JM. 1984. Behavioral electrophysiology of the prefrontal cortex. Trends Neurosci. 7:408–414.

Fuster JM, Alexander GE. 1971. Neuron activity related to short-term memory. Science. 173:652–654.

Gnadt JW, Andersen RA. 1988. Memory related motor planning activity in posterior parietal cortex of macaque. Exp Brain Res. 70:216–220.

Goldman-Rakic P. 1995. Cellular basis of working memory. Neuron. 14:477–485.

Horsley V, Clarke RH. 1908. The structure and function of the cerebellum examined by a new method. Brain Behav Evol. 31:45–124.

Jacob SN, Nieder A. 2014. Complementary roles for primate frontal and parietal cortex in guarding working memory from distractor stimuli. Neuron. 83:226–237.

Kang Y, Endo K, Araki T, Mitani A. 1986. Dual mode of projections from the parietal to the motor cortex in the cat. Exp Brain Res. 62:281–292.

Koch KW, Fuster JM. 1989. Unit activity in monkey parietal cortex related to haptic perception and temporary memory. Exp Brain Res. 76:292–306.

Kubota K, Niki H. 1971. Prefrontal cortical unit activity and delayed alternation performance in monkeys. J Neurophysiol. 34:337–347.

Lajoie K, Andujar J-E, Pearson KG, Drew T. 2010. Neurons in area 5 of the posterior parietal cortex in the cat contribute to interlimb coordination during visually guided locomotion: a role in working memory. J Neurophysiol. 103:2234–2254.

Lajoie K, Drew T. 2007. Lesions of area 5 of the posterior parietal cortex in the cat produce errors in the accuracy of paw placement during visually guided locomotion. J Neurophysiol. 97:2339–2354.

Leavitt ML, Mendoza-Halliday D, Martinez-Trujillo JC. 2017. Sustained activity encoding working memories: not fully distributed. Trends Neurosci. 40:328–346.

Lomber SG, Payne BR, Horel JA. 1999. The cryoloop: An adaptable reversible cooling deactivation method for behavioral or electrophysiological assessment of neural function. J Neurosci Methods. 86:179–194.

Ludwig KA, Miriani RM, Langhals NB, Joseph MD, Anderson DJ, Kipke DR. 2009. Using a common average reference to improve cortical neuron recordings from microelectrode arrays. J Neurophysiol. 101:1679–1689.

Mansouri FA, Rosa MGP, Atapour N. 2015. Working Memory in the Service of Executive Control Functions. Front Syst Neurosci. 9:166.

Marigold DS, Drew T. 2017. Posterior parietal cortex estimates the relationship between object and body location during locomotion. Elife. 6ie28143.

Markowitz DA, Curtis CE, Pesaran B. 2015. Multiple component networks support working memory in prefrontal cortex. Proc Natl Acad Sci. 112:11084–11089.

Marple-Horvat DE, Criado JM. 1999. Rhythmic neuronal activity in the lateral cerebellum of the cat during visually guided stepping. J Physiol. 518:595–603.

McVea DA, Pearson KG. 2006. Long-lasting memories of obstacles guide leg movements in the walking cat. J Neurosci. 26:1175–1178.

McVea DA, Pearson KG. 2007a. Stepping of the forelegs over obstacles establishes long-lasting memories in cats. Curr Biol. 17:R621–R623.

McVea DA, Pearson KG. 2007b. Long-lasting, context-dependent modification of stepping in the cat after repeated stumbling-corrective responses. J Neurophysiol. 97:659–669.

McVea DA, Taylor AJ, Pearson KG. 2009. Long-lasting working memories of obstacles established by foreleg stepping in walking cats require area 5 of the posterior parietal cortex. J Neurosci. 29:9396–9404.

Mohagheghi AA, Moraes R, Patla AE. 2004. The effects of distant and on-line visual information on the control of approach phase and step over an obstacle during locomotion. Exp Brain Res. 155:459–468.

Mori A. 1997. Cortico-cortical connections from somatosensory areas to the motor area of the cortex following peripheral nerve lesion in the cat. NeuroReport. 8:3723–3726.

Mori A, Fuwa T, Kawai A, Yoshimoto T, Hiraba Y, Uchiyama Y, Minejima T. 1996. The ipsilateral and contralateral connections of the fifth somatosensory area (SV) in the cat cerebral cortex. NeuroReport. 7:2385–2387.

Morton SM, Bastian AJ. 2006. Cerebellar contributions to locomotor adaptations during splitbelt treadmill walking. J Neurosci. 26:9107–9116.

Mountcastle VB, Lynch JC, Georgopoulos A, Sakata H, Acuna C. 1975. Posterior parietal association cortex of the monkey: command functions for operations within extrapersonal space. J Neurophysiol. 38:871–908.

Murata A, Gallese V, Kaseda M, Sakata H. 1996. Parietal neurons related to memory-guided hand manipulation. J Neurophysiol. 75:2180–2186.

Parkinson A, Condon L, Jackson SR. 2010. Parietal cortex coding of limb posture: in search of the body-schema. Neuropsychologia. 48:3228–3234.

Pasternak T, Greenlee MW. 2005. Working memory in primate sensory systems. Nat Rev Neurosci. 6:97–107.

Patla AE, Vickers JN. 1997. Where and when do we look as we approach and step over an obstacle in the travel path? NeuroReport. 8:3661–3665.

Pearson RC, Powell TP. 1985. The projection of the primary somatic sensory cortex upon area 5 in the monkey. Brain Res. 356:89–107.

Postle BR. 2015. The cognitive neuroscience of visual short-term memory. Curr Opin Behav Sci.

Poulet JF, Hedwig B. 2006. The cellular basis of a corollary discharge. Science. 311:518–522.

Quintana J, Fuster JM. 1999. From perception to action: temporal integrative functions of prefrontal and parietal neurons. Cereb Cortex. 9:213–221.

Quiroga RQ, Nadasdy Z, Ben-Shaul Y. 2004. Unsupervised spike detection and sorting with wavelets and superparamagnetic clustering. Neural Comput. 16:1661–1687.

Rainer G, Miller EK. 2002. Timecourse of object-related neural activity in the primate prefrontal cortex during a short-term memory task. Eur J Neurosci. 15:1244–1254.

Raposo D, Kaufman MT, Churchland AK. 2014. A category-free neural population supports evolving demands during decision-making. Nat Neurosci. 17:1784–1792.

Richardson AG, Borghi T, Bizzi E. 2012. Activity of the same motor cortex neurons during repeated experience with perturbed movement dynamics. J Neurophysiol. 107:3144–3154.

Riggall AC, Postle BR. 2012. The Relationship between Working Memory Storage and Elevated Activity as Measured with Functional Magnetic Resonance Imaging. J Neurosci.

Rigotti M, Barak O, Warden MR, Wang XJ, Daw ND, Miller EK, Fusi S. 2013. The importance of mixed selectivity in complex cognitive tasks. Nature.

Scannell JW, Blakemore C, Young MP. 1995. Analysis of connectivity in the cat cerebral cortex. J Neurosci. 15:1463–1483.

Shafi M, Zhou Y, Quintana J, Chow C, Fuster J, Bodner M. 2007. Variability in neuronal activity in primate cortex during working memory tasks. Neuroscience. 146:1082–1108.

Singhal A, Monaco S, Kaufman LD, Culham JC. 2013. Human fMRI reveals that delayed action re-recruits visual perception. PLoS One. 8:e73629.

Snyder LH, Batista AP, Andersen RA. 1997. Coding of intention in the posterior parietal cortex. Nature. 386:167–170.

Spaak E, Watanabe K, Funahashi S, Stokes MG. 2017. Stable and dynamic coding for working memory in primate prefrontal cortex. J Neurosci. 37:6503–6516.

Sperry RW. 1950. Neural basis of the spontaneous optokinetic response produced by visual inversion. J Comp Physiol Psychol. 43:482–489.

Stokes MG. 2015. “Activity-silent” working memory in prefrontal cortex: a dynamic coding framework. Trends Cogn Sci. 19:394–405.

Stokes MG, Kusunoki M, Sigala N, Nili H, Gaffan D, Duncan J. 2013. Dynamic Coding for Cognitive Control in Prefrontal Cortex. Neuron. 78:364–375.

Takeda K, Funahashi S. 2002. Prefrontal task-related activity representing visual cue location or saccade direction in spatial working memory tasks. J Neurophysiol. 87:567–588.

Takeda K, Funahashi S. 2004. Population vector analysis of primate prefrontal activity during spatial working memory. Cereb Cortex. 14:1328–1339.

Vogt BA, Pandya DN. 1978. Cortico-cortical connections of somatic sensory cortex (areas 3, 1 and 2) in the rhesus monkey. J Comp Neurol. 177:179–191.

von Holst E, Mittelstaedt H. 1950. Das Reafferenzprinzip. Naturwissenschaften. 37:464–476.

Wang L, Li X, Hsiao SS, Lenz FA, Bodner M, Zhou Y-D, Fuster JM. 2015. Differential roles of delay-period neural activity in the monkey dorsolateral prefrontal cortex in visual-haptic crossmodal working memory. Proc Natl Acad Sci USA. 112:E214–E219.

Watanabe K, Funahashi S. 2007. Prefrontal delay-period activity reflects the decision process of a saccade direction during a free-choice ODR task. Cereb Cortex. 17.

Westwood DA, Heath M, Roy EA. 2003. No evidence for accurate visuomotor memory: systematic and variable error in memory-guided reaching. J Mot Behav. 35:127–133.

Whishaw IQ, Sacrey LAR, Gorny B. 2009. Hind limb stepping over obstacles in the horse guided by place-object memory. Behav Brain Res. 198:372–379.

Wilkinson EJ, Sherk HA. 2005. The use of visual information for planning accurate steps in a cluttered environment. Behav Brain Res. 164:270–274.

Wong C, Lomber SG. 2017. Reversible cooling-induced deactivations to study cortical contributions to obstacle memory in the walking cat. J Vis Exp. 130:e5619.

Wong C, Pearson KG, Lomber SG. 2017. Contributions of parietal cortex to the working memory of an obstacle acquired visually or tactilely in the locomoting cat. Cereb Cortex. 1–16.

Wong C, Wong G, Pearson KG, Lomber SG. 2018. Memory-guided stumbling correction in the hindlimb of quadrupeds relies on parietal area 5. Cereb Cortex. 28:561–573.

Yumiya H, Ghez C. 1984. Specialized subregions in the cat motor cortex: anatomical demonstration of differential projections to rostral and caudal sectors. Exp Brain Res. 53:259–276.

Zhang CY, Aflalo T, Revechkis B, Rosario ER, Ouellette D, Pouratian N, Andersen RA. 2017. Partially Mixed Selectivity in Human Posterior Parietal Association Cortex. Neuron. 95:697–708.e4.

Chapter 6

6 General Discussion

6.1 Main findings and conclusions

The series of studies comprising this thesis are aimed to assess the role of parietal area 5 in working memory-guided obstacle locomotion in the cat. I sought to answer five main questions: (1) Can cats remember an obstacle over which the forelegs have tripped? (2) Is this memory-guided stumbling correction mediated by parietal area 5? (3) Does area 5 contribute similarly when the animal first sees the obstacle without tripping over it? (4) Is area 5 involved specifically in the acquisition or maintenance of obstacle information in working memory? And lastly, (5) what are the neural correlates of this area 5 contribution?

6.1.1 The ability to remember an obstacle over which an animal has tripped is mediated by parietal area 5

Using the tactile obstacle memory task first described in Chapter 2, I demonstrated the ability of cats to remember an obstacle over which their forelegs had tripped (Chapter 3). This working memory-guided behaviour is fairly reliable and robust, lasting for delays tested up to two minutes. Furthermore, cooling-induced deactivations of parietal area 5, but not the adjacent area 7, resulted in attenuated hindleg step height and altered trajectories indicating a disregard for the obstacle. Importantly, such alterations in hindleg stepping were absent for continuous obstacle locomotion. Hindleg step height attenuation was only observed in trials with a memory delay, and without any evidence of paw dragging, inability to lift the feet, or changes in peak step velocity to suggest impaired motor capabilities. Thus while the stumbling corrective reaction has been demonstrated previously in low spinal animals (Forssberg 1979), introducing a working memory component to this behaviour necessitates cortical control. Parietal area 5 mediates this working memory-dependent hindleg clearance above an obstacle over which the forelegs have tripped.

6.1.2 Area 5 contributes to obstacle memory regardless of whether an animal first sees or feels the obstacle

Obstacle memory deficits observed following deactivation of area 5 during the tactile, stumbling corrective task were similar to those observed in the visual task (Chapter 4). Thus area 5 contributes similarly to obstacle memory when the animal first sees the obstacle without tripping over it. Additionally, I assessed the laterality of area 5 contributions to visual obstacle memory by performing unilateral cooling. Such spatially restricted deactivations resulted in step height deficits selectively for the contralateral hindleg when the ipsilateral hindleg led. In contrast, step height deficits were evident for both hindlegs when the contralateral hindleg led. This pattern of deficits contingent on which hindleg was the first to step suggests a greater contribution of area 5 in one hemisphere for guiding leading contralateral hindleg clearance. Trailing hindleg clearance may be largely mediated by subcortical mechanisms, for example, within the spinal cord, that coordinate stepping between the two hindlegs (Pocratsky et al. 2017).

Furthermore, the ability to temporally restrict cooling-induced deactivations to distinct phases of testing permitted the assessment of area 5 contributions to approach and delay phases of both visual and tactile tasks. While approach phase deactivations interfering with obstacle memory acquisition resulted in only partial memory deficits, delay phase deactivation of area 5 interfering with working maintenance were sufficient in reproducing complete memory deficits. Thus area 5 contributions to obstacle memory may be more specialized for working memory maintenance rather than working memory acquisition. Additionally, when area 5 activity was restored following deactivation within the delay period, only partial memory deficits were observed. Thus despite disrupting area 5 function early during memory maintenance, information regarding the obstacle may have been partially restored later in the delay, facilitating the recovery, albeit partial or incomplete, of modulated hindleg stepping for obstacle clearance. Such recovery may be facilitated by regions beyond the locus of cooling that may similarly be responsible for maintaining or conveying information related to the obstacle to area 5 throughout the delay. Alternatively, disrupting area 5 function early during memory maintenance would not interfere with working memory mechanisms appearing later in the delay. However, within this potential framework, as hindleg stepping was elevated but inadequate for obstacle clearance, such late delay coding mechanisms are insufficient for reliable working memory-guided obstacle negotiation. Working memory processes occurring early in the delay are therefore essential for robust working memory encoding.

6.1.3 Diverse neural dynamics in parietal area 5 facilitate working-memory guided obstacle avoidance

Given the heterogeneity and complexity of neural responses frequently described in cortical regions involved in working memory tasks, the initial aim of characterizing the neural activity within the region of area 5 we previously cooled was an open-ended endeavour (Chapter 5). Assessing obstacle-modulated activity throughout the approach, delay, and continuation phases revealed a diverse population of neurons within cat area 5, with similar heterogeneity and mixed selectivity described in neural populations within the human posterior parietal cortex (Zhang et al. 2017), as well as macaque prefrontal cortex (Rigotti et al. 2013; Fusi et al. 2016). Only a small subset of neurons exhibited obstacle-modulated activity sustained throughout the delay period, demonstrating a classical neural correlate of working memory (Fuster and Alexander 1971). Delay period activity of a small proportion of these neurons was further correlated with foreleg stepping preceding the delay, or hindleg stepping following the delay. While delay activity related to antecedent foreleg stepping may represent proprioceptive or efference copy information, delay activity related to subsequent hindleg stepping demonstrates motor-related coding of impending actions. Thus the subset of delay-modulated neurons either generally signalled the presence or absence of the obstacle, or demonstrated greater motor specificity for guiding hindleg clearance. Furthermore, two additional subsets of neurons without sustained delay period modulation were obstacle-modulated selectively during early or late phases of the delay period. These neurons may contribute to the initial encoding of obstacle-related information in working memory early in the delay, or the planning of impending movements for clearance later in the delay, respectively.

Such responses may also provide insight into the debate as to the sensory versus motor nature of information retained in working memory. Numerous studies examining the delay activity of primate prefrontal and posterior parietal neurons during working memory-guided eye and arm movements support both sensory-related and motor-related coding. For example, previous work has shown the maintenance of a remembered target location regardless of whether a saccade or antisaccade was to be made following a delay in prefrontal (Funahashi et al. 1993) and parietal neurons (Gottlieb and Goldberg 1999). These results indicate the maintenance of relevant sensory information rather than specific motor plans in relation to the target. In contrast, delay-related activity in primate area 5 has been reported to vary with the instructed direction of an arm movement to a remembered visual target (Crammond and Kalaska 1989). Additionally, area 5 delay activity has also been shown to vary depending on whether a reach or saccade is to be made to a remembered visual target, demonstrating motor-related encoding (Snyder et al. 1997). However, a sharp delineation between a purely sensory or purely motor signal may not be applicable to area 5 (Graziano and Botvinick 2002) or other posterior parietal areas (Buneo and Andersen 2006), as these regions are likely involved in sensorimotor transformations (Andersen et al. 1987; Buneo et al. 2002). Accordingly, the coexistence of neurons with activity modulated generally by obstacle presence, or more specifically in relation to step height, demonstrates a propensity for both sensory-related and motor-related coding within this small region of area 5. As previously suggested in primate area 5, local circuitry within cat area 5 may facilitate the sensorimotor transformations required for working memory-guided movements, resulting in the diverse patterns of neural responses observed in the present work.

Interestingly, the coexistence of three groups of neurons demonstrating different patterns of delay period modulation may also underlie the pattern of deficits observed with temporally restricted cortical deactivations in Chapter 4. Cooling initiated at the delay phase disrupted the activity of sustained delay modulated neurons, early delay modulated neurons, as well as late delay modulated neurons. These deactivations resulted in complete memory deficits whereby hindleg movements resembled stepping in obstacle absent conditions. In contrast, due to the slow thermodynamic properties of cortical cooling, approach phase cooling likely unintentionally impaired the activity of sustained and early delay neurons. Thus residual functions of late delay modulated neurons may have been able to partially modify hindleg stepping. However, the failure to produce adequate clearance for successful obstacle avoidance demonstrates the necessity for early delay period processes.

In addition to these characterizations of individual neurons, cross-temporal discriminability analysis was used to assess the ability to decode trial type from population activity across the approach, delay, and continuation phases. While obstacle information was reliably discernable from population level activity across approach and continuation phases, discriminability was sporadic and relatively unreliable during the delay. However, within the subset of neurons demonstrating sustained delay period modulation, discriminability remained robust throughout all three phases of testing. Thus overall, working memory coding may not be a generalized function across all area 5 neurons. Instead, only a small subset of neurons reliably retains obstacle-related information throughout a working memory delay. This identification of such a limited proportion of working memory-related neurons within a population stands in stark contrast to numerous other studies reporting robust mnemonic activity across parietal and prefrontal cortical areas. Task-dependent, species-dependent, or brain region-dependent factors may underlie these differences. Alternatively, the use of single electrode recordings and specific inclusion or exclusion criteria in other studies can introduce sampling biases to a recorded neural population (Leavitt et al. 2017). In contrast, the sampled population of area 5 neurons demonstrating limited working memory-related activity in Chapter 5 was derived through the use of chronically implanted multi-electrode arrays and lacked specific preselection procedures. Arguably, these methods may provide a more holistic view of the neural activities and functions within this region of parietal cortex.

Altogether, the insights gained from this present work can be compiled with previously established concepts to consider the neural computations that occur as an animal avoids an expected obstacle visible several steps before clearance, or as an animal adapts stepping to an unexpected obstacle. I first consider an animal walking towards an obstacle in clear view. Visual information about its size, shape, and relative distance (Marigold and Drew 2017) is used to alter stepping two to three steps before the obstacle in anticipation for clearance (Wilkinson and Sherk 2005). Such information processed initially by visual areas is likely relayed to parietal area 5 to compute the necessary anticipatory gait modifications (Andujar et al. 2010; Lajoie et al. 2010). If forward locomotion is interrupted such that hindleg clearance is delayed, information about the obstacle, incomplete motor plans for elevated hindleg stepping, or both, must be maintained in working memory. Neurons within parietal area 5 demonstrating modulated activity during the delay mediate this retention, and may relay such information to other cortical or subcortical regions to ensure successful hindleg clearance following the delay (Chapter 5). This working memory circuitry can also be recruited if hindleg clearance is similarly delayed after an animal fails to observe an obstacle in its path and suddenly trips over it with their forelegs (Wong et al. 2017, 2018). Thus parietal area 5 also represents a point of convergence between visual and tactile sensory systems, wherein sensory information can be used to guide immediate and delayed behaviours and actions.

6.2 Conserved locomotor control mechanisms for quadrupeds and bipeds

The parietal cortex contributions to obstacle locomotion described here in the cat may be applicable to walking in the bipedal human. Despite obvious biomechanical differences between quadrupedal and bipedal locomotion, conserved control mechanisms are evident within the neural circuitry. In both cats (Miller et al. 1975) and humans (Nathan et al. 1996), long propriospinal neurons couple and coordinate control circuitries for the upper and lower limbs in the cervical and lumbar spinal cord, respectively. In quadrupeds, such connectivity is required to ensure successful interlimb coordination of the forelimbs and hindlimbs for normal walking. In bipeds, as humans can independently control the upper limb for skilled manual movements, cervical and lumbar neural circuitries can be functionally decoupled in a task-dependent manner (Dietz 2011). However, this connectivity is typically engaged during bipedal locomotion, as rhythmic arm swinging during walking is well coordinated with leg movements for stepping. Such coordinated arm movements are readily engaged to improve stability by counteracting torsional movements of the trunk (Ballesteros et al. 1965). This conserved upper and lower limb coupling within the spinal circuitry can be further demonstrated by bilateral reflex responses in the arm muscles evoked by stimulation of the tibial nerve in one leg (Dietz et al. 2001). Additionally, this reflex response is enhanced before and during the step over an obstacle (Michel et al. 2008). Thus in bipedal humans, an anticipatory quadrupedal limb coordination is augmented for obstacle negotiation, engaging muscles in both the legs and arms for obstacle clearance (Dietz and Michel 2009).

Conceptually, quadrupeds and bipeds also share commonalities for obstacle locomotion. Both cats (Wilkinson and Sherk 2005) and humans (Patla and Vickers 1997) rely on visual information acquired two to three steps ahead of an obstacle in order to coordinate clearance. Accordingly, foot placement is appropriately modified two steps preceding clearance (Matthis and Fajen 2014; Kunimune and Okada 2017). In humans, the obstacle and leading limb are typically visible in the lower visual field, permitting the online use of vision to guide leading step trajectories (Patla et al. 1996; Mohagheghi et al. 2004). In contrast, neither the obstacle nor the trailing limb is subsequently visible, necessitating the use of previously acquired information about the obstacle to guide trail limb trajectories (Heijnen et al. 2014). This reliance on internally maintained obstacle information for guiding trailing leg clearance in humans may be supported by neural mechanisms similar to those guiding hindleg clearance in cats.

The most directly comparable assessment of obstacle negotiation involving working memory in humans arises from Lajoie et al. (2012). In this study, subjects stepped over an obstacle with one leg and delayed clearance of their trailing leg. Measures of trailing step elevation were used to assess obstacle memory, similar to the visual and tactile paradigms employed in this thesis. As has been demonstrated in cats (McVea and Pearson 2006) and horses (Whishaw et al. 2009), obstacle memory guiding trailing leg clearance in humans appears to be fairly robust, lasting for delays tested up to two minutes (Lajoie et al. 2012). Trailing step height also scaled accordingly when clearance over obstacles of different heights was assessed. Furthermore, manipulation of proprioceptive feedback or efference copy signals by adding a mass or passively lifting the lead leg over the obstacle, respectively, did not affect trailing leg trajectories. However, visual occlusion during leading leg clearance resulted in reduced trailing leg elevation and increased variability, demonstrating the importance of acquired visual information for this task. Given the behavioural similarities between obstacle memory capabilities in humans and cats, homologous neural circuits, for example involving the PPC, may facilitate working memory-guided obstacle locomotion in both bipedal and quadrupedal mammals. However, such cortical contributions to obstacle negotiation remain to be assessed in humans.

6.3 Primate homology

6.3.1 Topographical considerations

In the rhesus macaque, Brodmann area 5 resides within the medial bank of the intraparietal sulcus (Figure 6.1), and extends onto the postcentral gyrus anteriorly, abutting area 2 (Krubitzer et al. 1995). In humans, area 5 occupies the superior parietal lobule, also extending anteriorly onto the postcentral gyrus, as well as medially into the cingulate sulcus comprising the precuneus on the medial surface of the brain (Scheperjans et al. 2008). In macaques, tactile stimulation to the limbs paired with electrophysiological recordings have demonstrated a somatotopy similar to that of the cat (Andujar and Drew 2007), whereby the lower limbs (i.e. hindlimbs of the cat) are represented medially in area 5, while the upper limbs (i.e. forelimbs of the cat) are represented laterally (Seelke et al. 2012). In humans, tactile stimulation paired with fMRI has been used to similarly demonstrate a lower-to-upper limb representational gradient along the medial-to-lateral axis (Huang et al. 2012).

6.3.2 Functional considerations

In both macaques and humans, area 5 is often subdivided into multiple regions for further anatomical and functional study. While variations in terminology and exact loci, and subsequently the attributed functions, vary between research groups, subdivisions containing or overlapping with Brodmann area 5 are generally involved in reaching and grasping movements involving the upper limb. This apparent lack of parietal area 5 contributions to obstacle locomotion involving the lower limb may simply be because, relative to cats, macaques and humans are more conducive to studies of instructed, well-coordinated, upper limb movements. Accordingly, most human and non-human primate

Figure 6.1 Diagram comparing the location of Brodmann area 5 within the parietal cortex in the human, macaque, and cat.

Abbreviations: lcf – lateral cerebral fissure, cs – central sulcus, pcs – postcentral sulcus, ips – intraparietal sulcus, sts – superior temporal sulcus, tos – temporal occipital sulcus, ls – lateral sulcus.

Figure 6.1

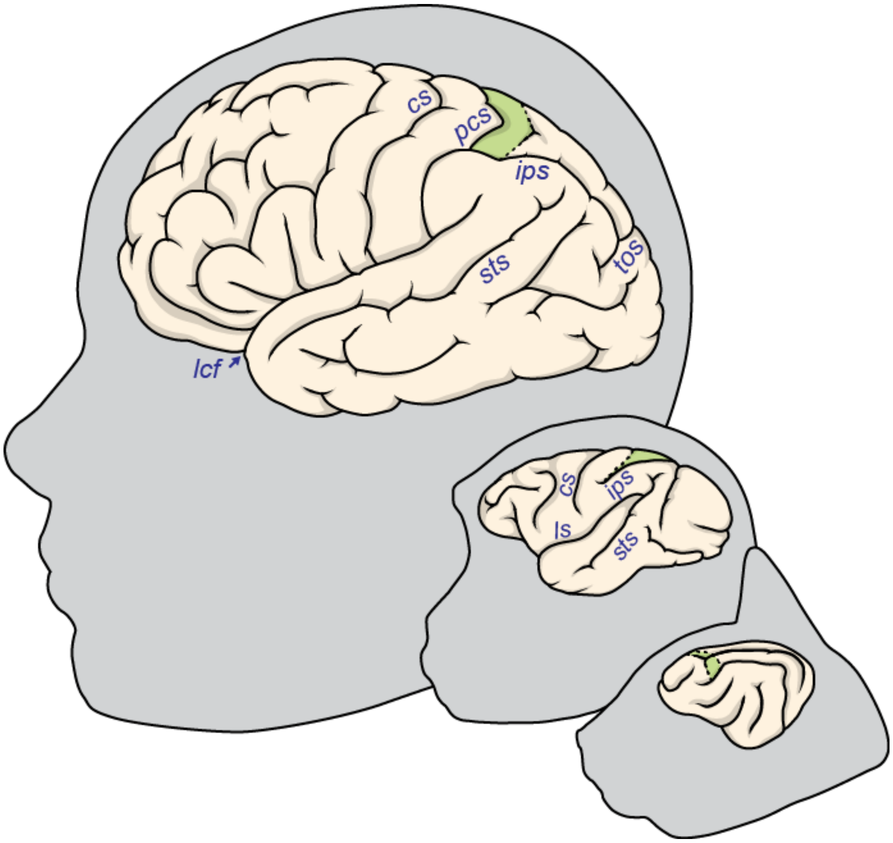

studies of area 5 function implicate more lateral regions where the upper limb is represented somatotopically. Note that the lack of assessment of area 5 contributions to obstacle locomotion does not imply the lack of contribution of area 5 to this behaviour.

Thus we presently lack the opportunity to directly compare cortical contributions to working memory-guided obstacle locomotion between cats and humans. However, a number of similarities exist between parietal cortex contributions to working memory-guided obstacle locomotion elucidated in this present work, and parietal cortex contributions to working memory-guided reaching movements. In macaques, projections from primary sensory areas, particularly from area 2, conveying proprioceptive information about limb position (Vogt and Pandya 1978; Pearson and Powell 1985), enables area 5 neurons to respond to changes in limb position and joint manipulation during reaching movements (Duffy and Burchfiel 1971; Mountcastle et al. 1975; Pellijeff et al. 2006; Shi et al. 2013). Additionally, area 5 neurons may also respond in anticipation of an arm movement, demonstrating sustained activity throughout the delay of memory-guided reaching tasks (Snyder et al. 1997; Batista and Andersen 2001; Buneo et al. 2002; Martínez-Vázquez and Gail 2018). In humans, regions of the PPC are similarly implicated in coordinating reaching movements (Culham et al. 2006; Busan et al. 2009; Vesia and Crawford 2012). Sustained delay period BOLD activity in the superior parietal lobule (Lindner et al. 2010a) as well as the precuneus (Gertz and Fiehler 2015) has been reported in human subjects performing memory-guided reaching tasks. Furthermore, PPC lesions affecting regions of Brodmann area 5 in humans result in severe optic ataxias, or misreaching, to visual targets (Schindler et al. 2004; Trillenberg et al. 2007; Caminiti et al. 2010).

Thus altogether, neural circuitry within Brodmann area 5 of the parietal cortex appears to support working memory capabilities for delayed movements of the limbs in both cats and primates. Such congruencies are somewhat unsurprising, as similarities between PPC contributions to visually-guided movements such as locomotion or reaching in cats or primates, respectively, may stem from evolutionarily conserved motor control mechanisms (Georgopoulos and Grillner 1989; Schmitt 2003). Thus in conjunction with avenues of working memory research in primates, further assessment of obstacle memory in the cat using paradigms similar to those evaluated in this thesis will help to complement and contribute to our understanding of how the brain controls memory-guided behaviours and actions.

6.4 Future Directions

The limitations and findings of this work prompt several possible avenues of future research. The studies comprising this thesis rely on relatively simple tasks involving the comparison of trials where the obstacle was present versus absent to assess working memory. In contrast, working memory-guided reaching and saccade tasks evaluated in humans and monkeys often feature multiple possible outcomes to probe the capabilities and specificity of working memory systems. For example, subjects may be required to remember one of sixteen possible remembered targets in an oculomotor delayed response task (Curtis et al. 2004). Additionally, varying the required movement in relation to a presented cue (i.e. pro-saccade or anti-saccade; Funahashi et al. 1993; Gottlieb and Goldberg 1999), or the effector for the delayed action (i.e. arm or eyes; Cui and Andersen 2007) has been used to examine the motor specificity of maintained neural representations. Furthermore, the comparison of a task involving both a memory and action component to a task requiring only a memory component can be used to determine whether a maintained neural representation encodes sensory information related to a remembered cue, or motor information related to the impending action (Lindner et al. 2010b). While the possible repertoire of experimentally testable behaviours in the cat may be relatively more limited, similar task manipulations may be evaluated. Future work involving clearance over multiple obstacles, obstacles of different sizes and shapes, or varying the locomotor path following the delay (i.e. by having the forelegs step backwards over the obstacle) may be useful for subsequently probing the complexity and capabilities of this system.

Additionally, while the studies comprising this thesis demonstrate the role of the parietal cortex in working memory-guided obstacle locomotion in the cat, this complex behaviour undoubtedly involves multiple regions of the brain. For example, in Chapter 4, interrupting area 5 function early in the delay does not completely attenuate hindleg stepping over a remembered obstacle. Other regions of the brain beyond the locus of cooling may drive such recovery of obstacle related information. Experiments involving simultaneous recordings from multiple regions of the brain can begin to elucidate the network of areas required for this complex behaviour. Additionally, pairing cooling-induced, optogenetic, or optoviral deactivations of one putative region with electrophysiological recordings from other regions may be used to demonstrate the functional relevance of candidate areas involved in working memory-guided obstacle locomotion.

6.5 References

Andersen RA, Essick GK, Siegel RM. 1987. Neurons of area 7 activated by both visual stimuli and oculomotor behavior. Exp Brain Res. 67:316–322.

Andujar J-E, Drew T. 2007. Organization of the projections from the posterior parietal cortex to the rostral and caudal regions of the motor cortex of the cat. J Comp Neurol. 504:17–41.

Andujar J-E, Lajoie K, Drew T. 2010. A contribution of area 5 of the posterior parietal cortex to the planning of visually guided locomotion: limb-specific and limb-independent effects. J Neurophysiol. 103:986–1006.

Ballesteros MLF, Buchthal F, Rosenfalck P. 1965. The pattern of muscular activity during the arm swing of natural walking. Acta Physiol Scand. 63:296–310.

Batista AP, Andersen RA. 2001. The parietal reach region codes the next planned movement in a sequential reach task. J Neurophysiol. 85:539–544.

Buneo CA, Andersen RA. 2006. The posterior parietal cortex: sensorimotor interface for the planning and online control of visually guided movements. Neuropsychologia. 44:2594–2606.

Buneo CA, Jarvis MR, Batista AP, Andersen RA. 2002. Direct visuomotor transformations for reaching. Nature. 416:632–636.

Busan P, Barbera C, Semenic M, Monti F, Pizzolato G, Pelamatti G, Battaglini PP. 2009.

Effect of transcranial magnetic stimulation (TMS) on parietal and premotor cortex during planning of reaching movements. PLoS One. 4:e4621.

Caminiti R, Chafee M V, Battaglia-Mayer A, Averbeck BB, Crowe DA, Georgopoulos AP. 2010. Understanding the parietal lobe syndrome from a neurophysiological and evolutionary perspective. Eur J Neurosci. 31:2320–2340.

Crammond DJ, Kalaska JF. 1989. Neuronal activity in primate parietal cortex area 5 varies with intended movement direction during an instructed-delay period. Exp Brain Res. 76:458–462.

Cui H, Andersen RA. 2007. Posterior parietal cortex encodes autonomously selected motor plans. Neuron. 56:552–559.

Culham JC, Cavina-Pratesi C, Singhal A. 2006. The role of parietal cortex in visuomotor control: what have we learned from neuroimaging? Neuropsychologia. 44:2668–2684.

Curtis CE, Rao VY, D'Esposito M. 2004. Maintenance of spatial and motor codes during oculomotor delayed response tasks. J Neurosci. 24:3944–3952.

Dietz V. 2011. Quadrupedal coordination of bipedal gait: implications for movement disorders. J Neurol. 258:1406–1412.

Dietz V, Fouad K, Bastiaanse CM. 2001. Neuronal coordination of arm and leg movements during human locomotion. Eur J Neurosci. 14:1906–1914.

Dietz V, Michel J. 2009. Human bipeds use quadrupedal coordination during locomotion. Ann N Y Acad Sci. 1164:97–103.

Duffy FH, Burchfiel JL. 1971. Somatosensory system: organizational hierarchy from single units in monkey area 5. Science. 172:273–275.

Forssberg H. 1979. Stumbling corrective reaction: a phase-dependent compensatory reaction during locomotion. J Neurophysiol. 42:936–953.

Funahashi S, Chafee M V, Goldman-Rakic PS. 1993. Prefrontal neuronal activity in rhesus monkeys performing a delayed anti-saccade task. Nature. 365:753–756.

Fusi S, Miller EK, Rigotti M. 2016. Why neurons mix: High dimensionality for higher cognition. Curr Opin Neurobiol.

Fuster JM, Alexander GE. 1971. Neuron activity related to short-term memory. Science. 173:652–654.

Georgopoulos AP, Grillner S. 1989. Visuomotor coordination in reaching and locomotion. Science. 245:1209–1210.

Gertz H, Fiehler K. 2015. Human posterior parietal cortex encodes the movement goal in a pro-/anti-reach task. J Neurophysiol. 114:170–183.

Gottlieb J, Goldberg ME. 1999. Activity of neurons in the lateral intraparietal area of the monkey during an antisaccade task. Nat Neurosci. 2:906–912.

Graziano MSA, Botvinick MM. 2002. How the brain represents the body: insights from neurophysiology and psychology. In: Prinz W,, Hommel B, editors. Common mechanisms in perception and action: Attention and performance. Oxford: Oxford University Press. p. 136–157.

Heijnen MJH, Romine NL, Stumpf DM, Rietdyk S. 2014. Memory-guided obstacle crossing: More failures were observed for the trail limb versus lead limb. Exp Brain Res. 232:2131–2142.

Huang R-S, Chen C -f., Tran AT, Holstein KL, Sereno MI. 2012. Mapping multisensory parietal face and body areas in humans. Proc Natl Acad Sci. 109:18114–18119.

Krubitzer L, Clarey J, Tweedale R, Elston G, Calford M. 1995. A redefinition of somatosensory areas in the lateral sulcus of macaque monkeys. J Neurosci. 15:3821–3839.

Kunimune S, Okada S. 2017. The effects of object height and visual information on the control of obstacle crossing during locomotion in healthy older adults. Gait Posture. 55:126–130.

Lajoie K, Andujar J-E, Pearson KG, Drew T. 2010. Neurons in area 5 of the posterior parietal cortex in the cat contribute to interlimb coordination during visually guided locomotion: a role in working memory. J Neurophysiol. 103:2234–2254.

Lajoie K, Bloomfield LW, Nelson FJ, Suh JJ, Marigold DS. 2012. The contribution of vision, proprioception, and efference copy in storing a neural representation for guiding trail leg trajectory over an obstacle. J Neurophysiol. 107:2283–2293.

Leavitt ML, Mendoza-Halliday D, Martinez-Trujillo JC. 2017. Sustained activity encoding working memories: not fully distributed. Trends Neurosci. 40:328–346.

Lindner A, Iyer A, Kagan I, Andersen RA. 2010a. Human posterior parietal cortex plans where to reach and what to avoid. J Neurosci. 30:11715–11725.

Lindner A, Iyer A, Kagan I, Andersen RA. 2010b. Human posterior parietal cortex plans where to reach and what to avoid. J Neurosci. 30:11715–11725.

Marigold DS, Drew T. 2017. Posterior parietal cortex estimates the relationship between object and body location during locomotion. Elife. 6ie28143.

Martínez-Vázquez P, Gail A. 2018. Directed interaction between monkey premotor and posterior parietal cortex during motor-goal retrieval from working memory. Cereb Cortex. 28:1866–1881.

Matthis JS, Fajen BR. 2014. Visual control of foot placement when walking over complex terrain. J Exp Psychol Hum Percept Perform. 40:106–115.

McVea DA, Pearson KG. 2006. Long-lasting memories of obstacles guide leg movements in the walking cat. J Neurosci. 26:1175–1178.

Michel J, van Hedel HJA, Dietz V. 2008. Obstacle stepping involves spinal anticipatory activity associated with quadrupedal limb coordination. Eur J Neurosci. 27:1867–

1875.

Miller S, Van Der Burg J, Van Der Meché F. 1975. Coordination of movements of the kindlimbs and forelimbs in different forms of locomotion in normal and decerebrate cats. Brain Res. 91:217–237.

Mohagheghi AA, Moraes R, Patla AE. 2004. The effects of distant and on-line visual information on the control of approach phase and step over an obstacle during locomotion. Exp Brain Res. 155:459–468.

Mountcastle VB, Lynch JC, Georgopoulos A, Sakata H, Acuna C. 1975. Posterior parietal association cortex of the monkey: command functions for operations within extrapersonal space. J Neurophysiol. 38:871–908.

Nathan PW, Smith M, Deacon P. 1996. Vestibulospinal, reticulospinal and descending propriospinal nerve fibres in man. Brain. 119 (Pt 6:1809–1833.

Patla AE, Rietdyk S, Martin C, Prentice S. 1996. Locomotor patterns of the leading and the trailing limbs as solid and fragile obstacles are stepped over: some insights into the role of vision during locomotion. J Mot Behav. 28:35–47.

Patla AE, Vickers JN. 1997. Where and when do we look as we approach and step over an obstacle in the travel path? NeuroReport. 8:3661–3665.

Pearson RC, Powell TP. 1985. The projection of the primary somatic sensory cortex upon area 5 in the monkey. Brain Res. 356:89–107.

Pellijeff A, Bonilha L, Morgan PS, McKenzie K, Jackson SR. 2006. Parietal updating of limb posture: an event-related fMRI study. Neuropsychologia. 44:2685–2690.

Pocratsky AM, Burke DA, Morehouse JR, Beare JE, Riegler AS, Tsoulfas P, States GJR, Whittemore SR, Magnuson DSK. 2017. Reversible silencing of lumbar spinal interneurons unmasks a task-specific network for securing hindlimb alternation. Nat Commun. 8:1963.

Rigotti M, Barak O, Warden MR, Wang X-J, Daw ND, Miller EK, Fusi S. 2013. The importance of mixed selectivity in complex cognitive tasks. Nature. 497:585–590.

Scheperjans F, Eickhoff SB, Hömke L, Mohlberg H, Hermann K, Amunts K, Zilles K. 2008. Probabilistic maps, morphometry, and variability of cytoarchitectonic areas in the human superior parietal cortex. Cereb Cortex. 18:2141–2157.

Schindler I, Rice NJ, McIntosh RD, Rossetti Y, Vighetto A, Milner AD. 2004. Automatic avoidance of obstacles is a dorsal stream function: evidence from optic ataxia. Nat Neurosci. 7:779–784.

Schmitt D. 2003. Insights into the evolution of human bipedalism from experimental studies of humans and other primates. J Exp Biol. 206:1437–1448.

Seelke AMH, Padberg JJ, Disbrow E, Purnell SM, Recanzone G, Krubitzer L. 2012. Topographic Maps within Brodmann’s Area 5 of macaque monkeys. Cereb Cortex. 22:1834–1850.

Shi Y, Apker G, Buneo CA. 2013. Multimodal representation of limb endpoint position in the posterior parietal cortex. J Neurophysiol. 109:2097–2107.

Snyder LH, Batista AP, Andersen RA. 1997. Coding of intention in the posterior parietal cortex. Nature. 386:167–170.

Trillenberg P, Sprenger A, Petersen D, Kömpf D, Heide W, Helmchen C. 2007. Functional dissociation of saccade and hand reaching control with bilateral lesions of the medial wall of the intraparietal sulcus: implications for optic ataxia. Neuroimage. 36 Suppl 2:T69–T76.

Vesia M, Crawford JD. 2012. Specialization of reach function in human posterior parietal cortex. Exp Brain Res. 221:1–18.

Vogt BA, Pandya DN. 1978. Cortico-cortical connections of somatic sensory cortex (areas 3, 1 and 2) in the rhesus monkey. J Comp Neurol. 177:179–191.

Whishaw IQ, Sacrey LAR, Gorny B. 2009. Hind limb stepping over obstacles in the horse guided by place-object memory. Behav Brain Res. 198:372–379.

Wilkinson EJ, Sherk HA. 2005. The use of visual information for planning accurate steps in a cluttered environment. Behav Brain Res. 164:270–274.

Wong C, Pearson KG, Lomber SG. 2017. Contributions of parietal cortex to the working memory of an obstacle acquired visually or tactilely in the locomoting cat. Cereb Cortex. 1–16.

Wong C, Wong G, Pearson KG, Lomber SG. 2018. Memory-guided stumbling correction in the hindlimb of quadrupeds relies on parietal area 5. Cereb Cortex. 28:561–573.

Zhang CY, Aflalo T, Revechkis B, Rosario ER, Ouellette D, Pouratian N, Andersen RA. 2017. Partially mixed selectivity in human posterior parietal association cortex. Neuron. 95:697–708.e4.

Curriculum Vitae

CARMEN WONG

EDUCATION

2018	Ph.D. Candidate, Neuroscience The University of Western Ontario, London, Ontario, Canada
2012	B.Sc., Honours Physiology The University of Western Ontario, London, Ontario, Canada

HONOURS

2016 – 2018	**Alexander Graham Bell Canada Graduate Scholarship** ($105,000) National Sciences and Engineering Research Council of Canada
2016 –2017	**Ontario Graduate Scholarship** ($15,000) - *declined* Ontario Ministry of Training, Colleges and Universities
2015	**Ontario Graduate Scholarship** ($15,000) Ontario Ministry of Training, Colleges and Universities
2014	**Frederick Banting and Charles Best Canada Graduate Scholarship** ($17,500) Canadian Institutes of Health Research
2013 –2013	**Ontario Graduate Scholarship** ($10,000) Ontario Ministry of Training, Colleges and Universities
2011	**Undergraduate Student Research Award** ($4,500) National Sciences and Engineering Research Council of Canada
2008 –2012	**Continuing Admission Scholarship** ($10,000) The University of Western Ontario

AWARDS

2018	**Travel Award for Federation of European Neuroscience Societies Forum of Neuroscience** ($2,000) Society for Neuroscience

2017	**G. Keith Humphrey Memorial Award for Outstanding Neuroscience Student** ($650) The University of Western Ontario
2016	**Doctoral Excellence Research Award** ($5,000) The University of Western Ontario
2014	**Travel Award for Federation of European Neuroscience Societies Forum of Neuroscience** ($2,000) Society for Neuroscience
2012	**Travel Award for Canadian Association for Neuroscience Annual Meeting** ($500) Canadian Association for Neuroscience

PUBLICATIONS

Wong C, Pearson KG, Lomber SG. 2017. Contributions of parietal cortex to visual- or tactile-mediated memory-guided obstacle locomotion in the cat. *Cerebral Cortex*. Published online 2017 Aug 2. PMID: 28981640.

Wong C, Lomber SG. 2017. Reversible cooling-induced deactivations to study cortical contributions to obstacle memory in the walking cat. *Journal of Visualized Experiments* (130), e56196. PMID: 29286402.

Stolzberg D, **Wong C**, Butler BE, Lomber SG. 2017. Catlas: An MRI-based three-dimensional cortical atlas and tissue probability maps for the domestic cat (felis catus). *Journal of Comparative Neurology*, 525(15): 3190-3206. PMID: 28653335.

Wong C, Wong G, Pearson KG, Lomber SG. 2016. Memory-guided stumbling correction in the hindlimb of quadrupeds relies on parietal area 5. *Cerebral Cortex*. Published online 2016 Dec 23. PMID: 28013232.

Wong C, Chabot N, Kok MA, Lomber SG. 2015. Amplified somatosensory and visual cortical projections to a core auditory area, the anterior auditory field, following early- and late-onset deafness. *Journal of Comparative Neurology*, 523(13):1925-1947. PMID: 25764419.

Wong C, Chabot N, Kok MA, Lomber SG. 2014. Modified areal cartography in auditory cortex following early- and late- onset deafness. *Cerebral Cortex*, 24(7): 1778-1792. PMID: 23413302.

SUBMITTED MANUSCRIPTS

Wong C, Lomber SG. Stable delay period representations in the posterior parietal cortex facilitate working memory-guided obstacle negotiation. *Current Biology*. Revision requested. Manuscript #CURRENT-BIOLOGY-D-18-00939.

Lomber SG, Meredith MA, **Wong C**, Kral A. Crossmodal plasticity in ventral auditory cortex of the deaf mediates enhanced face discrimination learning. *Nature Communications*. Revision requested. Manuscript #NCOMM-16-23355.

INVITED TALKS

“Parietal cortex contributions to working memory-guided obstacle avoidance.” Cortical Control of Locomotion and Posture Minisymposium, Society for Neuroscience Annual Meeting. November 2018.

“Neural correlates of sensory and motor information retained in parietal area 5 for memory-guided obstacle avoidance in the walking cat.” Canadian Action and Perception Network Satellite Meeting, Annual Canadian Neuroscience Meeting. May 2018.

CONFERENCE PRESENTATIONS

Wong C, Lomber SG. 2018. Neural correlates of sensory and motor information retained in parietal area 5 for memory-guided obstacle avoidance in the walking cat. Poster presentation at the FENS Forum of Neuroscience, Berlin, Germany.

Wong C, Lomber SG. 2017. Neural correlates of hindlimb obstacle memory revealed via chronic microelectrode array recordings in area 5 of walking cats. Poster presentation at the Neural Control of Movement Annual Meeting, Dublin, Ireland.

Wong C, Pearson KG, Lomber SG. 2016. Cooling-induced cortical deactivations reveal the contributions of area 5 to memory-guided stumbling correction in the walking cat. Poster presentation at the Neural Control of Movement Annual Meeting, Montego Bay, Jamaica.

Wong C, Pearson KG, Lomber SG. 2015. Dissociation of parietal cortex contributions to obstacle memory in walking cats. Poster presentation at the Society for Neuroscience Annual Meeting, Chicago, United States.

Wong C, Kral A, Lomber SG. 2014. Modified representations in auditory, visual and somatosensory cortices following deafness. Poster presentation at the 5th International Conference on Auditory Cortex, Magdeburg, Germany.

Wong C, Pearson KG, Lomber SG. 2014. Dissociation of parietal cortex contributions to obstacle memory in locomoting cats. Poster presentation at FENS Forum of Neuroscience, Milan, Italy.

Wong C, Kral A, Lomber SG. 2013. Duration of acoustic experience shapes development of auditory cortex cartography. Poster presentation at the Society for Neuroscience Annual Meeting, San Diego, United States.

Wong C, Kral A, Lomber SG. 2012. Modified areal cartography in auditory cortex following early- and late-onset deafness. Poster presentation at the Society for Neuroscience Annual Meeting, New Orleans, United States.

TEACHING EXPERIENCE

2014 **Teaching Assistant**
Neuroscience 4000: Honours Thesis in Neuroscience
The University of Western Ontario

2013 **Teaching Assistant**
Psychology 1000: The Psychology of Prosocial and Antisocial Behaviour
The University of Western Ontario

2012 **Teaching Assistant**
Psychology 2990: Applications of Psychology
The University of Western Ontario